The Mineralogy, Petrology and Geochemistry of the Port Mouton Pluton, Nova Scotia, Canada

by

Stephanie Leigh (Woodend) Douma

Submitted in partial fulfillment of the requirements
for the degree of Master of Science
at
Dalhousie University
Halifax, Nova Scotia
May, 1988

DALHOUSIE UNIVERSITY
DEPARTMENT OF GEOLOGY

The undersigned hereby certify that they have read and recommend to the Faculty of Graduate Studies for acceptance a thesis entitled " The Mineralogy, Petrology and Geochemistry of the Port Mouton Pluton, Nova Scotia, Canada.
by Stephanie Leigh (Woodend) Douma
in partial fulfillment of the requirements for the degree of Master of Science.

Dated August 31 | 88

Supervisor: Redacted

Readers:

D A L H O U S I E U N I V E R S I T Y

DATE August 6, 1988

AUTHOR Stephanie Leigh (Woodend) Douma

TITLE THE MINERALOGY, PETROLOGY AND GEOCHEMISTRY OF THE PORT MOUTON PLUTON, NOVA SCOTIA, CANADA

Department or School GEOLOGY

Degree M.Sc. Convocation Fall Year 1988

Permission is herewith granted to Dalhousie University to circulate and to have copied for non-commercial purposes, at its discretion, the above title upon the request of individuals or institutions.

Redacted

TABLE OF CONTENTS

Table of Contents iv

Figures, Photographs and Tables x

Abstract xix

Acknowledgements xx

Chapter 1 INTRODUCTION AND GEOLOGICAL SETTING 1

1-1 Introduction 1

1-2 Meguma Zone Granites (Northern vs Southern) 1

1-3 The Geological History of the Meguma Zone 3

1-4 Port Mouton Pluton 6

1-4-1 Purpose of Study 6

1-4-2 Location and Access 7

1-4-3 Physiography 8

1-4-4 Previous Work 9

1-4-5 Economic Potential 12

Chapter 2 FIELD RELATIONS, PETROLOGY AND STRUCTURE 13

2-1 Introduction 13

2-2 Description of Units 14

2-3 Structural Features Within the Pluton 77

2-3-1 Granite Dykes and Joints in Granite 77

2-3-2 Shear Zones and Shear Planes 81

2-3-3 Summary of Structural Data 81

2-4 Regional Structural Geology in the Meguma Group Metasediments 83

2-5 Discussion 84

Chapter 3 MINERALOGY 87

3-1 Introduction 87

3-2 Biotite and Phlogopites 87

3-2-1 Introduction 87

3-2-2 Composition of Biotite and Phlogopite within the PMP 88

3-2-3 Discussion 90

3-3 Muscovites 94

3-3-1 Introduction 94

3-3-2 Composition of Muscovites within the PMP 94

3-3-3 Discussion 94

3-4 Garnet 100

3-4-1 Introduction 100

3-4-2 Garnet Results 101

3-4-3 Discussion 104

3-5 Amphiboles 105

3-5-1 Introduction 105

3-5-2 Amphiboles from the Forbes Point Lamprophyre 106

3-5-3 Amphiboles from the MacLeod Cove Lamprophyre 107

3-5-4 Discussion 109

3-6 Plagioclase 111

3-6-1 Plagioclase Results 111

3-6-2 Discussion 113

Chapter 4 WHOLE ROCK CHEMISTRY 115

4-1 Introduction 115

4-2 Major Elements 115

4-2-1 Granitoid Rocks 115

4-2-2 Lamprophyres 117

4-3 Trace Elements 125

4-3-1 Introduction 125

4-3-2 Rubidium 128

4-3-3 Strontium 128

4-3-4 Barium 130

4-3-5 Yttrium 131

4-3-6 Zirconium 131

4-3-7 Vanadium 133

4-3-8 Niobium 133

4-3-9 Chromium 136

4-3-10 Nickel 136

4-3-11 Copper 137

4-3-12 Zinc 137

4-3-13 Gallium 137

4-3-14 Lead 137

4-3-15 Thorium 140

4-3-16 Lamprophyres 140

4-4 Rare Earth Elements 143

4-4-1 Introduction 143

4-4-2 REE's in the PMP 145

4-4-3 Discussion 148

4-4-4 Lamprophyre (NPM612) 149

4-5 Summary of Geochemical Data 152

Chapter 5 EMPLACEMENT, CHEMICAL MODELLING AND ORIGIN OF THE PMP 154

5-1 Mode of Emplacement..... 154

5-1-1 Introduction 154

5-1-2 PMP-Meguma Contacts 154

5-1-3 PMP Internal Contact Relations 154

5-1-4 Discussion 156

5-2 Depth of Emplacement of the PMP 159

5-3 Origin of the PMP Magma..... 167

5-3-1 Origin of Peraluminous Granites 167

5-3-2 Discussion 171

5-3-3 Origin of Tonalites 173

5-3-4 Discussion 175

5-3-5 Origin of Lamprophyre 176

5-4 Modelling the Whole Rock Chemistry of the PMP 176

5-4-1 Introduction 173

5-4-2 Fractional Crystallization 178

5-4-2-1 Methodology of the Fractional Crystallization Model 178

5-4-2-2 The Major Oxide Fractionation Model-XLFRAC 181

5-4-2-3 Limitations of this fractional crystallization model 182

5-4-2-4 Testing the XLFRAC models on the REE

and Trace Element analyses of the PMP 187
5-4-2-5 Discussion of Trace Element Fractionation Model Results 189
5-4-3 Restite Model 194
5-4-4 Batch Melting Model 196
5-4-5 Assimilation of Meguma Rocks 197
5-4-6 Assimilation of Earlier Plutonic Phases 197
5-4-7 Role of Fluids 198
5-4-8 Different Sources 199
5-5 Proposed Three Stage Model of the Evolutionary History of the PMP 199

Chapter 6 THE PORT MOUTON PLUTON IN RELATION TO SOUTHERN AND NORTHERN PERALUMINOUS GRANITOID BODIES IN SOUTHWESTERN NOVA SCOTIA 203
6-1 Introduction 203
6-2 Petrographic Variation between the Northern and Southern Plutons 204
6-3 $^{40}Ar/^{39}Ar$ Ages and Emplacement Histories 205
6-4 Metamorphic Grade 207
6-5 Oxygen and Sulfur Isotopes 210
6-6 Whole Rock Chemistry 210
6-6-1 Brief Description of the Nova Scotia Database 210
6-6-2 Separation of Northern and Southern Plutons by Multivariant Analyses 212

6-6-3 REE 212

6-7 Conclusions 215

Chapter 7 CONCLUSIONS AND RECOMMENDATIONS 219

7-1 Conclusions 219

7-2 Recommendatons for Future Work 222

Appendix A: Petrographic Descriptions..... 224

Appendix B: Microprobe Analyses 243

Biotite 244

Amphibole 255

Muscovite 255

Garnet 260

Plagioclase 263

Appendix C: Whole Rock Chemistry: Methods, Precision and Accuracy of Data 274

Appendix D: D-1 Whole Rock Major Element Analyses 283

D-2 Trace Element 290

D-3 REE 293

Appendix E: $^{40}Ar/^{39}Ar$ Laboratory Methods and Age Spectra.. 295

Reference 307

Map 1 - in back pocket

Map 2 - in back pocket

LIST OF FIGURES

Fig. 1-1 Location map of study area 2

Fig. 1-2 Peraluminous granitoid bodies in southwestern Nova Scotia Meguma Zone 4,5

Fig. 2-1 Ternary Qu-Ksp-Pl plot of modal analyses for Unit 1 20

Fig. 2-2 Schmidt stereographic projection - orientation of xenoliths and schlieren 29

Fig. 2-3 Schmidt stereographic projection -foliation in Unit 1 29

Fig. 2-4 Structural domains surrounding the PMP 32

Fig. 2-5 Ternary Qu-Ksp-Pl plot of modal analyses, Units 2 and 3 33

Fig. 2-6 Ternary Qu-Ksp-Pl plot of modal analyses, Unit 4 37

Fig. 2-7 Schmidt stereographic projection of banding in Unit 1 and Unit 4 48

Fig. 2-8 Schmidt stereographic projection of foliation in Unit 4 48

Fig. 2-9 Ternary Qu-Ksp-Pl plot of modal analyses of Units 5B, 6, 8 and 9 58

Fig. 2-10 Ternary Qu-Ksp-Pl plot of modal analyses of Unit 7 63

Fig. 2-11 Schmidt stereographic projections of orientation of aplite dykes 79

Fig. 2-12 Schmidt stereographic projections of orientation

of pegmatite dykes less than 1 metre wide 79

Fig. 2-13 Schmidt stereographic projections of orientation of pegmatite dykes greater than 1 metre in width ... 80

Fig. 2-14 Schmidt stereographic projections of orientation of granite veins 80

Fig. 2-15 Schmidt stereographic projection of orientation of joints in granite 82

Fig. 2-16 Schmidt stereographic projection of orientation of shear zones and shear planes in granites 82

Fig. 2-17 Schematic geological map of the Port Mouton Pluton 86

Fig. 3-1 Stability curve of phlogopite 89

Fig. 3-2 Biotite and phlogopite compositions- Al(vi) versus $Fe_T/ (Fe_T+Mg)$ 91

Fig. 3-3 Muscovite compositions Na/(Na+K+Ca) versus (Fe+Mg)/(Fe+Mg+Mn+Ti+Al(vi)) 98

Fig. 3-4 Muscovite compositions Ti versus Na versus Mg 99

Fig. 3-5 Garnet compositions Mn versus Fe versus Mg 103

Fig. 3-6 Garnet compositions Mg versus Fe_T+Mn versus Ca ... 103

Fig. 3-7 Metamorphic and magmatic fields of amphiboles from the St. Anthony Complex and PMP lamprophyres 110

Fig. 3-8 Anorthite composition of plagioclase -PMP 112

Fig. 4-1 Whole rock chemistry of the PMP -a- CaO vs SiO_2 .. 119

-b- MgO vs SiO_2 .. 119

-c- MnO vs SiO_2 .. 120

-d- FeO_T vs SiO_2 . 120

-e- K_2O vs SiO_2 .. 121

-f- Na_2O vs SiO_2 . 121

-g- P_2O_5 vs SiO_2 . 122

-i- TiO_2 vs SiO_2 . 122

-j- Al_2O_3 vs SiO_2 123

Fig. 4-2 Whole rock chemistry CIPW normative Qz vs Or vs Ab+An 124

Fig. 4-3 Shoshonitic and alkaline lamprophyre comositional fields 126

Fig. 4-4 Whole rock chemistry -PMP Na_2O + K_2O versus SiO_2 . 127

Fig. 4-5 Whole rock chemistry - PMP K_2O vs Rb 129

Fig. 4-6 Whole rock ehmistry -PMP Sr vs CaO 132

Fig. 4-7 Whole rock chemistry -PMP Rb vs Ba 132

Fig. 4-8 Whole rock chemistry- PMP Sr vs Ba vs Rb 134

Fig. 4-9 Whole rock chemitry -PMP Y vs D.I. 134

Fig. 4-10 Whole rock ehmistry -PMP Zr vs TiO_2 134

Fig. 4-11 Whole rock chemistry -PMP V vs D.I. 135

Fig. 4-12 Whole rock chemistry -PMP Cr vs D.I. 135

Fig. 4-13 Whole rock chemistry -PMP Cu vs D.I. 138

Fig. 4-14 Whole rock chemistry -PMP Zn vs D.I. 138

Fig. 4-15 Whole rock chemistry- PMP Pb vs D.I. 139

Fig. 4-16 Whole rock chemistry - PMP Pb vs K_2O 139

Fig. 4-17 Three lamprophyre dykes PMP, normalized to primitive earth crust 142

Fig. 4-18 REE whole rock analyses 146-147

Fig. 4-19 REE whole rock analyses average of each Unit 150

Fig. 4-20 Comparison of whole rock chemistry of lamprophyres: PMP vs Caledonian Kersantites 151

Fig. 5-1 Normative A-Ab-Or diagram. PMP (this study, data and de Albuquerque, 1977 161

Fig. 5-2 Plot of CIPW normative Ab-Qz-Or for the PMP 163

Fig. 5-3 Pressure-temperature diagram showing the path of metamorphism in the Port Mouton-Port Joli map area 164

Fig. 5-4 Composition of liquids generated within the melting interval of rocks of continental crust in the presence of H_2O (after Wyllie, 1977) 174

Fig. 5-5 Cartoon of the proposed petrogenetic model of the PMP 202

Fig. 6-1 Regional metamorphic map of Southwestern Nova Scotia 208

Fig. 6-2 Discriminant scores of Northern and Southern Plutons in Nova Scotia 214

Fig. 6-3 Whole-rock REE chemical analyses of selected samples from the SMB, Musquodoboit Batholith and PMP 216

LIST OF PHOTOGRAPHS

Photo 2-1 - Meguma/Unit 1 injection gneiss 21

Photo 2-2 - Migmatitic contact 22

Photo 2-3 - Biotite tonalite (Unit 1) 23

Photo 2-4 - Migmatitic contact 25

Photo 2-5 - Biotite tonalite (Unit 1) 26

Photo 2-6 - Thin section of tonalite (Unit 1) 27

Photo 2-7 - Thin section of biotite tonalite (Unit 1) 27

Photo 2-8 - Biotite schlieren 30

Photo 2-9 - Trondhjemite (Unit 2) 34

Photo 2-10- Thin section of trondjemite (Unit 2) 34

Photo 2-11- Leucomonzogranite (Unit 3) 35

Photo 2-12- Thin section of leucomonzogranite (Unit 3) 39

Photo 2-13- Inclusions of Unit 3 in Unit 4 39

Photo 2-14- Stringers of Unit 3 in Unit 4 40

Photo 2-15- Biotite granodiorite (Unit 4) 41

Photo 2-16- Biotite-muscovite monzogranite (Unit 4) 41

Photo 2-17- Thin-section of leucomonzogranite (Unit 4) 42

Photo 2-18- Thin section of Unit 4 monzogranite 42

Photo 2-19- Inclusions in Unit 4 44

Photo 2-20- Coarse banding in Unit 4 46

Photo 2-21- Coarse banding in Unit 46

Photo 2-22- Fine banding in Unit 4 47

Photo 2-23- Forbes Point lamprophyre (Unit 5A) 50

Photo 2-24- MacLeods Cove lamprophyre (Unit 5A) 50

Photo 2-25- Forbes Point lamprophyre (Unit 5A) 51

Photo 2-26- Thin section of Forbes Point lamprophyre 51
Photo 2-27- Plagioclase porphyritic phase of the Forbes Point lamprophyre 52
Photo 2-28- Thin section of Forbes Point lamprophyre (Unit 5A) 53
Photo 2-29- Thin section of Forbes Point lamprophyre (Unit 5A) 53
Photo 2-30- MacLeods Cove lamprophyre (Unit 5A) 54
Photo 2-31- Thin section of MacLeods Cove lamprophyre 55
Photo 2-32- Thin section of MacLeods Cove lamprophyre 55
Photo 2-33- Contact between Unit 5B breccia and Meguma Group metasediments 59
Photo 2-34- Thin section of breccia Unit 5B 60
Photo 2-35- Thin section of clasts in breccia (Unit 5B) ... 60
Photo 2-36- Banded leucomonzogranite (Unit 6) 62
Photo 2-37- Thin section of leucomonzogranite (Unit 6) 62
Photo 2-38- Thin section of biotite muscovite tonalite (Unit 7) 64
Photo 2-39- Thin section - granodiorite (Unit 7) 64
Photo 2-40- Biotite muscovite tonalite (Unit 7) 65
Photo 2-41- Biotite muscovite granodiorite (Unit 7) 65
Photo 2-42- Mafic dykes of Unit 7 -Type 1 67
Photo 2-43- Mafic dykes of Unit 7 -Type 2 67
Photo 2-44- Mesocratic dykes of Unit 7 -Type 3 68
Photo 2-45- Mafic dyke of Unit 7 -Type 4 68
Photo 2-46- Mafic dyke of Unit 7 -Type 5 70

Photo 2-47- Leucomonzogranite (Unit 8) 72

Photo 2-48- Thin section of a leucomonzogranite (Unit 8) .. 72

Photo 2-49- Leucomonzogranite (Unit 8) interbanded with aplite and pegmatite (Unit 9) 73

Photo 2-50- Banded leucomonzogranite (Unit 8) 73

Photo 2-51- Garnet-rich aplite (Unit 9) 75

Photo 2-52- Thin section of an aplite (Unit 9) 76

Photo 2-53- Green beryl in pegmatite 76

Photo 2-54- Garnet in pegmatite 78

LIST OF TABLES

Table 2-1 Summary of Units in the PMP 15

Table 2-2 Sample descriptions for each unit 16-19

Table 3-1 Chemistry of the biotites from the PMP 92-93

Table 3-2 Chemical analyses of muscovites from the PMP ... 96-97

Table 3-3 Petrological description of garnet samples 102

Table 3-4 Mineralogy of the garnet in the PMP and in the surrounding country rock 102

Table 3-5 Amphibole analyses - PMP 108

Table 4-1 Legend for the whole-rock geochemical plots 118

Table 4-2 Whole-rock chemistry of selected Caledonian kersantites and PMP lamprophyres 144

Table 5-1 Garnet-biotite geothermometry - PMP 166

Table 5-2 Table of ten whole-rock geochemical samples and their mineral phases used in the crystal fractionation modelling 179

Table 5-3 Database for the XLFRAC modelling of major elements 183

Table 5-4 Results of XLFRAC modelling of Major Oxides ... 184-186

Table 5-5 REE and Ba, Rb concentrations of initial and evolved magmas and mineral distribution coefficients 190

Table 5-6 Trace element crystal fractionation modelling using equilibrium fractionation models and Rayleigh fractionation models 191-192

Table 6-1 Discriminating northern and southern plutons on the basis of whole-rock geochemistry 213

ABSTRACT

The Port Mouton Pluton (PMP) is a complex, peraluminous, post-tectonic body located in southern Nova Scotia, that is distinct from the northern plutons and batholiths of the northeastern Meguma Terrane. The pluton consists of ten units, which collectively range in composition from tonalite, to trondhjemite, granodiorite, monzogranite, leucomonzogranite, aplite, pegmatite and lamprophyre.

The PMP evolved in three mafic-to-felsic cycles defined by the initial mafic end-members for each cycle (Units 1, 4 and 7). These three units are the most volumetrically abundant of the ten units and Unit 1 is the oldest of the ten units. Shoshonitic lamprophyres intruded mid-way through Cycle II and were subsequently intruded by phases in Cycle III.

The PMP is at least 352 million years old ($^{40}Ar/^{39}Ar$) but is demonstrably younger than the regional metamorphic age of 395 million years. The lamprophyre dykes are at least 328 million years old. Two distinct foliations observed within the pluton occur only in Units 1 and 4. The foliation in Unit 1 is perpendicular to the foliation of the country rock and is probably of igneous origin. The local foliation observed in Unit 4 is perpendicular to Unit 1 and parallel to the foliation in the country rock. Its origin is unknown.

Minor migmatization is present along some margins of the PMP but the contacts with the metasediments are predominantly sharp. The pluton was emplaced at a pressure of approximately 3.5 kilobars and temperatures of at least 650^{o}C.

Both mineral-chemistry and whole-rock chemical analyses suggest that Unit 1 is distinct from Unit 4. Simple, fractional crystallization cannot adequately explain the major and trace element variations observed between Unit 1 and Unit 4 but there is some evidence to support a crystal fractionation model evolving Unit 7 tonalites and granodiorites from Unit 1 tonalites.

ACKNOWLEDGEMENTS

I would like to thank the members of supervisory committee Drs. D.B. Clarke, R. Jamieson and R. Raeside and my external examiner Dr. S. Barr.

Field work was assisted by John Lerette and by the many discussions with Tracy Hope. Island mapping was possible with the assistance of Mr Davis and his fishing trawler. You made a great field assistance in the last week of the season Dad, thanks.

I would like to thank Linda Ham, Linda Richard and Heather Plint for their moral support and scientific discussions. They were greatly appreciated.

Thank you Bob MacKay for you patient help on the new microprobe, and Paul Smith and Dan Kontak for your interest and that last push in finishing this thesis.

I would like to acknowledge the abundant support from my families; the Woodends, the Doumas and in particular my husband Marten.

Chapter 1 INTRODUCTION AND GEOLOGICAL SETTING

1-1 Introduction

The purpose of this study is to investigate the geology of the Port Mouton Pluton, a peraluminous granitoid body situated in southern Nova Scotia (Fig. 1-1). Previous studies, and attempts to relate other satellite plutons of southern Nova Scotia to the well-studied South Mountain Batholith, have not included the Port Mouton Pluton (O'Reilly, 1976; MacDonald, 1981; Rogers, 1985, to name only a few).

1-2 Meguma Zone Granites (Northern versus Southern)

In the late Devonian to early Carboniferous, the Meguma Group was intruded by a number of peraluminous granitoid plutons (Elias, 1986; Dallmeyer and Keppie, 1986; Reynolds et al., 1981; Clarke and Halliday, 1980), the largest of which, at 10,000 km^2, is the South Mountain Batholith. The SMB and other peraluminous Meguma Zone plutons have been the object of intensive geological, geochemical and geophysical investigations over the past decade. Some of this work provided the necessary background for the discovery and development of the largest tin deposit of North America at East Kemptville, as well as the delineation of numerous prospects with appreciable tin, tungsten, and uranium mineralization (Clarke and Muecke, 1985) associated with the SMB.

The plutons intruding the Meguma Group were divided into two groups by Reynolds et al., (1981) on the basis of $^{40}Ar/^{39}Ar$ ages, and later by Kubilius (1983) on the basis of whole-rock sulphur isotope

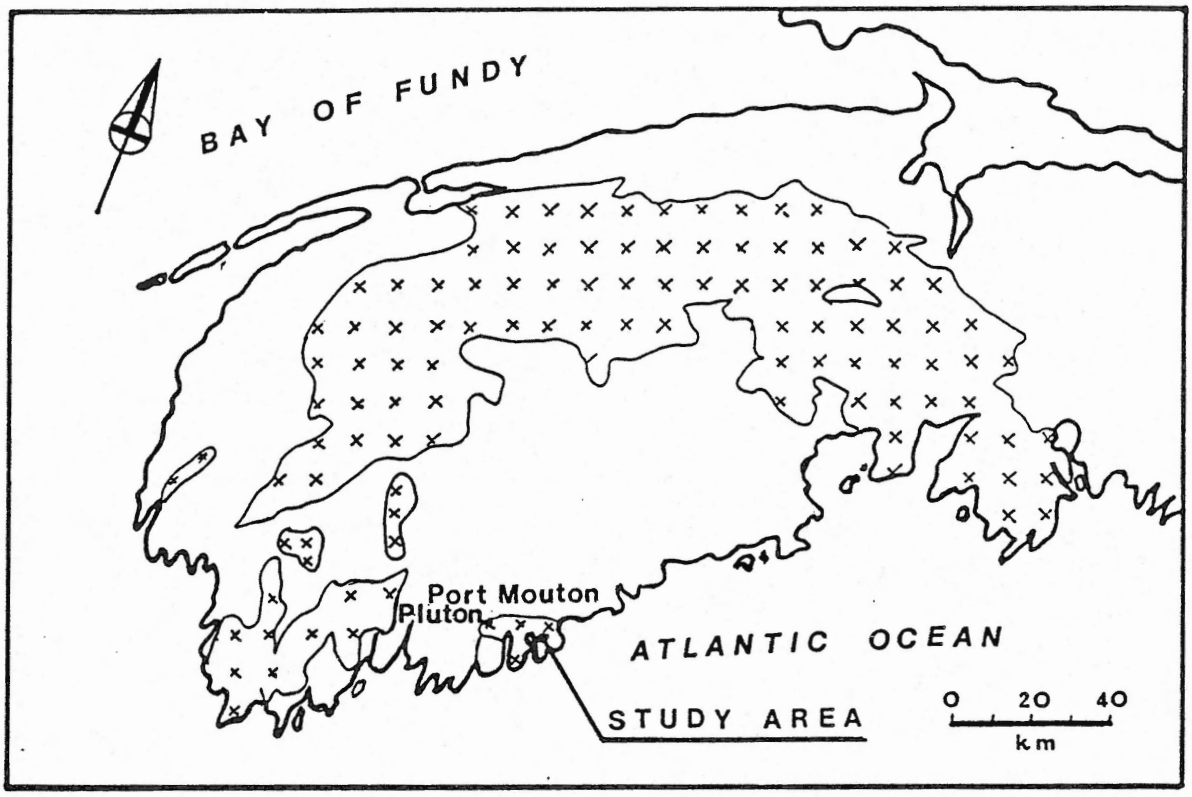

Figure 1-1: Map of southern Nova Scotia showing the location of the Port Mouton Pluton.

composition. The SMB was defined as a northern batholith, and the Barrington Passage, Shelburne and Port Mouton plutons were defined as southern plutons. In order to encompass as many of the documented peraluminous granites in the Meguma Zone as possible, these two groups are redefined and expanded in this study (Fig. 1-2).

Modern studies of peraluminous granites of the Meguma Zone suggest that the northern and southern plutons may be distinguished on the basis of $^{40}Ar/^{39}Ar$ ages (Reynolds et al., 1981; Elias, 1986), whole-rock chemistry (including isotopes) (Longstaffe et al., 1979; Kubilius, 1983; Richard, 1988), and petrology. Elaboration of the differences and similarities of the northern and southern plutons is documented in Chapter 6, and the position of the PMP is reconsidered in the light of new data presented in this thesis.

1-3 The Geological History of the Meguma Zone

The Meguma Zone is the easternmost lithotectonic terrane recognized in the Appalachian Orogen. It is situated south of the Avalon Zone of northern Nova Scotia and Newfoundland and consists largely of Paleozoic rocks (Williams, 1979). It differs from the adjacent Avalon Zone in its sedimentology (Schenk ,1970), plutonism (Clarke et al., 1980), tectonism (Webb, 1969; Eisbacher, 1969; Donohoe and Wallace, 1969) and metallogenesis (Zentilli, 1977). Stratigraphic, geochronological, structural, sedimentological, and paleomagnetic data exist for this terrane, but its origin is not yet established. Schenk (1983) suggested that possible source areas may be northwestern Africa, western Europe, western South America or even

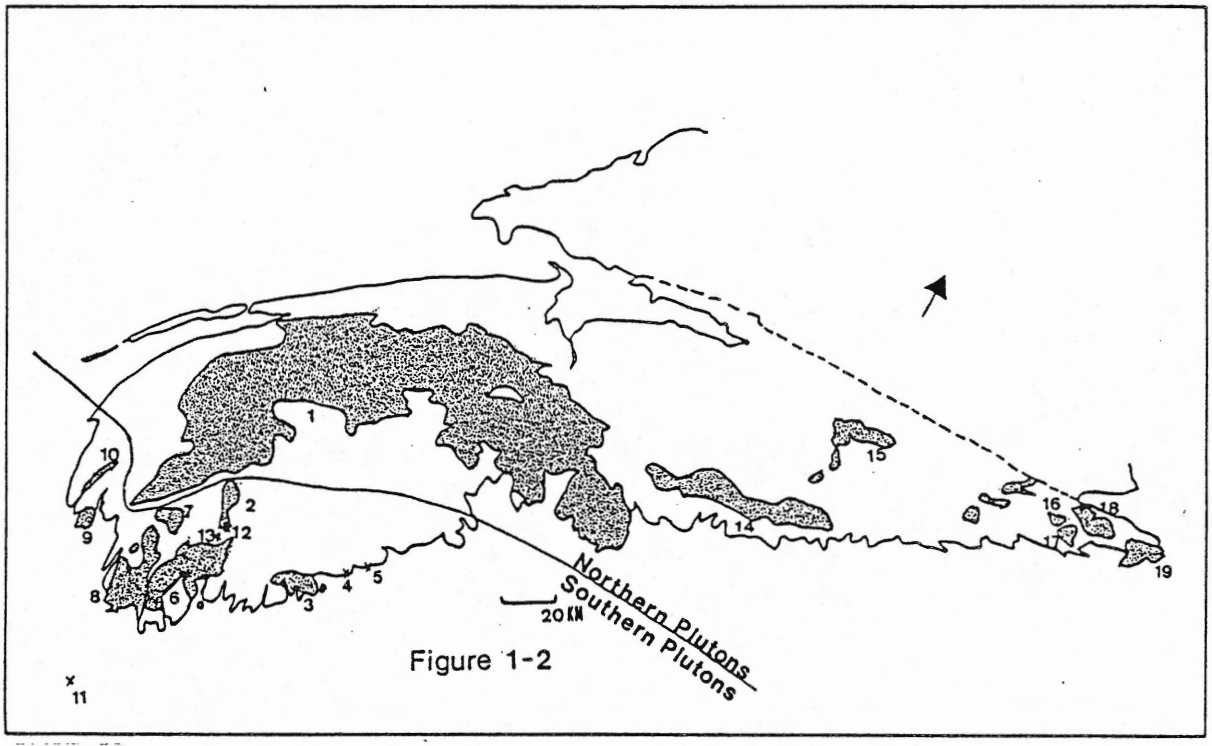

Figure 1-2

Figure 1-2: Peraluminous granitoid batholiths and plutons of Southwestern Nova Scotia Meguma Zone. Northern versus Southern Plutons as defined in this study. See page 5 for the map legend.

Figure 1-2
LEGEND:

-Southern Plutons-
2. Bald Mountain Pluton (Rogers, 1985)
3. Port Mouton Pluton (Faribault, 1913)
4. Moose Point Pluton (Weagle, 1983)
5. Strawberry Point Pluton (Weagle, 1983)
6. Shelburne Pluton (Rogers, 1985)
7. Quinan Pluton (Rogers, 1985)
8. Barrington Passage Pluton (Rogers, 1985)
9. Wedgeport Pluton (Rogers, 1985)
10. Brenton Pluton (O'Reilly, 1976)
11. Seal Island Pluton (Rogers, 1985)
12. Beach Hill Pluton (Rogers, 1985)
13. Deception Lake Pluton (Rogers, 1985)

-Northern Plutons-
1. South Mountain Batholith (McKenzie, 1974)
14. Musquodoboit Batholith (MacDonald, 1981)
15. Liscomb Pluton (Giles and Chatterjee, 1987)
16. Sangster Lake Pluton (O'Reilly, 1988)
17. Larry's River Pluton (O'Reilly, 1988)
18. Chedabucto Pluton (Halfway Cove and Queensport) (Ham, 1988)
19. Canso Pluton (Hill, 1986)
20. Bull Ridge Pluton (Richard, 1987)
21. Sherbrooke Pluton (Richard, 1987)
22. Ellison Lake Pluton (Richard, 1987)

the Canadian Shield.

The geological events affecting the Meguma Zone may be summarized as follows:

1) the deposition of the Meguma Group sediments (Goldenville and Halifax Formations) during the Cambrian and early Ordovician (Poole, 1971; Schenk, 1983);

2) the deformation of Meguma Group sediments into upright, isoclinal, east-west trending folds that were developed by regional deformation during the Acadian Orogeny at 415-385 Ma. (Reynolds and Muecke, 1978; Dallmeyer and Keppie, 1986 and Elias, 1986);

3) the intrusion of peraluminous granitoid bodies between 400-258 Ma. (Reynolds et al., 1984 and Dallmeyer and Keppie, 1986);

4) late Carboniferous deformation manifested by strike-slip faulting and/or thrusting of Carboniferous cover rocks and movement along the Minas Geofracture (Keppie, 1982; Giles, 1985; Dallmeyer and Keppie, 1986);

5) the deposition of mafic extrusive and intrusive rocks at 202 Ma (Poole et al., 1970) associated with the early phase of opening of the North Atlantic (Clarke, 1976; Wark and Clarke, 1980);

1-4 Port Mouton Pluton

1-4-1 Purpose of Study

Mapping of the PMP and the surrounding Meguma Group metasedimentary rocks was completed during the summer of 1985 (Hope and Woodend, 1986; Hope, 1987).

The purpose of this study is:

1) to produce a geological map of the pluton;

2) to describe the petrology of the various units observed in the pluton;

3) to standardize the nomenclature of the PMP with other granitoid bodies in the Meguma Zone;

4) to determine the cooling age of the PMP using $^{40}Ar/^{39}Ar$ ages;

5) using structural data, to determine if the PMP has been affected by any regional tectonic event and, if so, when;

6) to determine the mode of emplacement, depth of emplacement, and petrogenesis of the PMP;

7) to determine the variation in, and to search for possible genetic relationships between, the mapped units within the pluton using geochemistry (major, trace, rare earth elements);

8) to use trace elements and REEs to determine if Meguma Group sedimentary rocks could have been the source of melt for the pluton and also to determine if there is any evidence of a mantle component in the melt;

9) to classify the Port Mouton Pluton as either similar to Northern or Southern plutons in the Meguma Terrane.

1-4-2 Location and Access

The Port Mouton Pluton is a 160 km^2 body centred 12 km southwest of Liverpool, Nova Scotia. The town of Port Mouton is situated in the eastern quadrant of the pluton. The pluton underlies regions covered by the Port Mouton 1:50,000 NTS Map (20P/15,20P/10) and the Shelburne 1:50,000 NTS Map (20P/14). Henceforth the Port Mouton Pluton will be

referred to as the PMP.

The pluton crops out south of Highway 103, at Port Mouton Island, White Point, Hunts Point, Mouton Head, Black Point, St. Catherines River Beach, Port Joli Harbour, Haley Lake and at the head of Port LeHebert Harbour (Map 1). It is best exposed along shorelines, with sparse, small outcrops in the interior of the pluton and along the northern and western contacts.

Paved, gravel, and logging roads give good access to LeHebert Harbour, Port Joli Harbour, and the Western Channel. Footpaths extending from Southwest Port Mouton to Black Point allow access to the interior of the pluton and to the excellent shoreline outcrop at Black Point and St. Catherines River Beach area. Many brooks also allow access (by foot only) to the northern contacts of the pluton. A federal park has recently been established in the southern part of the PMP and encompasses the St. Catherines River Beach and Little Port Joli Harbour area.

1-4-3 Physiography

The southern sections of the pluton front on the Atlantic coastline. Drainage is by the Broad, Five, and Tidney Rivers and their tributaries and by smaller brooks flowing south to the Atlantic Ocean. The topography consists of a plateau with a generally southerly slope toward the Atlantic Ocean. Its elevation rarely exceeds 60-90 m above sea level.

The interior contains numerous peat bogs and swamps. The flow of water in the brooks and streams is reduced in summer making them

impossible to traverse by canoe.

Faribault (1913) reported that "much of the lowland is made up of coarse sandy material and loose pieces of rock with clay alluvium deposits along the depressions while the hills are largely composed of thick deposits of boulder clay and rock debris". Glacial striae recorded by Taylor (1967) show glacial motion towards the south.

Deeply incised ocean inlets cut into the mainland (Port Joli, Port LeHebert). The heads of these inlets contain abundant silt.

1-4-4 Previous Work

The Port Mouton Pluton was named by Faribault in 1913 in his study of the geology of Queens county. More recently Taylor (1967) completed a reconnaissance geological map of the Shelburne area in which he noted that the Port Mouton Pluton (referred to as the Port Joli Pluton in his report) intruded the Goldenville Formation of the Meguma Group. Contacts of the pluton with the sedimentary rocks were summarized as 'chiefly sharp but in part consisting of a mixed zone of biotite quartzite and granodiorite'. Taylor (1967) noted that migmatites crop out along the shore at White Point and west of White Point. The composition of the Port Mouton Pluton was mapped as granodiorite, with two small plugs to the west-northwest of the main pluton mapped as granites and granodiorites. Taylor (1967) mapped the pluton as primarily massive but found, in places, such as along the east side of Port Joli Bay, that biotite imparts a distinct foliation and sedimentary inclusions show a preferred orientation.

Detailed descriptions of beryl-bearing pegmatites of the Port

Mouton Pluton (including sketches) were made by Oldale (1959). Taylor (1967) also noted the occurrence of beryl in the pegmatites. Recent detailed work of a pegmatite within the PMP was completed by MacDonald (1988).

Two reconnaissance geochemical studies of the southern satellite plutons (including Port Mouton Pluton) were completed by Longstaffe et al., (1979) and Kubilius (1983). These studies used 'grab samples' from the pluton to compare ^{18}O and sulfur isotopes (respectively) of the Port Mouton Pluton (and other southern satellite plutons) with the SMB.

De Albuquerque (1977) in his brief geochemical and petrographic study of the PMP, described the pluton as a composite body composed of muscovite-biotite granodiorite and muscovite-biotite granite. Based on Qu-Or-Ab normative plots of samples taken from Port Mouton, de Albuquerque (1977) estimated pressure-temperature conditions of emplacement of the pluton at 4.5-5.5 kbars and 675-690 C. On the basis of similarities in major, trace, rare earth elements and mineralogy, he suggested that the PMP, the Shelburne Pluton and the Barrington Passage Pluton formed from partial melts of a metasedimentary source material.

Smith (1979) suggested that because of the similarity in major and trace elements between the PMP and the Halifax, New Ross and West Dalhousie plutons, that they were derived from the same source material. He also concluded that the same processes of differentiation of granite from granodiorite, suggested for the Halifax, New Ross and West Dalhousie plutons, are applicable to the

Port Mouton Pluton, specifically that the differentiation of granite from granodiorite resulted from the fractionation of plagioclase and biotite from the melt (Smith, 1974; McKenzie and Clarke, 1975).

There is uncertainty in the validity of the interpretations of Longstaffe et al., 1979; Kubilius, (1983), Cormier and Smith (1979), and de Albuquerque (1977) because no geological map detailing the magmatic units in the pluton was used as a basis for sampling, therefore the samples may not be representative of all units in the pluton.

Various radiometric ages have been recorded for the Port Mouton Pluton. Fairbairn et al., (1960) used a Rb/Sr model age of biotite from a granodiorite to date the pluton at 326 ± 5 Ma. Cormier and Smith (1973) obtained a three-point whole rock Rb/Sr isochron indicating an age of 349 ± 15 Ma, for a PMP granodiorite. Reynolds et al., (1981) used the $^{40}Ar/^{39}Ar$ total fusion method for a biotite from a 'monzonite' sample to obtain an age of 297 ± 8 Ma. Using the $^{40}Ar/^{39}Ar$ plateau-value method, Reynolds et al., (1981) obtained an age of 300 ± 8Ma for biotite from a 'monzonite' sample. Elias (1986) obtained four $^{40}Ar/^{39}Ar$ apparent ages from three mineral separate samples from the Port Mouton Pluton ranging from 255-321 Ma (see Chapter 6).

A structural study of the granites by Maksaev (1986) involved a detailed study of unusual fine and coarse banding observed in the granites on Port Mouton Island. He was able to show that multiple deformational events (of unknown magnitude or origin) had affected at least this section of the pluton during its cooling and consolidation.

Hope (1987) has studied the contact metamorphic aureole associated with the PMP for a comparison with the aureole associated with the Shelburne pluton. Detailed work on a migmatite in the northeast quadrant of the PMP has been completed by Merrett (1988).

1-4-5 Economic Potential

The Port Mouton Pluton has been assessed for its beryllium, tin, tungsten and uranium potential. Beryllium exploration by the Department of Mines (Oldale, 1959) indicates that the beryl is associated with pegmatites. In the Sandy Cove area some trenching and limited diamond drilling on pegmatite-hosted beryl have been done. In the southwestern section of Mouton Island a pit was sunk on the pegmatite dyke with the highest beryllium values. Unfortunately no drill-hole locations or drill-hole depths were given in the Department of Mines Report (1959).

Can-Lake Explorations Ltd. (Palmer, 1979) completed airborne radiometric, ground radiometric and geochemical (silt) surveys in an attempt to find uranium anomalies. The claim was dropped. Esso Minerals Canada (MacLeod, 1981) completed geochemical sampling and a reconnaissance geological study of the PMP areas in an attempt to locate tin and tungsten deposits. Tin anomalies in the Granite Brook and Wagner Brook area were described as "promising".

CHAPTER 2 FIELD RELATIONS, PETROLOGY AND STRUCTURE

2-1 Introduction

The Port Mouton Pluton is elliptical in plan view with axes approximately 20 km long (northeast-southwest) and 9 km across. The pluton has an area of approximately 160 km^2. Poor exposure along the northwestern contact and in the interior of the pluton has restricted mapping in these areas. The pluton contains at least ten distinct units showing cross-cutting relationships. Coded pie diagrams on Map 1 represent the relative abundances of the units within the vicinity of each symbol. Good coastal exposure in the southern sections of the pluton permitted identification of most of the field relationships of the ten units identified.

The pluton is locally very heterogeneous and, within a 100 square metre area, up to seven units have been mapped. Because of this heterogeneity, only two distinct units can be displayed at a scale of 1:50,000, as shown on Map 1. Around the perimeter of the pluton lies a zone which consists predominantly of coarse-grained foliated biotite tonalite (Unit 1). This unit makes up approximately 15% of the pluton and is the oldest intrusive phase exposed. In the central part of the pluton the predominant lithology is granodiorite to monzogranite (Unit 4), comprising about 50% of the intrusive material in the pluton.

With the exception of the pegmatitic Unit 9, all units in the Port Mouton Pluton have been examined petrologically. Stained slabs from 109 samples were point counted. All granitoid units have been

classified according to their modal abundances of quartz, plagioclase and K-feldspar after Streckeisen (1976). Table 2-1 is a summary of the field descriptions of the ten units, and Table 2-2 is a petrographic summary of selected samples from each of the units. Some units with a wide variation in composition (e.g. ranging from tonalite to granodiorite to monzogranite) are combined into a single unit because of their similar field relations. Lamprophyres have been classified after Rock (1977).

2-2 Description of Units

Unit 1, biotite tonalite

Unit 1 is a moderately well-foliated, biotite-rich tonalite and granodiorite (Fig. 2-1) comprising about 15% of the Port Mouton Pluton. It crops out mainly along the southern margin of the pluton and is the most common the intrusive material in direct contact with the Meguma Group metasedimentary rocks. The contacts between Unit 1 and the country rocks are typically sharp, although at Isaacs Harbour, at a locality 0.5 km north of Forbes Point, and at Scotch Point, abundant injection gneisses formed (Photo 2-1). Migmatites are prominent 1 km east of Summerville Beach, and at White Point, where the tonalite (Photo 2-2) has developed a subporphyritic texture (Photo 2-3) with plagioclase phenocrysts up to 8 mm long. Biotite tonalite dykes intruded along the bedding planes of the country rocks are prominent at the migmatitic contacts. Many xenoliths of the country rocks that have been incorporated in the tonalite have undergone

Table 2-1
Summary of Units in the Port Mouton Pluton

UNIT # (VOLUME% OF INTRUSION)	DESCRIPTION OF UNIT
9 (20-25%)	fine-grained aplite (± garnet, biotite, muscovite) and pegmatite (± biotite, tourmaline, beryl, garnet, fluorapatite)
8 (10%)	fine to medium-grained equigranular biotite-muscovite leucomonzogranite, intimately associated with Unit 9
7 (5-10%)	fine-grained equigranular, rarely porphyritic, mesocratic to melanocratic biotite-muscovite tonalite, granodiorite, rarely (5-10%) monzogranite.
	FORM and PERCENTAGE Of Unit 7 (not in order of age)
	1 (40%) pods, irregular meandering dykes
	2 (30%) dyke swarms with rounded biotite-rich xenoliths
	3 (<10%) dykes associated with pegmatites
	4 (1%) dykes with rounded biotite clots
	5 (20%) planar dykes with sharp contacts
6 (1%)	pegmatite, aplite and medium-grained equigranular leucomonzogranites (± biotite, muscovite, garnet)
5B (<1%)	fine-grained melanocratic biotite-muscovite tonalite breccia, with 50% clasts.
5A (<1%)	phlogopite and amphibole-rich lamprophyre dykes (younger than 4, older than 7)
4 (50%)	medium-grained, equigranular, biotite-muscovite granodiorite to monzogranite
3 (1%)	medium to fine-grained, equigranular, biotite-muscovite leucomonzogranite
2 (<1%)	coarse-grained, leucocratic trondhjemite with biotite schlieren
1 (15%)	coarse to medium-grained, foliated biotite tonalite and minor granodiorite

Note:
Grain size: fine < 1 mm, medium = 1 to 4 mm, coarse > 4 mm
Colour: leucocratic = mafic mineral content < 5%, mesocratic = mafic mineral content 5 - 20%, melanocratic = mafic mineral content > 20% .

Table 2-2

List of Abbreviations Used and Summary of Petrology of Collected Samples

(1) rock abbreviations: classification according to Streckeisen, 1976 and Rock, 1977
AL L=alkali lamprophyre
GRN=granodiorite
MNZ=monzogranite
MNZD+MNZG=monzodiorite+monzogabbro
SH L=shoshonitic lamprophyre
TON=tonalite
TRJ=trondhjemite
TON/L=tonalite/lamprophyre contact

(2) colour index:
= total biotite + phlogopite + amphibole content
(garnet is not included as a mafic mineral but as an accessory mineral)

(3) texture and grain size:
DUC DEF=ductile deformation
H G=hypidiomorphic granular
PANID=panidiomorphic
RECRYST=recrystallized
SUBPORP=subporphyritic
PORPHY=PORPHYRITIC
AVE=average

(4) mineral abbreviations:
ACT=actinolite
ACT HB=actinolitic hornblende
AP=apatite
BI=biotite
CHL=chlorite
EP=epidote
GT=garnet
KSP=potassic feldspar
MG HB=magnesio hornblende
MU=muscovite
PHL=phlogopite
PL=plagioclase
OP=opaque
QU=quartz
RUT=rutile
SPH=sphene
ST=staurolite
ZR=zircon

Table 2-2

SAMPLE	GRAIN SIZE	TEXTURE	MINERAL ASSEMBLAGE	NAME	AN	COLOUR INDEX
UNIT1						
NPM11	1-5mm	SUBPORP-H G	PL-BI-QU-MU-KSP-AP-EP-OP-ZR	TON	C=36 R=36	23
NPM2	1-5mm	SUBPORP-H G FOL	PL-QU-BI-MU-AP-ZR	TON	C=25 R=22	10
NPM487	1-6mm	H G	PL-QU-BI-MU-ZR	TON		12
NPM484	2-3mm	DUC DEF-H G	PL-QU-KSP-BI-MU-GT	GRN		11
NPM582	0.2-1mm	DUC DEF-H G	PL-QU-BI-MU-EP-OP	TON	C=37 R=29	21
NPM533	2-5mm	FOL-H G	PL-BI-QU-MU-EP-OP	TON	C=39 R=39	23
NPM544	0.5-6mm	H G	PL-QU-BI-MU-KSP-OP-EP-AP-ZR	TON		16
NPM593	1-6.5mm	H G	PL-QU-BI-KSP-MU-AP-ZR	GRN		12
NPM584	0.5-6.5mm	H G-FOL	PL-QU-BI-MU-EP-KSP-ZR	TON		16
UNIT 2						
NPM546	0.5-6mm	SUBPORP-H G	PL-QU-BI-MU-AP	TRJ	C=27 R=28	5-10
UNIT 3						
NPM468	0.5-1mm	DUC DEF-H G	PL-KSP-QU-MU-BI	MNZ	C=10 R=12	4
NPM542	0.5-3mm	DUC DEF-H G	PL-QU-KSP-MU-BI	MNZ	C=14 R=12	1
UNIT 4						
NPM549	1.5-6-5mm	H G	PL-QU-BI-KSP-MU-ZR-AP	GRN		15
NPM458	0.5-1.5mm	H G	PL-QU-BI-KSP-MU-AP-ZR	GRN	C=22 R=19	10
NPM558	0.5-3.5mm	SUBPORP-H G	PL-QU-BI-KSP-MU-AP-ZR	GRN	C=29 R=26	16

Table 2-2...

SAMPLE	GRAIN SIZE	TEXTURE	MINERAL ASSEMBLAGE	NAME	AN	COLOUR INDEX
UNIT 4						
NPM477	1-3.5mm	SUBPORP-H G	QU-KSP-PL-BI-MU-EP-AP-ZR	MNZ	C=12 R=10	6
NPM441	1-3.5mm	DUC DEF-H G	PL-QU-KSP-BI-MU-AP-ZR	MNZ	C=7.5 R=7.5	7
NPM580	1-4.5mm	SUBPORP-H G	KSP-QU-PL-BI-MU-ZR	MNZ	C=18 R=14	4
NPM32	1-5.5mm	DUC DEF-SUBPORP H G	PL-QU-KSP-BI-MU-AP-ZR	MNZ		5
NPM536	0.5-6mm	H G	PL-QU-KSP-BI-MU-AP-ZR	GRN		8
NPM543	0.5-3mm	H G	PL-BI-QU-KSP-MU-RUT-AP-ZR	GRN		26
NPM551	1-11mm AVE=4mm	SUBPORP H G	PL-QU-KSP-BI-MU-OP-ZR-AP	MNZ		13
NPM549	1.5-4mm	H G	PL-QU-BI-KSP-MU-ZR-AP	GRN		15
UNIT 5A						
FORBES POINT						
NPM405-NPM612	0.1-4.5mm	PANID	PHL-ACT-PLAG-OP-AP	SH L	C=54 R=29	82
NPM406-NPM615	0.5-2.5mm	PORPHY-H G	ACT HB PL-QU-PHL-AP-SPH-OP	AL L	C=47 R=43	65
CONTACT						
NPM407	0.5-6mm	PORPHY-H G	PL-PHL-MG HB-QU-KSP-AP-SPH-EP-OP	TON/L	C=46 R=44	50
MACLEOD COVE						
NPM485	0.03-0.4mm	RECRYST-GRANULAR CLUSTERS OF PHL	PL-PHL-ACT-SPH-AP QU	SH L	C=24 R=25	55

Table 2-2...

SAMPLE	GRAIN SIZE	TEXTURE	MINERAL ASSEMBLAGE	NAME	AN	COLOUR INDEX
UNIT 5						
MATRIX NPM486	0.2-1.5mm	RECRYST-GRANULAR	QU-PL-BI-CHL-MU-GT-AP-ZR-OP	TON		15
AVERAGE CLAST NPM486	0.2-0.5mm	SCHIST	QU-PL-BI-CHL-KSP-MU-GT-ST	BIOTITE SCHIST		25
UNIT 6						
NPM538	0.5-1mm	BANDED-DUC DEF H G	PL-KSP-QU-BI-MU-ZR	MNZ	C=15 R=15	4
UNIT 7						
NPM560	1mm	RECRYST-GRANULAR	PL-QU-BI-KSP-MU-OP-AP-ZR	TON	C=36 R=24	13
NPM539	0.5-2.5mm	SUBPORP-RECRYST H G	PL-QU-BI-KSP-MU AP	GRN	C=18 R=18	16
NPM583	0.5-1mm PLAG UP TO 3mm	SUBPORP-H G	PL-QU-BI-MU-KSP	TON	C=35 R=26	5
NPM566	0.1-1mm PLAG UP TO 3mm	SUBPORP-H G	KSP-PL-QU-BI-MU-ZR	MNZ	C=21 R=20	8
NPM464	0.2-1mm PLAG UP TO 5mm	SUBPORP-RECRYST H G	PL-BI-QU-KSP-MU-AP	MNZD-MNZG		16
UNIT 8						
NPM537	0.5-2.5mm	DUC DEF H G	PL-KSP-QU-BI-MU-ZR	MNZ	C=18 R=17	3
NPM361	0.5-3.5mm	H G	PL-QU-KSP-BI-MU-ZR	MNZ	C=13 R=13	1
NPM8A	2-4.5mm	H G	QU-KSP-PL-MU-BI-GT-CHL	MNZ		2
UNIT 9						
NPM491	0.1-1mm	BANDED APLITIC	PL-QU-MUS-KSP-GT-BI-AP	LEUCO TON	C=8 R=10	1

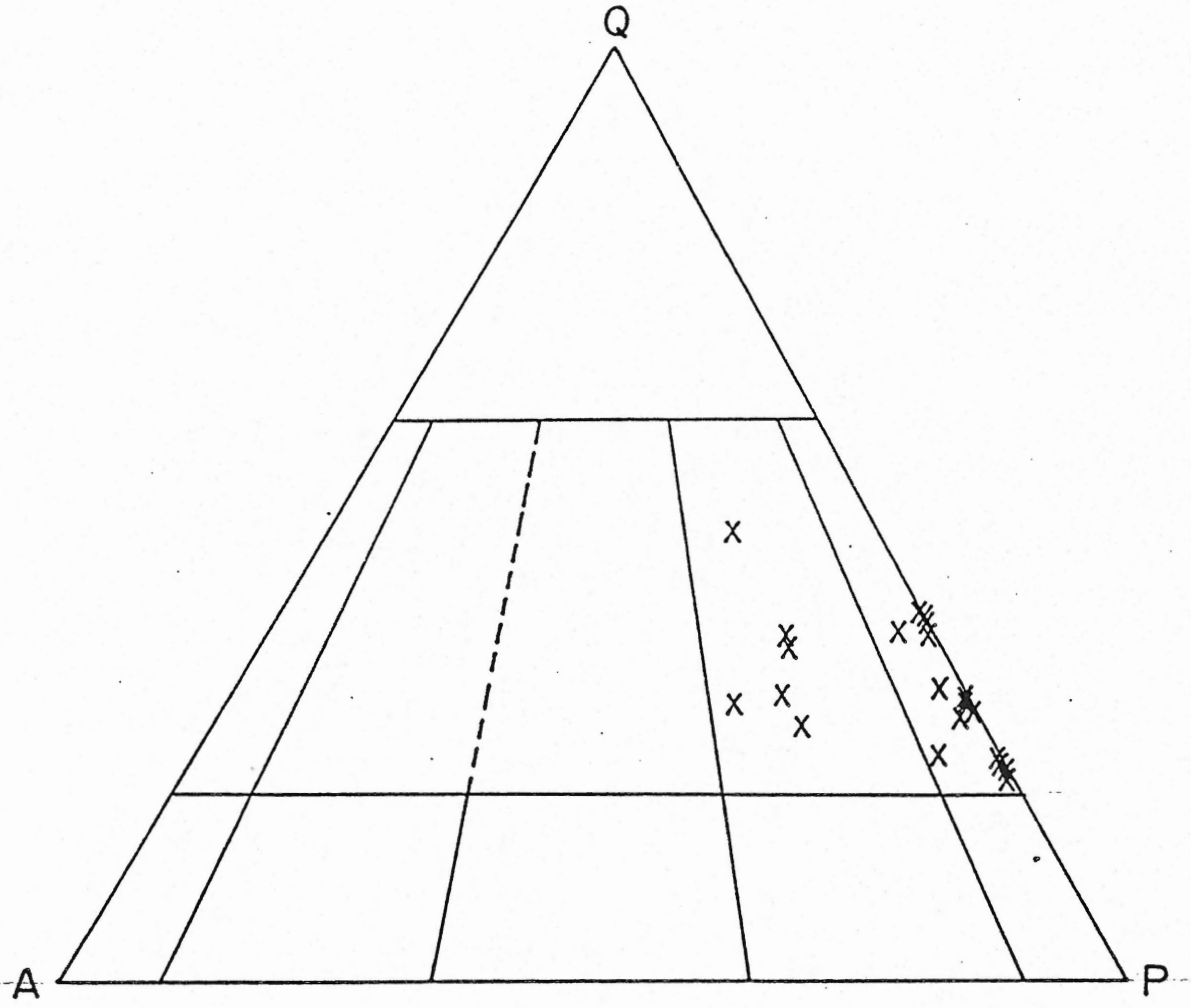

Figure 2-1: Ternary quartz-alkali feldspar-plagioclase plot of modal analyses of 22 samples of Unit 1.

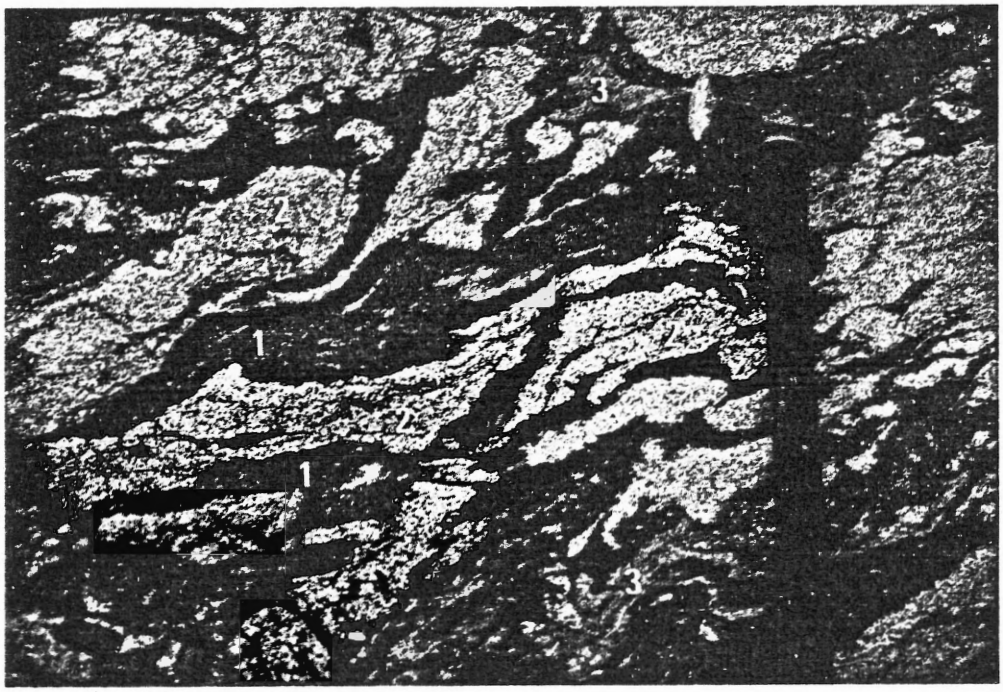

Photo 2-1: The Meguma/Unit 1 injection gneiss contact along St. Catherines River Beach. Note the ductile nature of the Meguma Group pelitic inclusions and host rock. The matrix consists of tonalite from Unit 1.

1 = pelite (Goldenville Formation)

2 = medium-grained to coarse-grained foliated biotite tonalite (Unit 1)

3 = psammite (Goldenville Formation)

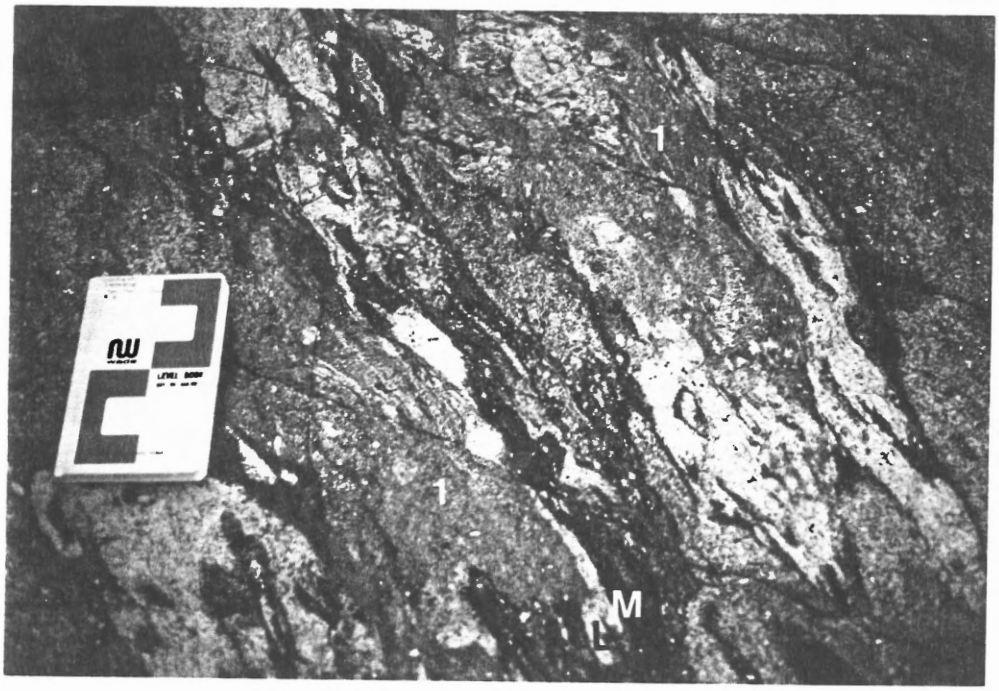

Photo 2-2: Migmatitic contact between Unit 1 (1) and Meguma (M) at White Point. The Meguma inclusions have undergone ductile deformation and there is a complex 'intermixing' of granitoid material and metasediment. Thin and wispy bands and pods of quartzo-feldspathic material may represent leucosomes (L).

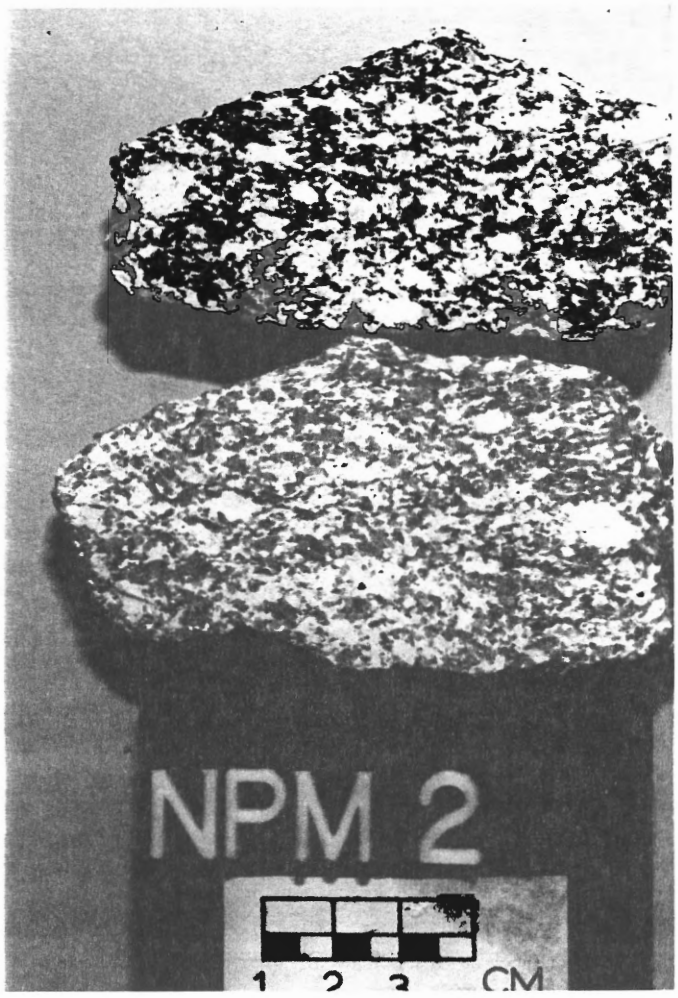

Photo 2-3: Stained hand specimen of medium-grained to coarse-grained subporphyritic, foliated, biotite tonalite of Unit 1 from a migmatite contact at east Summerville Beach. Note the elongation of some of the plagioclase phenocrysts.

ductile deformation and show evidence of anatexis in the formation of ptygmatically folded granitic bands (Merrett, 1987) (Photo 2-4). The injection gneiss contacts are similar to the migmatite contacts but lack leucosome and ptygmatically folded granitic bands.

The biotite tonalite is predominantly coarse-grained (Photo 2-5) with an average biotite content of 15%, rising to 23% near contacts with the country rock. Modal analyses of 22 slabbed and stained hand specimens show that the composition changes from a tonalite (dominant in the area shown as Unit 1 on Map 1) to a granodiorite toward the interior of the pluton. The major minerals are plagioclase (33-58%), quartz (20-40%), K-feldspar (0-20%), biotite (7-23%) and muscovite (1-11%) (Photos 2-6, 2-7). Apatite and zircon are common accessory minerals. Garnet observed in one sample of Unit 1 is probably xenocrystic from garnet-rich pelitic horizons in the nearby country rock.

In the interior of the pluton, Unit 1 resembles Unit 4, with a K-feldspar content as high as 15% , and muscovite up to 6% . Clear field relations identify Unit 1 and Unit 4 whereby inclusions of Unit 1 granodiorite in Unit 4, and dykes of Unit 4 cross-cutting Unit 1 granodiorite indicate that this granodiorite is part of Unit 1.

The types and percentages of inclusions in Unit 1 vary as a function of their distance from the edge of the pluton. At the contact, these xenoliths become less abundant and Unit 1 contain abundant xenoliths of psammite and pelite. At distances greater than 500 m from the contact, Unit 1 contains approximately 2% fine-grained, biotite-rich mafic inclusions. These inclusions are

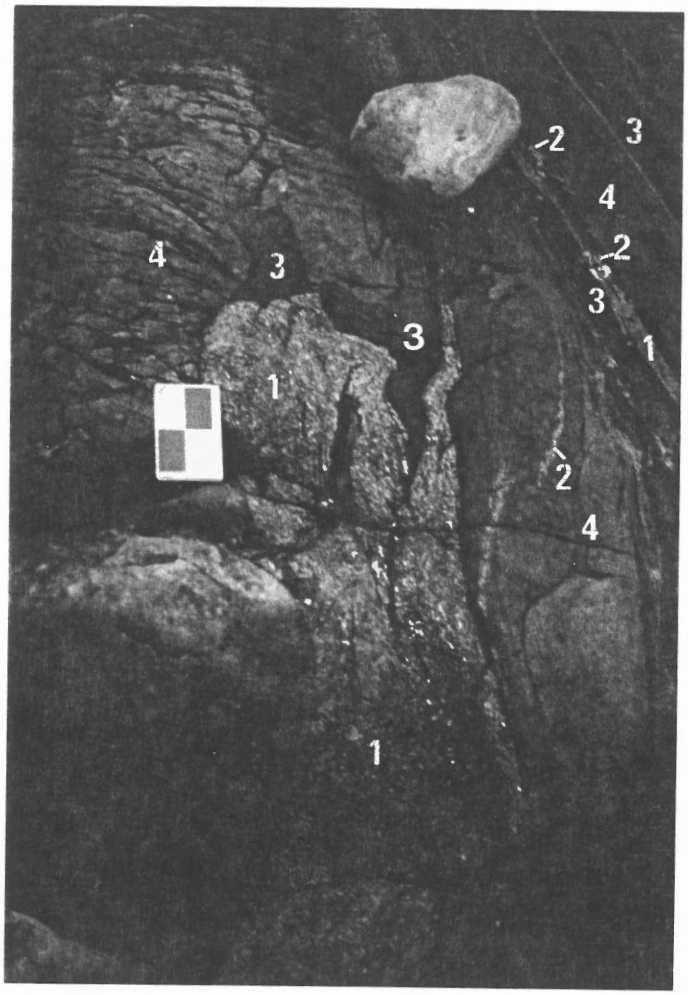

Photo 2-4: Migmatitic contact. Subporphyritic tonalite dykes intruding along the pelitic and psammitic Meguma bedding planes at White Point.

1 = Unit 1 medium-grained biotite porphyritic tonalite

2 = ptygmatic leucosomes, 'sweats'-predominantly quartz + feldspar

3 = pelite, Goldenville Formation

4 = psammite, Goldenville Formation

Photo 2-5: Stained hand specimen of coarse-grained, foliated, biotite tonalite of Unit 1 south of Forbes Point. The foliation lies horizontally across the photo.

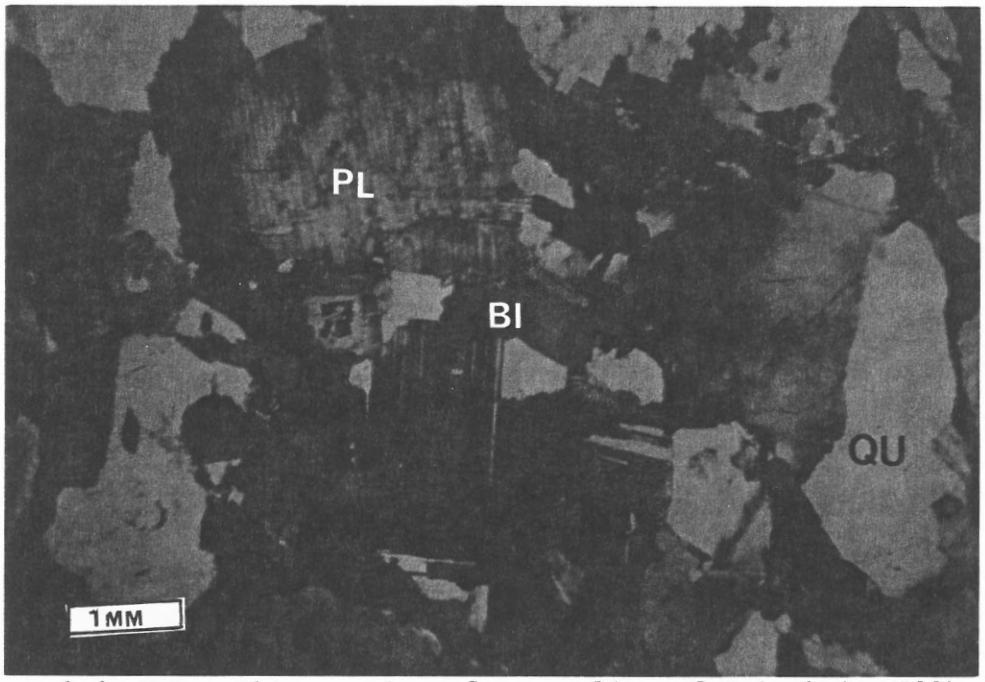

Photo 2-6: XNL. Thin-section of a tonalite of Unit 1 (NPM533). Mineralogy includes plagioclase, biotite, quartz, and minor muscovite (not visible in this field of view). Note the relatively large crystals and well-developed zonation in the plagioclase and the subhedral biotite grains. X 14

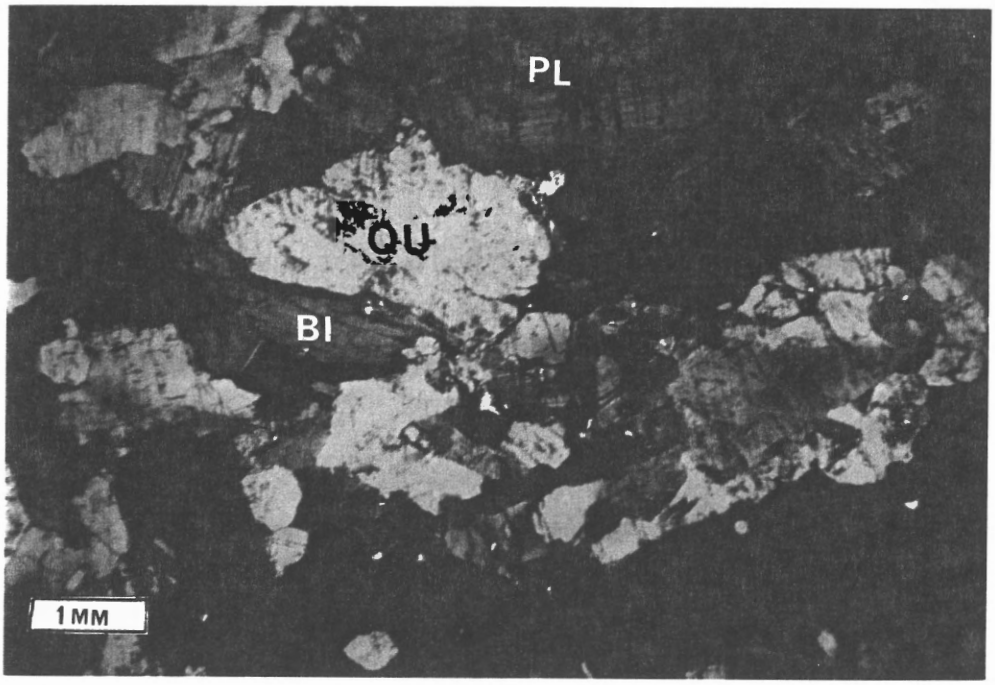

Photo 2-7: XNL. Thin section of Unit 1 (NPM11) from near the wharf south of Forbes Point. This is a medium-grained to coarse-grained subporphyritic biotite-tonalite. The mineralogy includes well zoned plagioclase, quartz, biotite and muscovite, with accessory zircon and apatite. Note the large well zoned plagioclase in the upper field of view.

typically rounded and elliptical to circular in shape. They range in composition from hornfels of Meguma Group country rock origin, to biotite schlieren, and ghost enclaves of unknown origin. Typically, the inclusions are finer grained than the host tonalite or granodiorite, and have a higher modal percentage of biotite. Locally, feldspar porphyroblasts occur in the inclusions. No microgranitoid enclaves (as described by Vernon, 1984) were identified in this unit, although xenoliths of Unit 1 commonly occur in the later units. In particular, large 10-15 m x 10 m blocks of Unit 1 occur in the younger, medium-grained, biotite-muscovite granodiorite and monzogranite of Unit 4. Outcrops at Forbes Point clearly illustrate the block-like inclusions of Unit 1 in Unit 4. The biotite foliation seen in Unit 1 is retained in the xenoliths, but occurs at high angles to the regional foliation, indicating that the blocks have been rotated.

The orientations of xenoliths of metasedimentary origin and biotite schlieren, collectively from Units 1 and 4, are shown on Figure 2-2. The irregular, wavy, biotite-rich schlieren in both Units 1 and 4 (Photo 2-8) are considered to be passive schlieren (Trent, 1981) and appear to have been passengers in the moving magma or crystal mush of enclosed rock. The maximum concentration of planes on the plot is about 140°, dipping moderately to the southwest.

Foliation in Unit 1 is displayed as a mild parallel alignment of biotite commonly detected only in fresh outcrop surfaces. It is moderately well developed in the vicinity of the contact with the country rocks, but poorly developed (or absent) in the interior of the

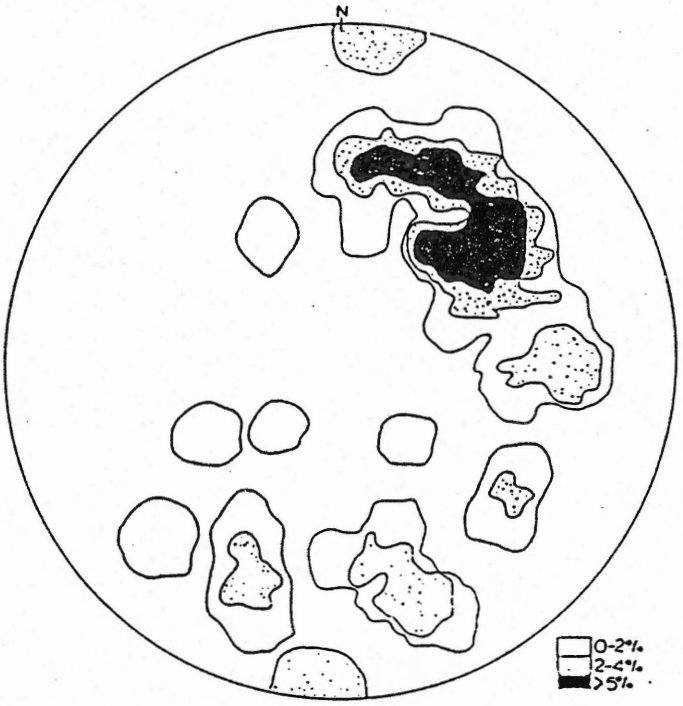

Figure 2-2: Orientation of xenoliths and schlieren in Units 1 and 4. Schmidt stereographic projections- plot of poles to planes percentages of 48 points in a 1% area if hemisphere.

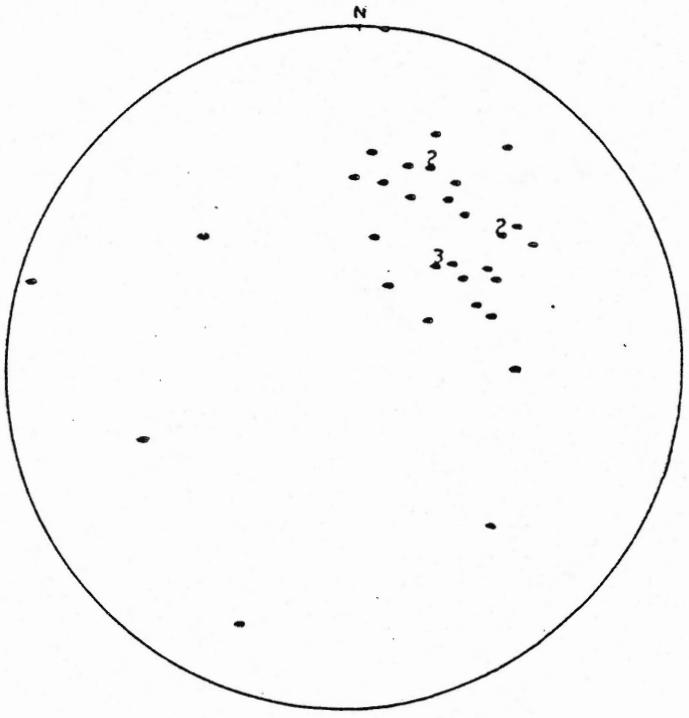

Figure 2-3: Foliation in Unit. Schmidt stereographic projections. A plot of 39 poles to planes.

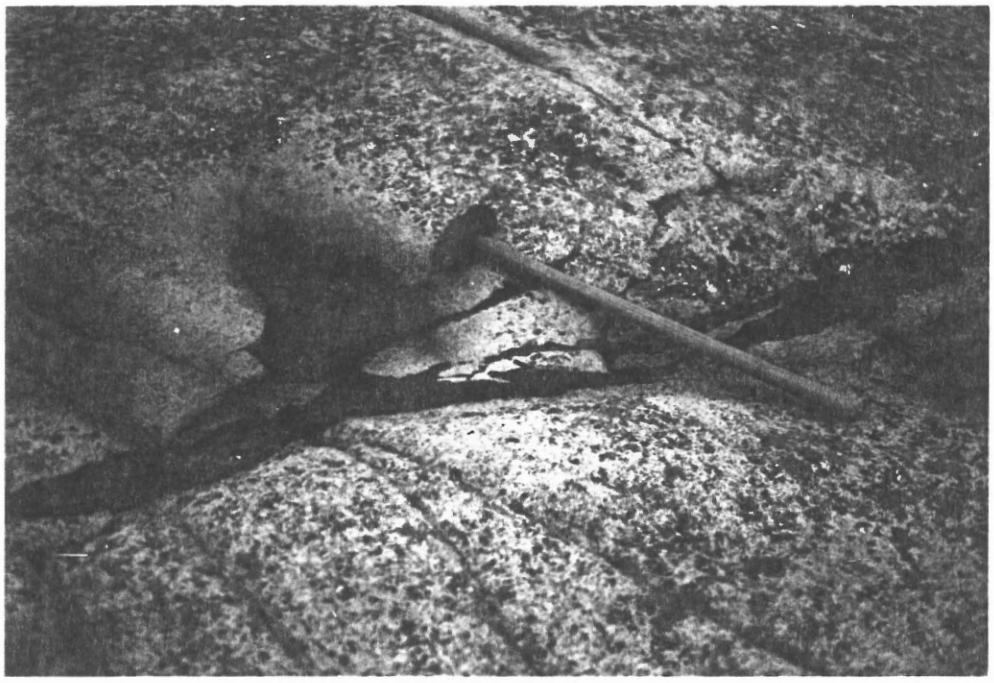

Photo 2-8: Biotite schlieren in Unit 4 located on the shoreline at Hunts Point wharf.

pluton. An equal area stereographic projection of foliations from Unit 1, predominantly from outcrops near St. Catherines River Bay, and within 1 km of the contact with the Meguma Group, show a concentration near 108°/60° SW (Fig. 2-3). This orientation is almost perpendicular to the 030°-040° regional foliation in the country rock (Fig. 2-4) and may reflect block movement of the country rock as a result of the intrusion of the pluton (i.e. a block of country rock is suspended by the granitoid intrusion).

Unit 2, trondhjemite

Unit 2 is represented by a single, 2 m wide, coarse-grained (5-8 mm), leucocratic trondhjemite dyke cutting Unit 1 near Black Point (Fig. 2-5). Its contacts with the tonalite are sharp and it contains a large tonalite xenolith. Although Unit 2 is only one dyke, its clear crosscutting relationship with Unit 1 indicates that it is a distinct unit from Unit 1. Its age relative to other units is not known. The trondhjemite contains euhedral and subhedral plagioclase phenocrysts (69%), quartz (20%), biotite (8%), and muscovite (3%) (Photos 2-9, 2-10). In places, the margins are rich in biotite, and thin biotite schlieren, up to 1 m long, lie parallel to the contacts.

Unit 3, monzogranite

Unit 3 makes up about 1% of the pluton. It is a medium-to fine-grained, leucocratic, biotite-muscovite monzogranite (Fig. 2-5) and contains 25-30% quartz, 25% K-feldspar, 35-45% plagioclase, and

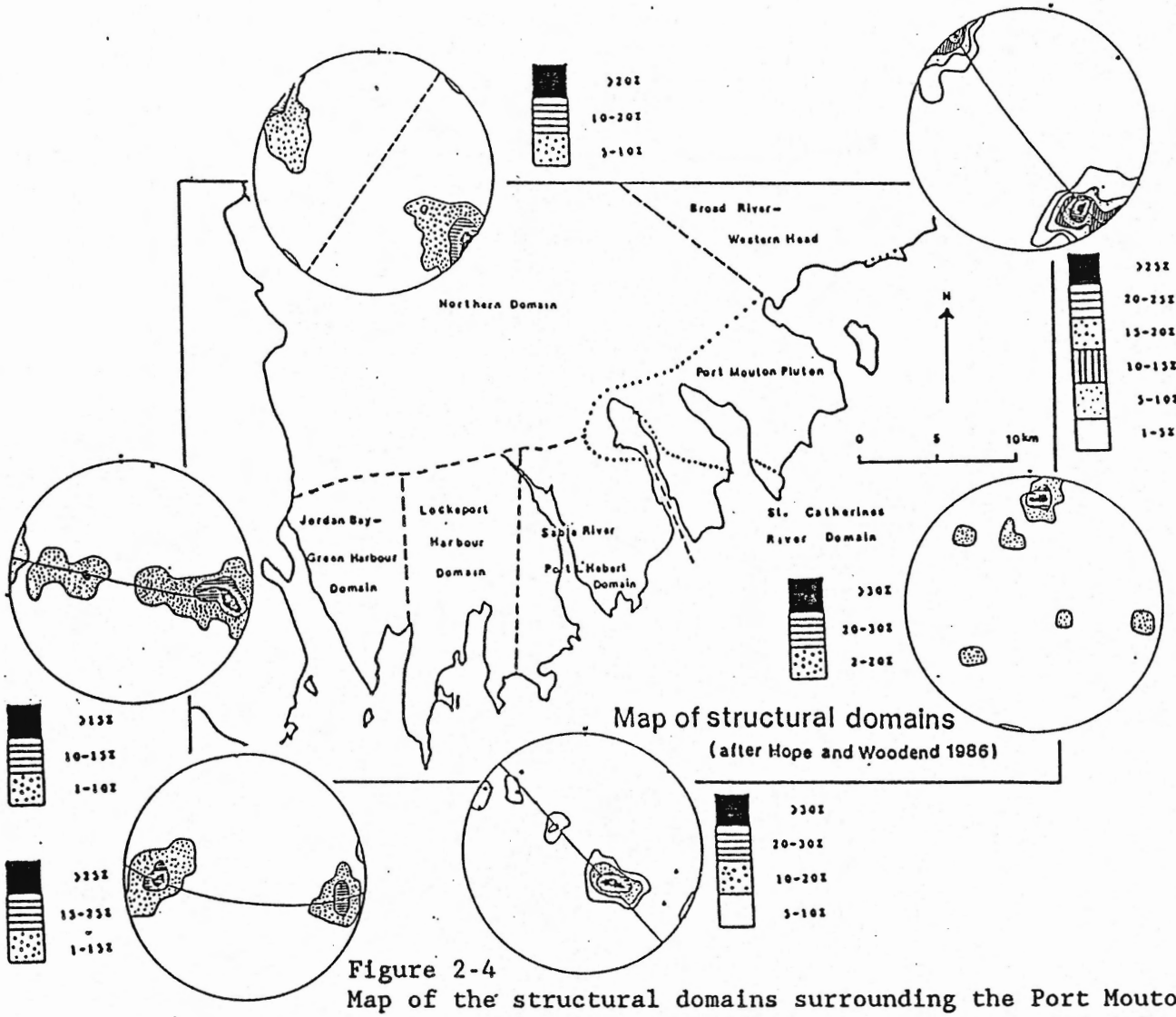

Figure 2-4
Map of the structural domains surrounding the Port Mouton Pluton with stereographic plots of bedding measurements recorded from within the domains (as mapped by Hope and Woodend, 1986).

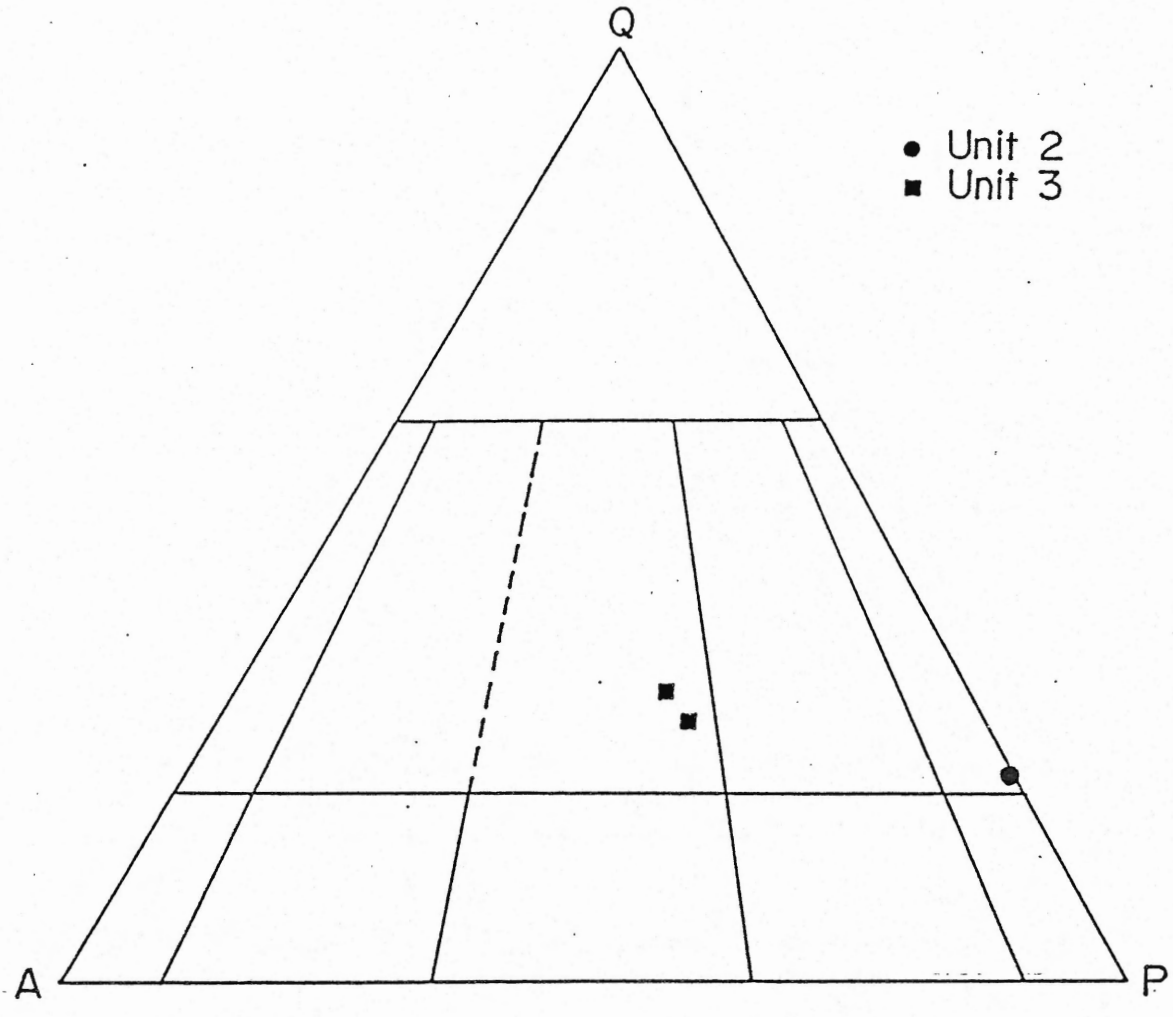

Figure 2-5: Ternary quartz-alkali feldspar-plagioclase plots of modal analyses of 2 samples of Unit 3 and one sample of Unit 2.

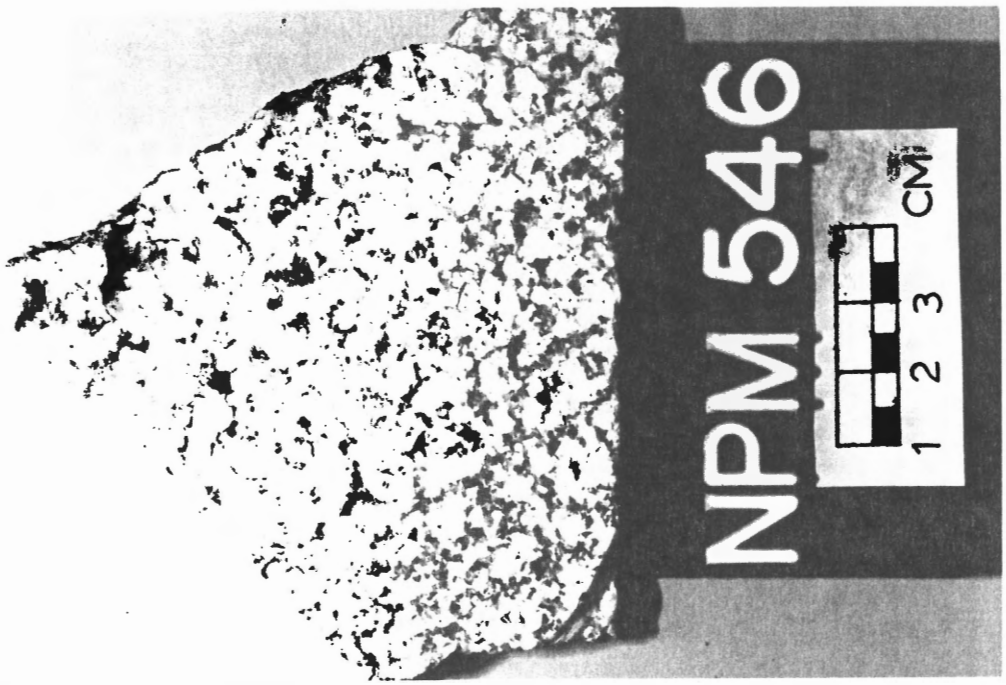

Photo 2-9: Coarse-grained subporphyritic trondhjemite of Unit 2 from Black Point.

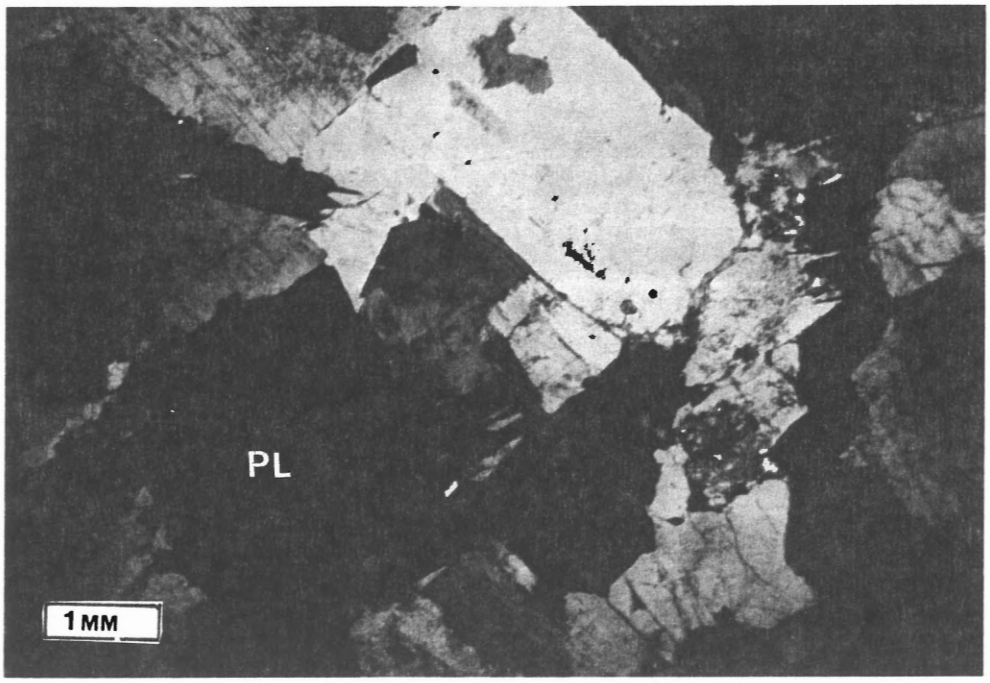

Photo 2-10: XNL. Thin-section of trondhjemite of Unit 2 (NPM546). Predominant mineralogy is zoned plagioclase and quartz. X 14

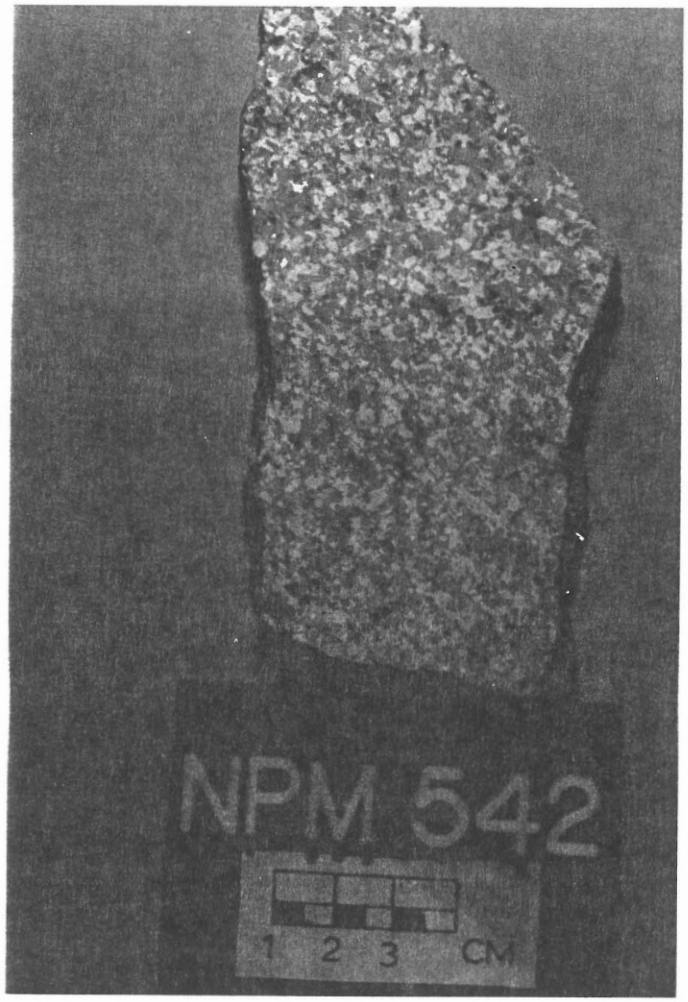

Photo 2-11: Fine-grained to medium-grained leucomonzogranite of Unit 3 located on Hwy 103 near the junction to Port Joli road.

less than 10% biotite and muscovite (Photos 2-11, 2-12). It occurs as inclusions (Photo 2-13) and as thin wispy bands in Unit 4 (Photo 2-14).Unit 4, granodiorite to monzogranite

Unit 4 is the dominant phase of the pluton, comprising about half of the body. It is a mainly equigranular, medium-grained, mesocratic, biotite-muscovite granodiorite to monzogranite (Fig. 2-6) that, in places, displays a mild foliation. Its grain size increases towards the interior of the pluton where it is the dominant phase. Contacts with the country rocks are sharp, but contacts with Unit 1 are sharp only near the periphery of the pluton and become indistinct toward the interior. In the northeastern section of the pluton (east of Summerville Beach), Unit 4 crosscuts migmatite banding.

Unit 4 appears to be spatially associated with Unit 3, where Unit 3 occurs as alternating flow bands within Unit 3 (Photo 2-14) and, in places Unit 4 contains inclusions of Unit 3 (Photo 2-13).

Unit 4 is composed of quartz (16-40%), K-feldspar (microcline and subordinate perthitic felspar, 5-33%), zoned plagioclase (24-59%), muscovite (1-14%) and biotite (3-26%) (Photos 2-15, 2-16, 2-17 and 2-18). Apatite and zircon are common accessory minerals and small, subhedral grains of rutile were found in one sample. The dominant texture is hypidiomorphic granular, commonly subporphyritic, with phenocrysts of inclusion-rich microcline and rarely plagioclase. The average muscovite content of Unit 4 is 4-5%, and the biotite content is 10%; however the total mica content of this unit can be up to 20-30%. There appears to be no systematic variation between the modal composition and the distance from the country rock contact.

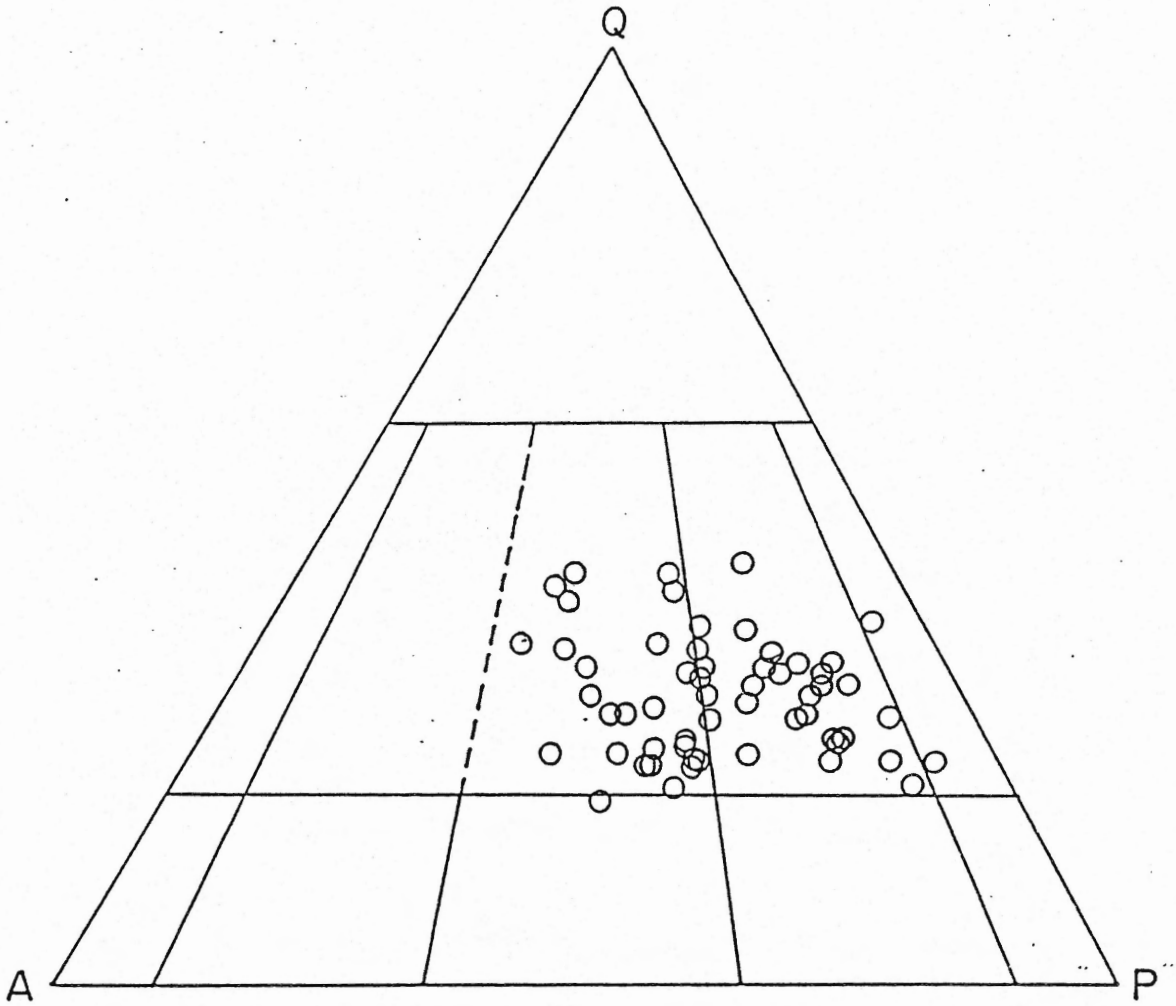

Figure 2-6: Ternary quartz-alkali feldspar-plagioclase diagram of modal analyses of 50 samples of Unit 4.

Where they are observed within the same outcrop, the main features used to distinguish this unit from the biotite tonalite of Unit 1 are:

1) the grain size of Unit 4 is less than that of Unit 1;

2) Unit 4 tends to display a less well-defined foliation than Unit 1,

3) in any one outcrop muscovite is more abundant in Unit 4 than in Unit 1;

4) Unit 1 is commonly found as inclusions in Unit 4;

5) dykes of Unit 4 cut dykes of Unit 1;

6) there are no tonalites in Unit 4 and no monzogranites in Unit 1.

In many cases positive identification of Unit 4 is difficult because of its variable appearance (modal mineral abundances of Units 1 and 4 overlap), and because in many areas, crosscutting relationships between the multiple dykes are so complex that correlation with any one unit is impossible without extensive geochemical work. In some outcrops only one unit is exposed, making identification on the basis of crosscutting relationships impossible, and in the interior of the pluton (e.g. at Black Point, Mouton Head, and Port Mouton Island) the differences in texture, grain size and modal mineralogy between Units 1 and 4 are less distinct. In the interior of the pluton Unit 1 is mainly a coarse-grained, mesocratic, biotite-muscovite granodiorite, whereas Unit 4 is a medium-grained, mesocratic, biotite muscovite granodiorite to monzogranite. The most reliable criteria for distinguishing Units 1 and 4, in the interior of

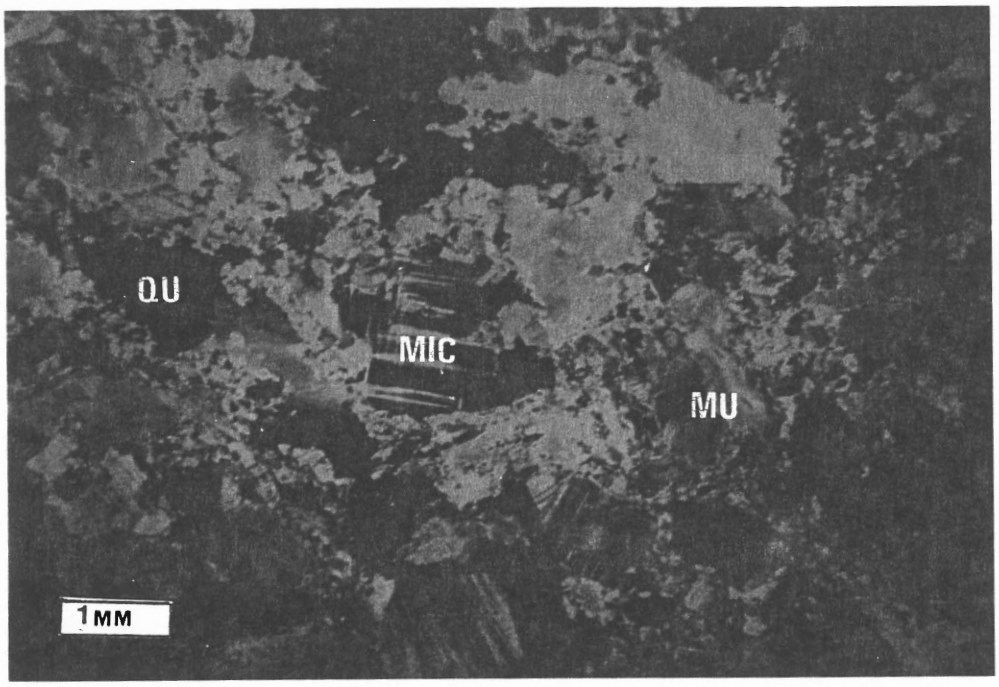

Photo 2-12: XNL Thin-section of Unit 3 leucomonzogranite (NPM542). Note the mortar texture of quartz and elongation of grains. Predominant mineralogy includes plagioclase, quartz, microcline, and muscovite.

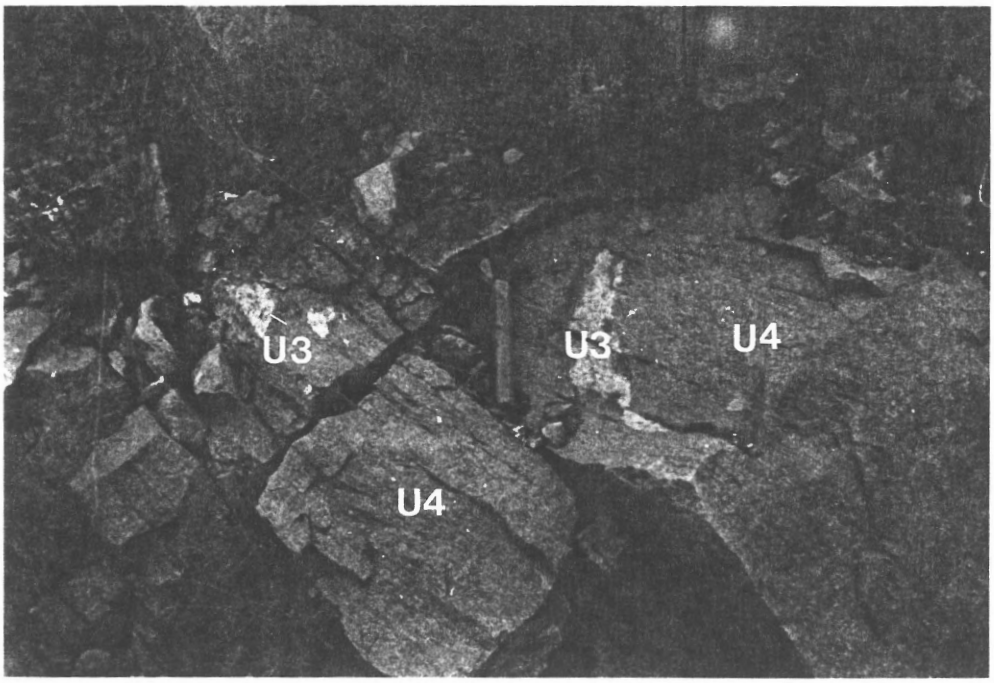

Photo 2-13: Irregular shaped inclusions of leucocratic granite (U3) in mesocratic granite (U4) in Unit 4, north of Robertson Lake near the junction of Hwy 103 and Port Joli Road.

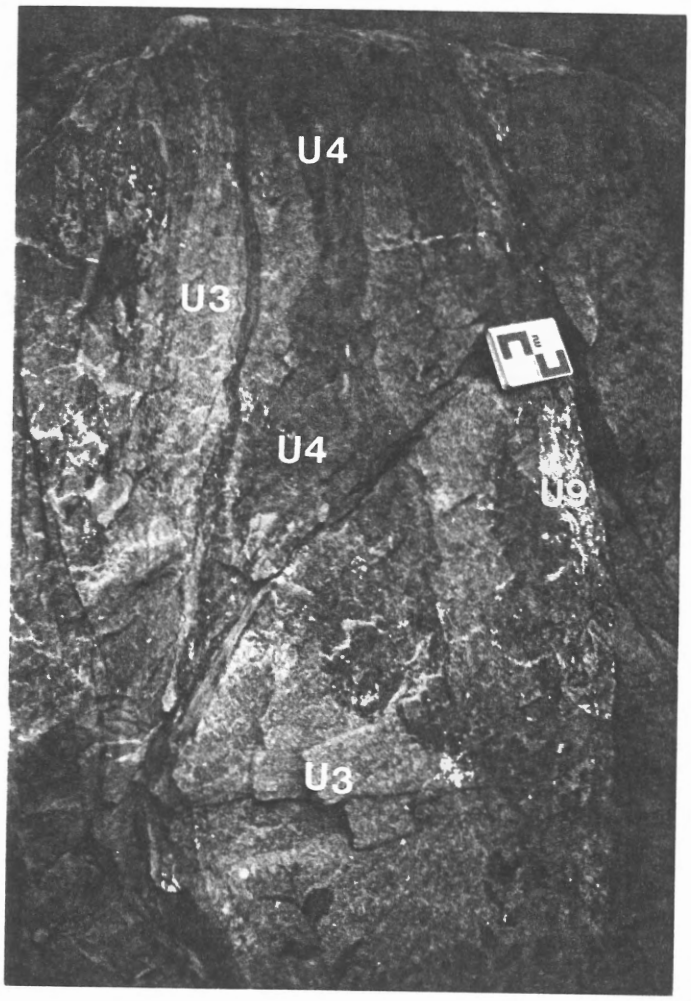

Photo 2-14: Stringers of Unit 3 in Unit 4. The relationship between these two units at this location north of Path Lake near Port Hebert/ Hwy 103 junction is unclear. In thin section sample Unit 3 exhibits evidence of ductile shearing parallel to Unit 4 contacts. A late phase (Unit 9) pegmatite dyke crosscuts this outcrop (right hand side of photograph).

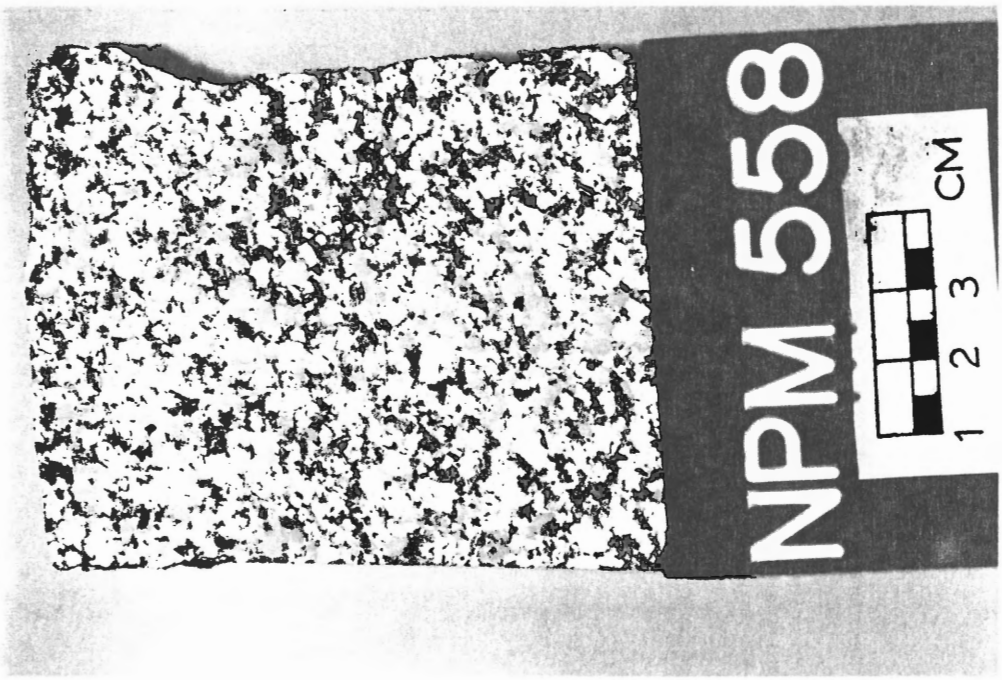

Photo 2-15: Stained hand specimen of medium-grained biotite granodiorite of Unit 4 from Port Mouton Head (interior of the pluton)

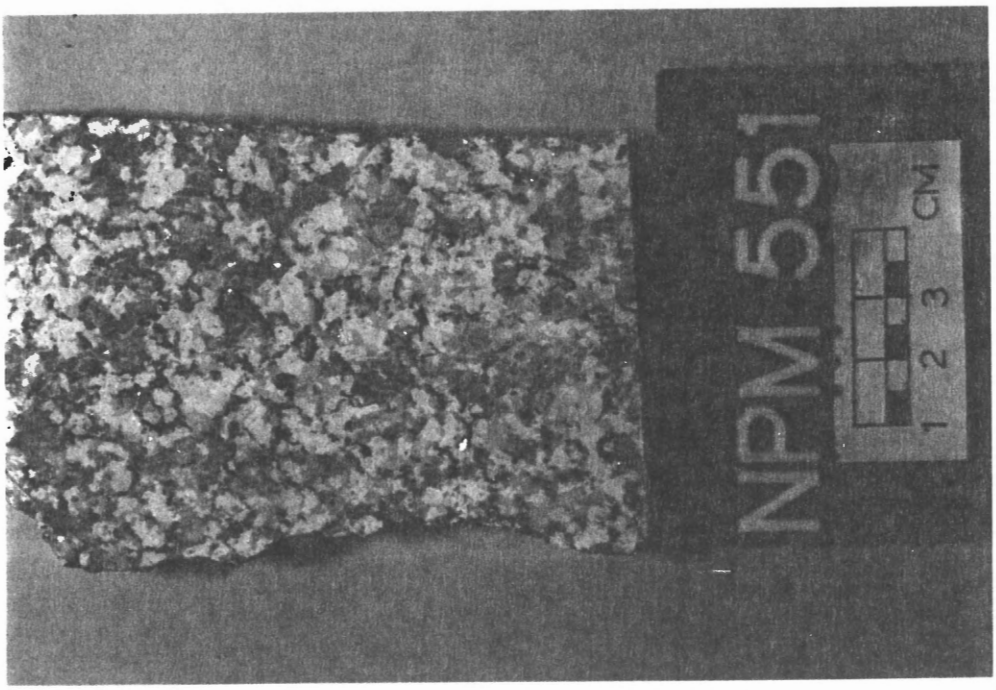

Photo 2-16: Stained hand specimen of coarse-grained, subporphyritic, biotite-muscovite monzogranite of Unit 4 from north of Black Point (interior of the pluton).

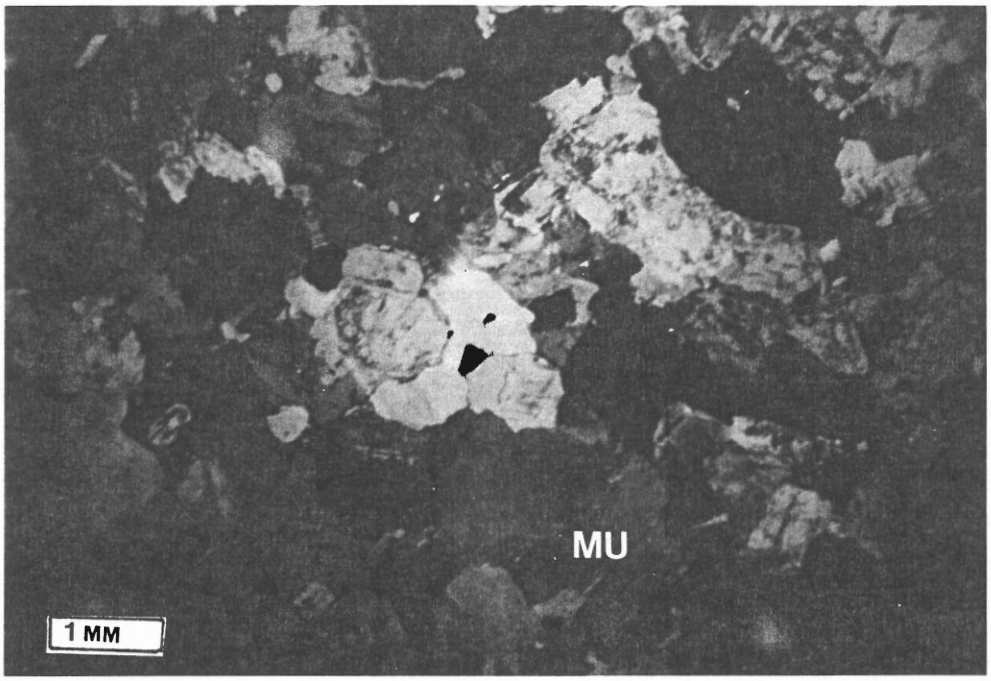

Photo 2-17: XNL. Thin-section of a medium-grained subporphyrtic leucomonzogranite of Unit 4 (NPM580). Dominant mineralogy includes microcline, quartz, zoned plagioclase, biotite and muscovite.

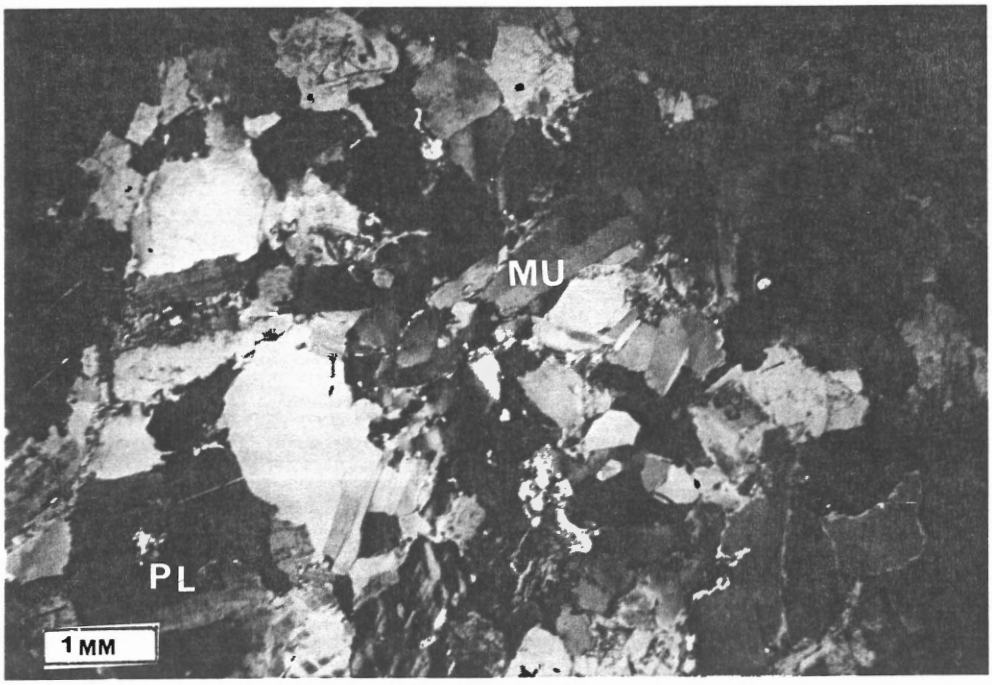

Photo 2-18: XNL. Thin-section Unit 4 (NPM32). This is a medium-grained monzogranite from Hunts Point. Evidence of ductile deformation in the form of quartz subgrain development and kinked muscovite.

the pluton, are cross-cutting relationships and the presence of inclusions of Unit 1 in Unit 4.

Enclaves of granitic, metasedimentary, and unknown affinity (possibly digested metasedimentary material) are common throughout Unit 4. The granitoid inclusions are inclusions of tonalite from Unit 1, and are most abundant near the contact with Unit 1 where they occur as blocks up to 10 m x 10 m. Approaching the interior of the pluton, inclusions of Unit 1 become smaller, less abundant, and more rounded. Unit 1 appears to have been solid before the emplacement of Unit 4, as indicated by the angularity of the xenoliths in Unit 4 near the contact, and by the preservation of well-developed foliation in the tonalite inclusions at oblique angles to the poorly-developed foliation in Unit 4.

Locally, Unit 4 contains rounded to convoluted inclusions of leucomonzogranite (Unit 3) and xenoliths of metasedimentary rocks. Inclusions of unknown origin are ubiquitous throughout the unit. These inclusions are rounded, fine-grained and biotite-rich, and range in size from 2 to 70 cm. In a typical section of Unit 4 (e.g. Black Point, Mouton Head, eastern Port Joli shore), these fine-grained xenoliths make up less than 5% of the outcrops. Locally, xenoliths cluster together in sections that are 1.5 to 2 m in diameter (Photo 2-19). The origin of such concentrations of rounded xenoliths is unknown. Photo 2-19 also illustrates the compositional variety of the xenoliths in Unit 4, including fine-grained, biotite-rich, quartzo-feldspathic inclusions, potassic feldspar porphyry inclusions, 'granitized' biotite-rich quartzofeldspathic inclusions and

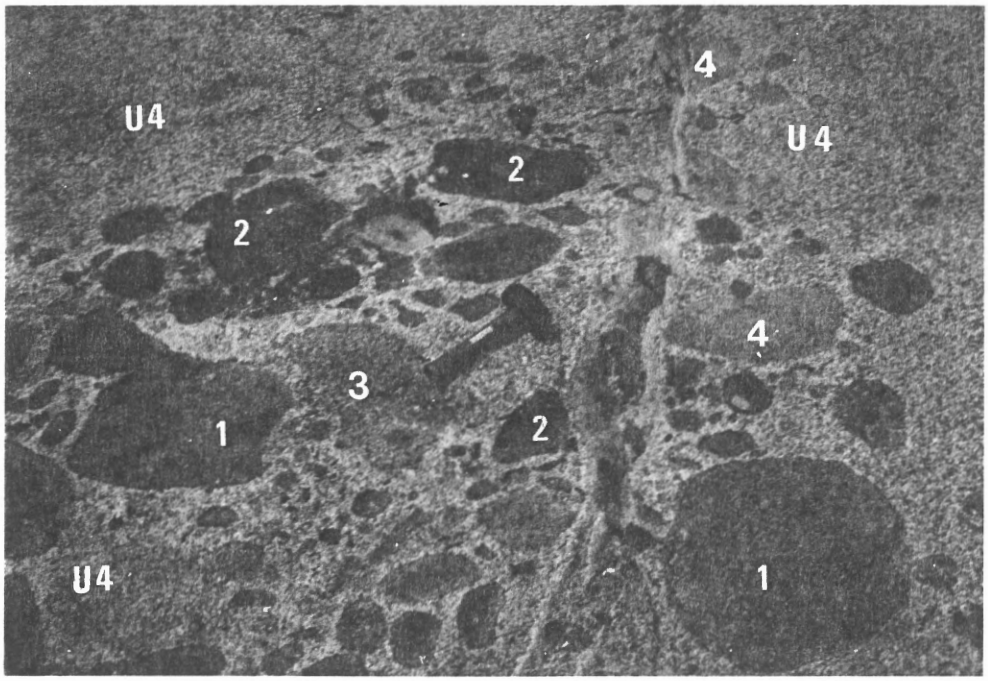

Photo 2-19: Inclusions in Unit 4 (U4) at Deadman's Rock, Little Port Joli Harbour.

1 = biotite quartzo-feldspathic inclusions with feldspar porphyries
2 = fine-grained biotite-rich quartz, feldspar-rich inclusions
3 = potassic-feldspar porphyry-rich fine-grained biotite-rich quartzo-feldspathic inclusions
4 = psammite (quartzo-feldspathic)
matrix : Unit 4= medium to coarse-grained biotite muscovite monzogranite

biotite-rich inclusions.

In the interior of the pluton, large blocks of easily recognizable country rocks are found in Unit 4. These blocks are up to 35 m long, 0.5 to 3 m wide, and have retained their pelitic and psammite interstratification. Prominent outcrops of these xenoliths occur at the southern tip of Black Point in Little Port Joli Bay, and at Darling Rock, north of Forbes Cove. Biotite-rich schlieren 1 to 3 m long and less than 25 cm wide are ubiquitous in the pluton, although they rarely make up less than 1% of Unit 4.

Rarely, Unit 4 displays bands of interlayered, medium-grained, melanocratic, biotite-muscovite granodiorite, and mesocratic, biotite-muscovite monzogranite. Both coarse and fine banding is displayed (bands from 30 to 150 cm and less than 10 mm thick, respectively). The coarsely banded granodiorite to monzogranite occurs at Bulls Point, Jackies Island, along Port Joli road, and along sections of the eastern and western shores of Port Mouton Island (Photos 2-20, 2-21). At Bulls Point the more melanocratic bands are enriched in biotite (12% versus 4%) and depleted in K-feldspar (13% versus 36%), relative to the mesocratic bands. In places, Unit 4 contains isolated pods of melanocratic material which are similar in appearance to the melanocratic bands and are probably of similar origin. The bands in all of these areas trend approximately 020°-040° (Fig. 2-7), parallel to the regional foliation in the country rock.

On the western shorelines of Port Mouton and Jackies Islands, there are small sections, less than 2 m wide, of fine-banded, granodiorite-monzogranite (Photo 2-22). This banding is parallel to the

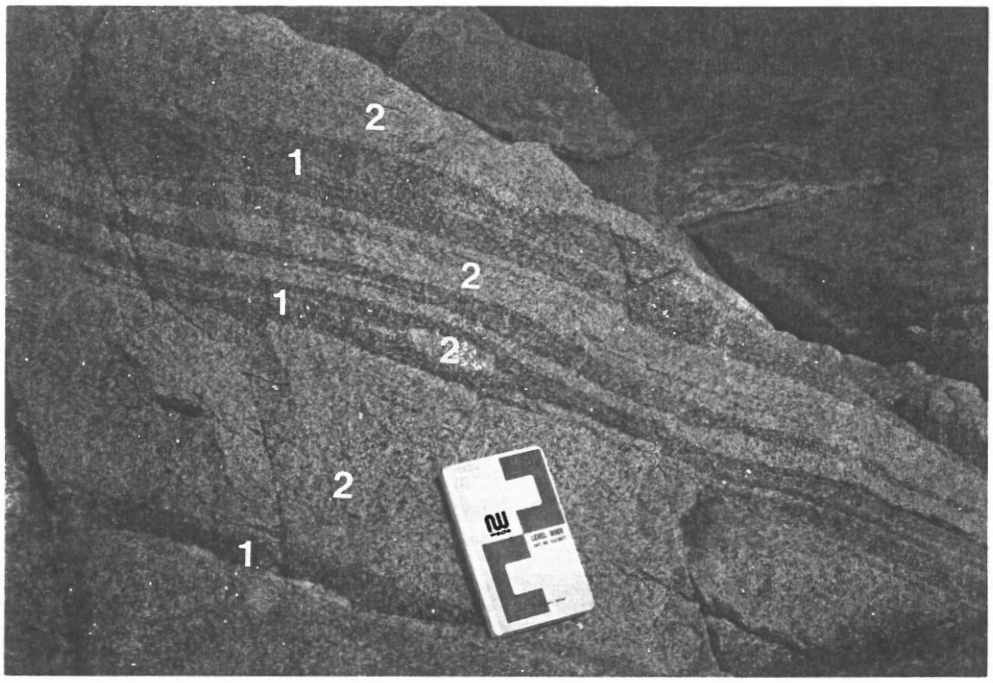

Photo 2-20: Type exposure of the Coarse Banding in Unit 4 at northeastern Mouton Island. 1= medium-grained biotite-muscovite melanocratic-granodiorite (Unit 4).2= medium-grained biotite-muscovite mesocratic-monzogranite (Unit 4).

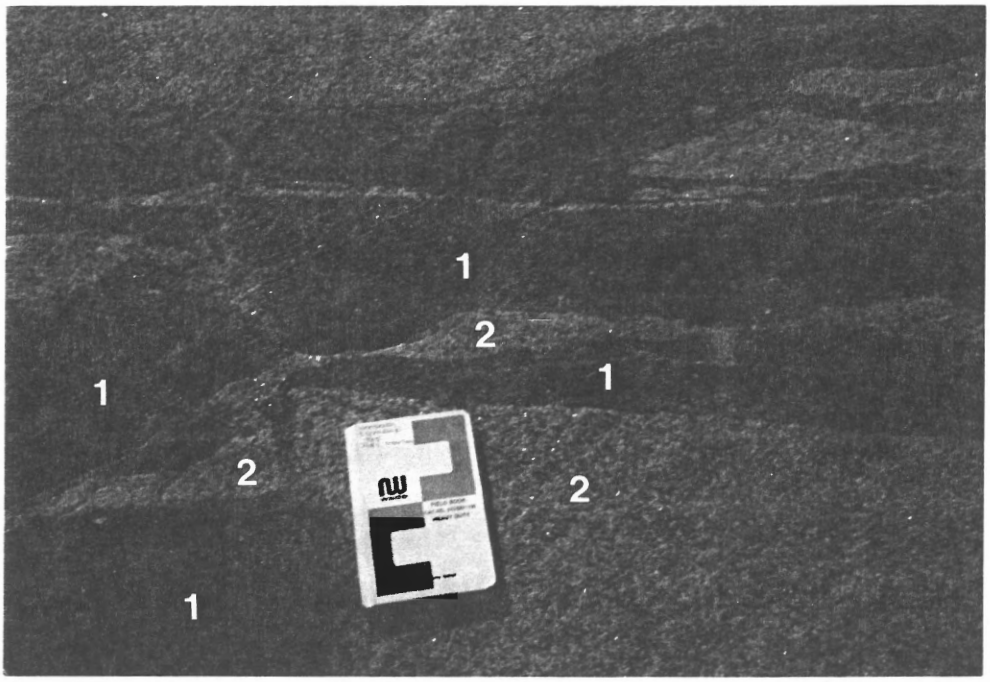

Photo 2-21: Coarse banding in Unit 4 at Bull Point, Western Channel
1=medium-grained biotite-muscovite melanocratic-granodiorite (Unit 4)
2=medium-grained biotite- muscovite mesocratic-monzogranite (Unit 4)

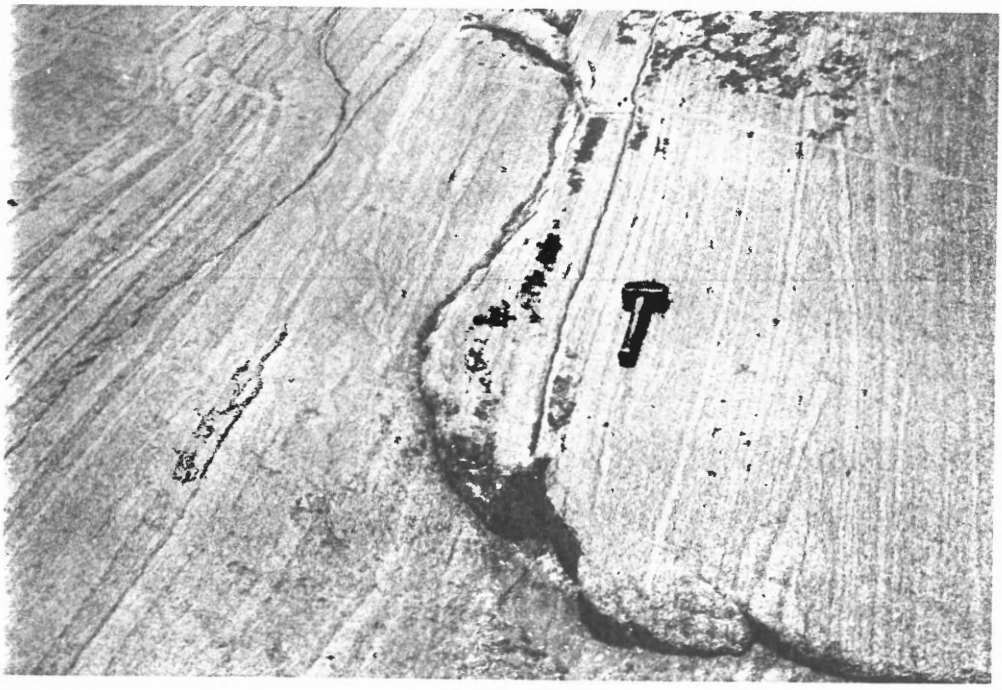

Photo 2-22: Fine Banding in Unit 4 granodiorite at the west shoreline of Mouton Island.

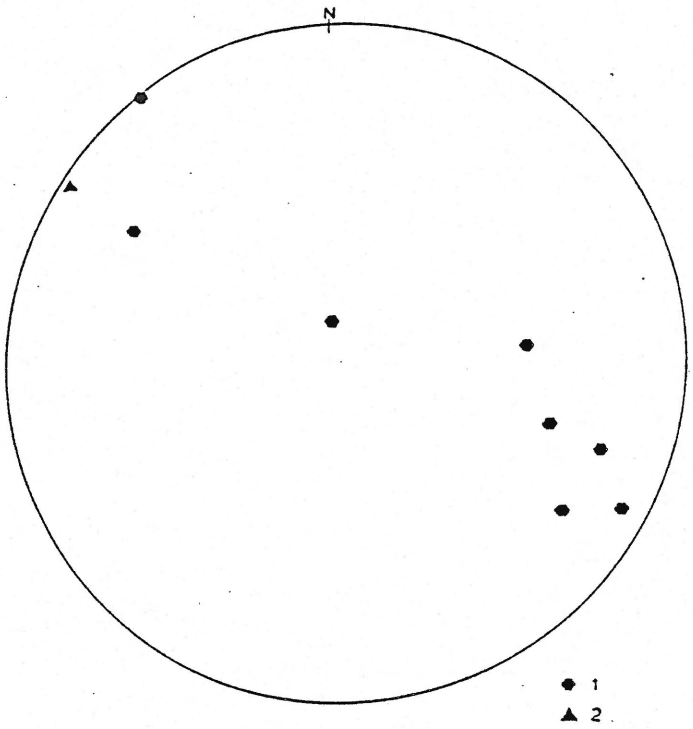

Figure 2-7: Poles to banding in Unit 1 and Unit 4 granites combined (10 points). Schmidt Stereographic Projection.

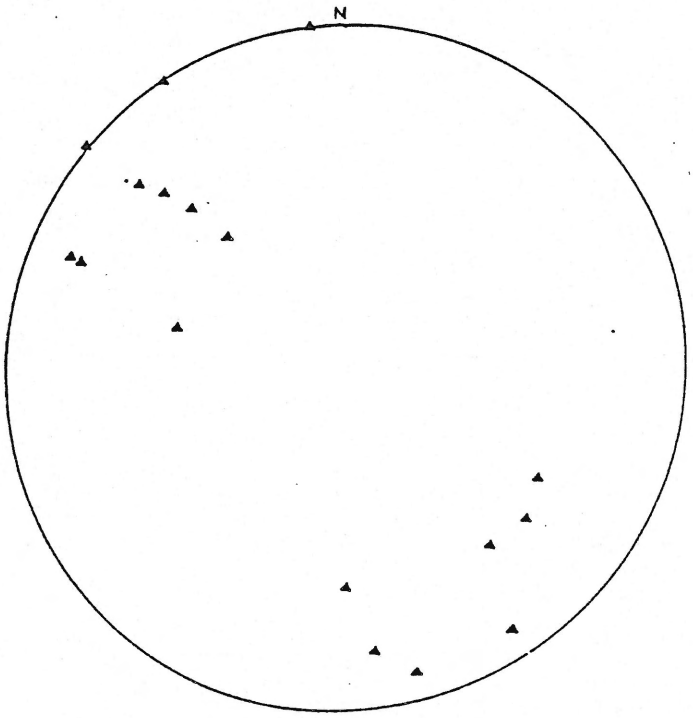

Figure 2-8: Foliation in Unit 4 (17 poles to planes). Schmidt Stereographic Projection.

coarser banding, but is distinct from it, being very thin (less than 10 mm), and with individual bands in the sequence dividing into two or more layers. The more melanocratic bands are enriched in biotite. Contacts with the coarsely banded monzogranites and granodiorites are abrupt.

In a field and petrographic study of banding on Port Mouton Island, Maksaev (1986) concluded that the fine and coarse banding were formed contemporaneously and by the same process, because of their parallelism, their adjacent location, and their compositional similarity. Both types of banding lack cumulate textures or current-related features such as grading, scour and fill structures, or slumps. He suggested that the banding formed as a result of stresses imposed during the crystallization and cooling of the Port Mouton Pluton. The banding is symmetrically oriented about an axis trending 035°, parallel to the regional foliation.

The foliation observed in Unit 4 is sporadic and varies in intensity. It is produced by an alignment of biotite and muscovite, but is difficult to measure in many places because of the lack of planar development. Only eighteen foliations were recorded and their trend is similar to the regional foliation (Fig. 2-8).

Unit 5A, lamprophyre

Unit 5A is a fine to coarse-grained phlogopite-amphibole lamprophyre. It has been observed at two locations in the Port Mouton Pluton - at Forbes Point on the eastern side of Port Joli Harbour (Photo 2-23) and at MacLeod Cove at St. Catherines River Bay (Photo 2-

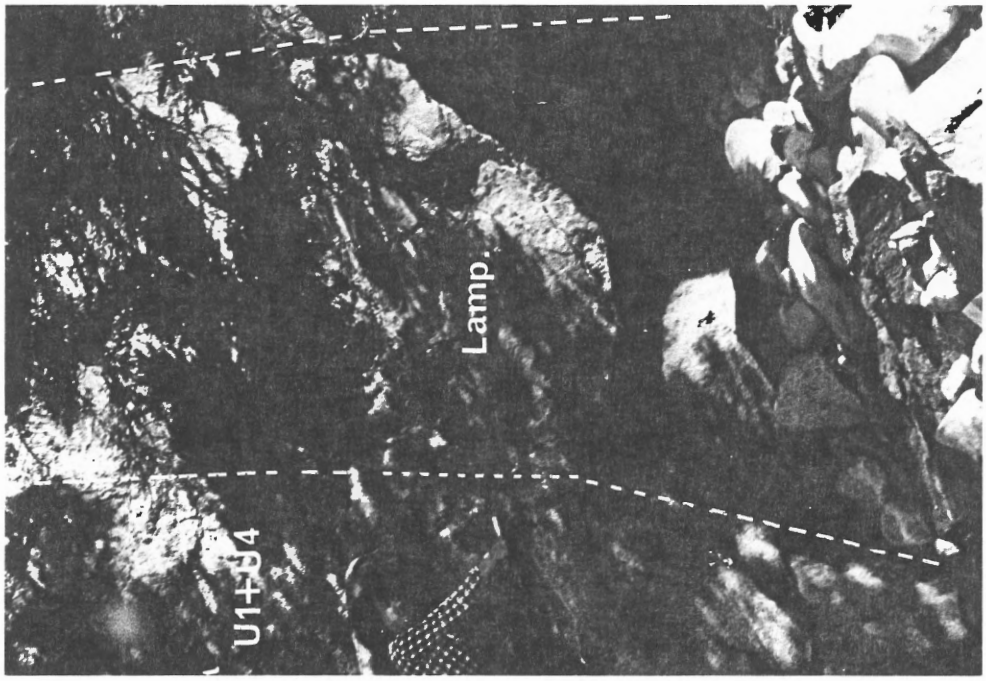

Photo 2-23: The Forbes Point lamprophyre dyke (Unit 5A) (Lamp) crosscutting Unit 1 and Unit 4 granitoids (U1 + U4).

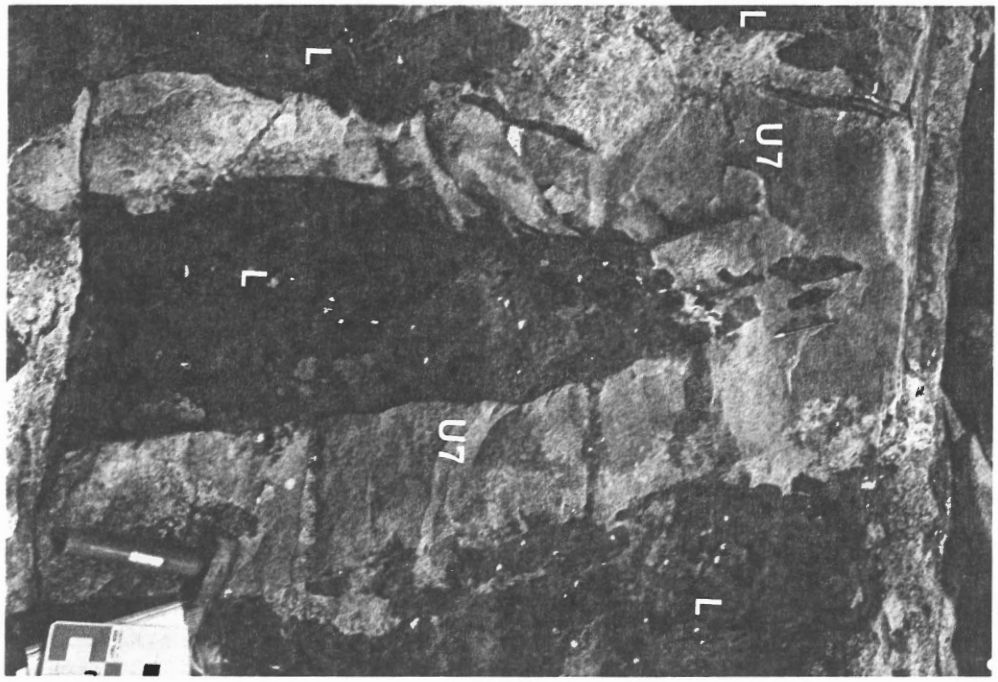

Photo 2-24: MacLeods Cove Lamprophyre (L), disseminated in a late-phase fine-grained biotite-muscovite Unit 7 dyke (U7).

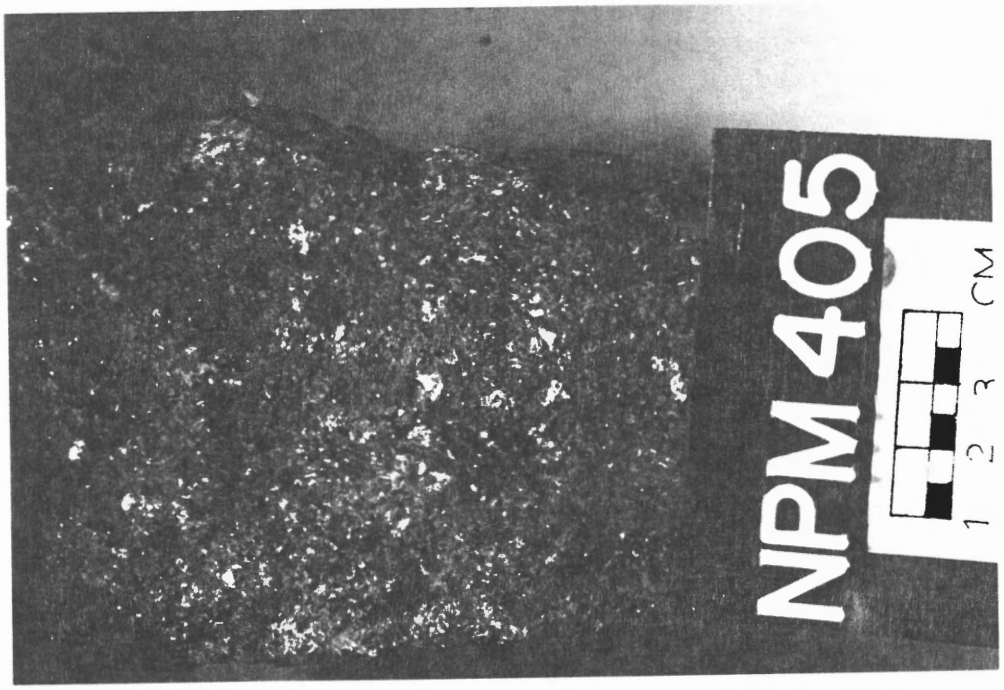

Photo 2-25: Unit 5A, Shoshonitic lamprophyre located at Forbes Point. This is a phlogopite-amphibole-rich zone.

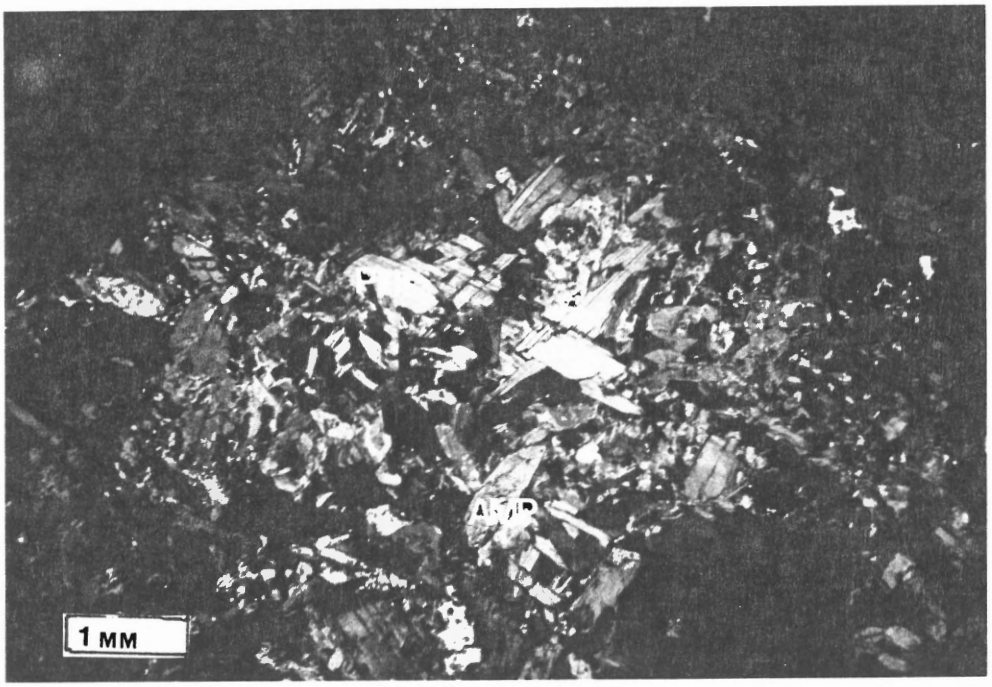

Photo 26: Thin section of NPM405. Unit 5A, shoshonitic lamprophyre located at Forbes Point. It has panidiomorphic texture with interlocking grains of euhedral phlogopite and actinolite in a matrix of phlogopite, actinolite, plagioclase, opaque minerals and apatite. XNL

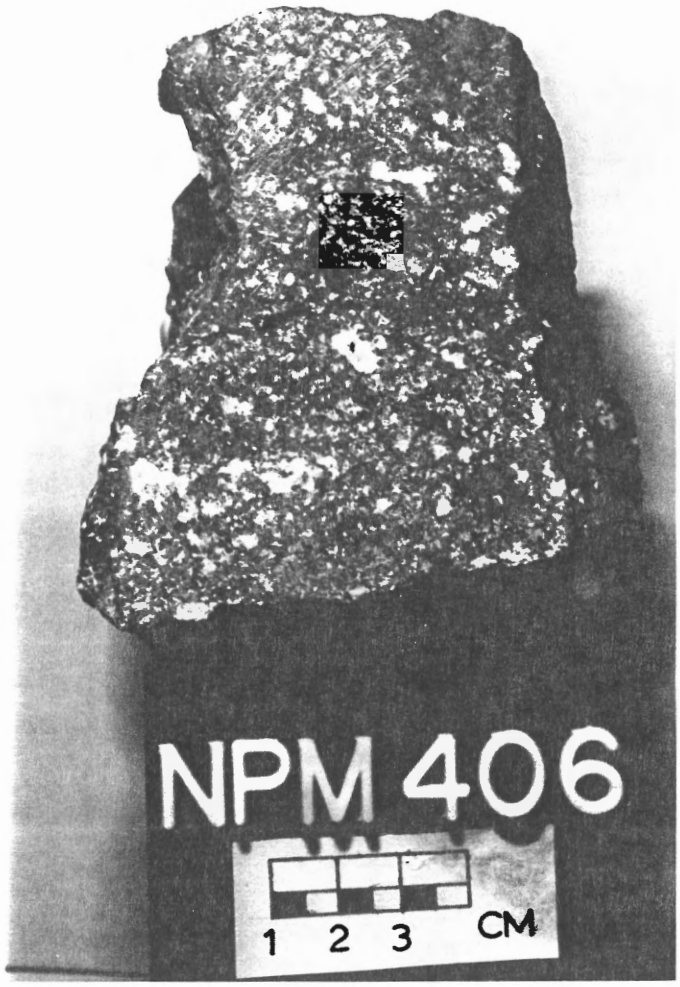

Photo 2-27: Unit 5A. Plagioclase porphryritic zone of the Forbes Point lamprophyre (plagioclase, amphibole-rich zone). This zone of the dyke is represented as large lenses in the main dyke.

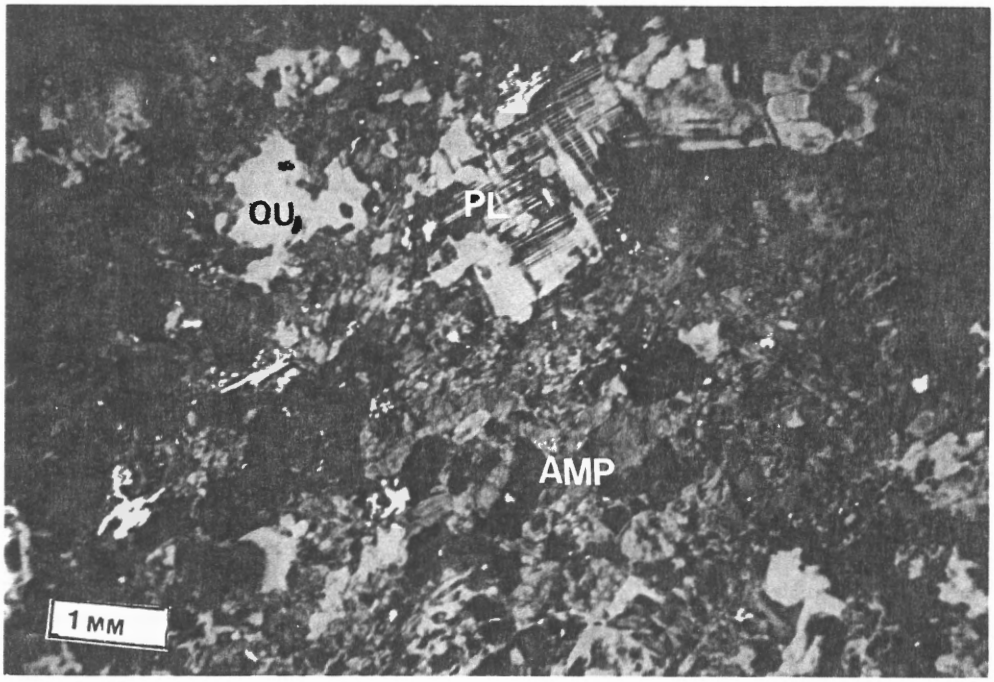

Photo 2-28: Unit 5A, Forbes Point. Thin-section of NPM406. This is the alkaline lamprophyre zone within the main dyke. Note the abundance of amphibole and the minor phlogpite alteration of the amphibole. The felsic minerals are calcic plagioclase and the needle shaped colourless minerals are apatites. PPL

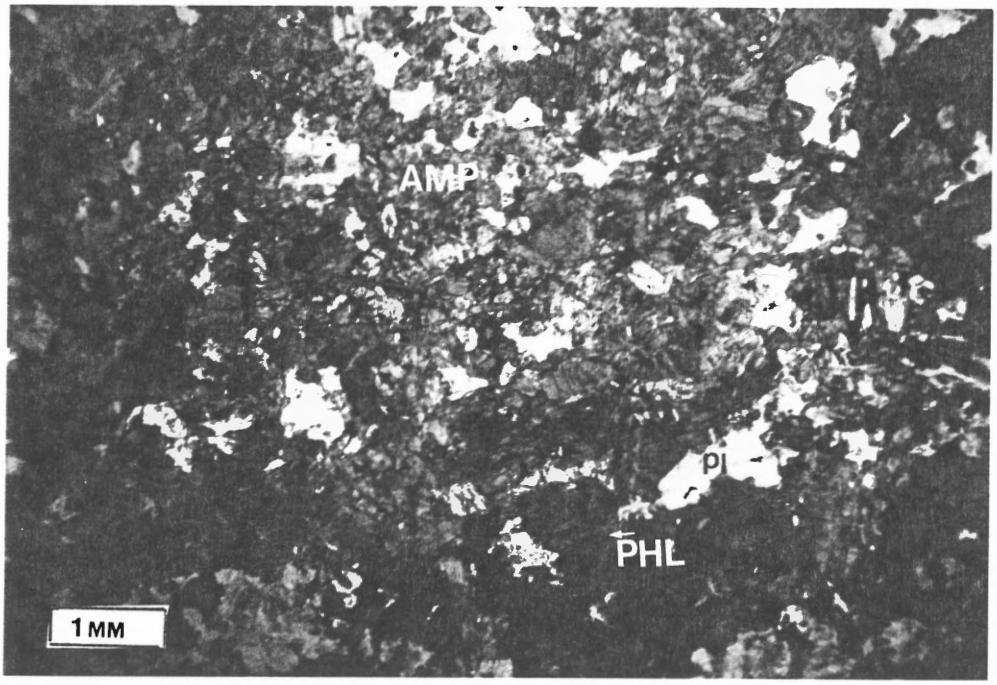

Photo 2-29: Unit 5A, Forbes Point. Thin section of NPM406. Plagioclase phenocrysts in a matrix of actinolitic hornblende, quartz, apatite, sphene, and opaques (there is minor phlogopite alteration of amphibole). XNL

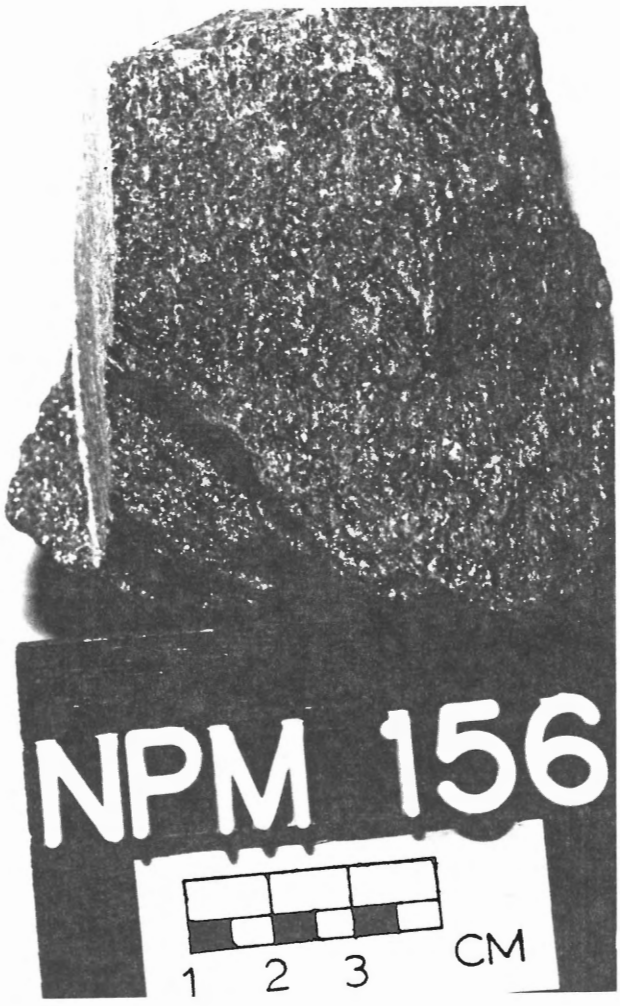

Photo 2-30: Unit 5A, MacLeods Cove, a shoshonitic lamprophyre. Note the fine-grained texture compared with the Forbes Point dyke and the distinct foliation. Note NPM156=NPM485

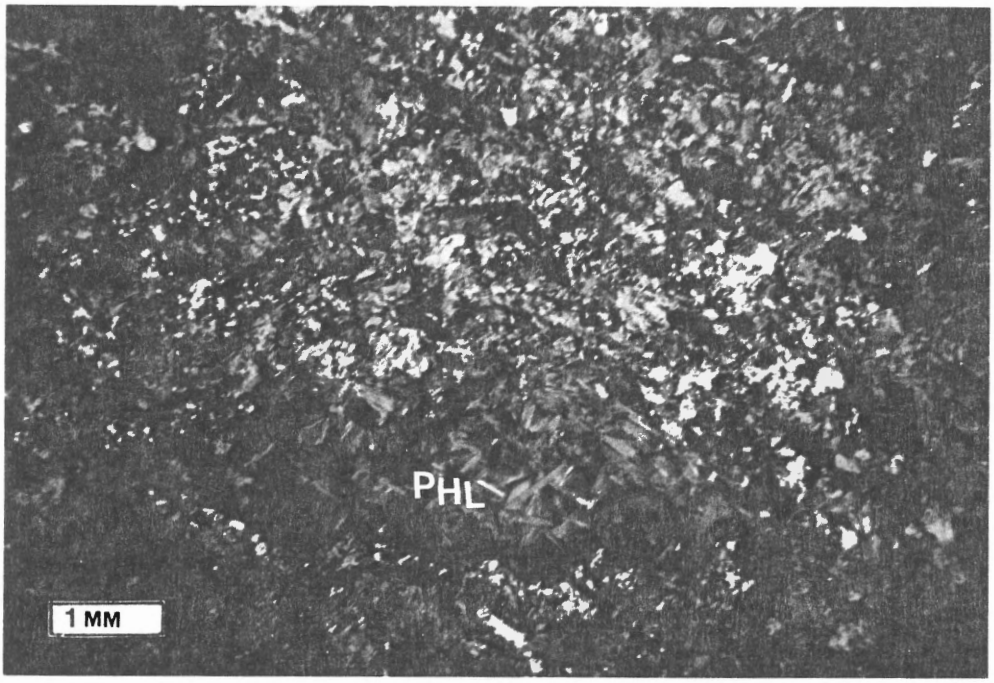

Photo 2-31: Unit 5A, MacLeods Cove lamprophyre. Thin-section of NPM485. Matrix= plagioclase, phlogopite, actinolite, sphene, apatite, and opaque minerals. Note the large cluster of phlogpite. PPL

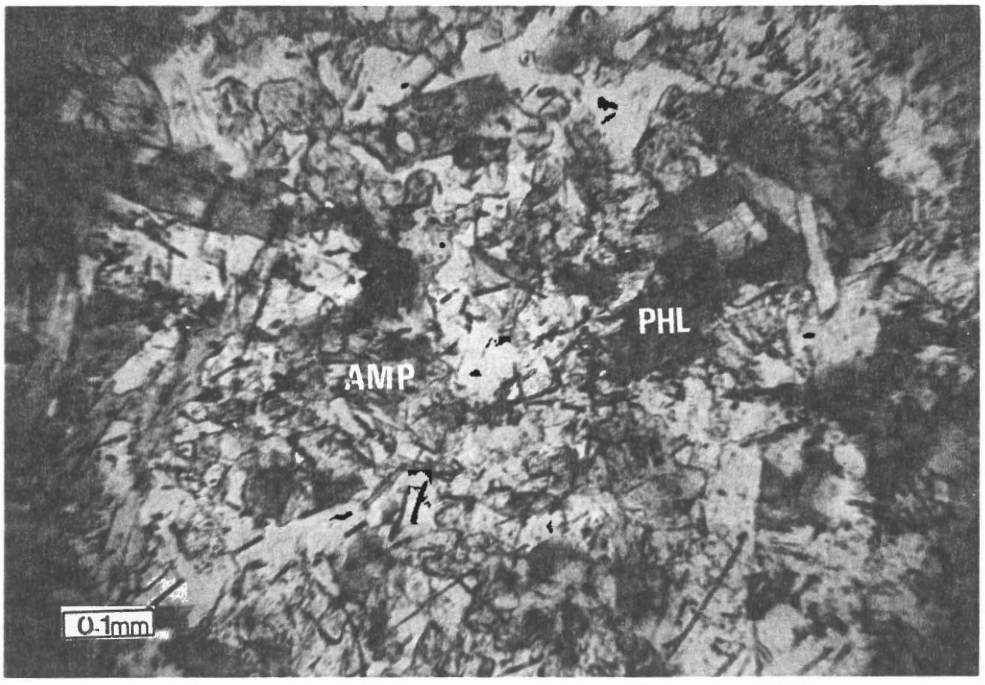

Photo 2-32: Unit 5A, MacLeods Cove lamprophyre. Thin section of NPM485. Note the needle-like apatite grains, the anhedral phlogpite and anhedral amphiboles (high relief, no colour in this photo). PPL

24). Although Unit 5A consists of only two dykes its clear intermediate relationship to the other units justify its being designated as a unit.

At Forbes Point a vertical dyke has intruded tonalite and monzogranite of Units 1 and 4. The dyke narrows from 6 m across at the base of the outcrop to 2 m at the top and contains three distinct units. The interior is a coarse-grained panidiomorphic phlogopite andactinolite-rich zone with subordinate sphene, apatite, plagioclase and opaque minerals (Photos 2-25, 2-26). A second zone occurs as lenses from 10 cm to 20 cm long and is particularly abundant near the margins of the dyke. The lenses are composed of a fine-grained, green, actinolitic hornblende matrix, with rare phlogopitic alteration, and contain approximately 20% plagioclase phenocrysts and subordinate quartz, apatite, sphene and opaque minerals defining a hypidiomorphic granular, plagioclase porphyritic texture (Photos 2-27, 2-28). The plagioclase phenocrysts range in size from 1 to 5 mm and are commonly zoned with dark brown to beige altered interiors (Photo 2-29). The third zone in the dyke is a coarse-grained mass of amphibole, plagioclase, and biotite that defines a 3 to 4 cm wide zone at the contact between the lamprophyre and the granite. In it, elongate amphibole crystals are aligned perpendicular to the contact. A 1.5 m rounded xenolith of fine grained biotite-rich quartzofeldspathic rock is included in the dyke.

The second mafic dyke is located at MacLeods Cove. This dyke is similar in composition to the main zone of the Forbes Point lamprophyre dyke but is more homogeneous and has been altered by

subsequent plutonic activity. The rock is fine-grained greenish grey, and contains phlogopite, green actinolite, plagioclase, sphene, apatite and quartz in a hypidiomorphic granular texture with scattered clusters of phlogopite (Photos 2-30, 2-31 and 2-32). Its dark green colour distinguishes it from the black pelitic layers of the Meguma Group country rocks. A marginal zone of aligned platy minerals, and the lack of euhedral grains (compared with the Forbes Point dyke) are the results of recrystallization during alteration.

The dyke is tabular, about 8 to 10 m long and at least 2 m wide. Its contact with the fine-grained, biotite-muscovite, mafic breccia of Unit 5B is sharp. No distinct contact aureole is associated with the dyke and it is unclear whether the dyke is a very large inclusion in the breccia (Unit 5B) or cuts across the breccia. Late stage, fine-grained tonalite to granodiorite dykes of Unit 7 (form 5) cut the dyke, and these in turn have been cut by pegmatites of Unit 9. The dyke has been fragmented into 2 to 5 m long blocks by the late phase dyking. Locally, fragments of the lamprophyre are found in Unit 7 dykes (e.g. Photo 2-24).

The actinolite-rich zone of the Forbes Point dyke is an alkaline lamprophyre and all other zones are shoshonitic lamprophyres (Rock 1977).

Unit 5B, tonalite breccia

A fine-grained, melanocratic, biotite-muscovite tonalite breccia dyke (Unit 5B, Fig. 2-9) is exposed at the southern contact of the pluton at MacLeod Cove (St. Catherines River Bay) (Photo 2-33). It is

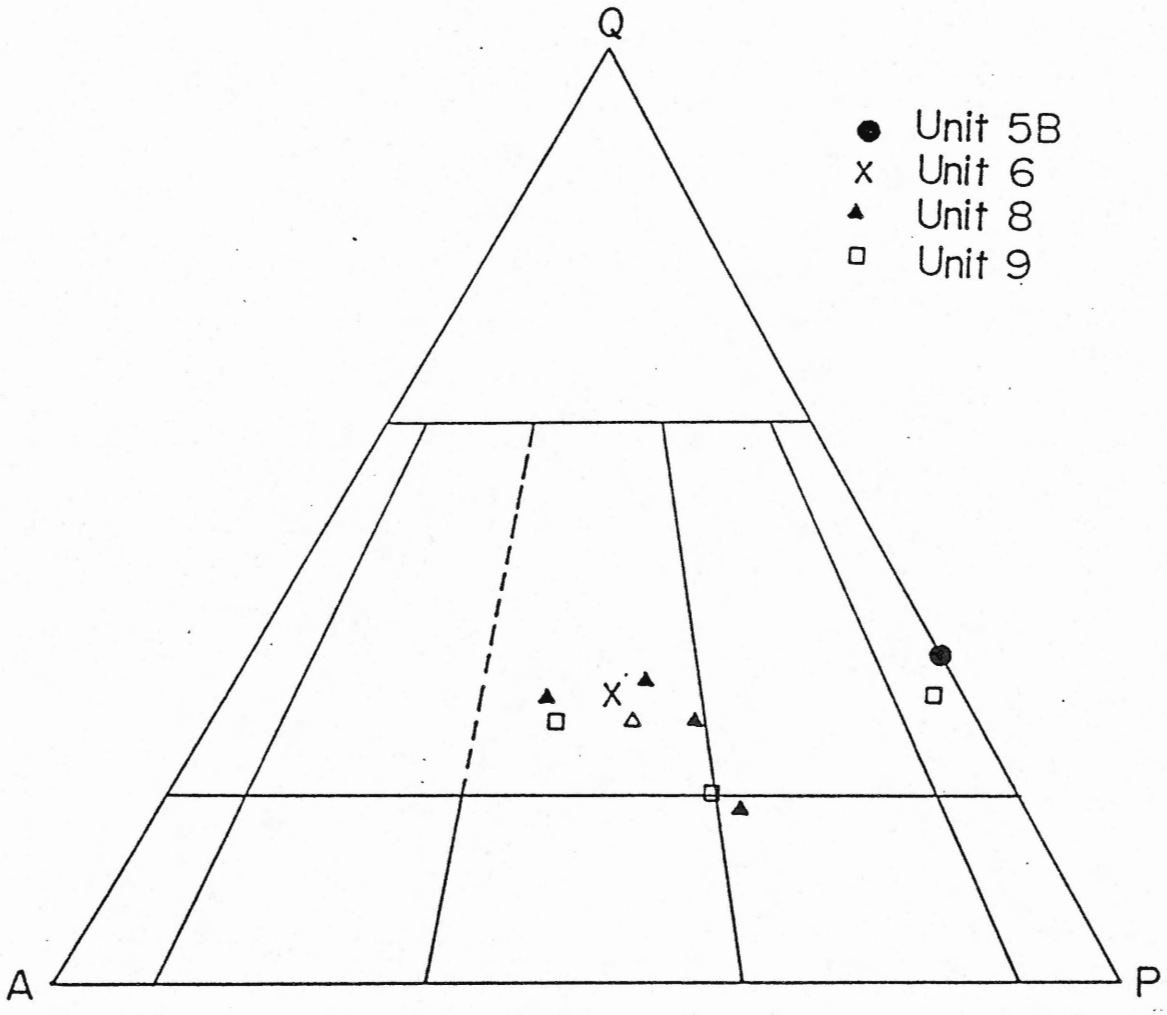

Figure 2-9: Ternary quartz-alkali feldspar-plagioclase diagram of modal anlyases of 10 samples of Units 5B, 6, 8 and 9.

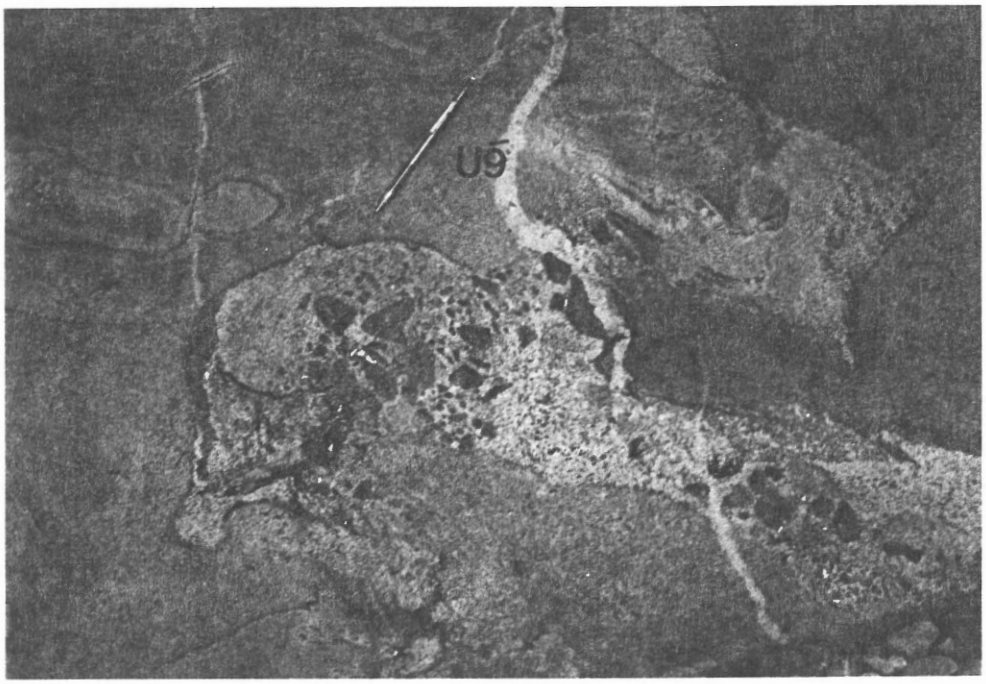

Photo 2-33: Contact relationship between the Unit 5B breccia and the Meguma Group country rock. Note the small angular inclusions within the meandering dyke. A late-stage aplite dyke (Unit 9) cuts the breccia dyke (trending from top to bottom of photograph).

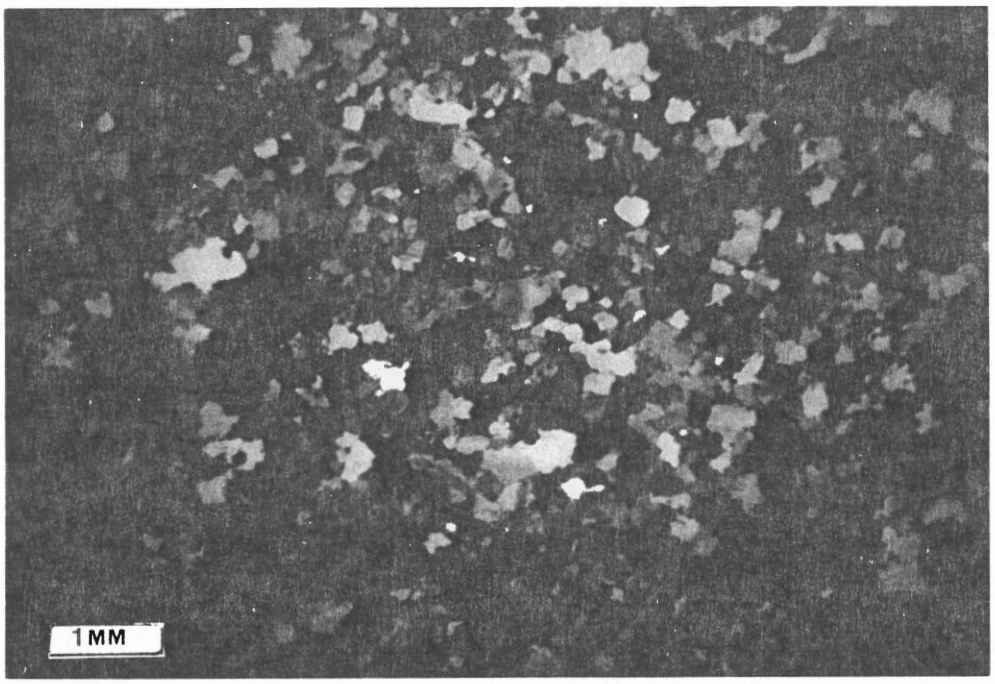

Photo 2-34: Unit 5B. Matrix of fine-grained biotite tonalite breccia. XNL. Thin-section NPM486.

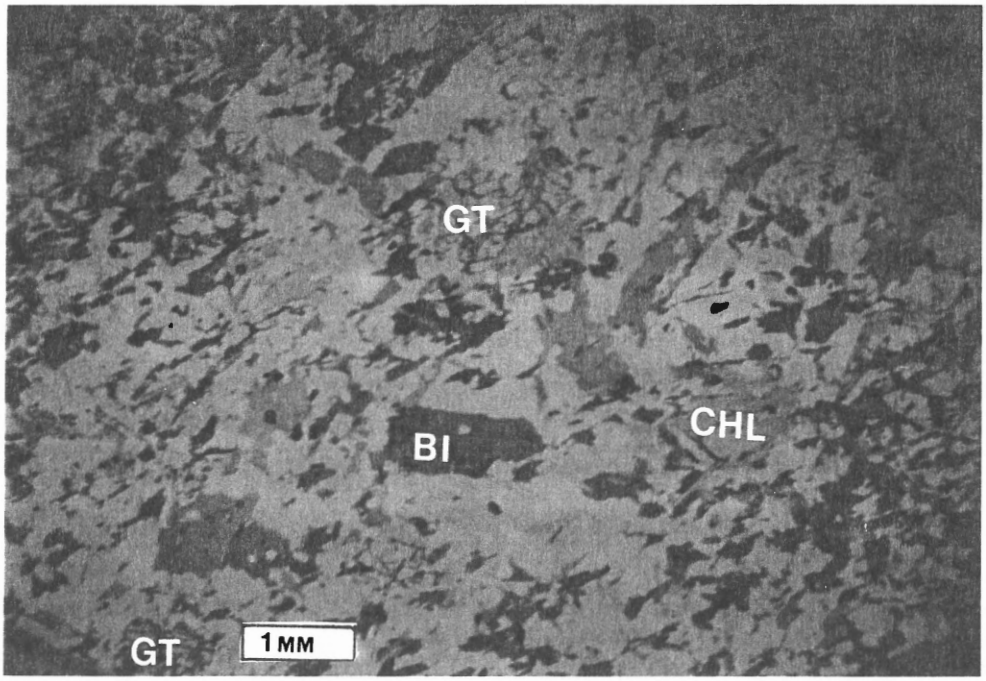

Photo 2-35: Typical clast in the fine-grained biotite tonalite breccia of Unit 5B (NPM486). Note the anhedral garnets and the chloritized biotite. PPL

distinguished by a large inclusion to matrix ratio (1:1), the composition and angularity of the inclusions, by its fine-grained, mafic composition, and its cross-cutting relationships. The breccia contains up to 50% angular to subangular inclusions and lenses of milky quartz grains, country rock, and tonalite to granodiorite, ranging in size from 5 to 50 cm. The matrix is hypidiomorphic-granular and consists of plagioclase (46%), quartz (23%), biotite (26%), muscovite (4%) and accessory amounts of apatite, zircon and garnet (probably xenocrysts) (Photo 2-34). Chloritization of the biotite is common in the metasedimentary clasts (Photo 2-35).

The breccia dyke was intruded along the contact between Unit 1 and the country rock as a meandering dyke of variable width. It contains xenoliths of Unit 1 as is cut by 0.3 to 4 m wide dykes of fine-grained, biotite tonalite (Unit 7), 5 to 10 cm wide dykes of fine-grained, leucocratic monzogranite (Unit 8) and pegmatites and aplites (Unit 9).

The contact between Units 1 and 5B is sharp, but its relationship to Unit 5A, also occurring in the outcrop, is unclear.

Unit 6, leucocratic dykes

Unit 6 includes fine-grained aplite dykes (some with garnet), medium-grained leucomonzogranite dykes and associated pegmatite dykes (Fig. 2-9). The leucomonzogranite dykes are commonly compositionally banded (Photo 2-36) and typically display a hypidiomorphic granular texture and contain quartz (17-29%), plagioclase (30-52%), microcline

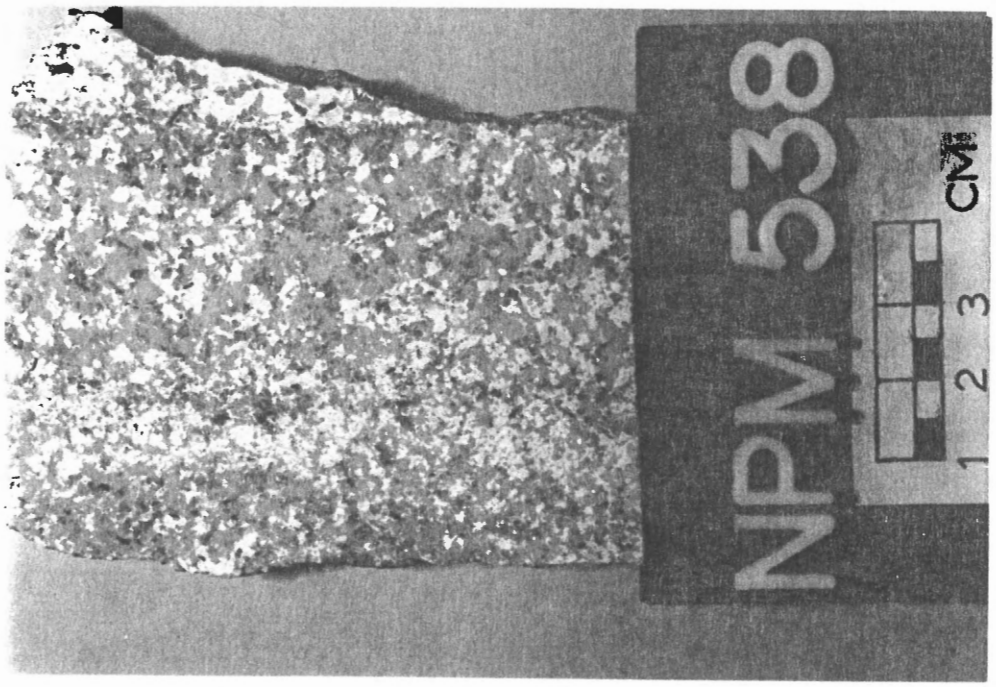

Photo 2-36: Stained hand specimen of banded leucomonzogranite of Unit 6 from eastern shore of Port Joli Harbour. Note the distinct alkali-feldspar-rich bands and plagioclase-rich bands.

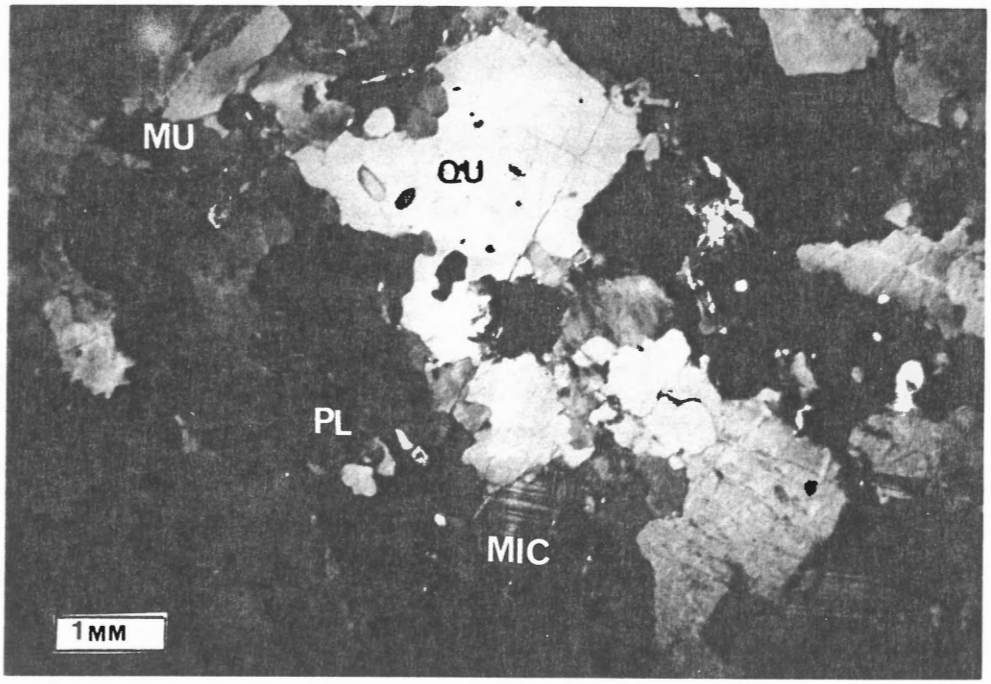

Photo 2-37: Unit 6, leucomonzogranite. Thin-section of NPM538. Note the well-developed microcline grains and minor quartz subgrains (mortar texture).

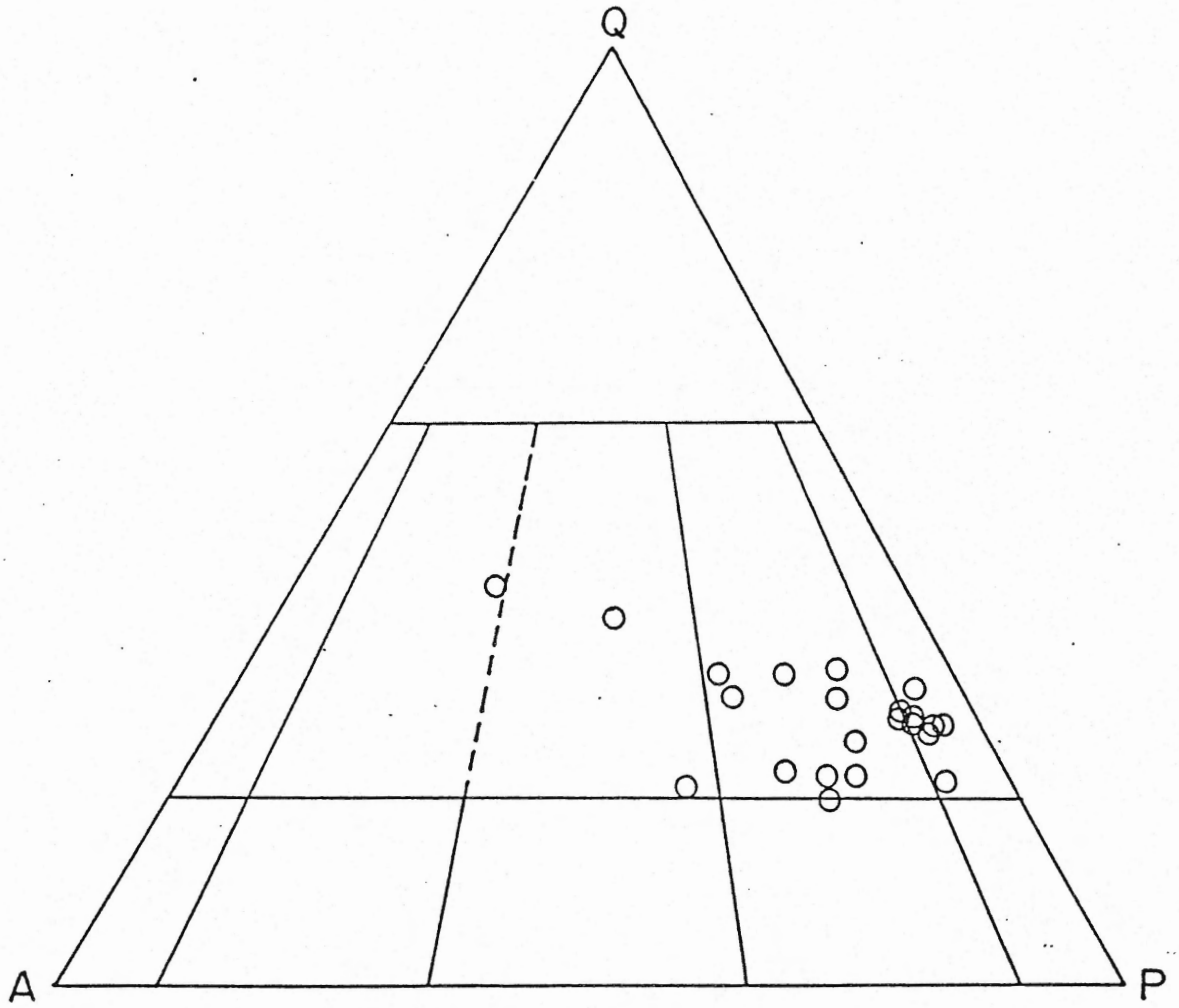

Figure 2-10: Ternary quartz-alkali feldspar-plagioclase diagram of modal analyses of 25 samples of Unit 7.

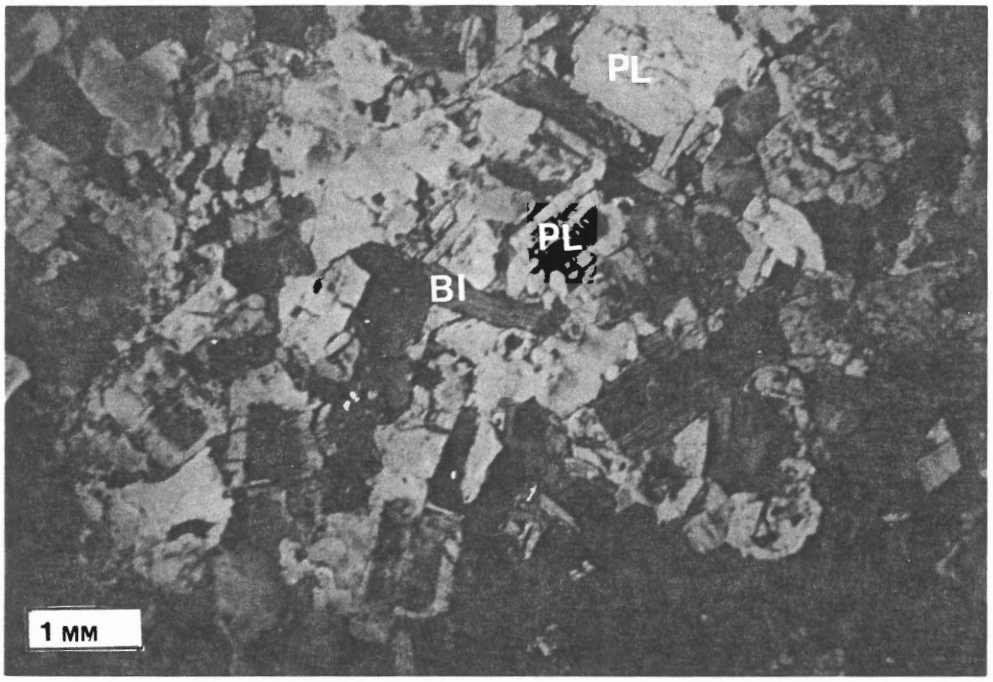

Photo 2-38: Stained hand specimen of Unit 7, from north of Port Mouton Head. Fine-grained biotite, muscovite tonalite (thin section of NPM560). Note the lath-like shape of the well-zoned plagioclase, and subhedral biotite.

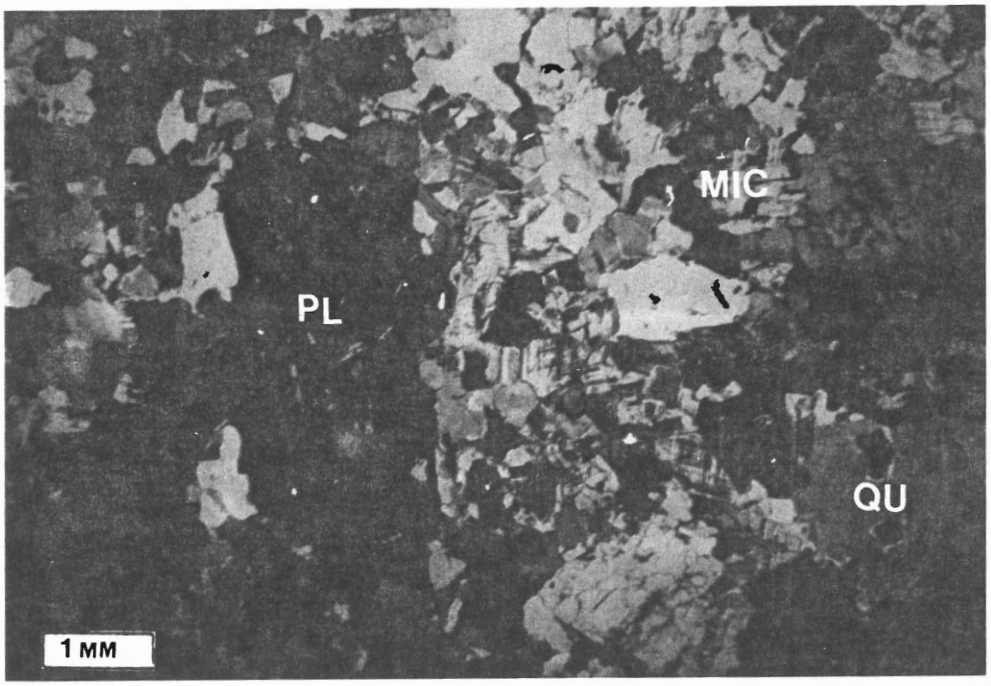

Photo 2-39: Medium-grained porphyritic granodiorite (Unit 7) (NPM539). Mineralogy includes biotite, muscovite, plagioclase, microcline, quartz, and accessory minerals of apatite and zircon. Note the large plagioclase phenocryst. XNL

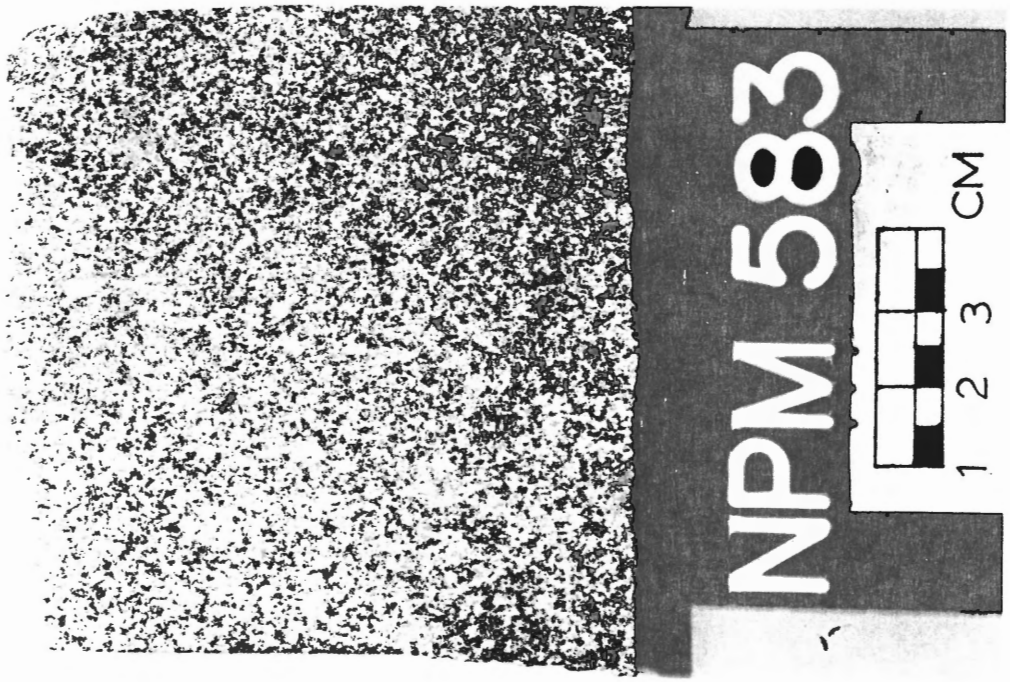

Photo 2-40: Stained hand specimen of Unit 7 from near the Meguma contact along Cadden Bay. Fine-grained biotite, muscovite tonalite (NPM583) with minor small phenocrysts of plagioclase.

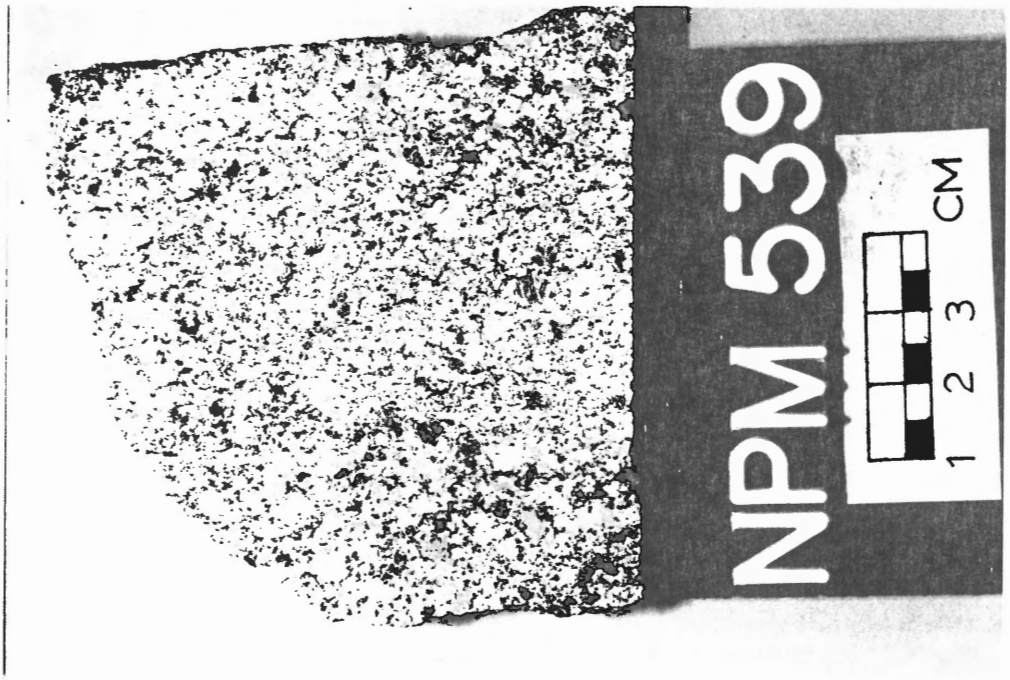

Photo 2-41: Unit 7, specimen from the eastern shore of Port Joli Harbour. Fine-grained subporphyritic, biotite-muscovite granodiorite.

and minor perthite (30-37%), biotite (up to 6%), muscovite (2-4%), and accessory zircon and subhedral to anhedral, commonly chloritized, garnet (Photo 2-37). This unit, which makes up less than 1% of the pluton, is similar in composition to Units 8 and 9 and is distinguished from them by being cut by Unit 7.

Unit 7, fine-grained tonalite to granodiorite

Unit 7, which comprises 5-10% of the pluton, ranges from mesocratic to melanocratic, and from biotite-muscovite tonalite, to granodiorite, and rarely to monzogranite (Fig. 2-10). This wide compositional variation may indicate a number of units are included in the unit, but because of its systematically similar spatial relationship to well-documented older and younger units it is considered as a single unit. It is mainly a fine-grained, hypidiomorphic granular rock, although medium-grained and plagioclase porphyritic varieties exist. It consists of plagioclase (18-62%), alkali feldspar (up to 44%), quartz (15-37%), biotite (6-27%), muscovite (up to 8%), and accessory apatite and zircon (Photos 2-38, 2-39, 2-40, and 2-41). It can be identified in the field by its grain size and texture (it is generally finer grained than Units 1 and 4),its greater biotite content, its crosscutting relationship with Units 4, 5A, 5B, and 9, and by the abundance of inclusions of country rocks, fine-grained, biotite-rich xenoliths, and granitoid xenoliths, which comprise up to 25% of the unit.

At least five morphological subdivisions of Unit 7 can be described:

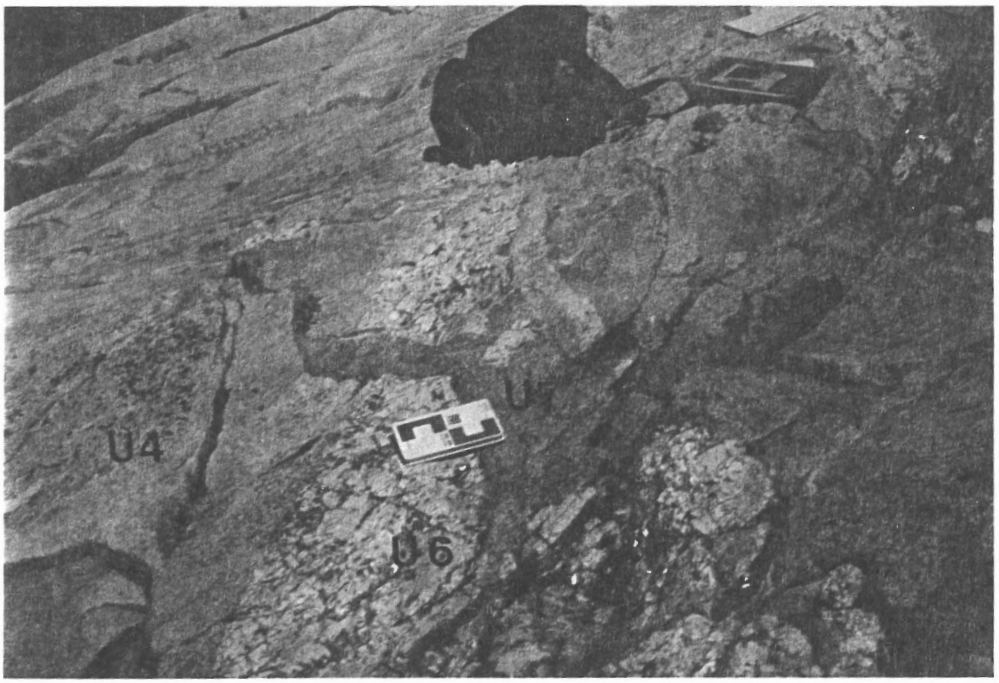

Photo 2-42: Fine-grained melanocratic dykes of Type 1 Unit 7 (see text) are cutting a wide pegmatite dyke of Unit 6 and monzogranites of Unit 4.

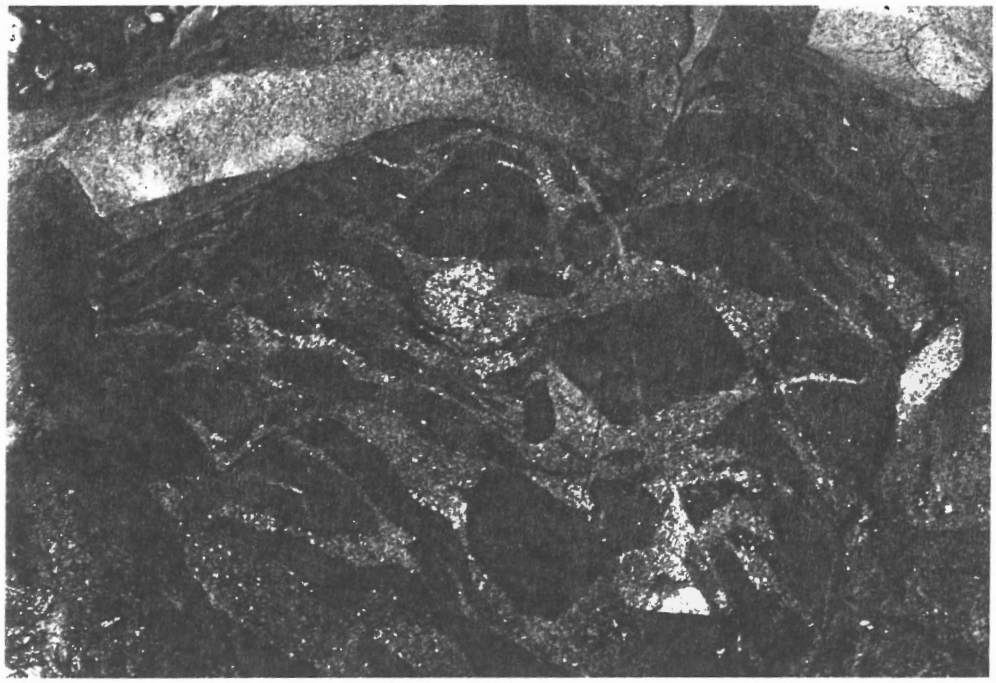

Photo 2-43: Fine-grained melanocratic dykes of Type 2, Unit 7 (see text). Fine-grained, biotite-rich quartzo-feldspathic inclusions (psammite?) are abundant (dyke swarms contain up to 20% rounded inclusions of fine-grained biotite-rich xenoliths).

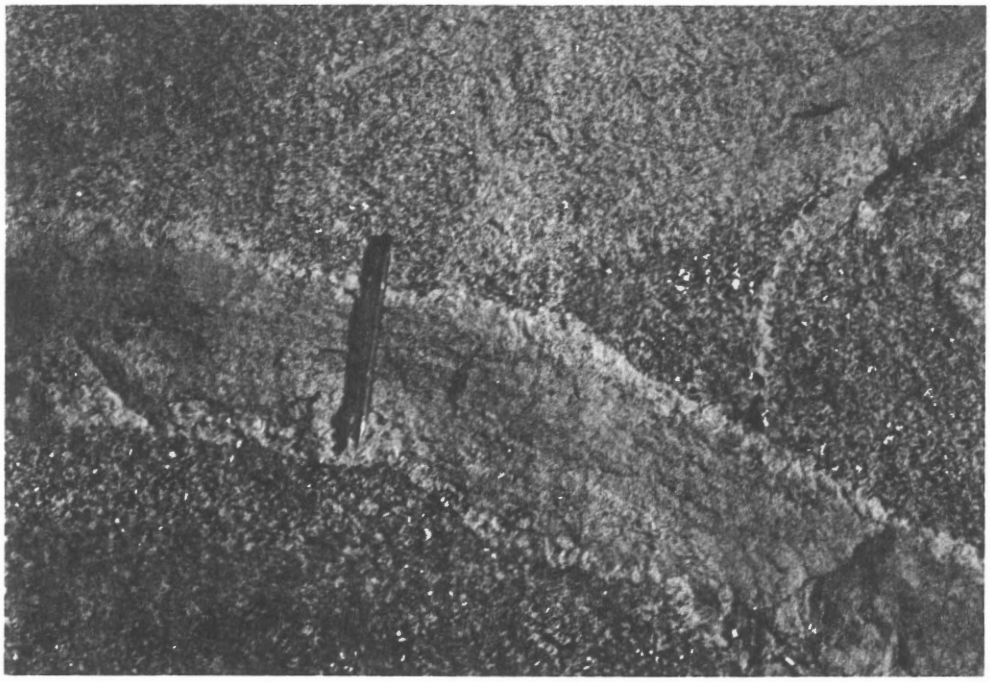

Photo 2-44: Fine-grained mesocratic dyke of Type 3 of Unit 7 (see text). This zone is penecontemporaneous with the 1-2 cm pegmatite margins. The dyke complex cuts Unit 1 and Unit 4 granites.

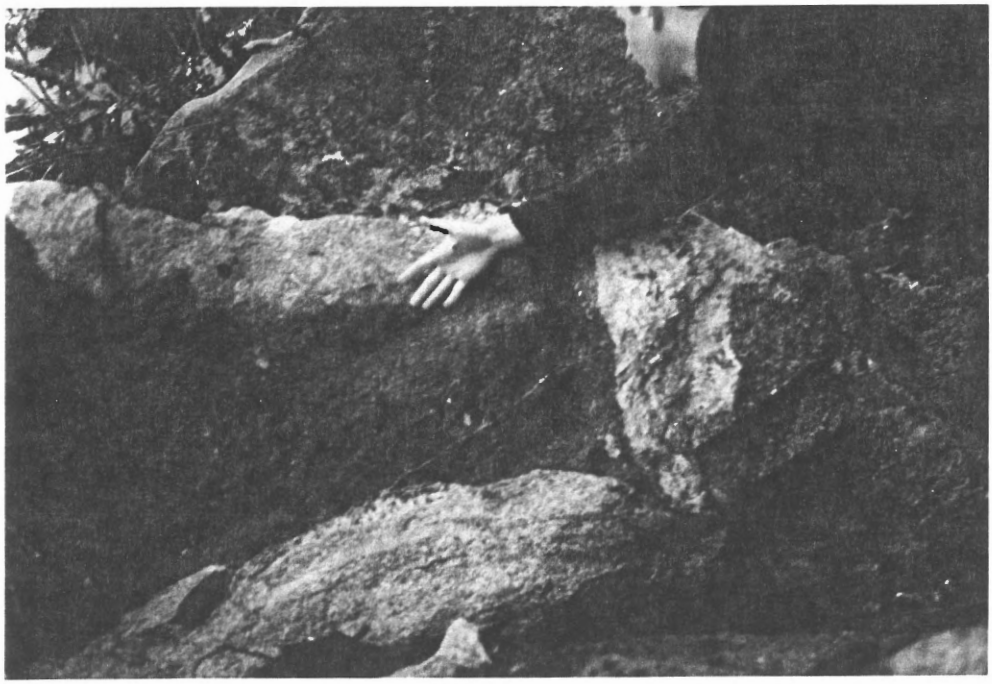

Photo 2-45: Fine-grained melanocratic dyke of Type 4 of Unit 7 (see text). Unit 7 contains 2-5 cm rounded biotite 'clots' (the dykes contain less than 10% rounded biotite 'clots'). Leucomonzogranite dyke of Unit 9 and biotite tonalite of Unit 1 are also exposed in this outcrop.

1) Pods and/or irregular meandering dykes.

Suites of dykes containing fewer than 5% inclusions of metasedimentary lithologies occur on Spectacle Island, at Black Point, Mouton Head, on the eastern shore of Port Mouton Island, and at St. Catherines River Bay (Photo 2-42). This variety of Unit 7 makes up roughly 40% of the Unit.

2) Inclusion-rich dyke swarms.

Swarms of dykes, up to 25 m wide, contain up to 20% rounded inclusions of fine-grained quartzofeldspathic material (probably psammitic country rock), fine-grained biotite-rich material, and less commonly coarse-grained granitoid lithologies (Photo 2-43). The inclusions are rounded and range in size from 10 to 40 cm. This variety of Unit 7 makes up 30% of the unit, and is well exposed at Black Point, Mouton Head.

3) Dykes intimately associated with zoned pegmatites.

Bands of Unit 7 occur within zoned pegmatites of Unit 9, parallel to the margins of the pegmatites. The bands are generally less than one metre wide, and appear to have been emplaced penecontemporaneously with the pegmatites. This variety is minor, comprising less than 10% of Unit 7, but ubiquitous (Photo 2-44). It is distinguished by its fine-grain size, its relatively high proportion of mafic minerals (greater than 10% biotite), and its crosscutting relationships to Units 1 and 4. With the exception of rare leucocratic inclusions of Unit 6, this variety is inclusion-free.

4) Dykes containing biotite clots.

A minor variety of Unit 7, comprising less than 1% of the unit,

Photo 2-46: Fine-grained melanocratic dyke of Type 5 of Unit 7 (see text). This dyke has a sharp planar contact with the older monzogranite of Unit 4. The black platy minerals abundant at the margins of the Unit 7 dyke are biotite.

outcrops along Port Joli Road and on East Port Mouton Island. It is distinguished by the occurrence of up to 10% of 2-5 cm rounded biotite clots (Photo 2-45). The outcrop along Port Joli Road is less than 5 m wide, although on Port Mouton Island this form of Unit 7 outcrops for almost 1 km.

5) Fine-grained tonalite/granodiorite with 5-20% biotite.

This form, which makes up about 20% of Unit 7, outcrops at Hunts Point, where it occurs as dykes ranging in width from 5-10 cm to 400m. The dykes are planar, distinguishing them from the meandering type described above, and contain fewer than 10% inclusions (Photo 2-46). These appear to have been derived from the country rocks and are rounded or ellipsoidal and range in diameter from 5 to 25 cm. Along St. Catherines River Bay, Unit 7 is locally porphyritic at the margins of the dykes, particularly where they are in contact with pegmatites. Feldspar phenocrysts range in diameter from 0.5 to 2 cm.

Unit 8, monzogranite

Unit 8 is a fine- to medium-grained, equigranular, leucocratic, biotite-muscovite monzogranite and comprises less than 10% of the pluton (Fig. 2-9). It consists of quartz (17-29%), plagioclase (30-52%), alkali feldspar (microcline and perthite, 25-37%), biotite (up to 6%), muscovite (2-4%) and accessory zircon and rare anhedral to subhedral garnet (Photo 2-47, 2-48). Often it is intimately associated with the pegmatites and aplites of Unit 9 and is more abundant along the margins of the pluton where dykes of Units 8 and 9 have invaded the country rocks. Dykes of Unit 8 are typically homoge-

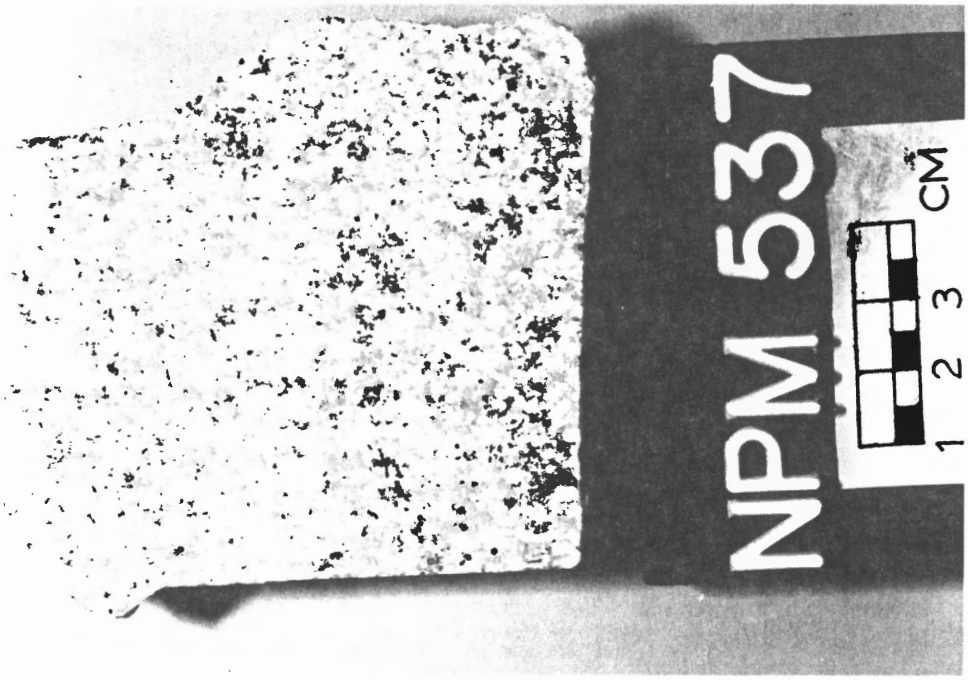

Photo 2-47: Stained hand specimen of Unit 8, fine-grained leucomonzogranite from the eastern shore of Port Joli Harbour. Mineralogy includes plagioclase, microcline, quartz, biotite and muscovite with accessory apatite.

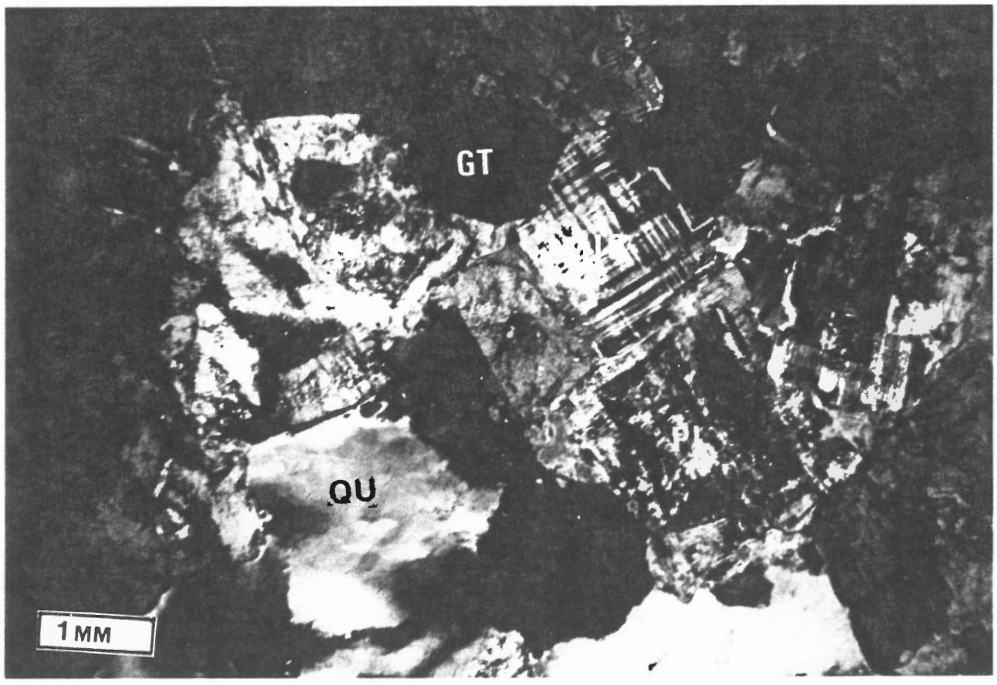

Photo 2-48: Unit 8, medium-grained hypidiomorphic granular leucomonzogranite (NPM8A). Note the euhedral garnets and the well developed microcline grains. XNL

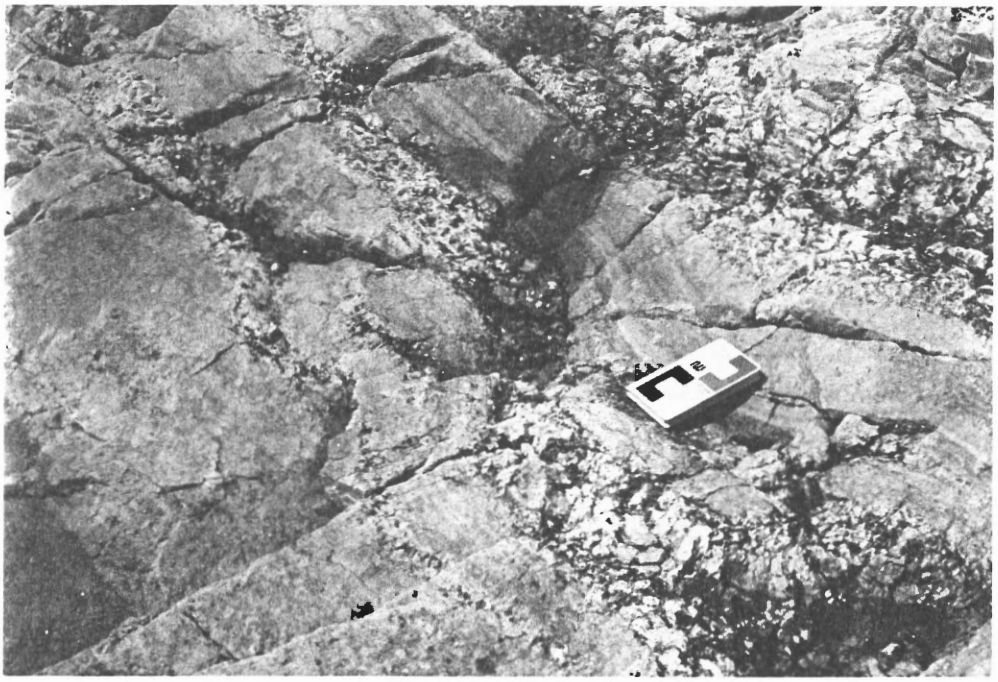

Photo 2-49: Unit 8 medium-grained leucomonzogranite interbanded with aplites and pegmatites of Unit 9

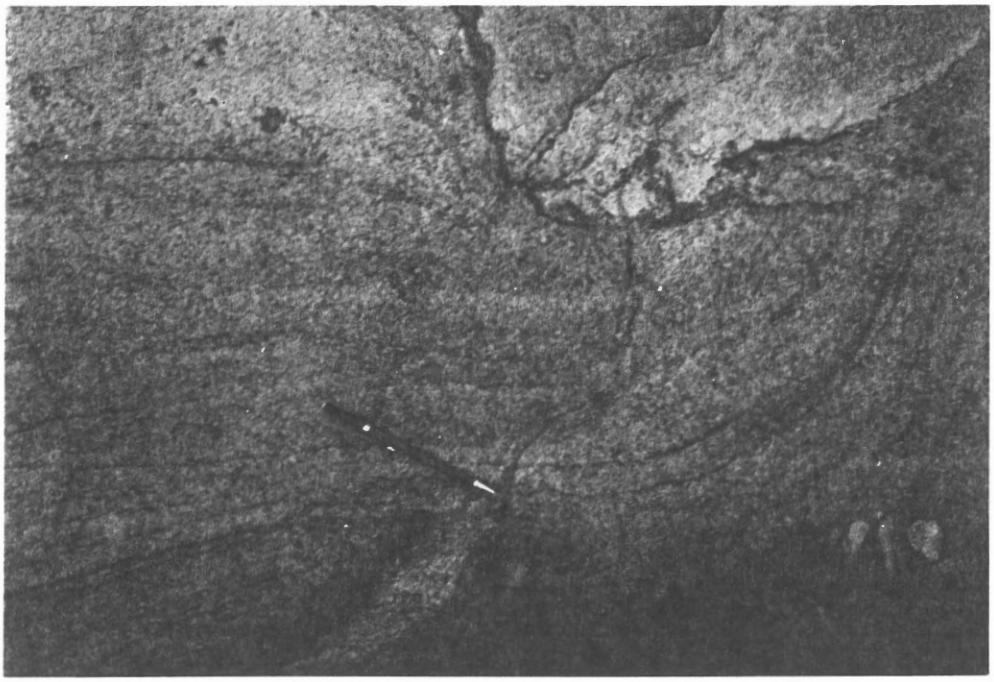

Photo 2-50: Banded Unit 8 (leucomonzogranite) dykes.

neous, and cut older pegmatites, or are interbanded with zoned pegmatites of Unit 9 (Photo 2-49). In places, however, Unit 8 is distinctly banded with the more melanocratic bands enriched in biotite (Photo 2-50). A typical dyke complex of Unit 9 contains a 1 m wide margin of banded Unit 8, a 50 cm band of garnet-rich aplite, and a core of coarse-grained pegmatite (Unit 9). Unit 8 commonly contains garnets where it is associated with pegmatite.

Unit 9, pegmatite and aplite.

Unit 9 is the youngest intrusive phase of the Port Mouton Pluton. It includes fine-grained aplite, commonly rich in garnet and pegmatites of variable grain size. Unit 9 makes up approximately 20-25% of the pluton (Fig. 2-9). The aplite consists of quartz (18-27%), plagioclase (31-59%), microcline (3-36%), muscovite (3-10%), biotite (1-5%) and accessory subhedral garnet (Photos 2-51, 2-52). Pegmatite dykes are abundant throughout the pluton and are particularly concentrated at the contact with the country rocks. Unit 9 is commonly associated with Units 7 and 8; the three units often forming zoned pegmatite complexes attaining widths of over 7 m, and tens of metres in length. Dykes of fine-grained aplite (with or without garnet) and/or pegmatite of Unit 9 extend into the country rock for many hundreds of metres. The contacts between Unit 9 and the granitoid units that it has intruded are typically sharp. The pegmatites contain quartz (< 1 cm to 1.5 m long), perthitic feldspar, plagioclase, graphic feldspar, and muscovite. Accessory minerals include biotite, tourmaline, garnet, fluorapatite, beryl (Photo 2-

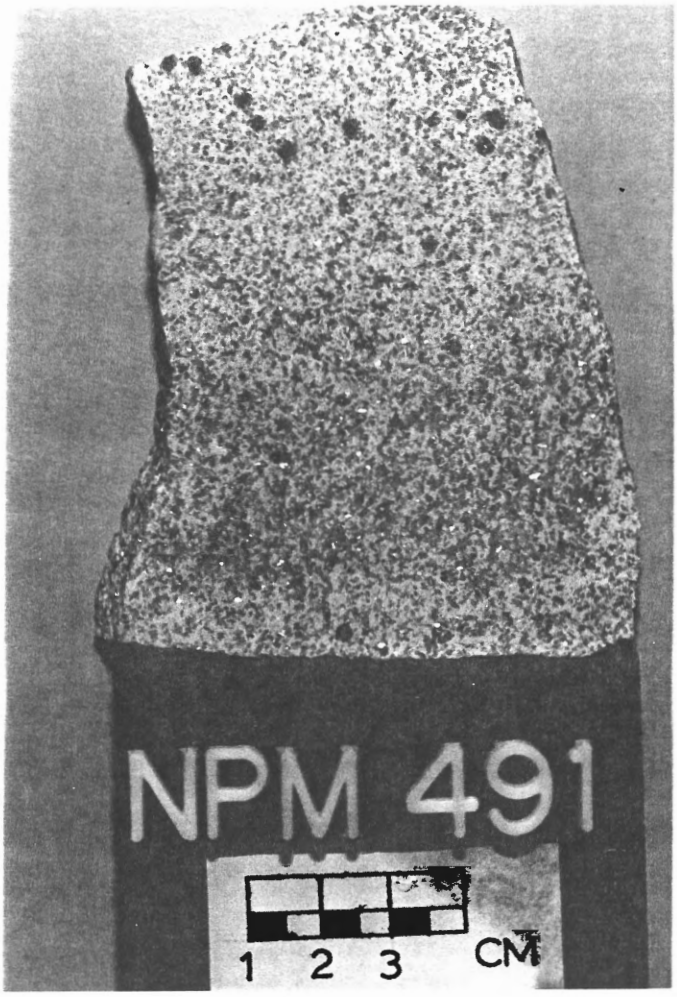

Photo 2-51: Unit 9, garnet-rich aplite from a large dyke in the Meguma Group at Sandy Cove. Note the mineralogical zonation in the sample. The bottom zone is enriched in potassic feldspar, quartz,and muscovite relative to the plagioclase-rich upper zone.

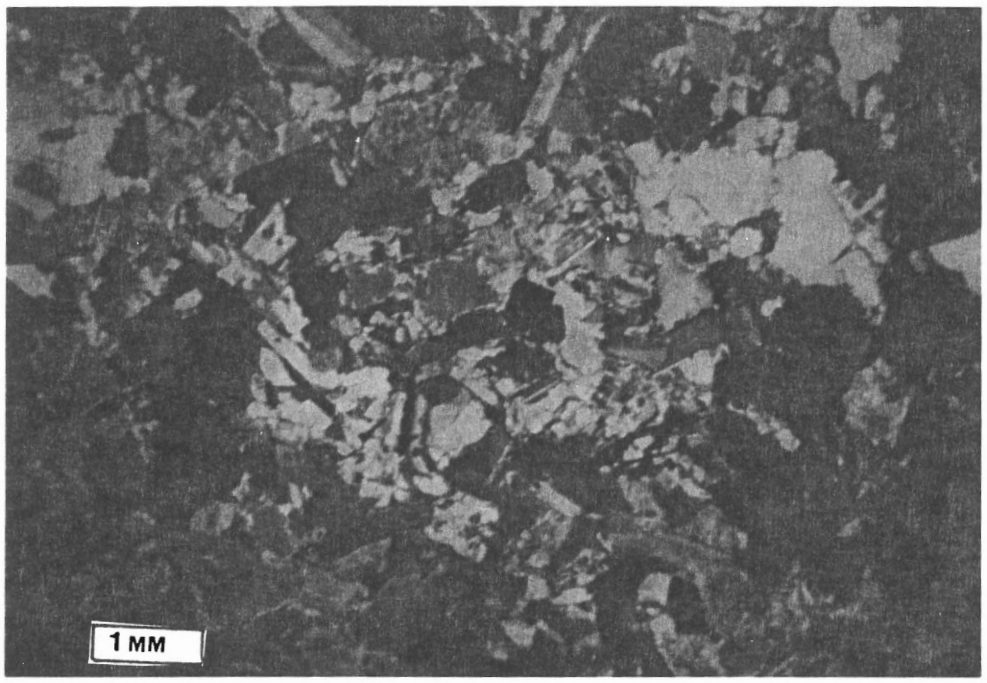

Photo 2-52: Unit 9 aplite. Thin section of NPM491. Note the subgrain development surrounding the quartz and the abundance of muscovite (secondary?). XNL.

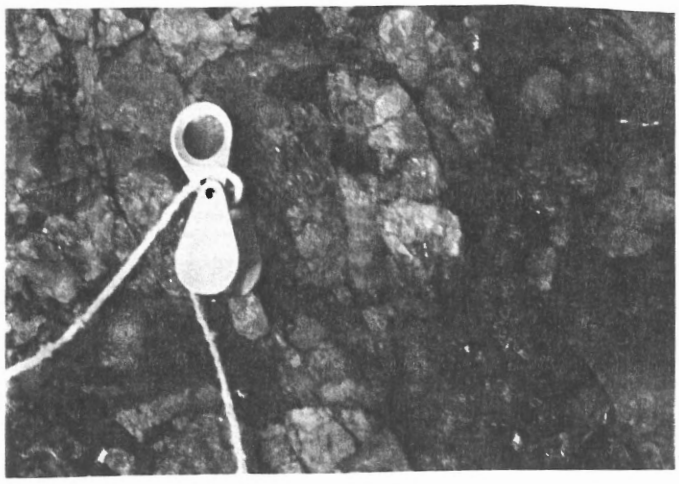

Photo 2-53: A euhedral crystal of light green beryl in quartz in a coarse-grained pegmatite (Unit 9).

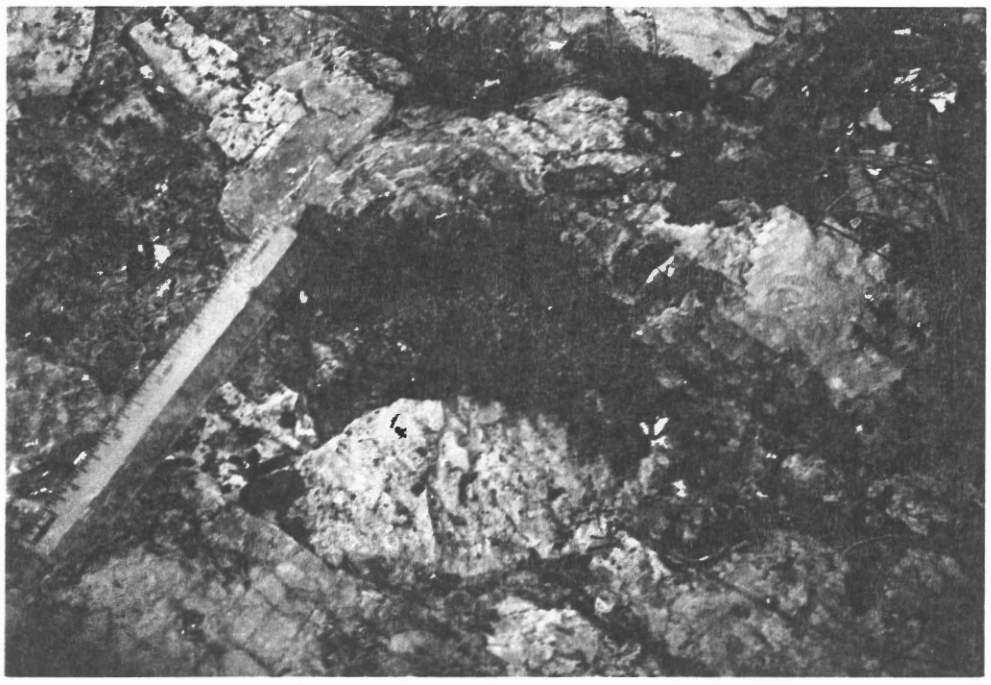

Photo 2-54: Garnet (12 cm diameter) with quartz inclusions, in a coarse-grained pegmatite (Unit 9).

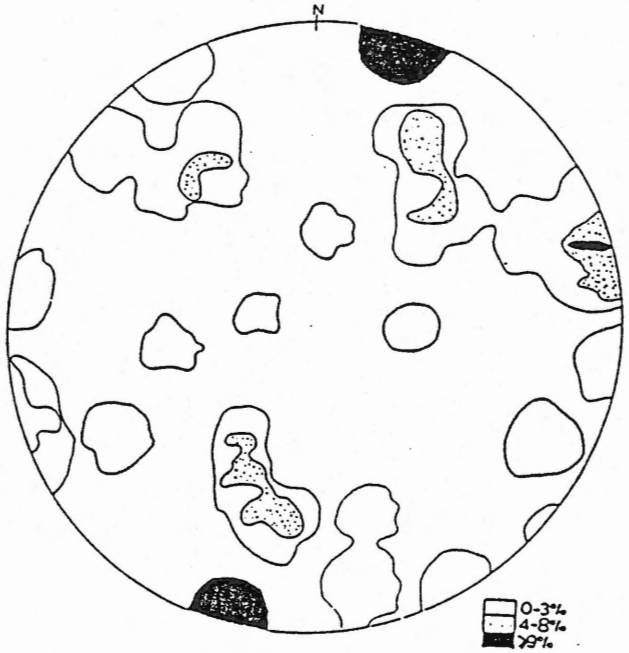

Figure 2-11: Aplite dykes. Schmidt stereographic projections- plot of poles to planes. Contours represent the percentage of 31 points in a 1% area of the hemisphere.

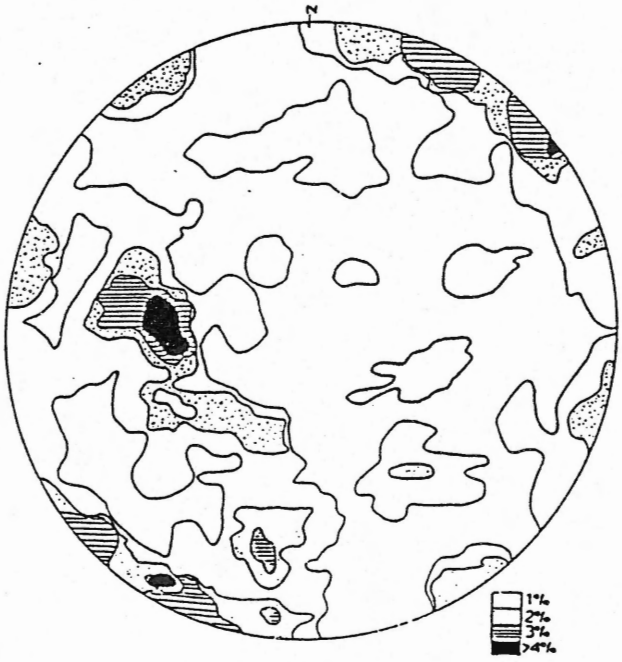

Figure 2-12: Pegmatite dykes less than one meter in width. Schmidt Stereographic Projection -plot of poles to planes. Contours represent percentages of 256 points in a 1% area of the hemisphere.

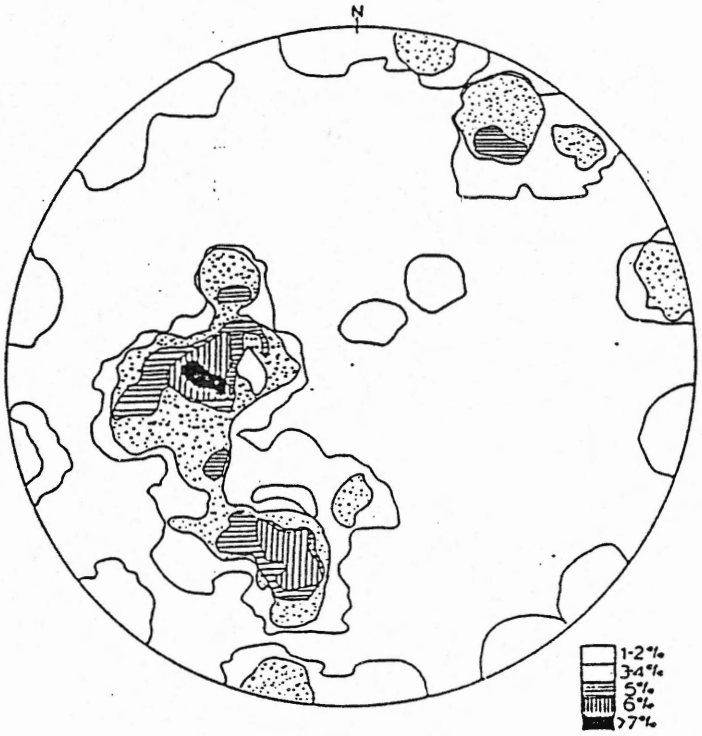

Figure 2-13: Pegmatites greater than one meter in width. Schmidt Stereographic Projections- plot of poles to planes. Contours represent percentage of 53 points in a 1% area of the hemisphere.

Figure 2-14: Granite veins (Veins of Unit 4, 5, and 8). Schmidt Stereographic Projection- plot of poles to planes. Contours represent percentage of 67 points in a 1% area of hemisphere.

dipping dykes. Similarly, a stereographic projection of the orientations of 183 unfilled joints in granite (Fig. 2-15) shows very few horizontal joints, and a girdle of data points rimming the perimeter of the plot.

2-3-2 Shear Zones and Shear Planes

Shear planes and protomylonitic shear zones occur throughout the pluton in isolated 0.3 to 1.5 m wide zones. Evidence for ductile shearing has been observed in thin section and in hand specimen. Quartz grains have been broken into subgrains, quartz and feldspars have been elongated, and some micas are kinked. The shear zones appear to be uniformly distributed throughout the pluton, although north of Haley Lake, along Highway 103, there is a 0.5 km wide zone in which entire granitic outcrops display a sheared fabric, trending 225°/66°-75° to the west.

A plot of 69 poles to shear planes (Fig. 2-16) shows a concentration at 060°/90°.

2-3-3 Summary of Structural Data

The foliation orientations of Units 1 and 4 are distinctly different, with maxima at 108°/60° SW and 040°/70 W to 80° E, respectively (Figs. 2-3 and 2-8). The foliation of Unit 4 does not appear to be superimposed on that of Unit 1 (Unit 1 has only one foliation and it is defined by the orientation of biotite). The orientation of the foliation of Unit 4 is similar to that of the layering observed sporadically throughout the unit, suggesting a

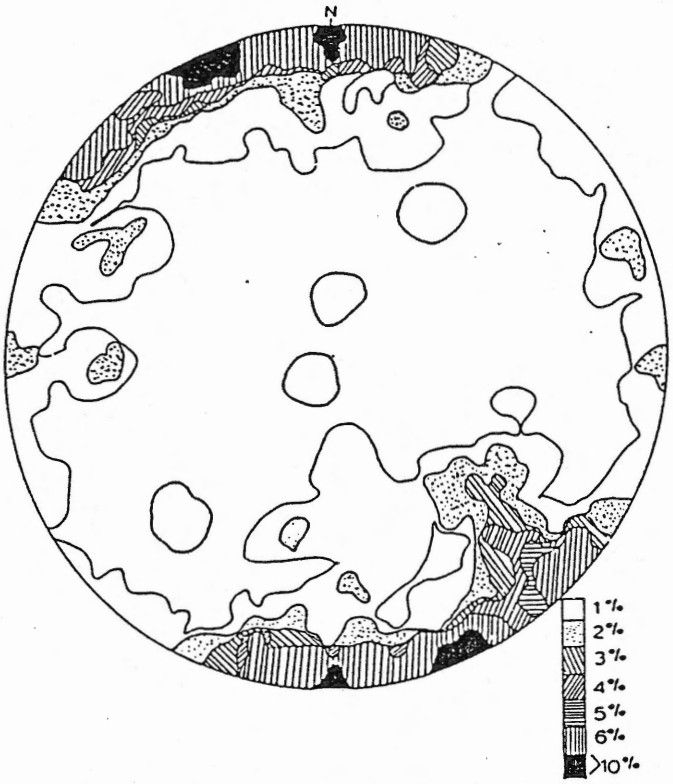

Figure 2-15: Joints in Granite. Schmidt stereographic projection - plot of poles to planes. Contours represent the percentage of 183 points in a 1% area of the hemisphere.

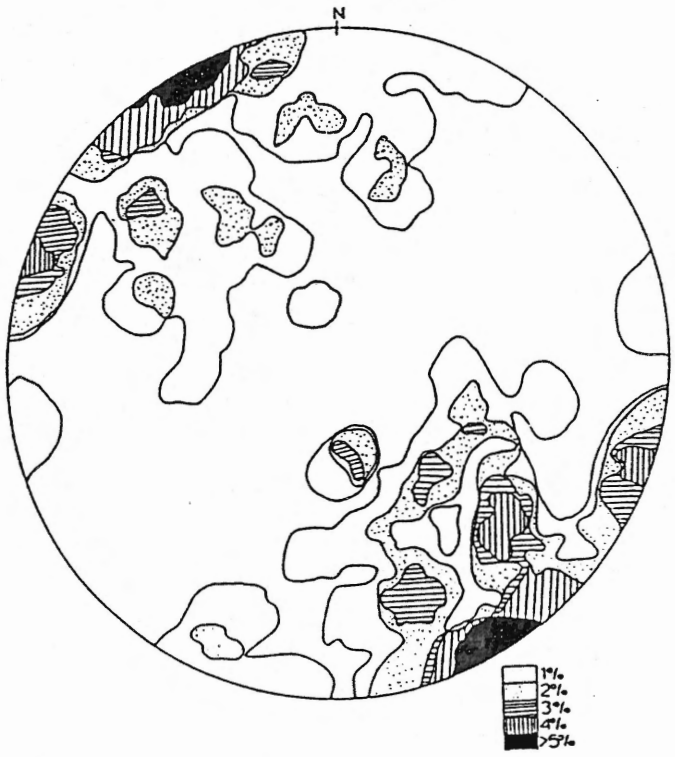

Figure 2-16: Shear Zones and Shear Planes. Schmidt stereographic projections. Contours represent percentage of poles to planes of 69 points in 1% area of the hemisphere.

relationship in their formation. The foliation in Unit 1 may be magmatic in origin, based on the dissimilarity in orientation with the Unit 4 foliation and the regional foliation (see discussion below), and by the lack of ductile deformation.

2-4 Regional Structural Geology in the Meguma Group Metasedimentary Rocks.

In the vicinity of the PMP, the Meguma Group country rock has major F1 folds that range from open to isoclinal, and upright to inclined. The wavelengths range from a few meters to 10 km. "F1 folds vary in orientation from 010° to 045° and plunge gently (1 to 16°) to the northeast. These folds have an associated axial planar cleavage (S1) that strike between 012° and 052°, with dips ranging from 70° southeast to 70° to the northwest" (Hope and Woodend, 1986, p21-22). Hope and Woodend (1986) also noted that the foliations and bedding orientations are deflected by or deflected around, the intrusion of the Port Mouton Pluton in the St. Catherines River Domain. As well, in the Broad River-Western Head Domain at Black Point, the bedding is subparallel to the contact with the pluton, having been deflected 20° to 30° clockwise towards the east (Fig. 2-4). The PMP has a sillimanite- grade contact aureole (Hope, 1987). This sillimanite zone is concentric around the pluton and ranges in width from 500 m to 1 km. (Hope, 1987). The pluton has overprinted staurolite-cordierite-andalusite zone assemblages with sillimanite zone assemblages (Hope, 1987). The Port Mouton Pluton occurs at the centre of the regional metamorphic culmination, and it therefore

appears that, rather than the pluton being responsible for the metamorphism, the metamorphism and plutonism may both be manifestations of locally increased thermal activity (Hope, 1988). See Hope (1987) for a detailed discussion of the local structure and metamorphism associated with the Meguma Group metasediments surrounding the PMP.

2-5 Discussion

The PMP is a complex intrusive body made up of at least 10 distinct units. Figure 2-17 illustrates the observed field relationships chracterising each of the 10 units.

The intrusive history of the PMP can be subdivied into a series of three mafic to felsic cycles (Units 1 to 3, 4 to 6, and 7 to 9, respectively) based on field relations. Unit 1 (the mafic end-member of Cycle I) consists of a coarse to medium-grained foliated biotite tonalite and minor granodiorite. Unit 2 (a single trondhjemite dyke) crosscuts Unit 1. Unit 3, the felsic end-member of this first cycle, makes up only 1% of the pluton volumetrically and is a medium to fine-grained biotite-muscovite leucomonzogranite. The mafic end-member of Cycle II is initiated by Unit 4, a medium-grained, biotite-muscovite granodiorite to monzogranite which makes up the largest percentage volumetrically of the pluton at 50%. Unit 4 is crosscut by the mafic lamprophyre dykes and tonalitic breccias of Units 5A and 5B (respectively). These are small dykes making up less than 1% of the pluton volumetrically and are not considered to be mafic end-members in the three defined cycles. The felsic end-members of Cycle II are

the pegmatite, aplite and leucomonzogranites of Unit 6 (making up 1% of the pluton volumetrically). The final cycle (Cycle III) is initiated by the mafic end-member Unit 7 (comprising 5-10% of the pluton) which consists of fine-grained mesocratic to melanocratic biotite-muscovite tonalite, granodiorite and rarely monzogranite. This is the most compositionally diverse unit within the pluton. The felsic end-members of Cycle III consist of biotite-muscovite leucomonzogranites of Unit 8 and aplite and pegmatite dykes of Unit 9 (Units 8 and 9 making up almost 35% of the pluton in total).

This idea of three mafic to felsic cycles will be further developed in subsequent chapters.

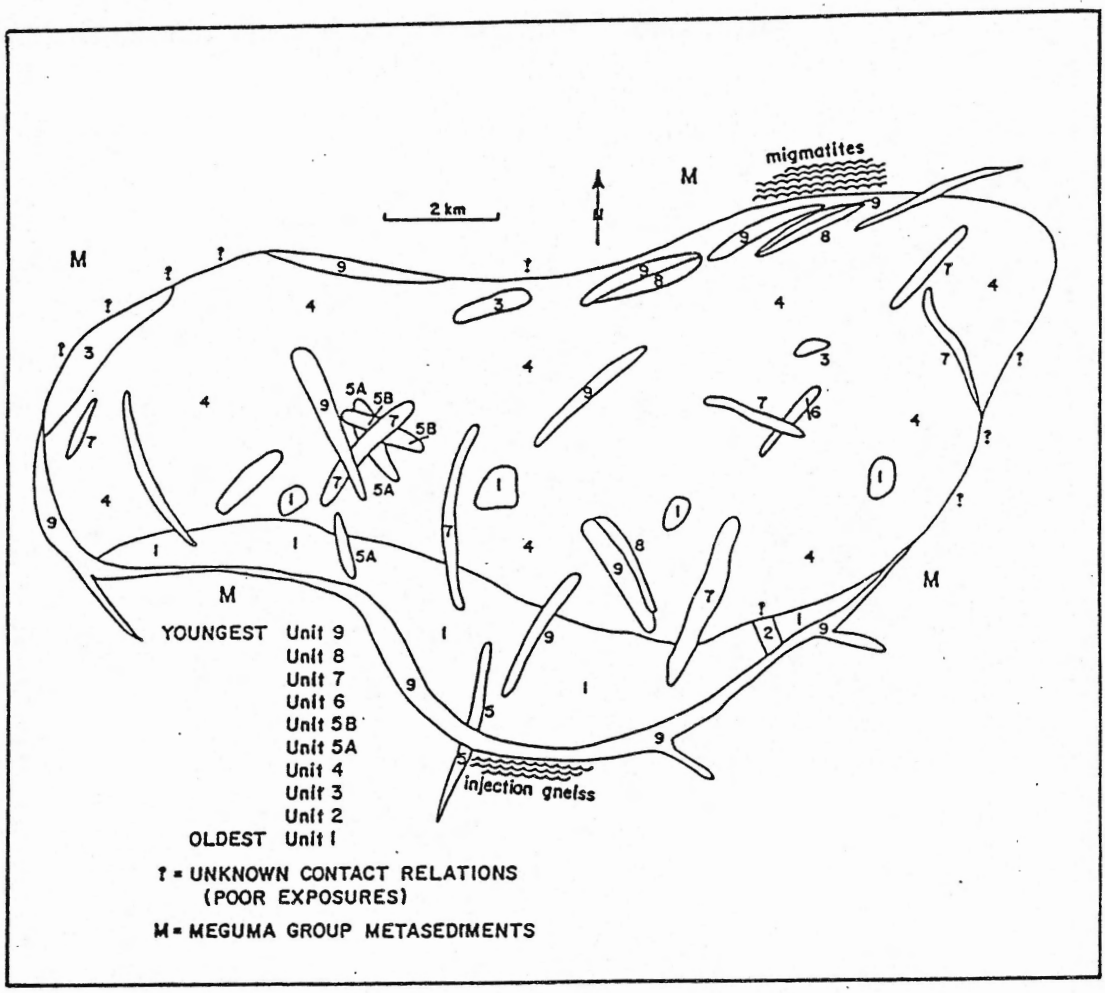

Figure 2-17: A schematic geological map of the Port Mouton Pluton illustrating the observed field relationships.

CHAPTER 3 MINERALOGY

3-1 Introduction

Peraluminous granites contain essential quartz, two feldspars, and one or more characteristic phases such as biotite, muscovite, garnet, cordierite, the alumino-silicates (Al_2SiO_5), mullite, topaz, tourmaline, spinel, and corundum (Clarke, 1981). The granitoid phases of the PMP contain some minerals that are characteristic of peraluminous granites: biotite, muscovite (of uncertain origin), garnet, and tourmaline. In order to compare the composition of the peraluminous minerals of the PMP with other peraluminous granites, biotite, muscovite and garnet were analysed. Plagioclase was also analysed (Fig. 3-8) in order to determine if each mappable unit in the PMP had a distinctive plagioclase composition, and to help distinguish between granodiorites of Unit 1 and granodiorites of Unit 4. Amphiboles (from the metaluminous lamprophyre dykes of Unit 5A) were analysed in order to determine their composition.

3-2 Biotite and Phlogopite

3-2-1 Introduction:

Biotite is an iron-rich trioctahedral mica, which is arbitrarily differentiated from phlogopite by Mg:Fe less than 2:1 (Deer et al., 1966).

Biotite is perhaps the most common sink for excess alumina in granitoid rocks, regardless of the A/CNK ratio of the host rock (Clarke, 1981). Most biotite is of magmatic origin (Clarke, 1981),

although some may occur as mafic remnants from the source region (White and Chappell, 1977), or as refractory mafic schlieren resulting from the assimilation of country rock. 'For peraluminous magmas, prior to the appearance of such minerals as muscovite or garnet, biotite is the only peraluminous mineral and its modal abundance relative to the other precipitating minerals may be critical in determining whether a mildly peraluminous magma can evolve into magmas of higher aluminum saturation index' (Zen, 1986, p. 1117).

Deer et al., (1962) observed that the ratio of Al_2O_3: (MgO + total Fe as FeO) is dependent on the degree of differentiation or contamination of the magma from which the biotite crystallized. Minerals formed at higher temperatures tend to have more Al in four-fold coordination (Deer et al., 1962).

'Phlogopites are critical phases in most lamprophyres but especially in minettes (K-feldspar lamprophyres) and kersantites in which they are the dominant ferromagnesian mineral' (Bachinski and Simpson, 1984). In Figure 3-1 the phlogopite stability curve lies above the granite melting curve for all but the lowest pressures, and crosses the basalt solidus at 2-3 kbars. In a basic rock, phlogopite is stable at depth but would become unstable on extrusion.

3-2-2 Composition of Biotite and Phlogopite within the PMP

The composition of the oxides and cations for the analysed biotite are recorded in Appendix B-1. Table 3-1 includes a brief description of the biotites from samples selected for analysis and Fe_T:(Fe_T+ Mg) ratio of the analysed biotites. Biotite is an abundant

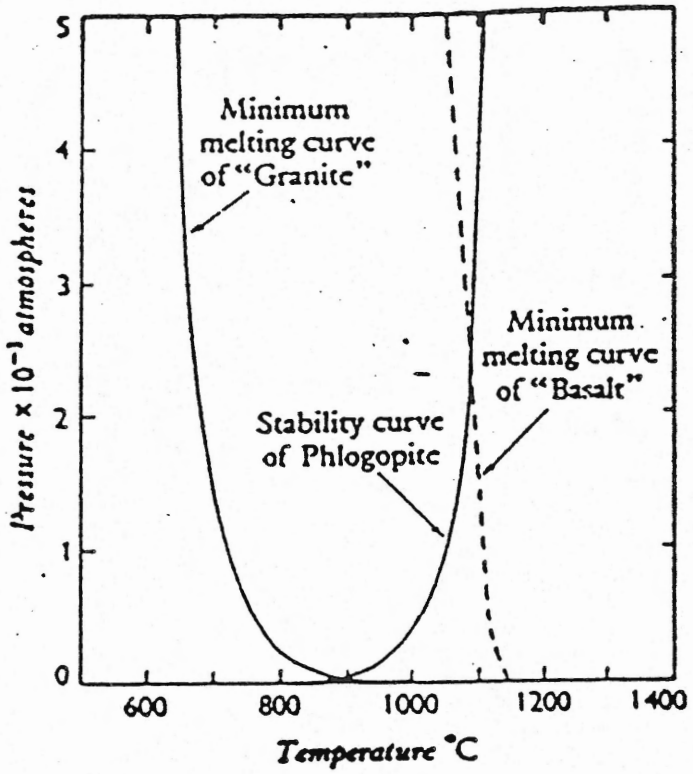

Figure 3-1: From Deer et al., 1966. Relation of upper stability curve of phlogopite to the determined minimum melting curve of granite (Bowen and Tuttle, 1953, p.50) and the estimated minimum melting curve of basalt (after Yoder and Eugster, 1954).

mineral in Units 1, 4 and 7 of the PMP and a subordinate mineral in Units 2, 3, 6, 8 and 9. The lamprophyre dykes of Unit 5A contain abundant phlogopite but no biotite.

On a plot of tetrahedral aluminium against $Fe_T/(Fe_T+Mg)$ (Fig. 3-2), Unit 5A plots close to the phlogopite end member, whereas Units 1, 2, 4, 6, 7, 8 and 9 plot in the region of higher tetrahedral aluminium contents and with $Fe_T/(Fe_T+Mg)$ ratios closer to the eastonite-siderophyllite join. Based on Figure 3-2, the following observations were made on the biotite compositions of the PMP Units:

1) micas from Unit 5A (the lamprophyres) have distinct chemical compositions defined by a lower Al^{iv} and $Fe_T/(Fe_T+Mg)$ values than any of the biotites from the analysed granitoid units;

2) the biotites in Units 6 and 8 are comparable in composition to those in Unit 4;

3) biotites from Units 1, 4 and 7 (mafic end-members of Cycles I, II and III, as discussed in Chapter 2) have very similar Al^{iv} and $Fe_T/(Fe_T+Mg)$ values, although there is an increase in the average FeT/(FeT+Mg) ratio from a low in Unit 1, intermediate in Unit 7, and to the highest values in Unit 4;

4) the composition of biotite from the trondhjemite of Unit 2 is comparable to those of Unit 1.

3-2-3 Discussion

The $Fe_T/(Fe_T+Mg)$ of biotite has been used in the SMB as an indicator of differentiation (Stallard, 1975) where it was found to increase with differentiation. Applying this ratio to the PMP, it can

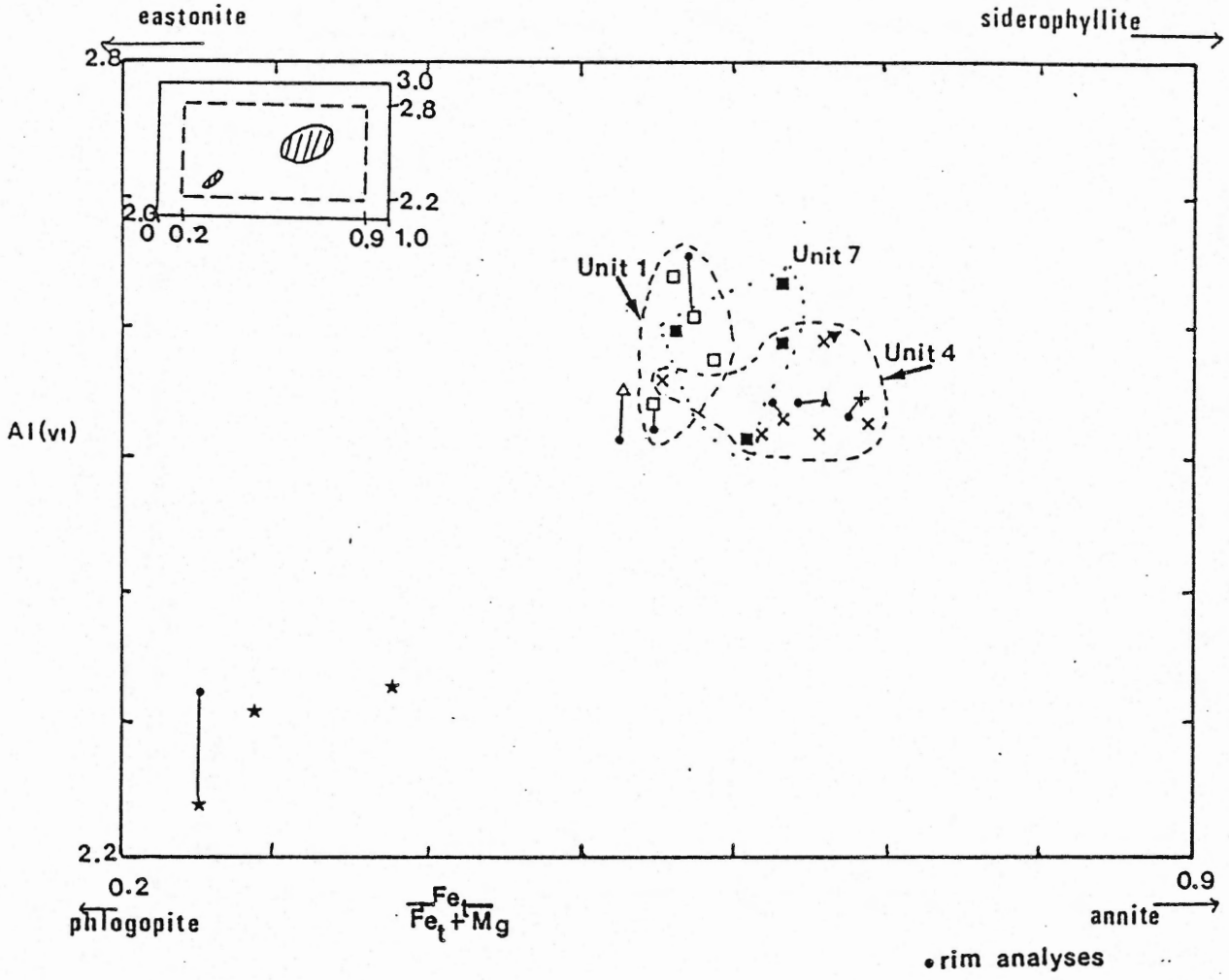

Figure 3-2: Biotite-phlogopite compositions from the PMP (cores and rims).

Table 3-1 Chemistry, Inclusions, Habit and Alteration of the Biotites (cores) from the PMP

LEGEND:
(1) NAME: references- Streckeisen, 1975; Rock, 1977
GRN=granodiorite
LAMP=lamprophyre
L MNZ=leucomonzogranite
MNZ=monzogranite
TON=tonalite
TRJ=trondhjemite

(2) INCLUSIONS: refers to the inclusions found in the biotite-phlogopite grains
AMP=amphibole
AP=apatite
OP=opaque
SPH=sphene
ZR=zircon

(3) MODAL % OF BIOTITE: refers to the modal percentage of biotite or phlogopite found in the specimens

(4) HABIT:
anhed=anhedral
euhed=euhedral
subh=subhedral

(5) ALTERATION: alteration affecting the biotite or phlogopite grains

minor=less than 10% of the grain altered
mod=between 10-5-% alteration of the grain

CHL=chlorite
EP=epidote
MU=muscovite
OP=opaque

(6) $Fe_T/(Fe_T+Mg)$:
refers to the total Fe cations to Fe_T + Mg ratio of the biotites or phlogopites (based on 24 oxygens).

Table 3-1

SAMPLE	NAME/NO.	INCLUSIONS	MODAL% OF BIOTITE	HABIT	ALTERATION	CORE ANALYSES Fe_T/ FeT+Mg)
UNIT 1						
NPM11	TON-3	AP,ZR	23	subh	minor MU	0.57
NPM2	TON-3	AP,ZR	10	some kinked subh	minor CHL	0.56
NPM533	TON-2	AP,ZR	23	subh	minor EP,MU	0.55
NPM582	TON-3	OP,AP,ZR	21	anhed	minor MU,CHL	0.59
UNIT 2						
NPM546	TRJ	ZR,AP	5-10	anhed ragged	minor MU,CHL	0.53
UNIT 3						
NPM542	L MNZ-3		1	ragged	CHL	0.68
UNIT 4						
NPM441	MNZ-3	ZR	7	ragged	minor MU,CHL	0.66
NPM458	GRN-3	ZR,AP	10	ragged	minor MU	0.66
NPM468	MNZ-3	ZR	4	ragged	mod CHL,MU	0.69
NPM477	MNZ-3	ZR	6	ragged	mod CHL,MU	0.62
NPM558	GRN-3	ZR,AP	16	subh	mod CHL	0.55
NPM580	L MNZ-3		4	ragged	minor CHL,MU	0.63
Unit 5A						
NPM405 (NPM612)	LAMP-3	AP,OP,AMP	40	euhed	assoc AMP	0.25
NPM407 (CONTACT)	LAMP-3	SPH,AP, AMP,ZR	40	subh	" "	0.38
NPM485	LAMP-3	SPH,OP,AP	30	subh	"	0.29
UNIT 6						
NPM538	L MNZ-3	ZR	3	ragged	minor MU,CHL	0.63
UNIT 7						
NPM539	GRN-3	ZR	16	subh	minor MU	0.56
NPM560	TON-3	ZR,AP	13	subh to anhed	minor CHL	0.61
NPM566	MNZ-3	ZR	8	ragged	minor MU	0.63
NPM583	TON-3	ZR	5	ragged	minor CHL	0.63
UNIT 8						
NPM361	L MNZ-3		1	ragged	mod CHL,MU	0.66
NPM537	L MNZ-3	ZR	3	ragged	minor MU	0.64

be concluded that Units 1, 2, 4, 6, 7 and 8 are more differentiated than the lamprophyres of Unit 5A. Unit 4 is more evolved than Units 1 and 7 and Unit 7 is more evolved than Unit 1 (Fig. 3-2).

3-3 Muscovites

3-3-1: Introduction

According to Miller et al., (1981) muscovite is the most common mineralogical indicator of strongly peraluminous plutonic rocks. The minimum pressure at which primary igneous muscovite can crystallize directly from a granite melt is 3 kbars (Miller et al., 1981). Data from 41 samples representing 16 plutons in North America and Europe yield a formula of:

$K_{(0.91)}Na_{(0.07)}Fe^{3+}_{(0.20)}Fe^{2+}_{(0.05)}Mg_{(0.10)}Ti_{(0.03)}Al_{(2.6)}Si_{(3.10)}O_{10}(OH_{1.9}F_{0.07})$

with very slight trioctahedral substitutions (2.00 to 2.04 octahedral cations) (Miller et al., 1981).

Muscovite is the most problematic mineral of peraluminous granitoid rocks because there are few textural and/or chemical means of distinguishing between the magmatic and subsolidus modes of origin (Saavedra, 1978). Clarke (1981) observed that muscovite can occur as euhedral books in the groundmass of granites, aplites, and pegmatites, or as obvious breakdown products of feldspar, biotite, aluminosilicates and corundum. Miller et al., (1981) noted several compositional characteristics that distinguish most of the texturally magmatic-looking muscovite from subsolidus muscovite. They found that most magmatic micas are richer in Ti, Al and Na and poorer in Mg and

Si than subsolidus micas, and are typically somewhat closer to ideal muscovite than their secondary mica counterparts, because of their lower Mg. Zen (1987) agreed that the Ti content of muscovite is a useful indicator of magmatic origin (if it has at least 0.4-0.6 weight percent TiO_2). 'One reason that Ti is useful may be that it does not readily undergo subsolidus exchange or oxidation reactions as Mg, Fe and the alkali cations do' (Zen, 1987 p.7).

3-3-2 Composition of Muscovite within the PMP

Muscovite in the PMP granitoid rocks occurs as an alteration of feldspars, intergrowths with/and replacing biotite, and as large subhedral grains overgrowing the quartz-feldspar matrix. These different modes of muscovite are not differentiated in Table 3-2.

Muscovite analyses from Units 1, 2, 3, 4, 6, 7, 8 and 9 are listed in Appendix B-3. Table 3-2 lists the muscovite samples analysed and their modal percentage, habit, $(Fe_T+Mg)/(Fe_T+Mg+Mn+Ti+Al^{vi})$ and Na/(Na+K+Ca) contents. According to Clarke (1981), muscovite compositions from peraluminous granitoid rocks have values of $Fe_T+Mg/(Fe_T+Mg+Mn+Ti+Al^{vi})$ less than 0.2 and Na/(Na+K+Ca) less than 0.1. Figure 3-3 shows that all PMP muscovites (except one tonalite sample) meet these criteria.

Ham (1983) attempted to differentiate primary muscovite from secondary muscovite in samples of the Musquodoboit Batholith and the SMB. Figure 3-4 shows that primary muscovite cannot be distinguished from secondary muscovite on the basis of Ti, Mg and Na cations (Ham, 1983). Superimposed on this plot are samples from the PMP. The PMP

Table 3-2: Chemical Analyses of Muscovites (cores) from the PMP

LEGEND:

(1) NOMENCLATURE:
GRN=granodiorite
L MNZ=leucomonzogranite
L TON=leucotonalite
MNZ=monzogranite
TON=tonalite
TRJ=trondhjemite

(2) HABIT:
summary of habit of muscovite in the various Units
MATRIX=large muscovite grains overgrowing the matrix
#= number of analyses

SAMPLE	MODAL	% HABIT	$\frac{Fe+Mg}{Fe+Mg+Mn+Ti+Al^{IV}}$	$\frac{Na}{Na+K+Ca}$	#
UNIT 1					
NPM11 (TON)	2	intimate association with BI alteration of PL	0.11	0.03	1
NPM2 (TON)	10	assoc with BI,PL matrix	0.06	0.10	3
NPM533 (TON)	2	assoc with BI,PL	0.21	0.03	3
NPM582 (TON)	4	assoc with BI matrix	0.10	0.03	3
UNIT 2					
NPM546 (TRJ)	3	assoc with BI,PL	0.11	0.04	3
UNIT 3					
NPM468 (MNZ)	5	assoc with PL	0.08	0.06	3
NPM542 (MNZ)	3	assoc with BI,PL matrix	0.08	0.05	3
UNIT 4					
NPM441 (MNZ)	5	assoc with BI,PL matrix	0.05	0.08	3
NPM477 (MNZ)	2	assoc with PL incl of QU,PL, BI, in matrix	0.11	0.06	3
NPM558 (GRN)	5	assoc with BI,PL matrix	0.09	0.05	3

Table 3-2 ...,

SAMPLE	MODAL	% HABIT	$\frac{Fe+Mg}{Fe+Mg+Mn+Ti+Al^{iv}}$	$\frac{Na}{Na+K+Ca}$	#
UNIT 4 ...					
NPM580 (L MNZ)	4	matrix, and assoc. with BI	0.07	0.06	3
UNIT 6					
NPM538 (L MNZ)	2	matrix, assoc. with KSPAR, PL matrix	0.08	0.08	3
UNIT 7					
NPM539 (GRN)	3	assoc with BI,PL	0.08	0.05	3
NPM566 (MNZ)	4	assoc with BI matrix,incl of QU PL,BI	0.07	0.06	3
NPM583 (TON)	<5	assoc with BI matrix, incl of QU	0.07	0.05	3
UNIT 8					
NPM361 (L MNZ)	3	assoc with BI,PL matrix	0.04	0.07	3
NPM537 (L MNZ)	3	assoc with BI,PL	0.09	0.05	3
UNIT 9					
NPM491 (L TON)	10	matrix	0.07	0.05	3
NPM8B (L MNZ)	6	assoc with feld-spathic matrix	0.06	0.04	3

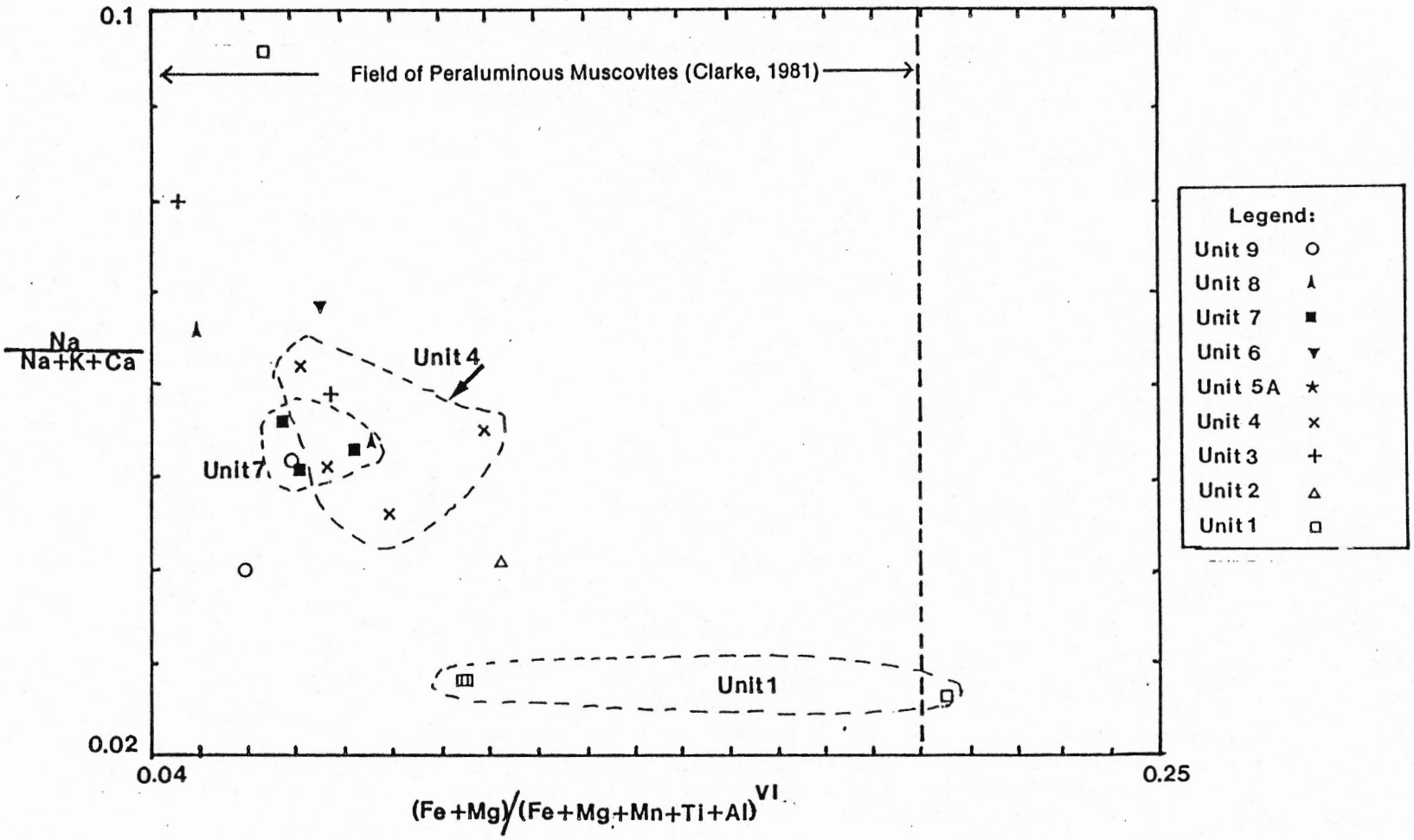

Figure 3-3: Composition of muscovites from the PMP (cores)

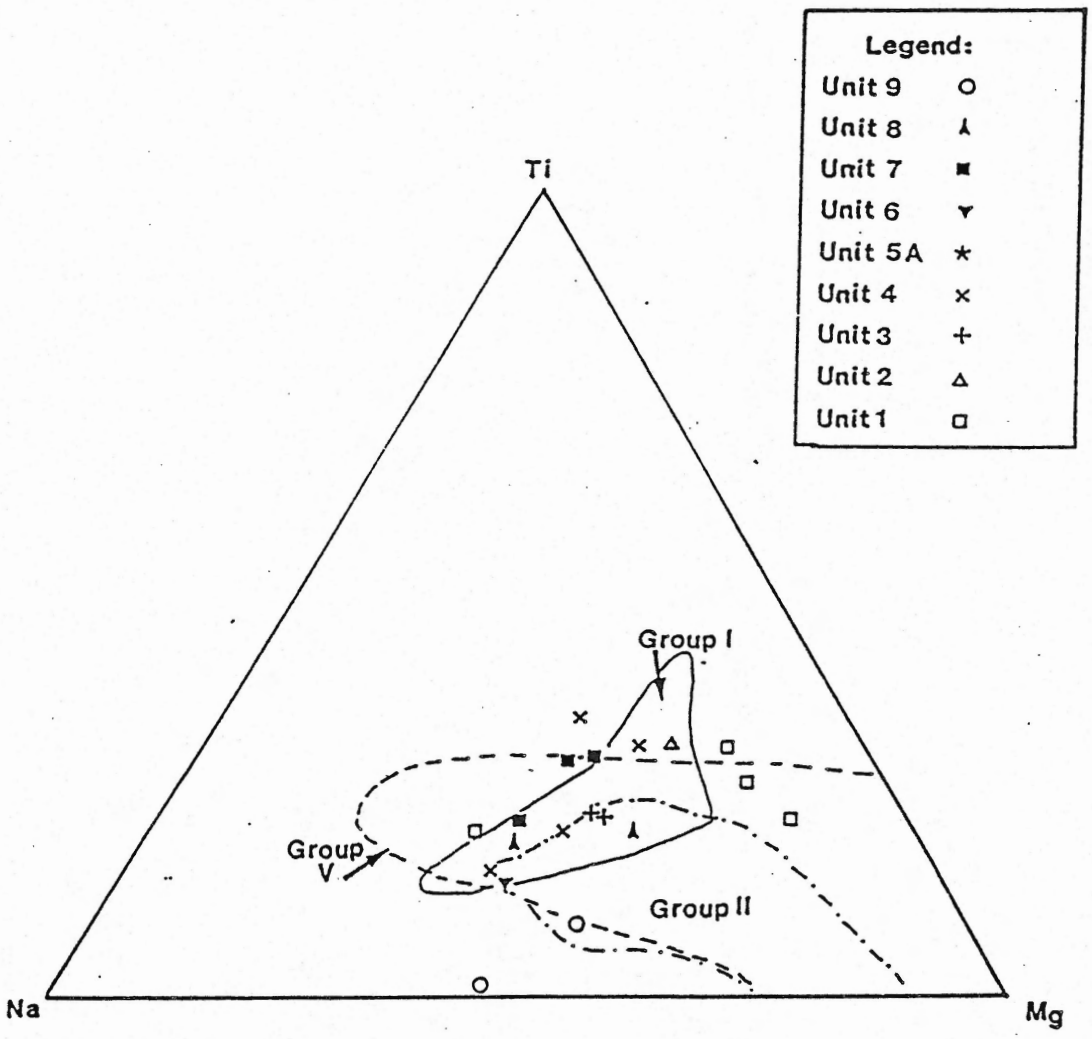

Figure 3-4: Composition of muscovite from the PMP (cores)

Muscovite compositional fields after Ham (1983).
Alteration of feldspars (group V)
Possible Primary Muscovite (group I)
Intergrowth with biotite (group II)

samples are similar in chemical composition to the primary muscovite (Group I), muscovite replacing feldspars (Group V), and muscovite intergrown with biotite (Group II).

3-3-3 Discussion

According to Figure 3 of Clarke (1981), muscovite compositions from the PMP are similar to those from average peraluminous granitoid rocks. Chemical characteristics cannot determine if the muscovites from the PMP granitoids are secondary or primary. Primary muscovite, as defined by Ham (1983), occurs in thin section, although Zen (1987) disputes the existence of an unambiguous textural basis for identifying magmatic muscovite. Considerable overlap in muscovite compositions does not allow the separation of the three predominant Units in the PMP (Units 1, 4 and 7). Of these, Unit 1 is the most chemically distinctive. Three of the four Unit 1 muscovite samples have lower Na/(Na+K+Ca) ratios and higher Mg and Ti compared with Na than any of the other Units.

3-4 Garnet

3-4-1 Introduction

Clarke (1981) compiled possible origins of garnet in granitoid rocks: (1) refractory xenocrysts from porphyroblasts (Allan and Clarke, 1981); (2) refractory restite phase from the zone of partial melting (White and Chappell, 1977); (3) generation in marginal facies of a granite body as a result of reaction between magma and pelitic xenoliths rich in Al and Mn relative to the melt (Jamieson,1974; Allan

and Clarke, 1981); (4) nucleation directly from the silicate melt: (5) reaction between early formed phases and silicate melt.

"Garnets from peraluminous granites can have highly variable compositions with most of the variation occurring in the ratio of Mn:Fe:Mg" (Clarke 1981, p. 9). According to Clarke (1981), normal zoning in the garnets (Ca-Mn cores, Fe-Mg rims) is generally attributed to their growth in a metamorphic environment during prograde conditions. Reverse zoning (Fe-Mg cores, Ca-Mn rims), may indicate either growth during retrograde metamorphism or, in the case of igneous garnets, falling temperature and fractional crystallization.

3-4-2 Composition of Garnet within the PMP and Surrounding Country Rock

The composition of the oxides and cations for the garnets analysed are listed in Appendix B-4. The garnet analyses were originally intended to be used only for garnet-biotite geothermometry; the garnets analysed, therefore, are those that have biotite associated with them. Garnet in Unit 9 was not analysed because this unit lacks biotite. Six garnet-bearing samples were analysed, five from granodiorite rocks (Unit 8, Unit 1) and one from a biotite schist from the surrounding country rock (NPM108). Tables 3-3 and 3-4 briefly describe the habit, alteration, and relative proportions of almandine, spessartine, pyrope and grossular. Figure 3-5 illustrates the relative abundance of spessartine, almandine and pyrope and Figure 3-6 illustrates the relative proportion of Ca, Mg and Fe+Mn in the

Table 3-3

Habit and Alteration Characteristics of Garnet Samples Analysed

Legend for Tables 3-3 and 3-4:
L MNZ=leucomonzogranite
GRN=granodiorite
NPM108=biotite muscovite schist (Meguma Group metasediment)

SAMPLE+ NO. OF ANALYSES	NAME	HABIT+ABUNDANCE	ALTERATION
UNIT 8			
NPM107 C=2,R=2	L MNZ	anhedral,<1%	core missing, garnet fractured moderate chloritization matrix texture=cataclastic
NPM611 C=1,R=1	L MNZ	subhedral,<1%	minor chloritization, matrix subcataclastic, fracture garnet grains
NPM344 C=3,R=3	L MNZ	subhedral,<1%	some garnet grains fractured
NPM8A C=3,R=3	L MNZ	anhedral,<1%	garnet fractured, minor chloritization
UNIT 1			
NPM484 C=3,R=3	GRN	anhedral,<1%	fractured, grains associated with chlorite. Garnets are inclusion-free
NPM108 C=3,R=3	BIOTITE MUSCO-VITE SCHIST	euhedral,5%	poikioblastic, unaltered

Table 3-4
Mineralogy (averages) of the Garnets in the PMP and Surrounding Country Rock. Legend the same as in Table 3-3

SAMPLE	NAME	ALMANDINE CORE:RIM	SPESSARTINE CORE:RIM	PYROPE CORE:RIM	GROSSULAR CORE:RIM
NPM107	L MNZ	56.3:59.15	37.7:35.3	4.5:4.3	1.3:1.2
NPM611	L MNZ	63.3:64.5	27.9:27.2	7.2:6.6	1.5:1.6
NPM344	L MNZ	53.3:60.8	37.5:30.4	7.03:6.8	2.2:2.0
NPM8A	L MNZ	71.4:68.9	19.9:23.5	6.9:5.9	1.6:1.6
NPM484	GRN	80.5:78.4	12.5:15.1	4.4:3.7	2.6:2.8
NPM108	MEGUMA	64.1:63.9	20.5:21.4	9.3:8.8	5.7:5.8

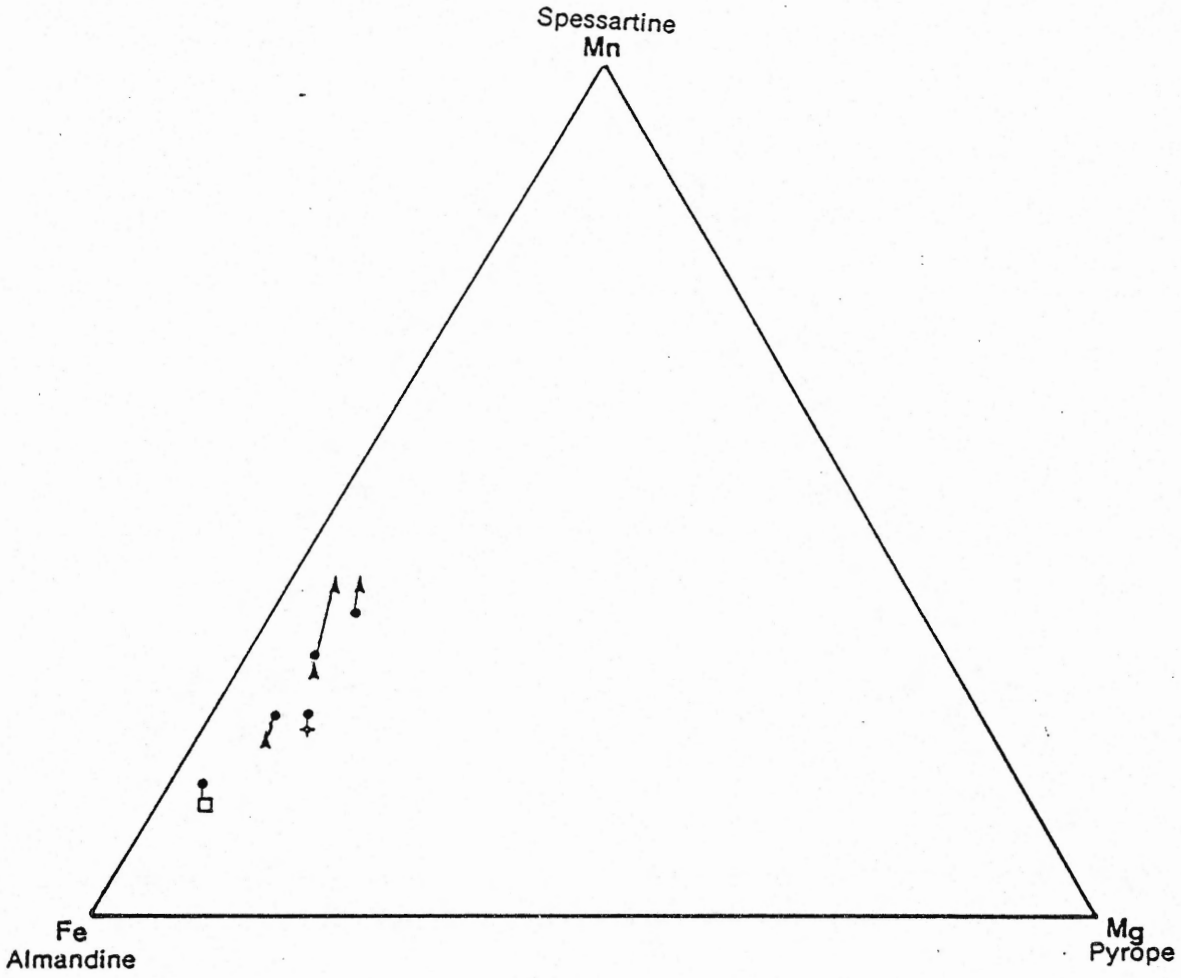

Figure 3-5: Composition of garnet from the PMP (cores and rims)

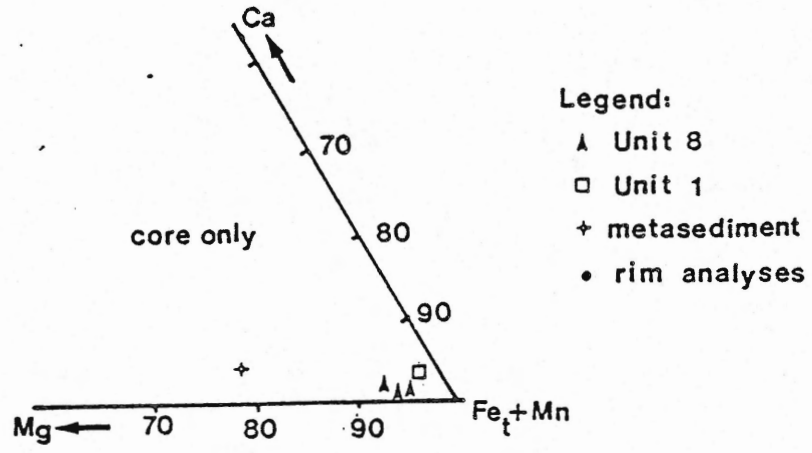

Figure 3-6: Composition of garnets from the PMP (cores)

analysed garnets. All garnets analysed are almandine and spessartine-rich.

Three of the four Unit 8 garnets (NPM344,-107,-8A) exhibit significant concentric zonation. Two samples (NPM107,-344) display normal zonation typified by enrichment of Ca and Mn in the cores and Fe and Mg in the rims.

3-4-3 Discussion

Conflicting observations bearing on the origin of the Unit 8 garnets support both primary magmatic and subsolidus (metamorphic) origin for these garnets. The observations about Unit 8 are as follows:

1) xenoliths are absent. 'If magma-country rock reaction has been responsible for the nucleation of these garnets, then no other trace of the xenoliths remains' (Allan and Clarke, 1981 p. 22);

2) the spessartine content of the Unit 8 garnets is greater than 10%, and in the range normally considered to be magmatic (Miller and Stoddard, 1978);

3) the Unit 8 garnets are normally zoned, characteristic of progressive metamorphism of metasedimentary rocks (Kretz, 1973; Green, 1977);

4) the MnO content (8.6-18.0 wt. %) is in the range characteristic of magmatic garnets (Miller and Stoddard, 1978).

Conflicting observations bearing on the origin of the Unit 1 garnets (one sample, 3 grains) are:

1) garnet-enriched xenoliths are abundant in the granodiorite

suggesting that the garnets in Unit 8 may be xenocrysts;

2) Unit 1 garnets have lower spessartine compositions than those of Unit 8, but are still higher than the 10% range normally considered as magmatic (Miller and Stoddard, 1978);.

The Mn concentration in garnet may not only be dependent on magmatic processes, but may also be dependent on the bulk composition of the rock. Therefore, it is questionable whether the spessartine criterion, stated by Miller and Stoddard, (1978) is a valid one.

3) the garnets are inclusion-free, a common feature in igneous garnets.

3-5 Amphiboles

3-5-1 Introduction

Amphiboles are divided into four principal groups on the basis of B-site cation occupancy (Leake, 1978):

1) $(Ca+Na)_B < 1.34$ Iron-magnesium-manganese group

2) $(Ca+Na)_B \geqslant 1.34$ Calcic amphibole group
   and $Na_B < 0.67$

3) $(Ca+Na)_B \geqslant 1.34$ Sodic-calcic amphibole group
   and $0.67 \leqslant Na_B < 1.34$

4) $Na_B \geqslant 1.34$ Alkali amphibole group

These four groups are represented both in igneous and metamorphic amphiboles (Gilbert and Popp, 1982; Gilbert, 1982). In the PMP the amphiboles are only associated with the the lamprophyre dykes (Unit 5A) and are from the calcic amphibole group. Four subgroups represented in the calcic amphibole group are actinolite,

ferro-actinolite, actinolitic hornblende and magnesio-hornblende. The analyses of the amphiboles are listed in Appendix B-2.

3-5-2 Amphiboles from the Forbes Point Lamprophyre

Analyses were made of amphibole samples from three zones within the dyke.

1) a phlogopite-amphibole-rich zone (NPM612) within the dyke (predominant zone);

2) an amphibole-rich zone (NPM615) which occurs as lenses (up to 0.5m long and 0.2-0.3m wide) within the main lamprophyre dyke;

3) an amphibole from the contact aureole (NPM407) which is superimposed on intruded Unit 1 and Unit 4.

The phlogopite-amphibole zone contains 40% amphiboles that are euhedral to subhedral, often contain minor inclusions of apatite and opaque minerals and have pale green pleochroism. Large subhedral to euhedral phlogopites commonly overgrow and enclose the amphibole and appear to replace the amphibole. The amphiboles contain minor inclusions of apatite and opaque minerals. Chemically, three amphiboles of this zone are actinolite. Two of the three grains analysed are zoned chemically and display both a chemical progression from a core of actinolite to a rim of actinolitic hornblende and the reverse zonation.

The amphibole-rich (67 modal %) zone contains plagioclase. The dark, moss-green, pleochroic, amphiboles are closely packed (mat-like texture) subhedral grains that show minor alteration to phlogopite. Large plagioclase phenocrysts are common and sphene and anhedral

opaque minerals are common inclusions in the amphiboles. Analyses of three amphiboles in this sample identify them as a magnesio-hornblende, based on an index devised by Miller and Stoddard (1978). One of the three minerals analysed is zoned, with an actinolitic hornblende core and a magnesio-hornblende rim.

The amphiboles from the contact aureole (NPM407) are anhedral, ragged grains that appear to be in disequilbrium with the quartz (with irregular grain boundaries), in a plagioclase-rich matrix. The dark, moss-green, pleochroic amphiboles contain minor inclusions of apatite, sphene and anhedral opaque minerals, and make up 40% of the mineralogy. Chemically, the average of the cores of three grains of the amphiboles place it as magnesio-hornblende. Two of the three grains analysed show significant chemical zonation from core to rim. One grain has an actinolitic hornblende core, grading to a magnesio-hornblende rim. The other grain shows a higher Si and Mg in the rim compared with the core.

3-5-3 Amphiboles from the MacLeods Cove Lamprophrye

The MacLeods Cove lamprophyre (NPM485) is a relatively homogenous dyke. The amphiboles within the dyke occur in two habits, as anhedral to subhedral matrix minerals extensively replaced by phlogopite, or as concentrated clusters of subhedral to anhedral grains also altered to phlogopite. The amphiboles are pale-green and have poor crystal terminations. The amphiboles make up 25% of the sample and contain minor inclusions of sphene, apatite and opaque minerals. Chemically the average of the cores of three amphibole grains is actinolite.

Table 3-5

Cores Analyses of Amphiboles from the Lamprophyre Dykes of the PMP

SAMPLE # OF ANALYSES	MODAL% + NOMENCLATURE	HABIT OF AMPHIBOLE	INCLUSIONS
MACLEODS COVE LAMP			
NPM485 4	25 actinolite	mats of crystals altered by phlogopite -anhedral,ragged grain boundaries	sphene and apatite + opaques
FORBES COVE LAMP			
NPM612 (NPM405) 3	40 actinolite	euhedral to subhedral grains altered by phlogopite	minor apatite + opaques
NPM615 (NPM406) 3	67 magnesio-hornblende	closely packed subhedral grains altered by phlogopite	sphene and anhedral opaques
NPM407 contact aureole 3	10 magnesio-hornblende	intimately assoc with phlogopite, subhedral to anhedral up to 0.75mm long	apatite and sphene and opaque

Note: complete petrological descriptions of samples NPM612,615, and 485 are included in Appendix B-2

Only two of the three grains were analysed in both the core and rim, and both of these grains are zoned chemically (both with an increase in Si and Mg in the rim compared with the core).

3-5-4 Discussion

In summary, the amphiboles from the PMP lamprophyres show a wide range in chemistry, ranging from ferro-actinolite to actinolite and magnesio-hornblende. The amphiboles from the lamprophyres are either primary (magmatic) or secondary (developed as a product of hydrothermal alteration). On the basis of their euhedral habit and interlocking grains, some appear to be primary (NPM612-actinolite and NPM615-magnesio-hornblende). Others appear to be subsolidus (NPM485-actinolite and NPM407-magesio-hornblende) because of their poor crystal development (indicating disequilibrium?) and extensive phlogopitic alteration.

Actinolite is considered to be a metamorphic mineral (Yamaguichi, 1985; Oba, 1980; Cameron, 1975; Deer et al., 1962) and is a member of the tremolite-actinolite-ferroactinolite series. Hornblendes can be either metamorphic or igneous (Hammarstrom and Zen, 1986; Laird and Albeel, 1981; Raase, 1974; Mason, 1968; Deer et al., 1966). In an attempt to determine the origin of the PMP amphiboles, their compositions were compared with metamorphic and magmatic amphibole fields defined by Jamieson (1981) (Fig. 3-7), metamorphic hornblendes (mafic schists) from Vermont (Laird and Albee, 1981), and igneous hornblendes from five calc-alkaline plutonic complexes (Hammarstrom and Zen, 1986).

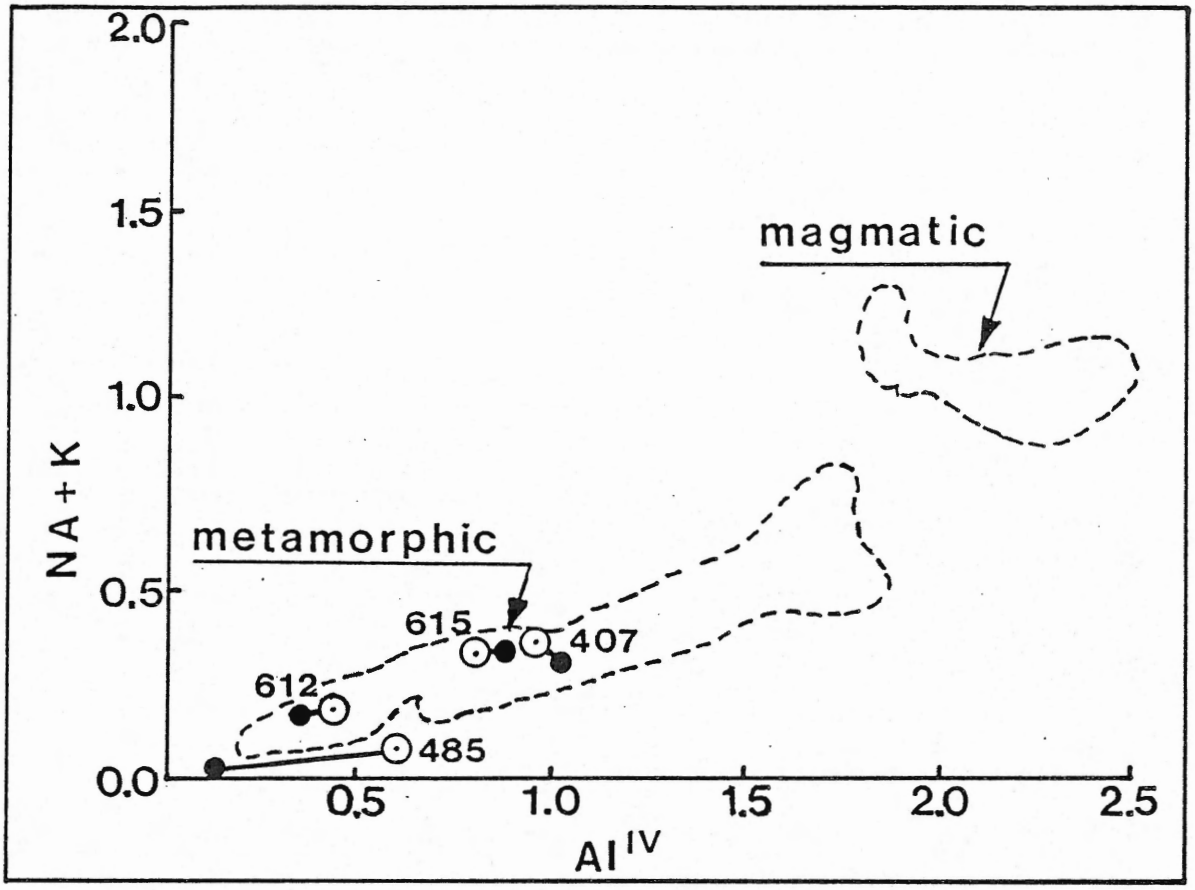

Figure 3-7: Metamorphic and magmatic fields of amphiboles from the St. Anthony Complex, Newfoundland (after Jamieson, 1981). The PMP lamprophyres are labelled, NPM-612-615-407 and 485).
⊙ =core, ● =rim

Conflicting chemical evidence supports either magmatic or metamorphic origin for the PMP amphiboles. The magnesio-hornblendes and the actinolitic-hornblende of the Forbes Cove lamprophyre plot in the high pressure field defined by the hornblendes in a tonalite pluton (Hammarstrom and Zen, 1986), as metamorphic amphiboles (fields defined by Jamieson, 1981) and in the field of medium pressure calcic-amphiboles in mafic schists (Laird and Albee, 1981).

The origin of the amphiboles in the PMP lamprophyres remains resolved.

3-6 Plagioclase

3-6-1 Composition of Plagioclase within the PMP

Microprobe analyses of plagioclase from Units 1, 2, 3, 4, 5A, 6, 8 and 9 are listed in Appendix B-5. Plagioclase is ubiquitous in all units although its relative abundance varies among the units; it dominates in Units 1, 2, 4, 5A, 5B and 7 but is subordinate in the more potassic Units 3, 6, 8 and 9. The plagioclase in the mafic end members (tonalites and granodiorites) of Units 1, 4 and 7 and the trondhjemite dyke of Unit 2 is subhedral to anhedral and distinctly zoned (An 42-18); both normal and reverse zoning occur in any one sample (Fig. 3-8). In these units, plagioclase occurs in the matrix (grain size 0.5-2 mm) and occasionally as larger phenocrysts (grain size 2-6 mm).

Plagioclase in the more felsic end members of Units 4 and 7 and in the leucocratic Units 3, 6, 8 and 9 occurs mainly in the matrix and occasionally has a perthitic texture. Zoning is less distinct and

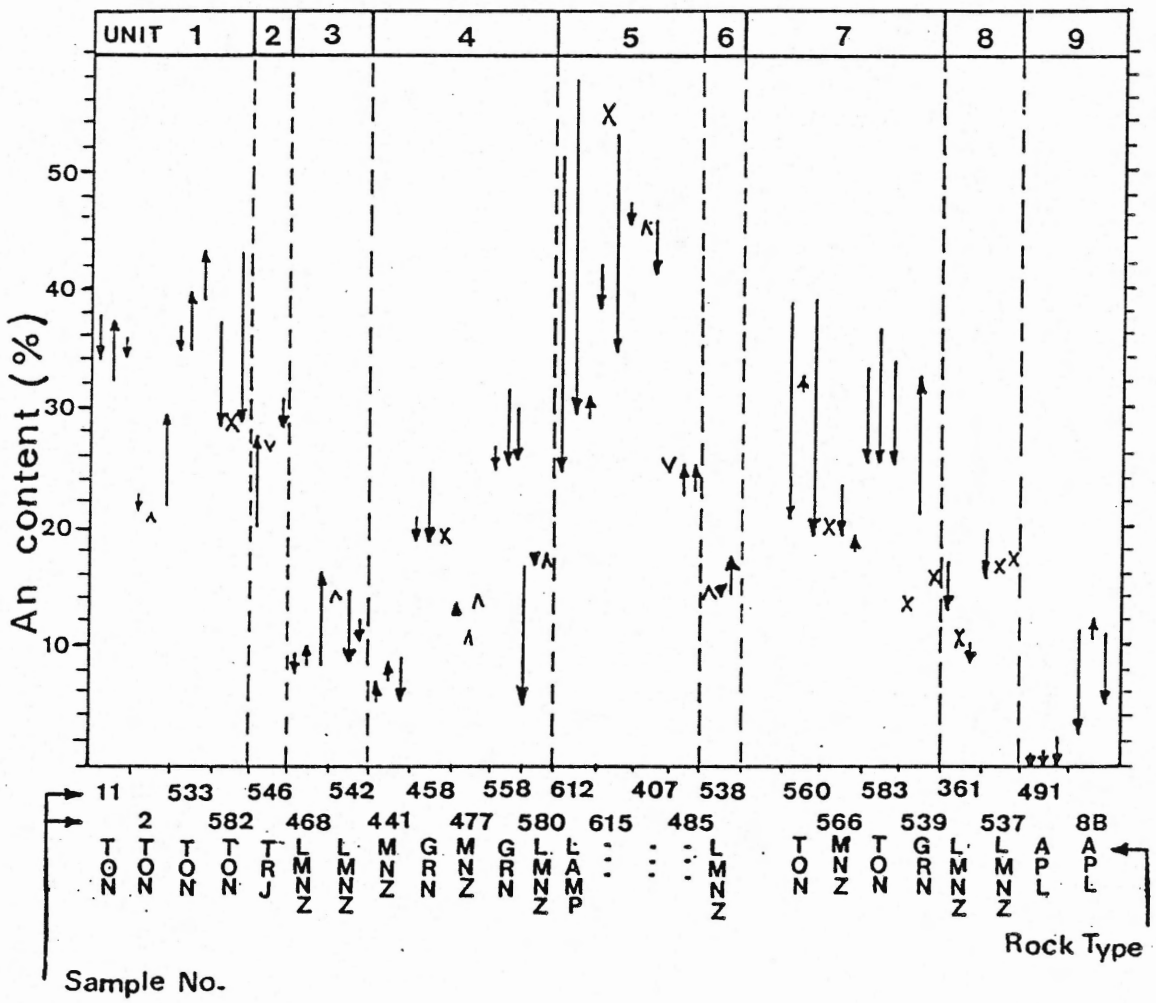

Figure 3-8: Anorthite composition of plagioclase from the PMP.
LEGEND:

TON=tonalite
TRJ=trondhjemite
L MNZ=leucomonzgranite
GRN=granodiorite
MNZ=monzogranite
LAMP=lamprophyre
APL=aplite
core=x
core ——————→ rim
rim= ∧

anorthite compositions are lower (An 9-23) than in the mafic end-member described above. Some plagioclase in Units 1, 2, 3, and 7 show reverse zonation.

Plagioclase in the lamprophyres is the most calcic within the pluton and is distinctly zoned from An 23-57 (cores) to An 25-35 (rims). In the Forbes Point lamprophyre, plagioclase occurs as subhedral phenocrysts and anhedral matrix, elements of which are more distinctly zoned and more calcic than plagioclase in the MacLeods Cove lamprophyre (Fig. 3-8).

The relatively low anorthite composition of the plagioclase in the MacLeods Cove lamprophyre (An 24), the lack of plagioclase phenocrysts, the reverse zoning observed in these grains and the foliation developed in the dyke by amphiboles suggest that the MacLeods Cove dyke has been altered relative to the Forbes Point dyke of the same relative age.

3-6-2 Discussion

The anorthite composition of the plagioclase in the granitic phases (tonalite, granodiorite and monzogranite) decreases with decreasing plagioclase abundance, and from mafic to felsic members within previously defined Cycles (i.e. a decrease from Unit 1 to Unit 3 = Cycle I; a decrease from Unit 7 to Units 8 and 9 = Cycle III). The anorthite composition of the plagioclase from the mafic granodiorite and tonalite end members of Units 1 is similar to Unit 7 (Fig. 3-8). The anorthite compositions of plagioclase in granodiorites from Units 1, 4 and 7 are similar (An 18-40) and cannot

be used to distinguish between granodiorite samples from different units (Fig. 3-8).

Considerable disequilibrium is evident by the reverse zonation of the plagioclase, particularly in Unit 1. Reversed zonation implies an introducton of heat possibly suggesting mixing of two melts of differing temperatures to produce Unit 1. Reversed zonation (although sporadic in abundance) is also apparent in Units 2, 3, 7. This may suggest that these units may also have involved hybridization of more than one melt.

The anorthite compositions of the plagioclase associated with the lamprophyres are distinct from the granitoid units.

CHAPTER 4 WHOLE-ROCK CHEMISTRY

4-1 Introduction

The whole-rock chemistry of fifty-one samples collected from the Port Mouton Pluton (Map # 2) is presented in this chapter. All samples were analysed for major elements (wt. %), and fourteen trace elements (all values in ppm) (Ba, Rb, Sr, Y, Zr, Nb, Th, Pb, Ga, Zn, Cu, Ni, V and Cr in ppm). Thirteen of these samples were analysed for ten rare earth elements (Ce, Nd, Sm, Eu, Gd, Tb, Yb, Lu, Hf and Ta in ppm)(Appendix C, D1-D3).

Major element and trace element analyses were obtained for samples from nine of the ten units mapped in the PMP. Unit 5B (the tonalitic breccia) was not analysed because of the difficulty in separating the matrix material from the clasts. The number of analyses per unit was intended to reflect the volume of that unit in the PMP. Twenty-two samples of Unit 4, ten samples of Unit 1, eight samples of Unit 7, three samples of the Unit 5A lamprophyres, three samples of Unit 8, two samples of Unit 9 and one sample from each of Units 2, 3 and 6 were analysed. Three samples each of Units 1 and 4, four samples of Unit 7, and one sample each of Units 3, 9 and 5A were analysed for REEs. The geochemistry is discussed in terms of the three mafic to felsic cycles (I, II and III) discussed in Chapter 2.

4-2 Major Elements

4-2-1 Granitoid Rocks

With the exception of the lamprophyre dyke rocks (section

4-2-2) the PMP is a peraluminous granitoid complex that ranges in SiO_2 content between 63 and 76 wt. %. All but one of the 49 granitoid samples analysed are alumina oversaturated. Average CIPW normative corundum contents of the three dominant phases of the pluton (Units 1, 4, and 7) are indistinguishable at 2.3%, 2.3% and 2.0% respectively (see Table D-1).

From the Harker diagrams (Fig. 4-1) and ternary CIPW plot (Fig. 4-2) the following generalizations about the whole-rock major chemistry of the PMP granitoid rocks can be made.

There is a roughly linear decrease in TiO_2, Al_2O_3, FeO_T, MgO and CaO with increasing SiO_2 within each mafic to felsic cycle (I to III). A similar trend exists among the more mafic Units from 1 to 7 to 4, but it is difficult to define distinct fields for the three mafic units because of their chemical overlap. There appears to be no linear relationship in MnO, Na_2O and P_2O_5 versus SiO_2 contents in the three predominant units (1, 4 and 7) making the distinction difficult between the three units on the basis of these elements. The K_2O contents of Units 1 and 7 are distinctly lower than those of Unit 4. Figure 4-2 illustrates that the three mafic end members of Cycles I, II and III plot in overlapping geochemical fields in the normative quartz, orthoclase and albite + anorthite space. Unit 1 contains higher normative albite and anorthite compared with Unit 4.

Units 3, 6 and 8 (the felsic end members of Cycles I, II and III) show close similarity in SiO_2, Al_2O_3, FeO(total), MnO, MgO, CaO, K_2O and P_2O_5 contents. There is considerable variation in Na_2O contents among Units 3, 6, 8 and 9. Unit 9 samples contain anomalously high

MnO contents and higher Al_2O_3 values than Units 3, 6 and 8. This is consistent with the abundant garnet observed in Unit 9 samples.

4-2-2 Lamprophyres

The lamprophyres from the PMP are shoshonitic and alkaline lamprophyres. Because their chemical signature is distinct from the granitoids they are discussed separately. 'Shoshonitic lamprophyres are porphyritic dyke rocks, richer in amphibole, biotite, ultramafic elements (Mg,Cr,Ni) and incompatible elements (K, F, P, Rb, Sr, Zn, Nb, Ba, REE, Th, U) than other rocks of comparable weight% SiO_2 (46-57)' (Rock, 1984, p.193). Unlike the peraluminous granitoid rocks of the PMP, the lamprophyres are alumina-undersaturated (A/CNK values of 0.7 (NPM485), 0.6 (NPM612) and 0.5(NPM615)), A/NK values range between 2 and 3.2, and they are not peralkaline.

The whole-rock, major element compositions of each of the two zones within the Forbes Point lamprophyre are significantly different from one another. The plagioclase porphyritic zone (NPM615) has higher SiO_2, Al_2O_3, MnO, CaO and NaO contents and lower FeO(total), MgO and K_2O values than the phlogopite-actinolite-rich lamprophyre (NPM612). The plagioclase porphyritic zone contains only minor phlogopite and is diopside and hypersthene normative. The phlogopite-actinolite zone contains abundant phlogopite (40%) and is olivine, hypersthene and hematite normative. According to the classification of Rock (1977) the phlogopite-actinolite zone (NPM612) is typical of shoshonitic lamprophyres which are often spatially associated with post-orogenic granites.

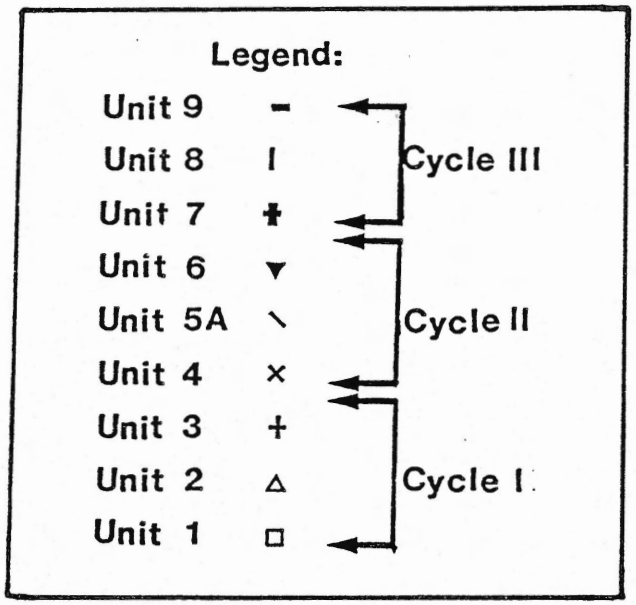

Table 4-1: Legend for the whole-rock geochemical plots in this chapter. Unit 1, 4 and 7 (dominant units volumetrically) are outlined by solid, dotted and dashed lines respectively.

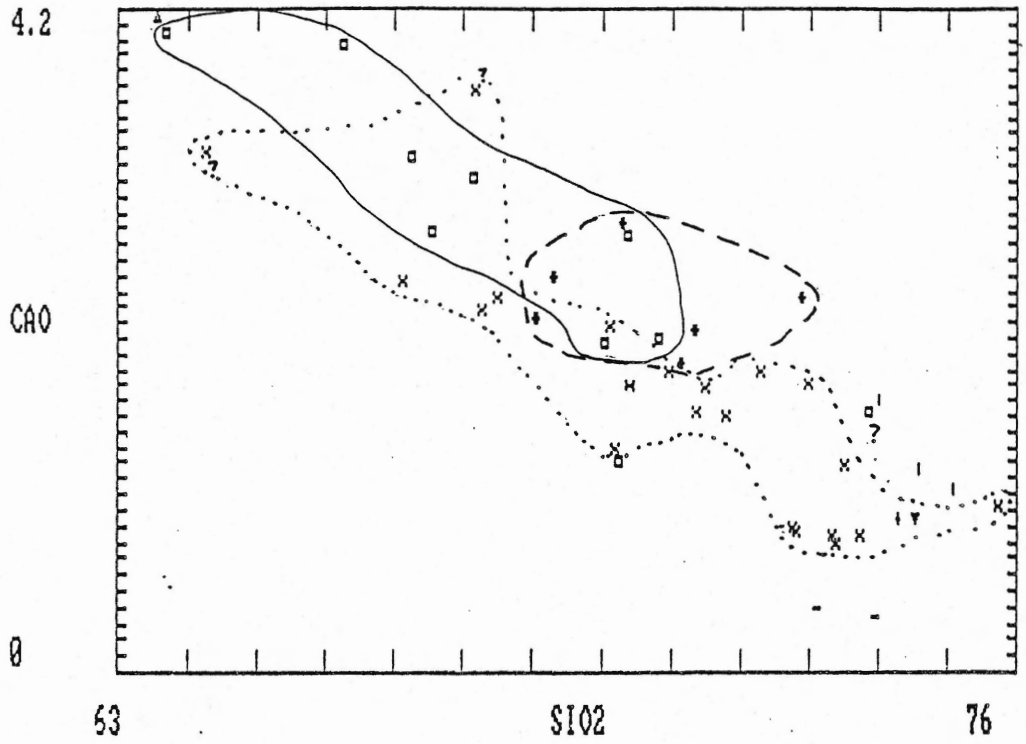

Figure 4-1a: Whole-rock chemistry of granitoid rocks: CaO (wt. %) compared with SiO_2 (wt. %) .

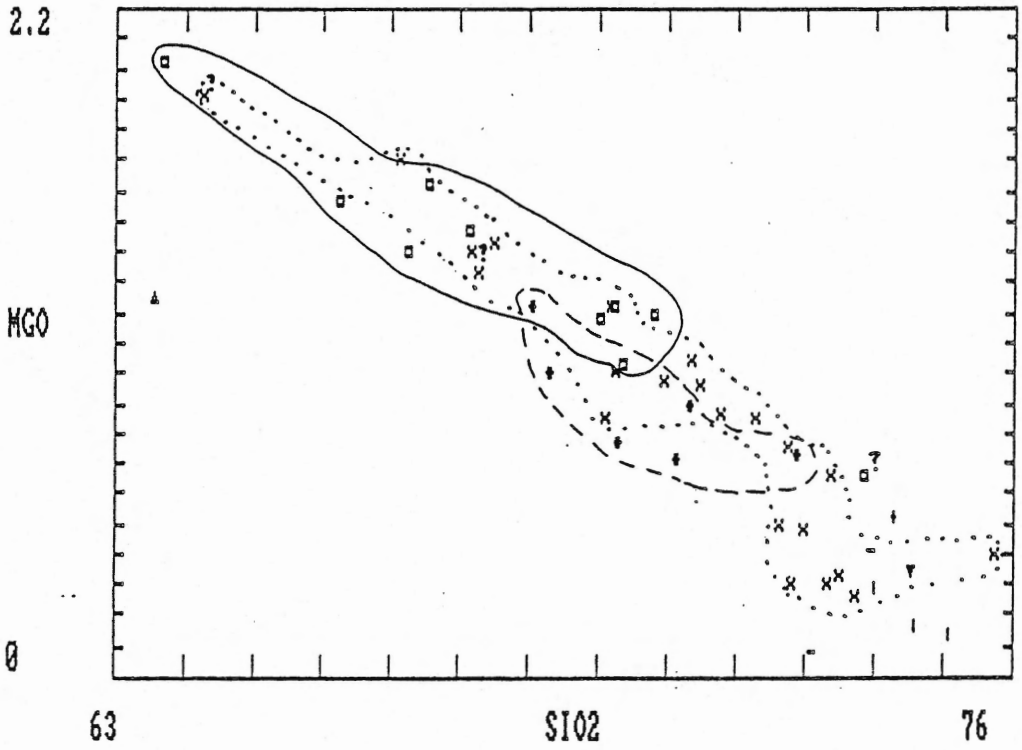

Figure 4-1b: Whole-rock chemistry of granitoid rocks: MgO(wt. %) compared with Si_2O (wt. %).

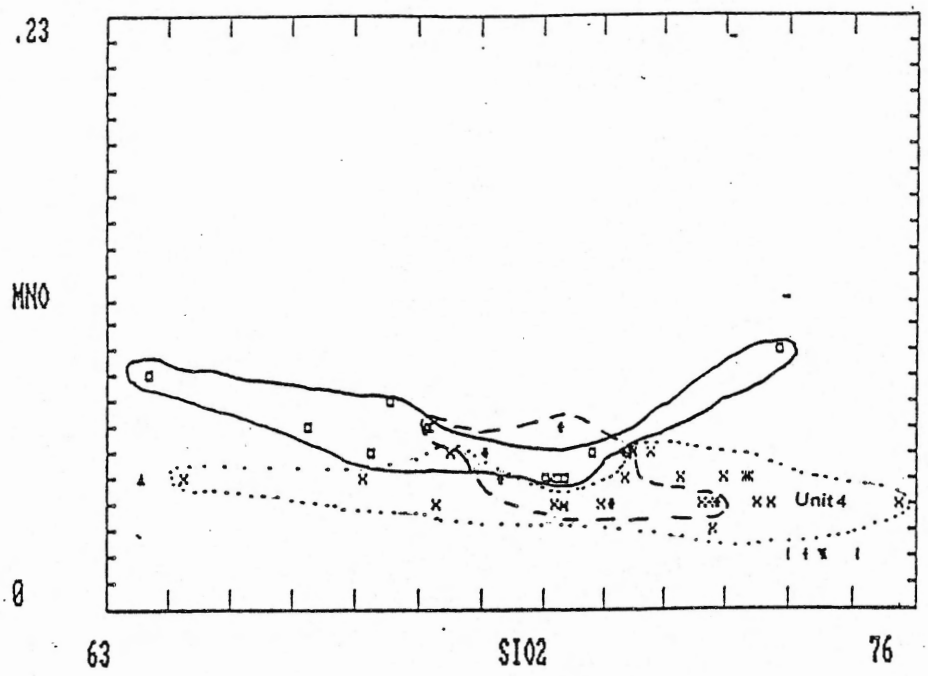

Figure 4-1c: Whole-rock chemistry of granitoid rocks: MnO (wt. %) compared with SiO_2 (wt. %).

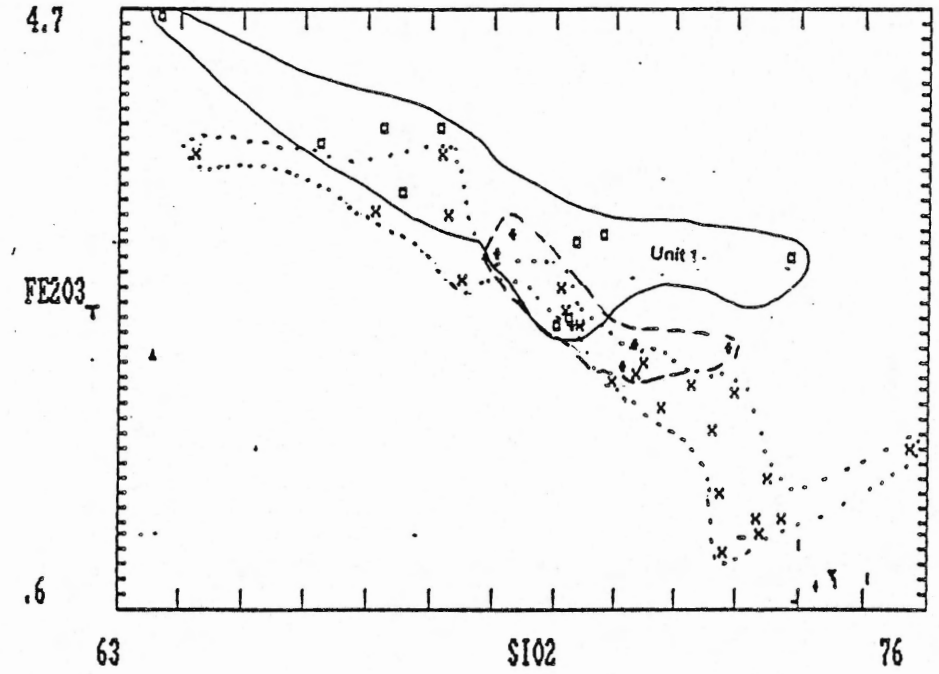

Figure 4-1d: Whole-rock chemistry of granitoid rocks: Fe_2O_{3T} (wt. %) compared with SiO_2 (wt. %).

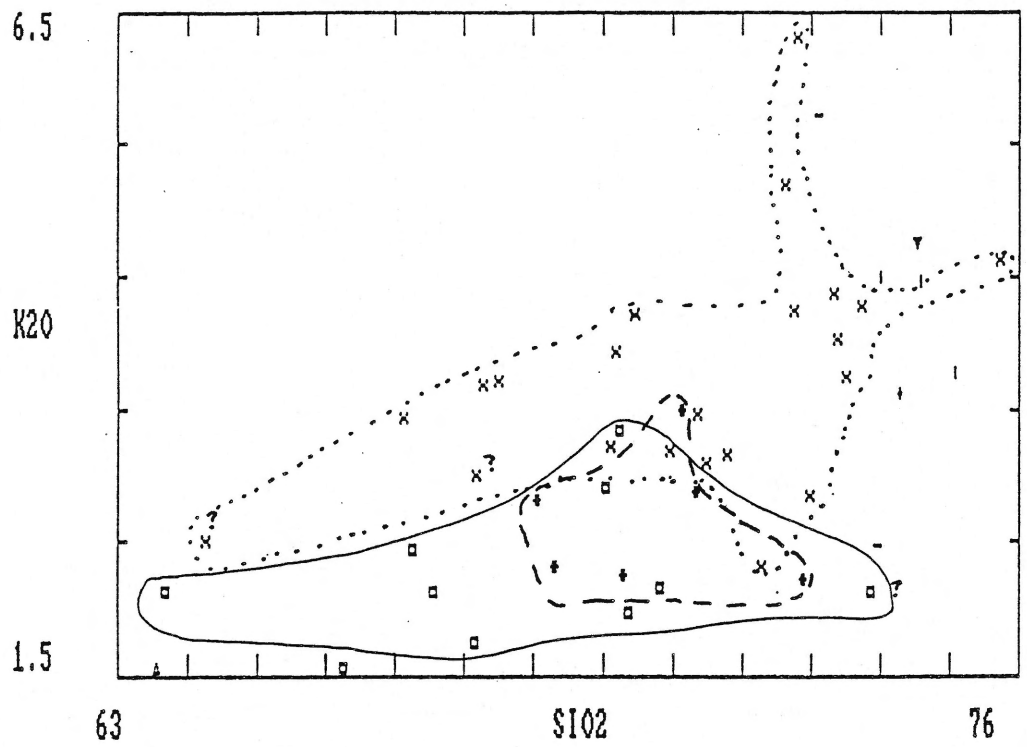

Figure 4-1e: Whole-rock chemistry of granitoid rocks: K_2O (wt. %) compared with SiO_2 (wt. %)

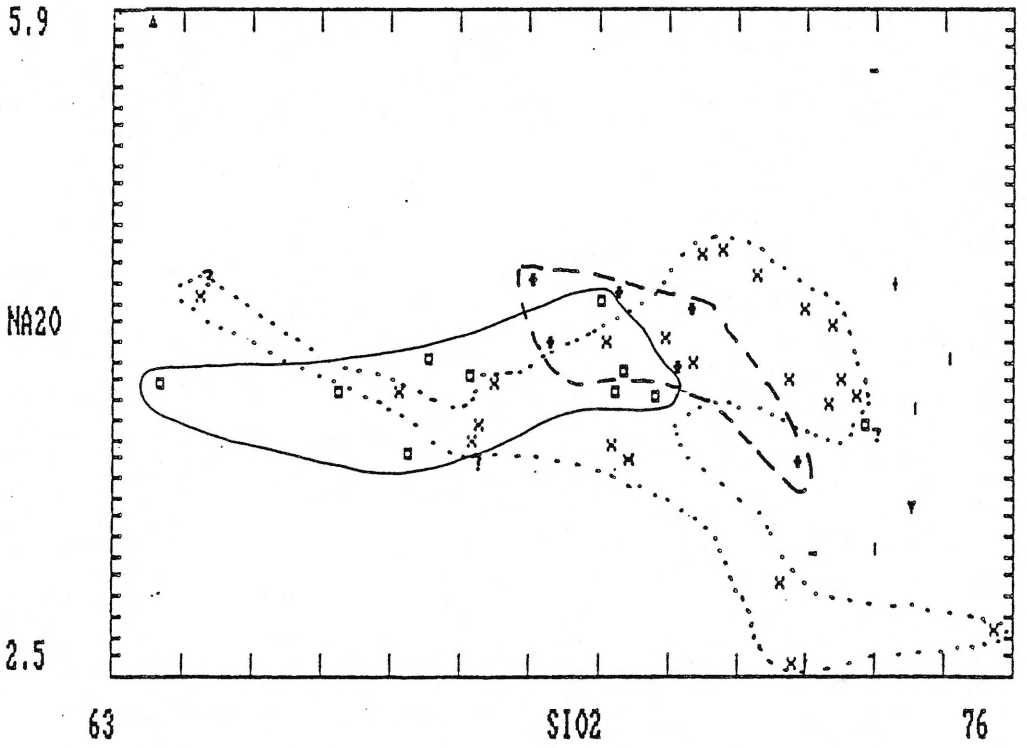

Figure 4-1f: Whole-rock chemistry of granitoid rocks: Na_2O (wt. %) compared with SiO_2 (wt. %).

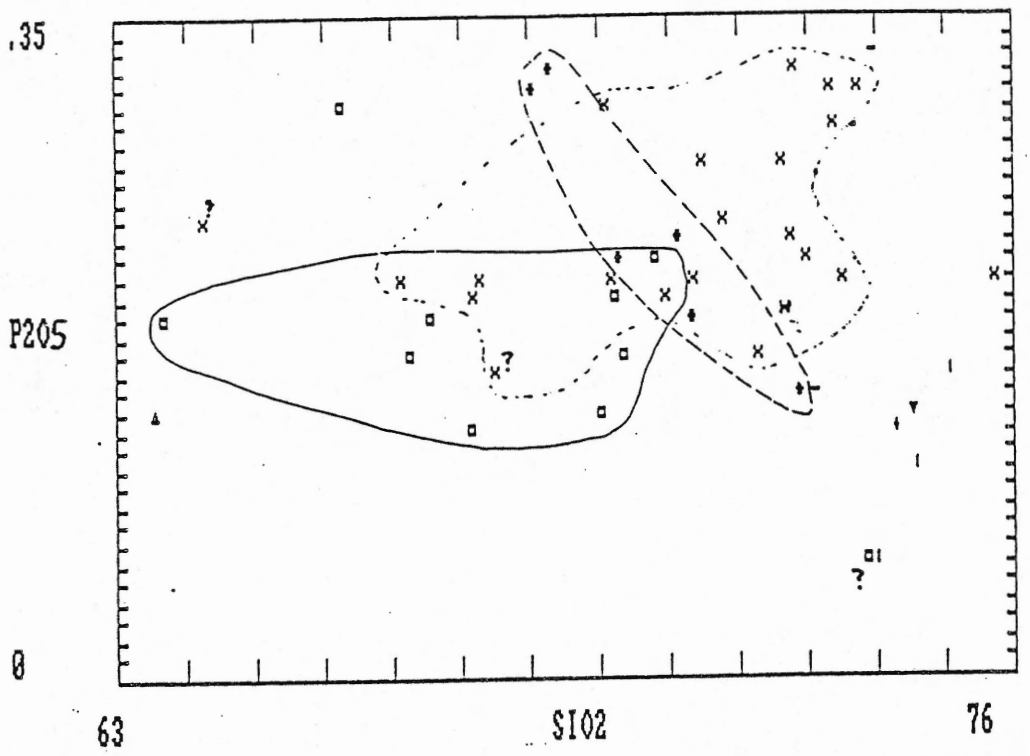

Figure 4-1g: Whole-rock chemistry of granitoid rocks: P_2O_5 (wt. %) compared with SiO_2 (wt. %).

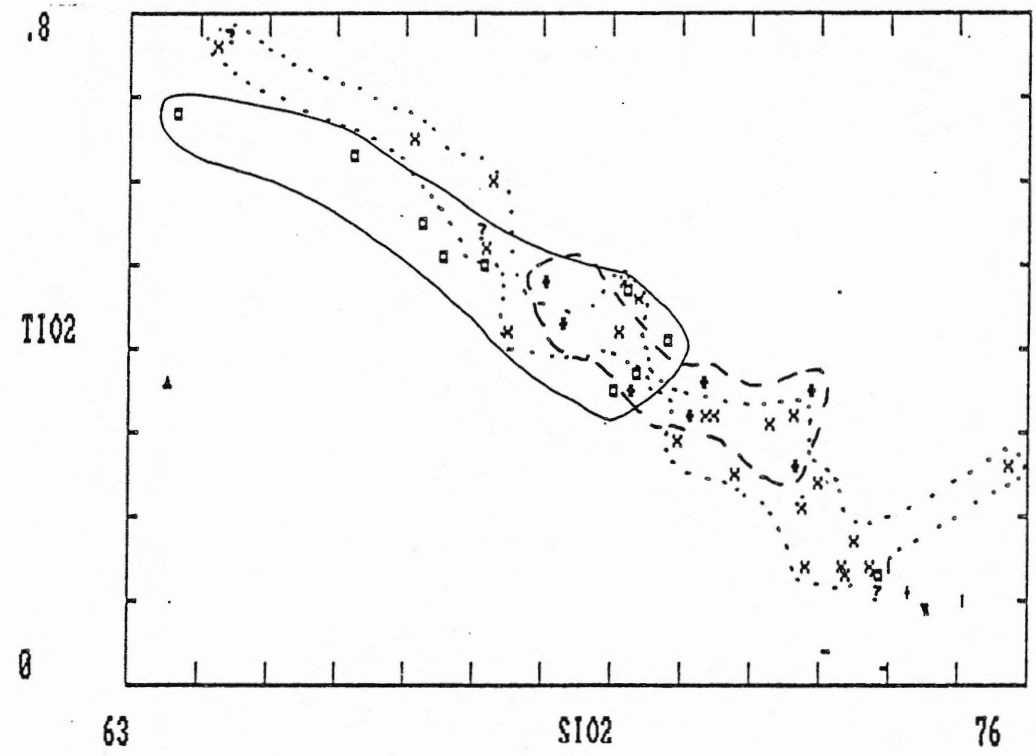

Figure 4-1h: Whole-rock chemistry of granitoid rocks: TiO_2 (wt. %) compared with SiO_2 (wt. %).

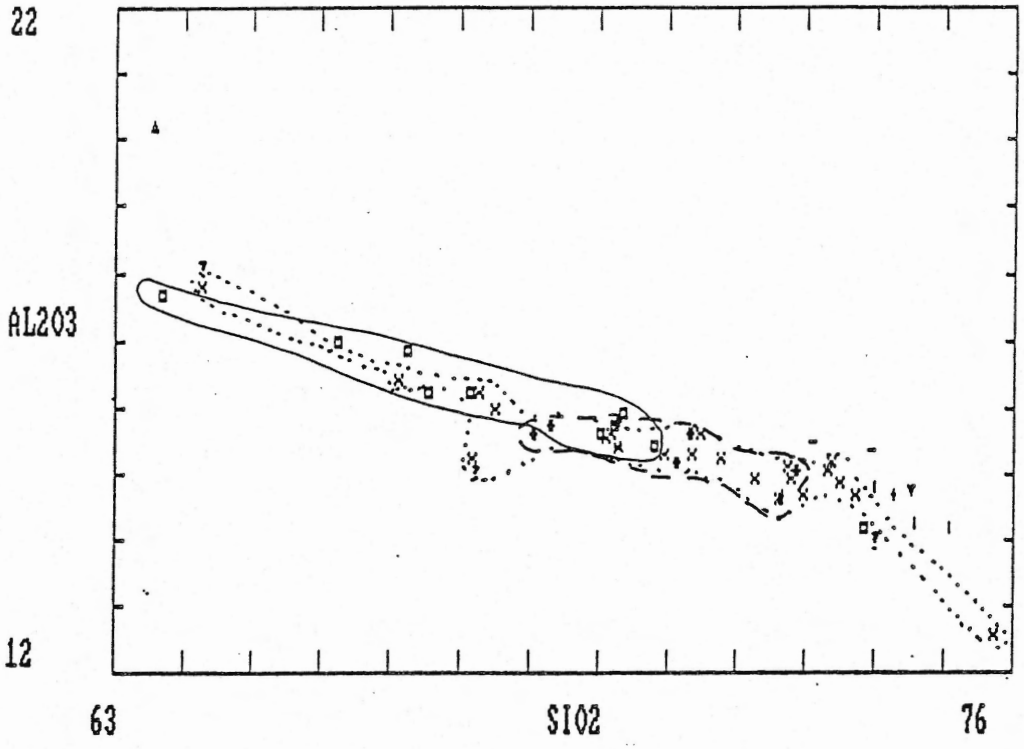

Figure 4-1i: Whole-rock chemistry of granitoid rocks: Al_2O_3 (wt. %) compared with SiO_2 (wt. %).

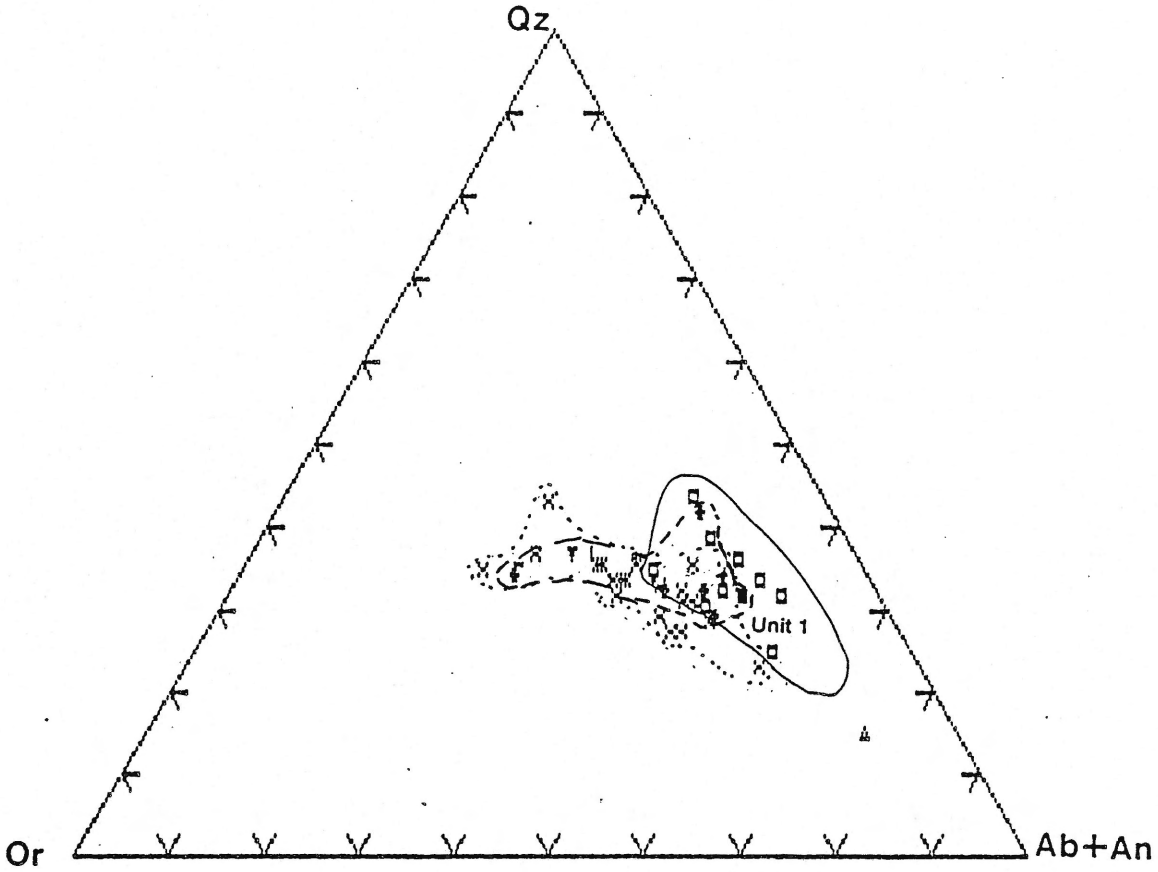

Figure 4-2: Whole-rock chemistry of granitoid rocks within the PMP: CIPW plot of normative quartz (Qz), orthoclase (Or) and albite and anorthite (Ab + An).

The plagioclase porphyritic lamprophyre (NPM615) is classified as an alkaline lamprophyre (Rock, 1977) and has a whole-rock, major element composition similar to a typical alkali basalt (Karlo, 1982) except that the total iron, Al_2O_3 and TiO_2 contents are slightly less in the lamprophyre (Fig. 4-3).

The MacLeods Cove lamprophyre (NPM485) is classified as a shoshonitic lamprophyre, and its normative composition is very similar to sample NPM612 of the Forbes Point lamprophyre (Fig. 4-3). The Forbes Point lamprophyre has lower SiO_2 and Al_2O_3 and higher FeO(total), MgO and CaO than the MacLeods Cove lamprophyre (NPM612).

The shoshonitic dykes at MacLeods Cove and Forbes Point have lower Al_2O_3, Na_2O and significantly higher MgO (12-15 wt. %) compared with 'typical' shoshonitc lamprophyres (6-6.3 wt. % MgO) defined by Metais and Chayes (1962). In comparison with the mafic granitoids rocks of the PMP (tonalite NPM533), the three lamprophyre samples from the PMP have sigificantly greater concentrations of FeO(total), MgO, CaO, K_2O (except NPM615), P_2O_5, TiO_2, MnO and lower Al_2O_3, Na_2O, SiO_2 contents. A plot of (Na_2O+K_2O) versus SiO_2 (Fig. 4-4) illustrates the differences in concentration of these elements in the PMP granitoids and the PMP lamprophyres.

4-3 Trace Elements

4-3-1 Introduction

The geochemical behaviour of fourteen trace elements is summarized for the Port Mouton Pluton samples. The chemistry of the lamprophyre dykes is described separately from the granitic samples

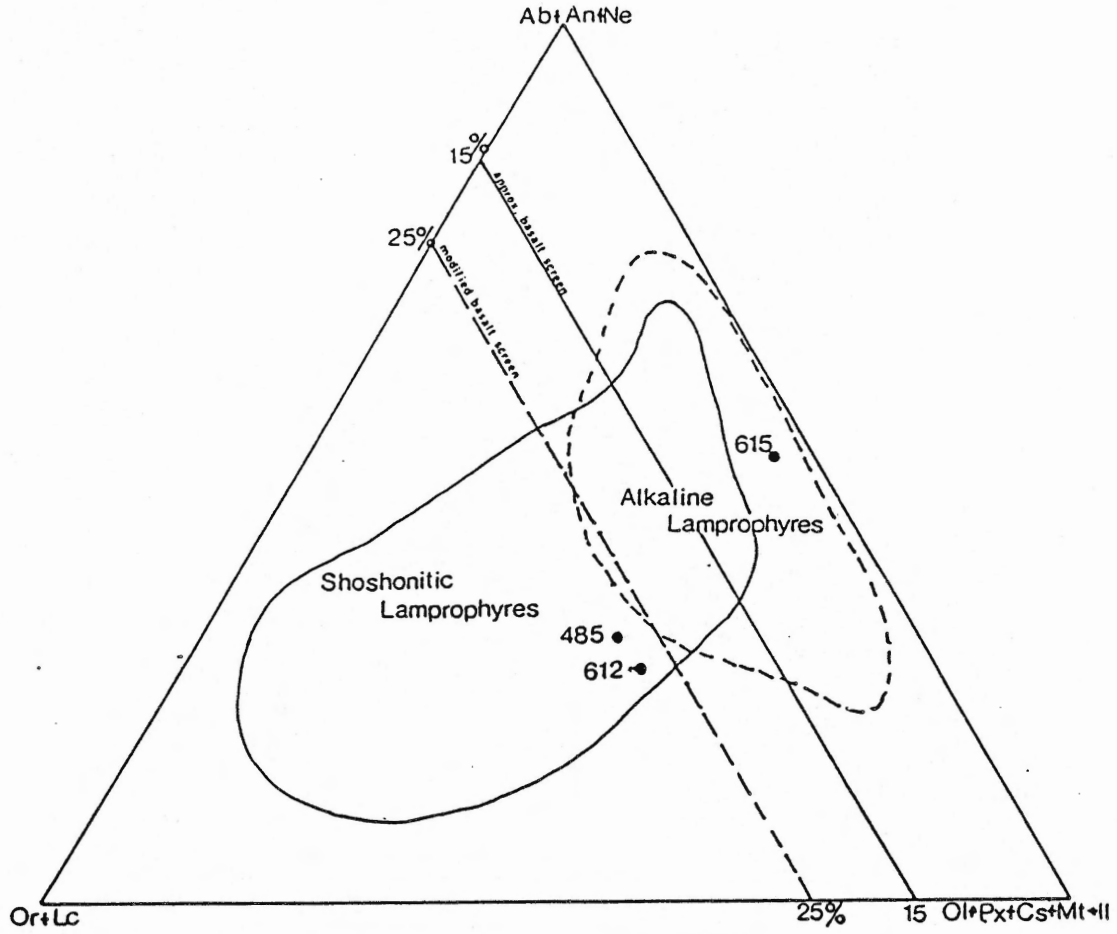

Figure 4-3: CIPW triangular plot, defining the zones of shoshonitic and alkaline lamprophyre composition (after Rock, 1977). The approximate basalt screen from 0 to 15% is after Manson (1967) and the modified basalt screen from 0 to 25% is after Rock (1977).

485= NPM485, shoshonitic lamprophyre MacLeods Cove
612= NPM612, " " of Forbes Point
615= NPM615, alkaline lamprophyre of Forbes Point

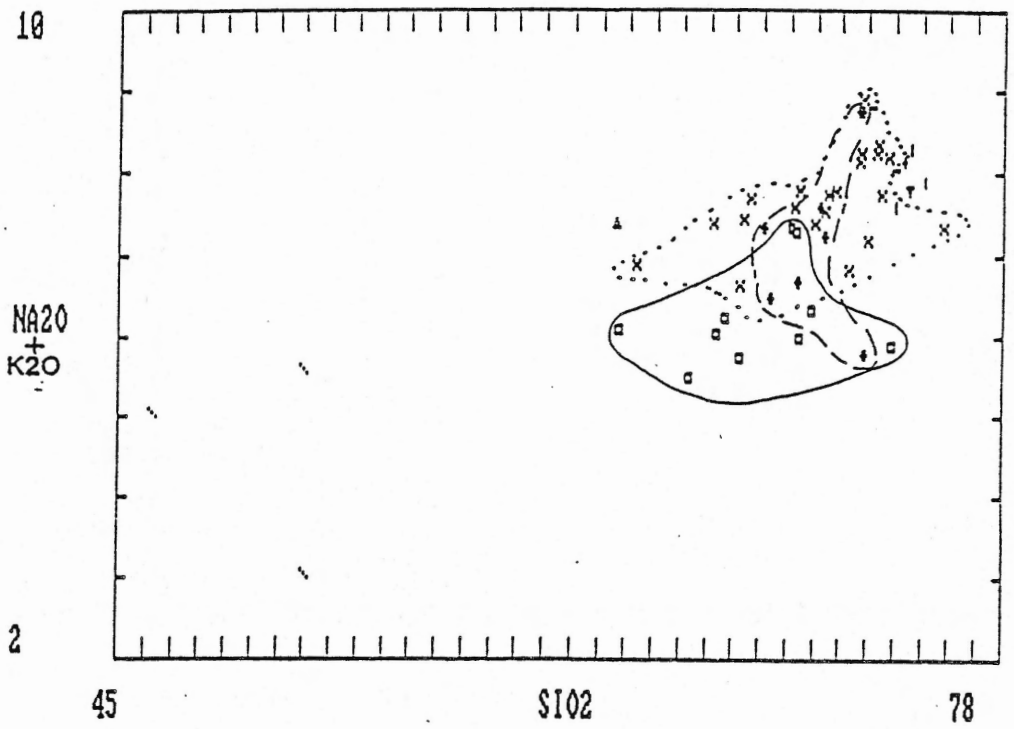

Figure 4-4: Whole-rock chemistry Na_2O+K_2O (wt. %) versus SiO_2 (wt. %) of the PMP granites and lamprophyres. Symbols as in Table 4-1.

because of the extreme variation in trace element contents.

Alkali Metals

4-3-2 Rubidium

The geochemistry of Rb is dominated by its extensive diadochic relation with K, and for this reason Rb is usually discussed with respect to K (Reynolds, 1972). Important Rb carriers in igneous rocks are muscovite and biotite, which commonly contain several thousand ppm Rb (Reynolds, 1972). Igneous differentiation causes a slight relative enrichment of Rb and a decrease in the K /Rb ratio (Mason, 1982).

Rubidium in the PMP granitoids displays a progressive enrichment (in mean values for each unit) from Units 1 to 4, although there is some overlap in values. Unit 4 has a higher Rb content than Unit 1. Unit 7 has average Rb values intermediate between Unit 1 and 4 (Fig. 4-5). The K/Rb plot of Figure 4-5 indicates that there is a moderately well-defined, progressive decrease in the K/Rb ratio with decreasing age among Units 1, 4 and 7. The K/Rb ratios start at magmatic values (Unit 1) of approximately 250, and drop to values of less than 155. The low values may indicate fluid involvement (excess Rb and therefore low K/Rb values) for Unit 1, 4 and 7. This is similar to the decrease noted by MacDonald (1981) in the Musquodoboit Batholith samples.

Alkaline Earth Metals

4-3-3 Strontium

Strontium is admitted to the lattice of Ca minerals or captured

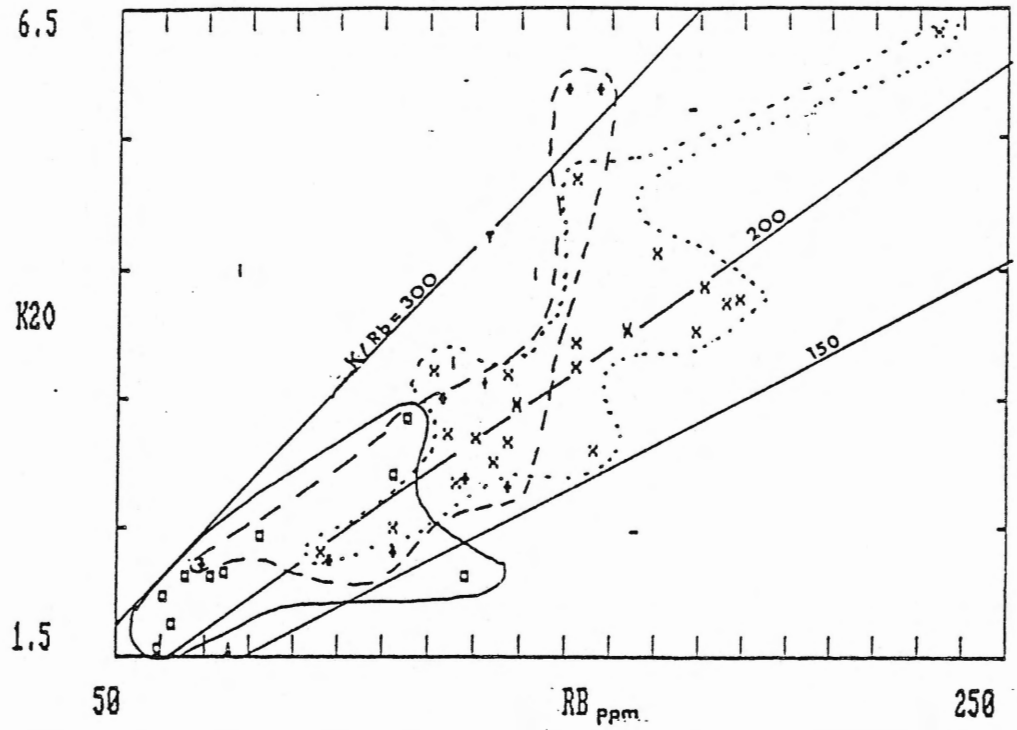

Figure 4-5: Whole-rock analyses of granitoid rocks- K_2O (wt.%) compared with Rb (ppm).

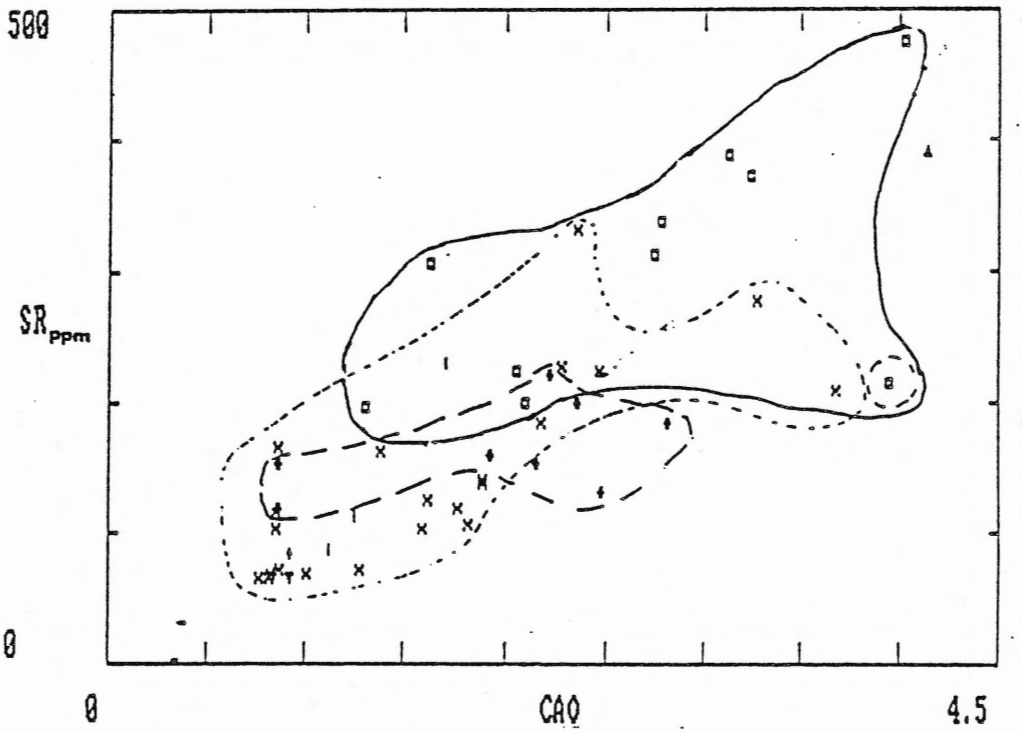

Figure 4-6: Whole-rock analyses of granitoid rocks- Sr (ppm) compared with CaO (wt. %).

by K minerals (Mason, 1982). The concentration of Sr is highest in calcium-rich minerals and, to a lesser extent, in K-rich minerals. The average concentration of Sr is 282 ppm in granitic rocks and 465 ppm in basaltic rocks (Turekian, 1956). Plagioclase and potash feldspar are Sr-enriched, relative to the silicate melt. Strontium concentration in the silicate melt decreases as crystallization proceeds (Mason, 1982). Pegmatites and aplites are usually depleted compared with granites (Faure, 1970).

Strontium increases with CaO content in PMP granitoid (Fig. 4-6). In the PMP granitoids there is an overall increase in Sr with an increase in CaO (Fig. 4-6). There is a wide scatter in the data and considerable overlap in the fields of Units 1, 4 and 7, although Unit 1 shows higher Sr/CaO ratios than Unit 4 (Fig. 4-6). The felsic units, 3, 6 and 9 have relatively low Sr and CaO concentrations compared with Units 1, 2, 4 and 7.

4-3-4 Barium

Barium occurs as a divalent cation which, in terms of overall geochemistry, closely resembles Sr. Barium is able to substitute for K^+ due to their similar ionic radii (1.35 A^o and 1.33 A^o, respectively)(Pilkey, 1972). Barium is often enriched in early-formed potassium minerals, and occurs in orthoclase, muscovite and biotite. Portions of a granitic magma that crystallize first are commonly enriched in Ba (Puchelt, 1978). Orthoclase from the late-stage pegmatite rocks is typically depleted in Ba. In general, felsic igneous rocks contain more Ba than basic rocks because of the

relatively higher abundance of orthoclase in the felsic rocks (Pilkey, 1972).

Figure 4-7 illustrates the relationship of Rb and Ba in samples from the PMP. There is no linear correlation between these elements. A plot of Ba, Sr and Rb (Fig. 4-8) illustrates that the PMP granitoids are preferentially enriched in Ba (except Unit 2 and 9) with respect to Sr and Rb, and that a distinction can be made between Units 1 and 4. Unit 7 is intermediate to Units 1 and 4 in this plot. Unit 9 samples plot with the strongly differentiated granites.

Group IIIB Metals

4-3-5 Yttrium

Yttrium content in the PMP granitoid rocks is not a useful discriminator between Units 1, 4, 7, 8 and 9 (Fig. 4-9). Plots of SUMREE/Y, Ce/Y and Y/Yb are equally uninformative as the units do not define distinct geochemical domains. Note that the trace element plots are plotted against the differentiation index (DI) because of the better resolution (distribution) of the points. Differentiation index is a better discriminator than SiO_2.

4-3-6 Zirconium

Group IVB Metals

Zirconium does not occur in the main rock-forming minerals because of its high oxidation state (4+), (McNally, 1972). Zirconium is found principally in the mineral zircon. Zirconium is concentrated in residual magmas resulting from fractional crystallization. This

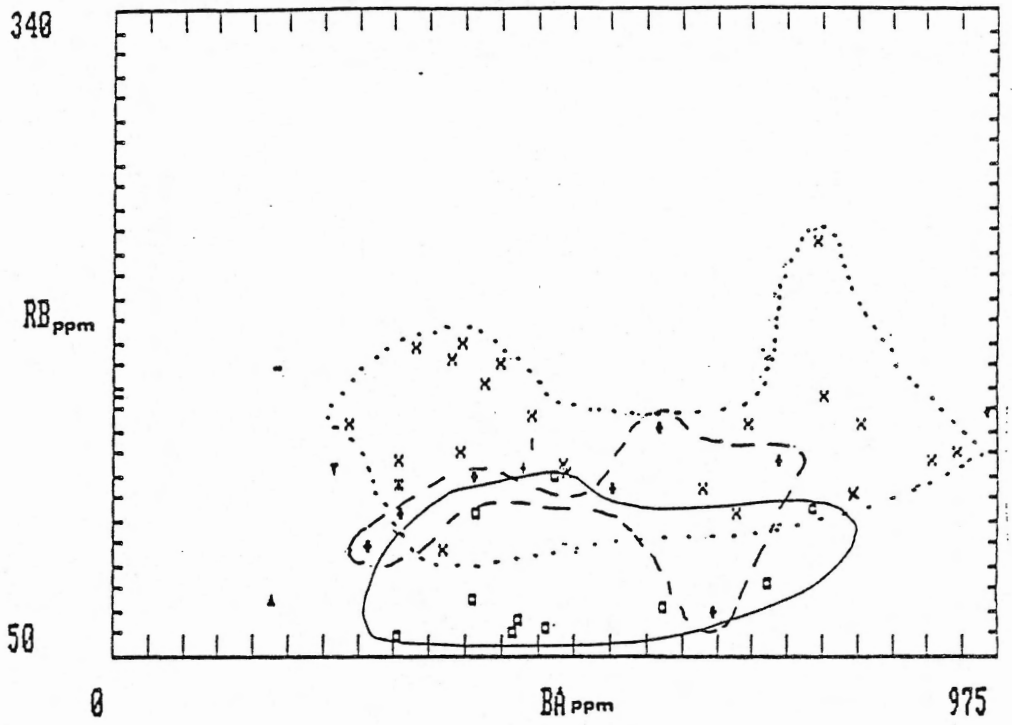

Figure 4-7: Whole-rock analyses of granitoid rocks. Rb (ppm) versus Ba (ppm)

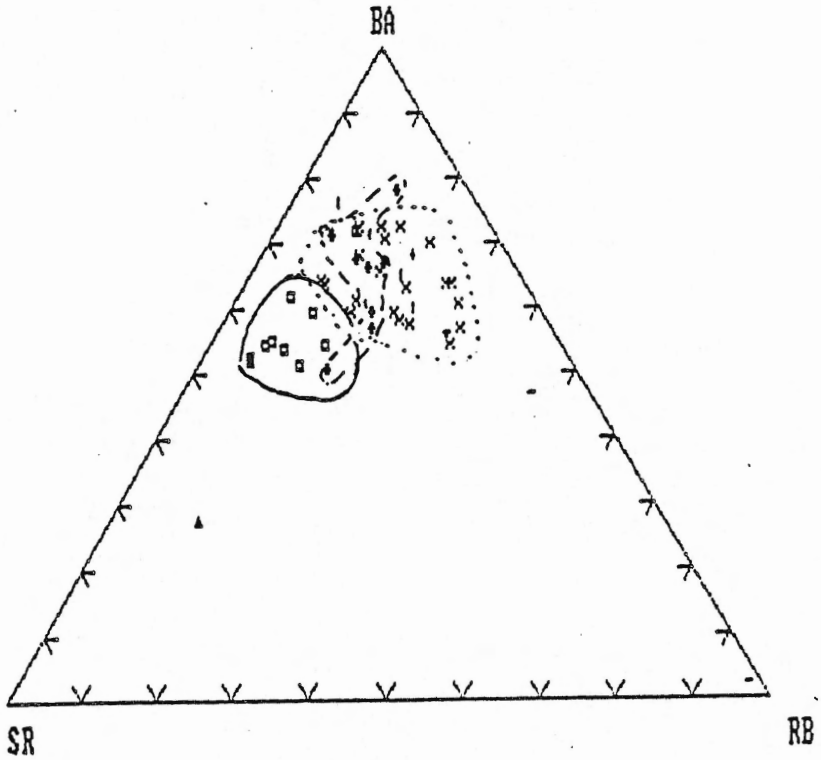

Figure 4-8: Whole-rock analyses of granitoid rocks. Sr (ppm) versus Ba (ppm) versus Rb (ppm).

may be especially true in the case of residual magmas with a high concentration of alkali minerals (McNally, 1972).

There is a poorly-developed correlation between Zr and TiO_2 in the PMP samples (Fig. 4-10). The felsic units, 3, 6, 8 and 9, exhibit similar Zr concentrations that are lower than their respective mafic precursors (Units 1, 4 and 7). The Zr contents of Unit 4 and Unit 7 are slightly higher than Unit 1 (Fig. 4-10).

Group VB Metal

4-3-7 Vanadium

Vanadium occurs with valences of $2^+, 3^+, 4^+$ and 5^+. V^{3+} (ionic radius=0.64-0.74 A^o) substitutes for Fe^{3+} in minerals of magmatic origin such as pyroxenes, amphiboles and biotites. The concentration of V in basaltic rocks is 250 ppm compared with 88 and 44 ppm in the Ca-rich and Ca-poor granites respectively (Burkart-Baumann, 1972).

Figure 4-11 is a plot of V (in ppm) and the TT-DI of the PMP granitoid samples. There is a moderately well-defined linear inverse relationship between V and TT-DI (Thornton-Tuttle differentiation index). The linear correlation becomes more diffuse at high V and low TT-DI values. The V content of Unit 4 samples is lower than those of Unit 1, and Unit 7 has average V values intermediate between those of Units 1 and 4.

Group VB Metal

4-3-8 Niobium

Naturally-occurring Nb exists only in the form Nb^{5+} and has an

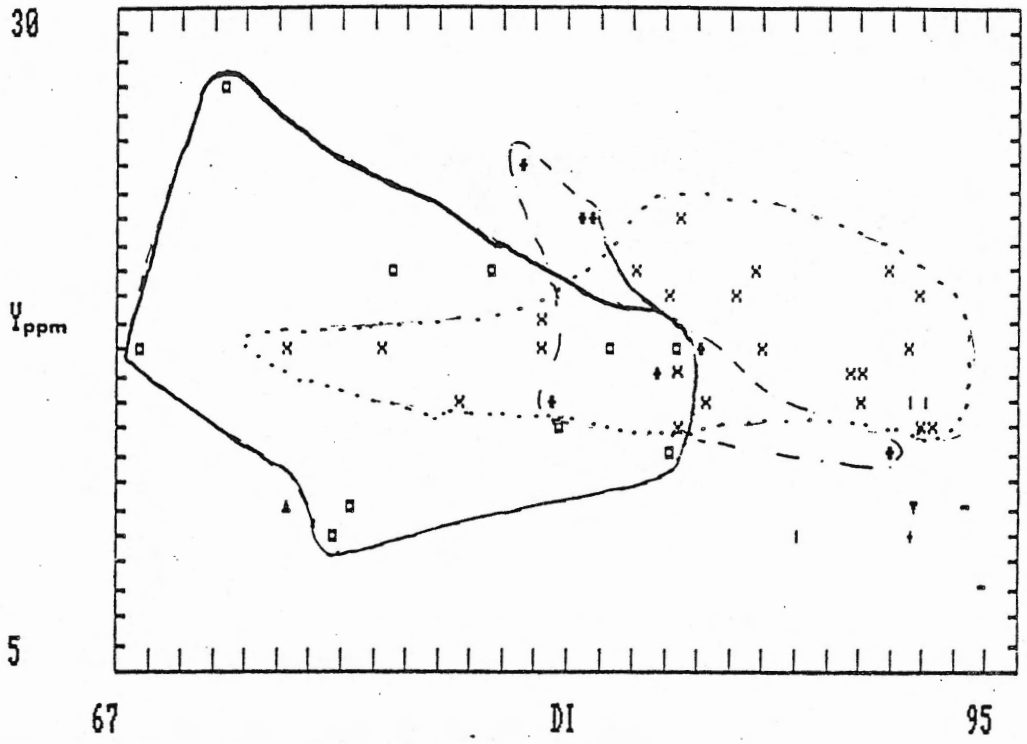

Figure 4-9: Whole-rock analyses of granitoid rocks. Y(ppm) versus Thornton-Tuttle differentiation index.

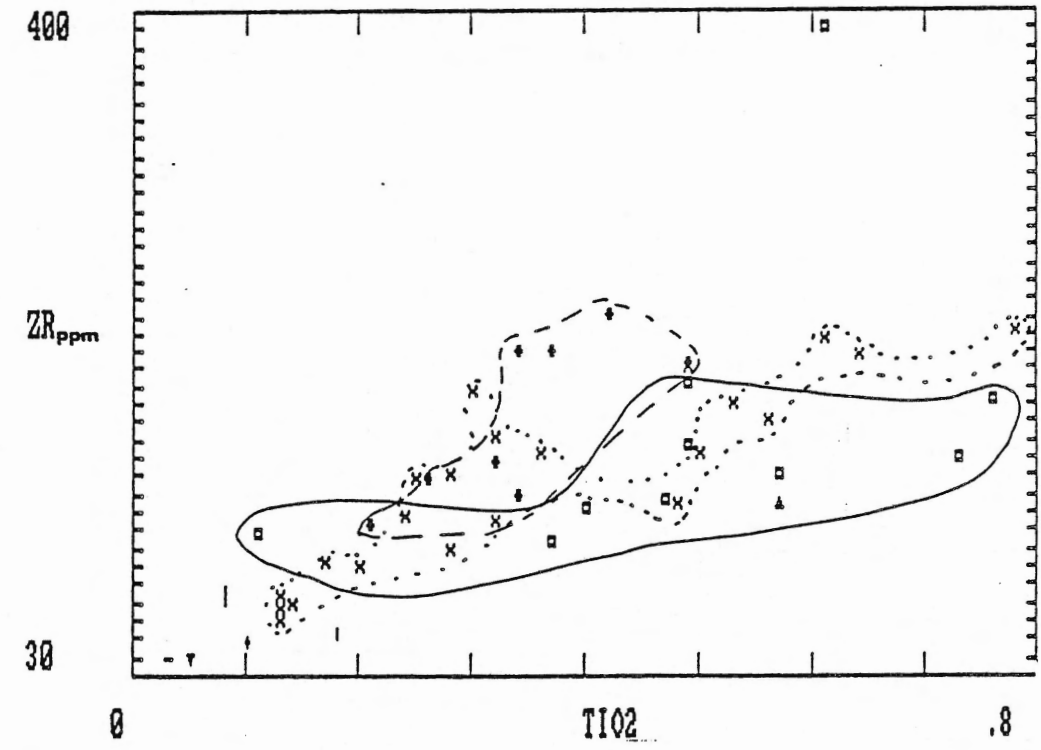

Figure 4-10: Whole-rock analyses of granitoid rocks. Zr (ppm) versus TiO_2 (wt. %).

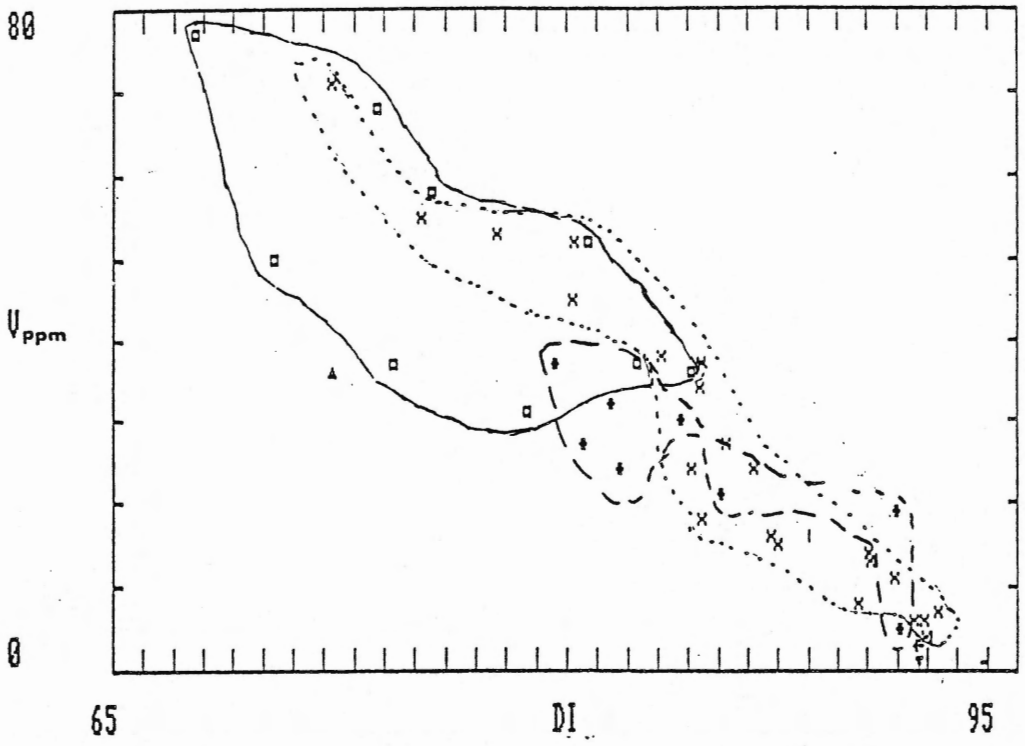

Figure 4-11: Whole-rock analyses of granitoid rocks. V (ppm) versus Thornton-Tuttle differentiation index.

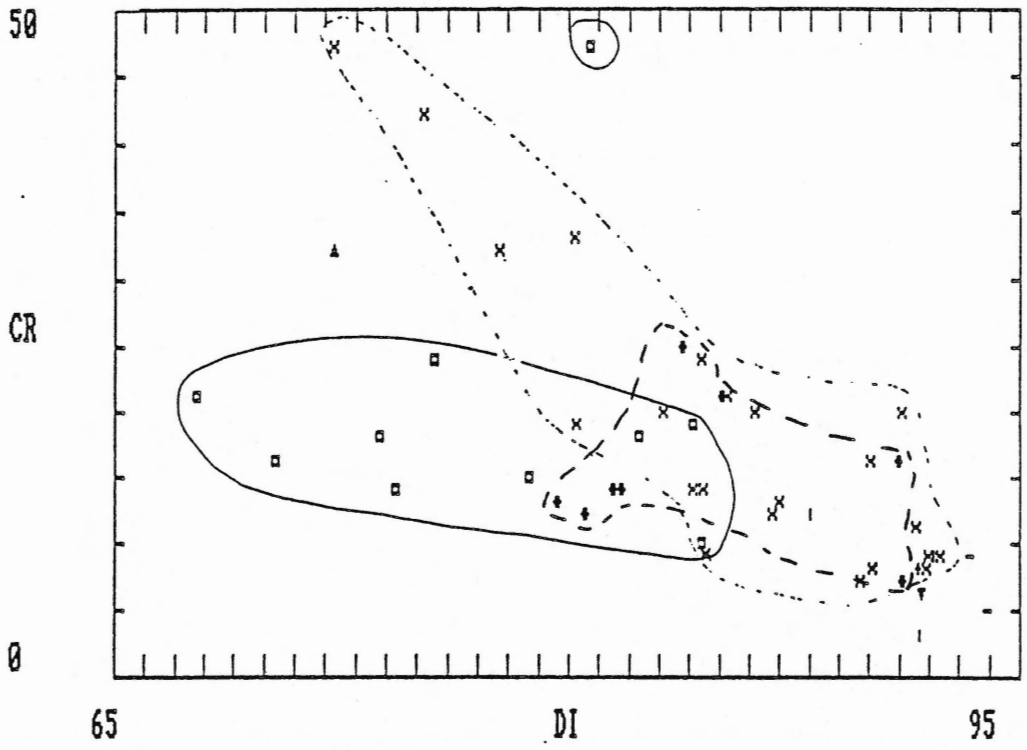

Figure 4-12: Whole-rock analyses of granitoid rocks. Cr (ppm) versus Thornton-Tuttle differentiation index.

ionic radius of 0.69 A°. It is found substituting for Ti (Ti^{4+} radius=0.64 A°) in Ti-bearing minerals such as ilmenite, rutile and sphene. Niobium will also substitute for Zr in zircon. Niobium becomes concentrated in the later stages of magmatic crystallization in granitic pegmatites (Gornitz, 1972).

Niobium has no correlation with the TT-DI in the PMP samples.

Group VIB metal

4-3-9 Chromium

In nature, chromium occurs principally as the trivalent ion, Cr^{3+} (ionic radius=0.64 A°). It readily substitutes for Fe^{3+} (0.67 A°) andA°1^{3+} (0.56 A°) during crystallization. Typically Cr is precipitated from a magma at an early stage in its evolutionary history, either in chromium spinel or in silicate minerals, particularly clinopyroxene (Smith, 1972).

Chromium displays a negative correlation with the TT-DI (Fig. 4-12).

Group VIII Metal

4-3-10 Nickel

No correlation between Ni concentrations and the TT-DI is apparent. The concentration of Ni in all units ranges from 2 ppm (NPM584-Unit 1) to 18 ppm (NPM580-Unit 4).

Group IB metal

4-3-11 Copper

No detectable Cu in samples from the felsic zones (Units 3,6,8 and 9) of the PMP (Fig. 4-13). There is considerable overlap in the Cu values for Units 1, 2, 4 and 7 which range from 1 to 10 ppm. Two Unit 1 samples, NPM11 and NPM582, show anomously high Cu values of 16 and 19 ppm respectively.

Group 11B Metal

4-3-12 Zinc

The concentration of Zn does not appear to have a strong correlation with TT-DI in the PMP (Fig. 4-14). The leucomonzo-granite-leucotonalite zones of Units 3, 6, 8 and 9 have the lowest Zn concentrations (at 17 to 43 ppm).

Group IIIA Metal

4-3-13 Gallium

Ga appears to have no correlation with the TT-DI in the PMP samples. The range in Ga concentration varies from 14 to 26 ppm.

Group IVA Metal

4-3-14 Lead

The occurrence of Pb in magmatic rocks is governed primarily by its relationship to potassium. Divalent lead has an ionic radius of 1.2 A^{o}, slightly smaller than that of K (1.33 A^{o}). Lead substitutes for K in micas and potassium feldspars, and may to a smaller degree,

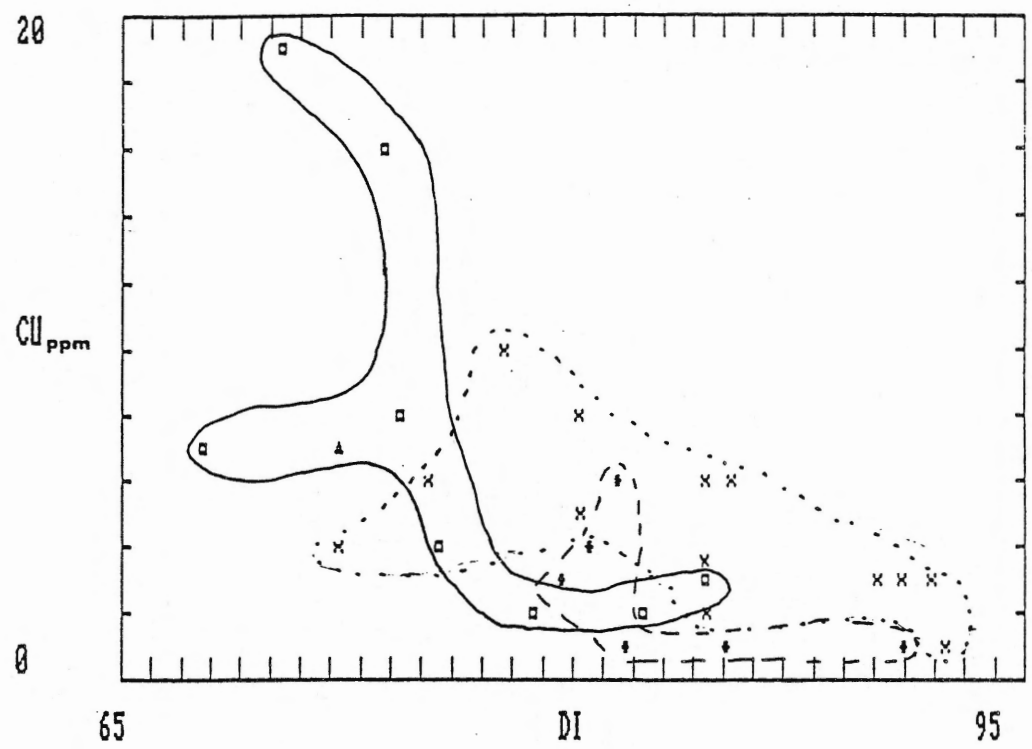

Figure 4-13: Whole-rock analyses of granitoid rocks. Cu (ppm) versus Thornton-Tuttle differentiation index.

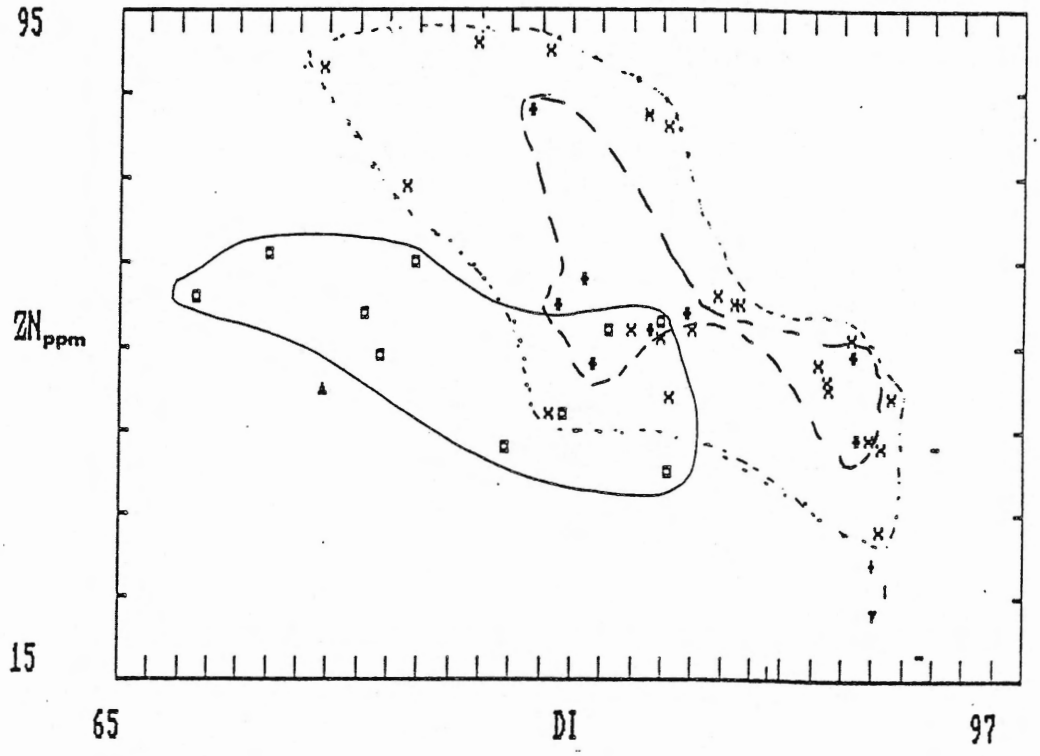

Figure 4-14: Whole-rock analyses of granitoid rocks. Zn (ppm) versus Thornton-Tuttle differentiation index.

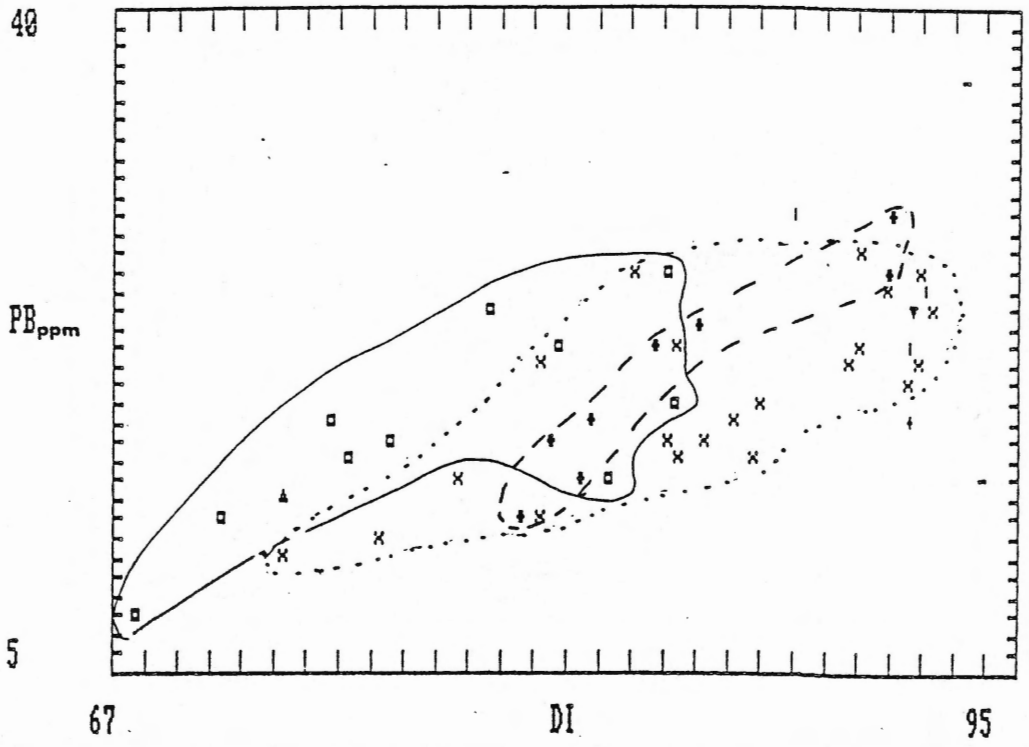

Figure 4-15: Whole-rock analyses of granitoid rocks. Pb (ppm) versus Thornton-Tuttle differentiation index.

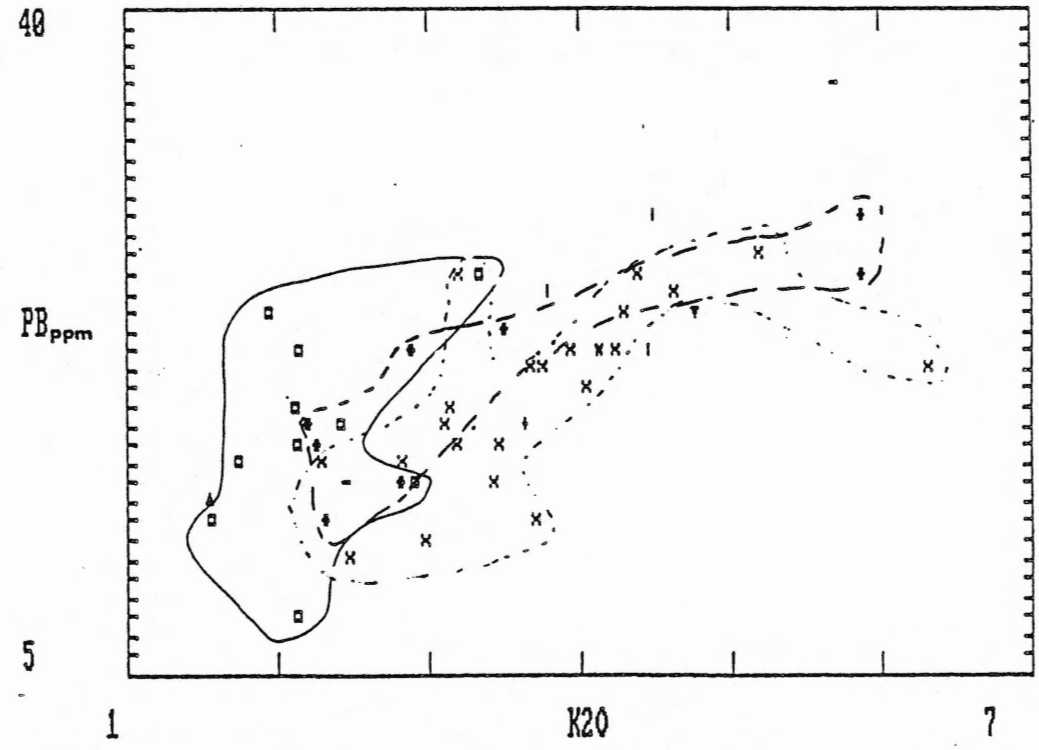

Figure 4-16: Whole-rock analyses of granitoid rocks. Pb (ppm) versus K_2O (wt. %).

substitute for Ca^{+2} (0.99A) in plagioclase, amphiboles and pyroxenes. Of the common types of igneous rocks, granites contain the highest abundance of Pb at 20 ppm (Wampler, 1972).

There is a weak positive correlation between Pb and the TT-DI for the PMP samples (Fig. 4-15). Figure 4-16 illustrates a positive correlation between Pb and K_2O. Unit 1 has a higher Pb/K_2O ratio than Unit 4. Unit 7 has Pb/K_2O ratios intermediate between Units 1 and 4.

Actinide Series

4-3-15 Thorium

Thorium occurs as a quadrivalent ion with a radius of 0.99 A^o. It is concentrated in the late stages of magmatic crystallization (Moore and Swami, 1972) where it substitutes for REEs in monazite, Zr in zircon, and Ca in apatite and sphene. Uranium follows a similar path during crystallization of magmas. Late-stage Th concentration did not occur in the SMB of Nova Scotia (see Chatterjee and Muecke, 1982).

The felsic units 2, 3, 6, 8 and 9 have Th concentrations less than 10 ppm. Unit 7 contains between 0 and 14 ppm Th. Units 1 and 4 show the greatest variations in Th, ranging from 0-44 ppm.

4-3-16 Lamprophyres

The two PMP lamprophyre dykes (three samples) exhibit trace element compositions, relative to the granitic bodies of the PMP. The two shoshonitic lamprophyres (NPM612 and NPM485) have higher concentrations of Ba, Cu, Ni and lower concentrations of V and Cr than the alkaline lamprophyre (NPM615).

The shoshonitic dykes have dissimilar trace element chemistry. The MacLeods Cove lamprophyre has significantly higher Sr (at 2567 vs 420 ppm), Zr (at 421 vs 135 ppm), Nb (at 30 vs 12 ppm) and Cr (957 vs 551 ppm) and lower Ba (1311, 1920 ppm) and Ni (79,194 ppm) than the Forbes Point dyke. The alkaline zone of the Forbes Point dyke shows significantly lower Ba, Rb, Cu and Ni values than the shoshonitic zone. The alkaline zone is significantly higher in Sr, Zr, Nb, Zn, V, Cr and Y than the shoshonitic zone.

The three PMP lamprophyre analyses are plotted on a spidergram and normalized to the primitive earth crust composition in order to compare their chemistry with that of the average crustal rocks (Taylor, 1980) (Fig. 4-17). As can be seen in Figure 4-17, the composition of the three lamprophyres of the PMP are significantly different from the primitive earth crustal composition. The PMP lamprophyres have significantly higher Ba concentrations than average granites 1311 to 1920 ppm and 400-500 ppm (Pilkey, 1972) respectively. The alkaline zone (NPM615) of is slightly lower, at 394 ppm, than the average granite. Strontium concentration in the PMP lamprophyres is high (420 and 2567 ppm) compared with basaltic rocks (465 ppm). Average granites (282 ppm, Turekian,1956) show significantly lower Sr concentrations than either basalts or PMP lamprophyres. The concentration of Ni in the PMP lamprophyres ranges from 22 ppm in the alkaline lamprophyre zone (NPM615) to 194 ppm in the MacLeod Cove lamprophyre (NPM485). The average Ni concentration in igneous rocks is 80 ppm (Avias, 1972). The concentration of V in the PMP lamprophyres from 144 to 240 ppm is close to its concentration in

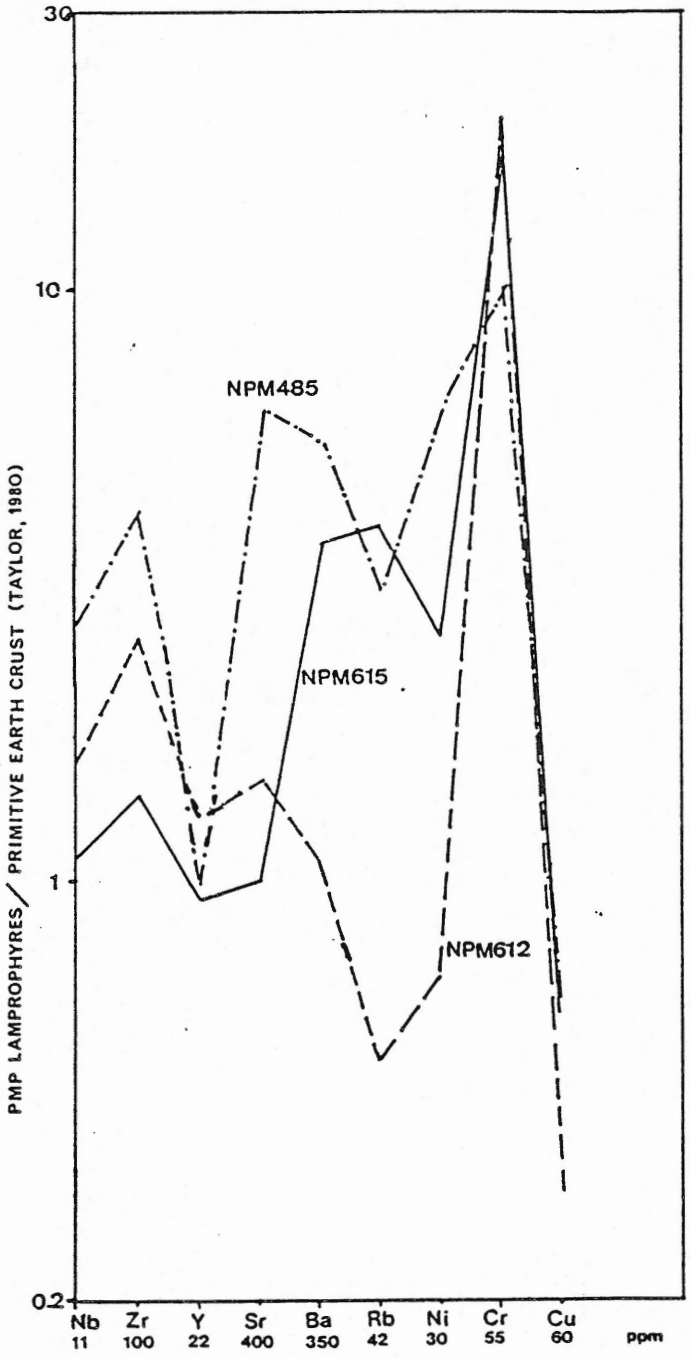

Figure 4-17: Plot of three lamprophyre zones from the PMP normalized to primitive earth crustal composition (normalization values after Taylor, 1980).

average basic rocks, defined by Burkart-Baumann (1972) to be 250 ppm.

The PMP shoshonitic dykes (NPM612 and NPM485) are similar to the Caledonian kersantite lamprophyres (phlogopite-plagioclase-rich shoshonites) of northern England (MacDonald et al., 1985) in their Ba, Cr, Nb, V, Sr (NPM485), Y and Zr trace element concentrations (Table 4-1). Noteworthy differences are evident in the concentrations of Ni, Rb and Th. Some of these relationships are shown in a rock/MORB plot of the PMP lamprophyre (NPM612) compared with the English Caledonian lamprophyres (Fig. 4-20). Majors, traces and rare earth elements are shown, using Pearce (1982, 1983) element ordering and MORB normalization values. Values from a 'primitive' tonalite from Unit 1 (NPM584) is also included on the diagram (see also Table 4-1).

4-4 Rare Earth Elements

4-4-1 Introduction

The REEs La to Lu (atomic numbers 57-71) are members of Group IIIA in the periodic table and have similar chemical and physical properties. Although the REEs are generally trivalent, some exhibit other oxidation states, including Ce^{4+} and Eu^{2+} which are important in geological processes (Ahrens,1964). The REEs exhibit a steady decrease in ionic radius of the REEs with increasing atomic number (La^{3+}=1.14A, Lu^{3+}=0.85A) (Henderson, 1984). The large ionic radii of the REEs preclude their significant substitution into minerals except where the substituted cation is also large. Substitutions of trivalent REE are observed for Ca^{2+}, Y^{3+}, Th^{4+}, U^{4+}, Mn^{2+} and Zr^{4+} (Eu^{2+} has a similar radius to that of Sr^{2+}). If REE concentrations

4-2

Whole-rock chemistry of Caledonian kersantites of northern England (MacDonald et al., 1985) compared with the PMP lamprophyres and a PMP tonalite sample from Unit 1.

	NPM584 Unit 1 tonalite	NPM612 Shosh. Lamp.	NPM615 Alkaline Lamp.	NPM485 Shosh. Lamp.	MacDonald et al., 1985 Caledonian kersantites
SiO2	68.14	46.23	52.01	51.95	45 +/-6
TiO2	0.50	1.08	1.08	1.22	1.25 +/-0.33
Al2O3	16.25	10.71	12.01	12.07	12.92 +/-2.3
Fe(t)	3.86	10.01	8.03	7.89	8.62 +/-0.74
MnO	0.07	0.15	0.21	0.12	0.21 +/-0.10
MgO	1.46	15.63	10.05	12.98	9.09 +/-2.37
CaO	3.12	6.69	10.80	5.92	9.05 +/-2.2
Na2O	4.02	1.01	2.38	1.29	1.74+/-0.79
K2O	1.73	4.01	0.67	4.29	2.61+/-0.82
P2O5	0.13	0.75	0.64	0.84	0.81+/-0.22
Ba	475	1311	394	1920	2191+/-149
Rb	62	167	19	132	54+/-17
Sr	385	420	598	2567	2111+/-2305
Y	11	21	28	23	26+/-9
Zr	156	435	248	421	212+/-48
Nb	9	12	18	30	17+/-4
Th	10	4	3	-	-
Pb	16	7	2	-	-
Ga	18	16	15	19	-
Zn	54	89	110	105	-
Cu	8	38	16	41	-
Ni	2	79	22	194	291+/-173
V	37	181	240	144	86+/-28
Cr	14	957	1046	551	570+/-355

*major oxides record in %, trace element values record in ppm.

are high enough, monazite, allanite, or other REE-rich may form. Otherwise, REEs become incorporated in the lattices of major rock-forming minerals such as apatite, zircon, plagioclase, potassic feldspar, garnet and biotite.

REEs are important because the degree of REE fractionation in a rock or mineral can indicate of its genesis. 'The REEs have their greatest utility in that, although the values for the Kd's for a given mineral may vary widely as a function of temperature or composition, in general, the shape of the pattern for a given mineral is consistent. Thus a given mineral will have a characteristic effect on a REE pattern of a melt which allows identification of that mineral as having been a residual zone.' (Hanson,1978 p.34).

The importance of REE-complexing in late-stage supercritical melts is unclear (Hanson, 1978). Muecke and Clarke (1981) suggested that fluorine may have been effective as complexing agent of REEs under magmatic conditions during the late-stage greisenization of the South Mountain Batholith.

4-4-2 REEs in the PMP

There is a marked variation in the SUM7REE (excluding Gd from analyses) between the Units analysed. The SUM7REE of Unit 1 (the oldest zone in the PMP) ranges from 64.6 to 105.2. Unit 4 has SUM7REE values ranging from 96.2 to 196.5. Only one of the three Unit 4 samples analysed has lower SUM7REE values than Unit 1 (NPM458). SUM7REEs of Unit 7 are variable (Fig. 4-18) and have values ranging from 24.8 (NPM560-monzogranite) to 91.3 (NPM583-tonalite). The Forbes

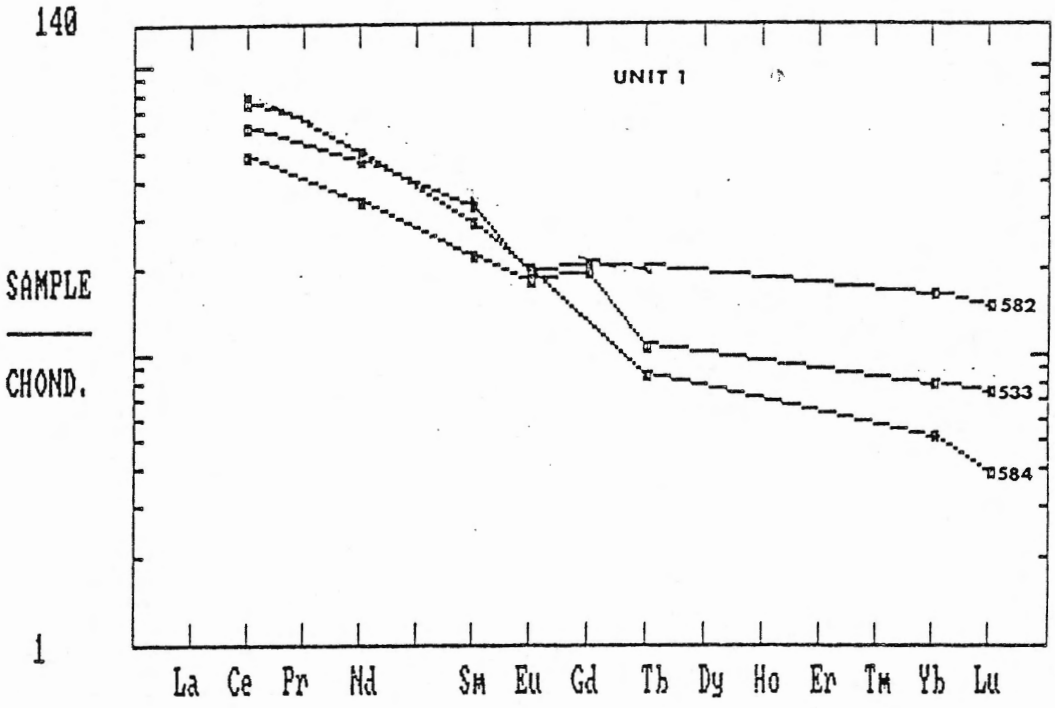

Figure 4-18: REE whole-rock analyses. Chondrite normalized (Haskin et al., 1966) samples from the PMP. Unit 1

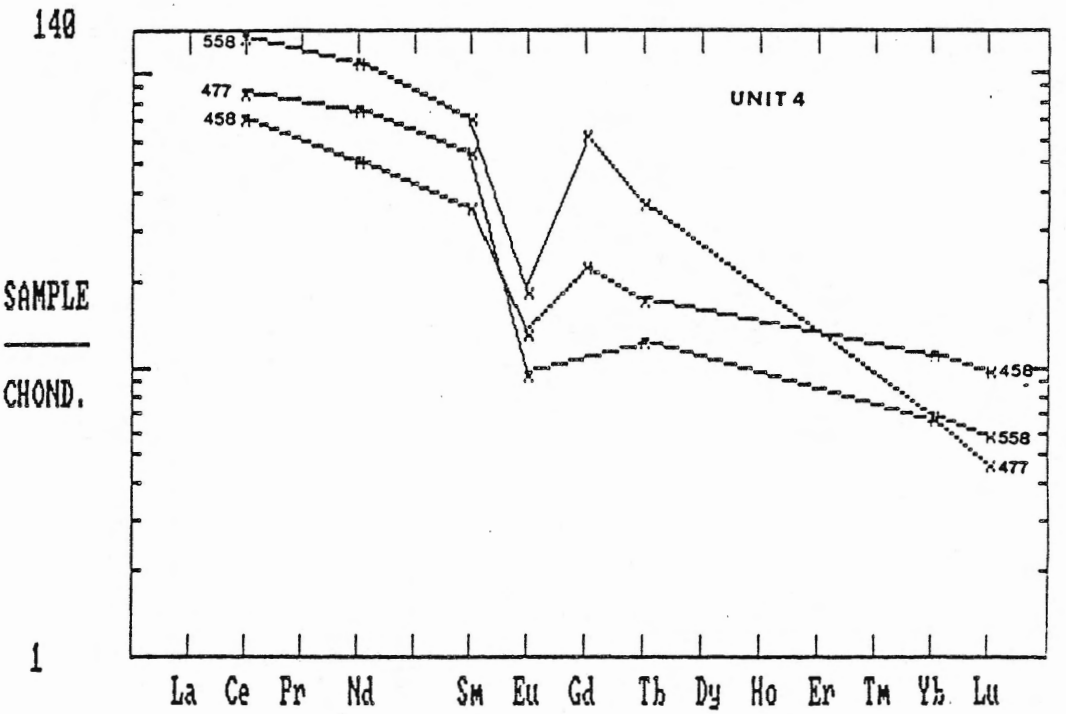

Figure 4-18: REE whole-rock analyses. Chondrite normalized (Haskin et al., 1966) samples from Unit 4.

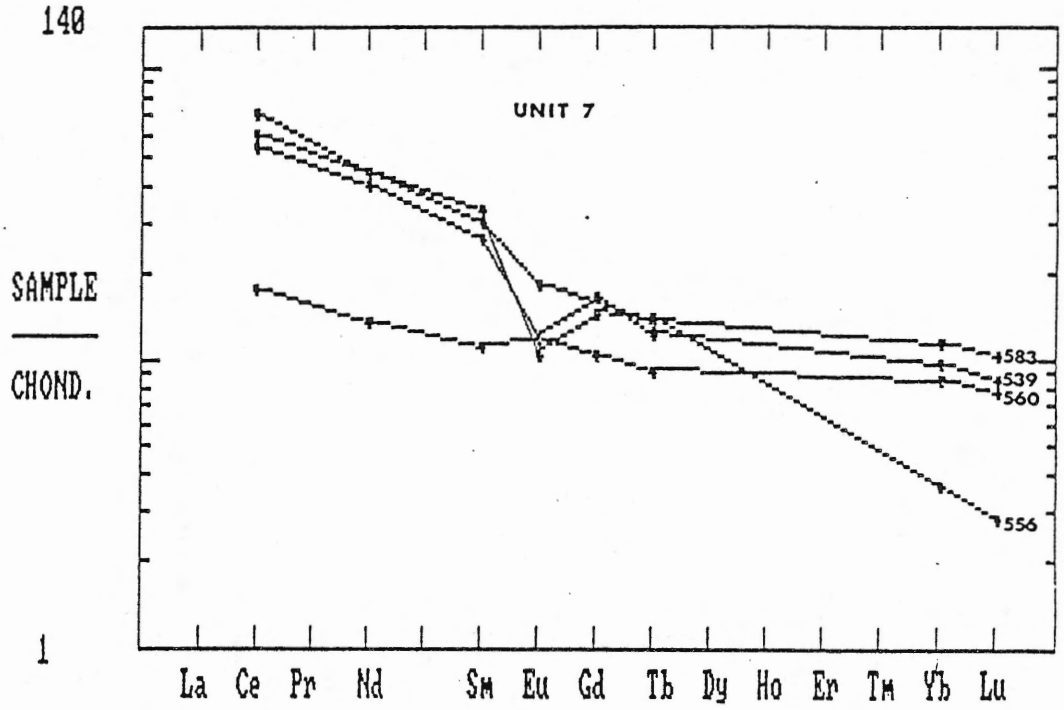

Figure 4-18: REE whole-rock analyses. Chondrite normalized (Haskin et al., 1966) samples from Unit 7.

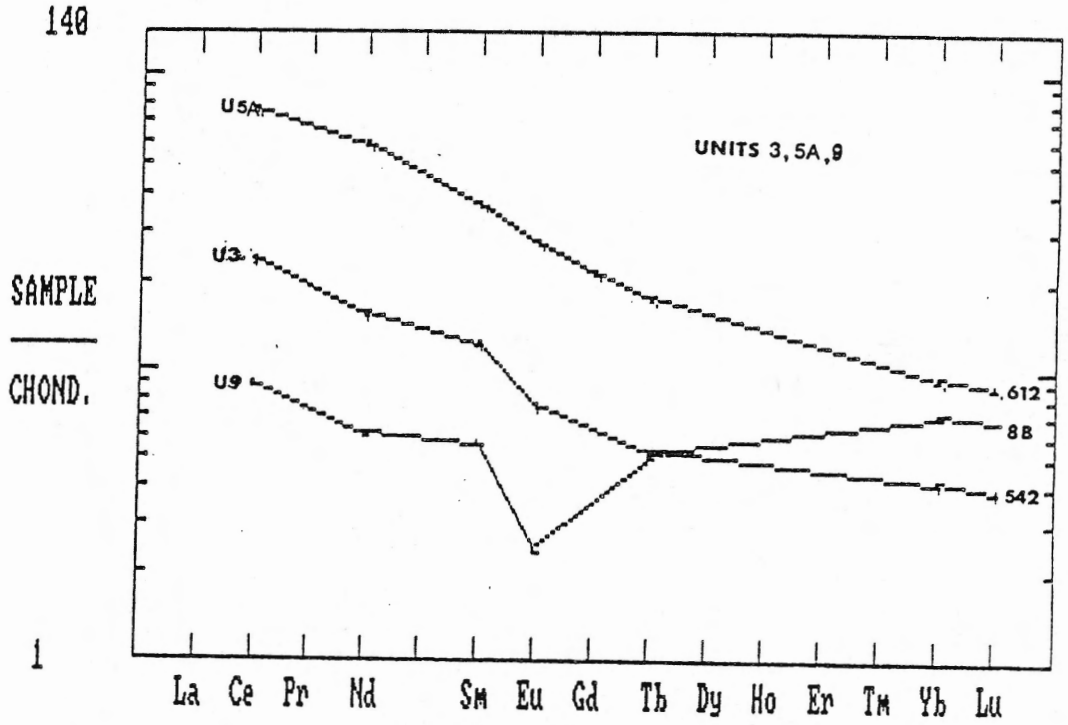

Figure 4-18: REE whole-rock analyses. Chondrite normalized (Haskin et al., 1966) samples from Units 3, 5A and 9.

Point shoshonitic lamprophyre sample (NPM612) has a low SUM7REE value of only 105.3. This is within the upper range of Unit 1 and intermediate to the values of Unit 4.

The Eu/Eu^* values of Unit 1 vary from 0.8 to 1.3. The Unit 3 sample appears to have no Eu anomaly ($Eu/Eu^*=1$). Unit 4 samples have Eu/Eu^* values ranging from 0.2 to 0.4. The negative Eu anomaly is more pronounced in Unit 4 than in Unit 1. The samples of Unit 7 have Eu/Eu^* values of 0.5 (NPM566), 0.6 (NPM539) to 1.1 (NPM560) and 0.9 (NPM583). Two of the Unit 7 samples have a negative Eu anomaly comparable to those of Unit 4 (NPM566,-539) and two of the Unit 7 samples are comparable to Unit 1 (NPM583,-560). The aplite sample of Unit 9 has a Eu/Eu^* of 0.4. The Forbes Point lamprophyre dyke (NPM612) has a Eu/Eu^* value of 1.0 (no anomaly).

All of the samples analysed have a LREE enrichment relative to the HREEs. The (Ce/Sm)cn (where cn = chondrite normalized) for the Unit 1 samples ranges from 1.4 (NPM582) to 2.8 (NPM533). Unit 3 has a (Ce/Sm)cn value of 2.0 within the range of Unit 1. The Unit 4 value ranges from 1.7 (NPM477) to 2.1 (NPM458). Similar values were obtained for Unit 7 at 1.7 (NPM560) to 2.5 (NPM583). The aplite of Unit 9 has a (Ce/Sm)cn value of 1.6, the lowest value obtained of the thirteen samples analysed. Yb and Lu are enriched relative to Tb in the Unit 9 aplite. This feature is common in garnet-bearing igneous rocks (Hermann, 1970).

4-4-3 Discussion

Unlike the SMB (Muecke and Clarke, 1981), the average values of

SUMREE, La/Sm (Ce/Sm) and Eu/Eu* do not show a systematic decrease from the oldest zone (Unit 1) to the youngest zone (Unit 9). There is a systematic decrease in SUM7REE from Units 4 (Cycle II) to 7 (Cycle III) to 9 (Cycle III), but Unit 1 has intermediate SUM7REE values between Units 4 and 7 (Fig. 4-19). There is a pronounced negative europium anomaly for Units 4 and 9 but not for Unit 7. Based on the average REE analyses shown in Figure 4-19, there may have been more than one parental source magma for the observed units in the PMP.

4-4-4 Lamprophyre (NPM612)

The REE content of the shoshonitic lamprophyre at Forbes Point shows lower SUMREE values than the two Caledonian kersantite lamprophyres of northern England (MacDonald et al., 1985). The PMP has lower Ce (60.8 ppm compared with 120-217 ppm), Nd (33.5 ppm compared with 55-93 ppm), Sm (6.5 ppm compared with 9-13.3 ppm), Eu (1.8 compared with 2.3-2.9 ppm), Tb (0.7 ppm compared with 1.0-1.1 ppm) concentrations and similar Yb (1.7 ppm compared with 2.4-2.4 ppm) and Lu (0.4 ppm compared with 0.4 ppm) concentrations.

Figure 4-20 shows MORB-normalized incompatible trace elements, plus compatible elements from the shoshonitic PMP lamprophyre. The ordering of the elements and normalizing values are after Pearce (1982, 1983). Key features observed are that:

1) the alkalies, Ba (alkaline earth), LREE, and Th show variable but strong enrichment (6.83X);

2) the high field strength (HFS) elements Zr, Hf, Nb and Ta show only modest enrichment (1.7-3.4X). The alkaline earth element Sr shows

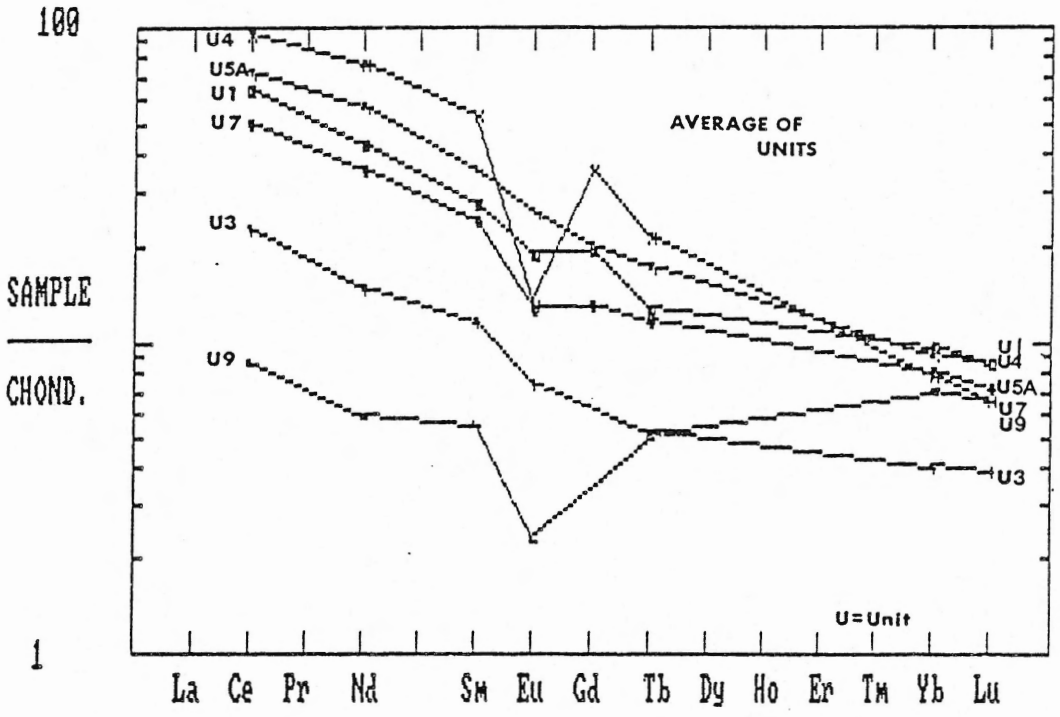

Figure 4-19: REE whole-rock analyses. Chondrite normalized (Haskin et al., 1966) samples. Average of each Unit analysed. U=Unit

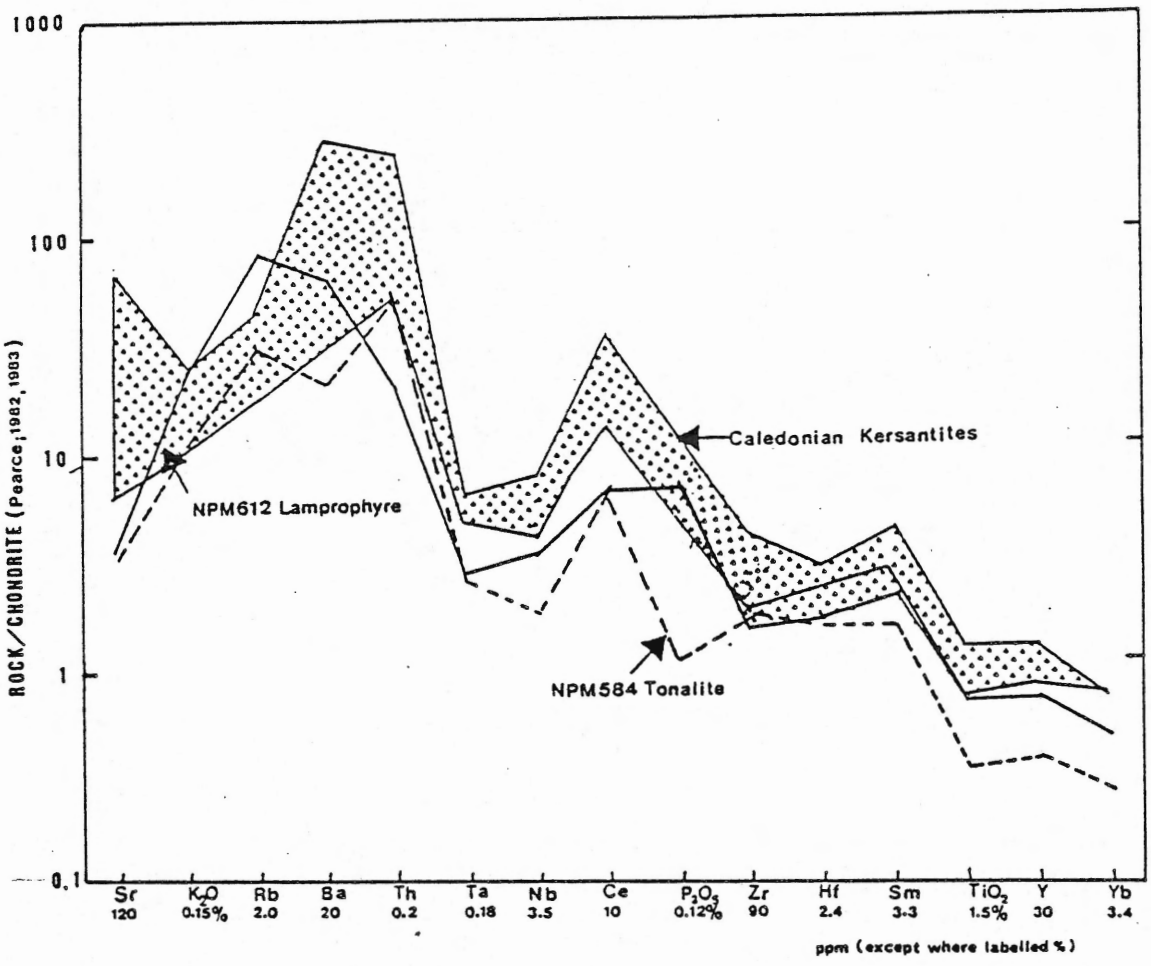

Figure 4-20: Comparison of the whole-rock chemistry of lamprophyres: PMP compared with Caledonian kersantites (MacDonald et al., 1985).

only modest enrichment (3.5X);

3) Ti, Y and the HREE values are lower than those in the standard MORB (0.5-0.7X). Sm is slightly enriched with respect to MORB (2X).

4-5 Summary of Geochemical Data

Based on the whole-rock chemistry results, there is support for three distinct intrusive mafic to felsic cycles in the PMP. There is a geochemical distinction between Unit 1 tonalites and granodiorites and Unit 4 granodiorites and monzogranites.

The following major element, Harker diagrams show the difference in whole-rock chemistry among Units 1, 4 and 7 and the intermediate relationship of Unit 7 with Units 1 and 4: TiO_2 (Fig. 4.1h), Al_2O_3 (Fig. 4.1i) , FeO_T (Fig.4.1d), MgO (Fig. 4.1b), CaO (Fig. 4.1a), K_2O (Fig. 4.1e) and the Thornton Tuttle differentiation index. MnO and P_2O_5 Harker diagrams (Figs. 4.1c and 4.1g respectively) display poor resolution among these three units. The following trace elements can be used to distinguish among Units 1, 4 and 7, and to define an intermediate relationship for Unit 7 between Units 1 and 4: Sr-CaO, Rb, Sr-Ba-Rb, Zr-TiO_2, V-TT-DI, Pb, Cr and Pb-K_2O.

Units 1, 4 and 7, show distinctive SUM7REE and Eu/Eu^* values. The lamprophyre dykes (Unit 5A) have exotic whole-rock chemistry compared with any other zone in the PMP.

In summary, whole-rock chemistry shows that:

1) some of the major, trace and REE elements can be used to discriminate between Units 1, 4 and 7;

2) Units 1 and Unit 4 have distinctly different whole-rock

compositions (particularly supported by their SUMREEs and Eu/Eu* contents);

3) average Unit 7 analyses tend to have intermediate compositions compared with Units 1 and 4;

4) the PMP can be described as having evolved in three mafic-to-felsic eruptive cycles.

Chapter 5 EMPLACEMENT, CHEMICAL MODELLING AND ORIGIN OF THE PMP

5-1 Mode of Emplacement

5-1-1 Introduction

The mode of emplacement of the PMP can be determined by the character of the exo- and endo-contacts associated with the pluton. The exposure of the exo-contact in the northern sector of the PMP is poor, but the contact is well exposed in the southern contact.

5-1-2 PMP-Meguma contacts

The PMP is characterized by both sharp and migmatitic granite-metasedimentary contacts. Emplacement after the deformation of the host Meguma Group metasediments into tight isoclinal northeast-southwest trending folds is supported by:

1) a sillimanite contact aureole overprinting the amphibolite facies rocks of the Meguma Group;

2) the lack of pervasive and uniformly oriented foliation within the pluton (Unit 1 foliation has a distinctly different orientation than Unit 4);

3) the local dislocation of the Meguma Group structure in the Broad River-Western Head and St. Catherines River Domains (Hope, 1987).

5-1-3 PMP Internal Contact Relations

Internal contact relations between the units give some evidence as to the relative stages of consolidation of each phase during emplacement of subsequent units. In deducing the emplacement history

of the PMP, the following observations should be considered:

1) angular inclusions of Unit 1 in Unit 4 are common near the perimeter of the PMP;

2) in the interior of the pluton, inclusions of Unit 1 in Unit 4 are more rounded and the contacts between the two units are more diffuse and irregular than at the perimeter of the pluton;

3) locally within the pluton, Unit 4 contains 'coarse' and 'fine' banded zones;

4) the Unit 2 trondhjemite dyke contains a large subangular fragment of Unit 1;

5) the lamprophyre dykes of 5A appear to have intruded along fractures and have superimposed an aureole (amphibole-phlogopite enrichment of the granitoids) on Units 1 and 4 at Forbes Point;

6) the breccias of Unit 5B contain abundant, angular fragments of milky quartz, granitoid rocks (Unit 1) and Meguma-like clasts;

7) the Unit 7 mafic dykes may have intruded granitoid rocks. Multiple dilation dykes ('pinch and swell' dykes), appear in the interior of the pluton (form #1- see Chapter 2) and may represent dykes that have intruded only partially consolidated melt. The non-dilating, straight-sided Unit 7 dykes with local fragmental inclusions of granitoids probably intruded consolidated granites;

8) the late dykes (Unit 8 and 9) are characterized by sharp intrusive contacts with Units 1, 4 and 7;

9) in the southeastern and western sectors of the pluton, wide dykes of Unit 9 pegmatites and Unit 8 leucomonzogranites contain slabs of Goldenville psammites.

5-1-4 Discussion

The PMP was clearly formed by the active emplacement of magma as is supported by the dislocation of the country rock. The emplacement history of the PMP is further complicated by deformation throughout its emplacement history (e.g. Maksaev, 1986). The following interpretation divides the emplacement history of the PMP into a sequence of six steps:

STAGE 1: Emplacement of Unit 1 subsequent to the deformation of the country rock.

evidence: -contact aureole

-local deflection of regional structure

STAGE 2: Emplacement of Units 2 and 3. Unit 1 was consolidated prior to the intrusion of Unit 2.

evidence: -the trondhjemite dyke (Unit 2) contains a large subangular fragment of Unit 1

STAGE 3:a) Emplacement of Unit 4 and subsequent development of 'coarse' and 'fine' banding in Unit 4 and later deformation of banding.

evidence: -small scale 'z' patterns in the banding, some dextral shear surfaces, mineral alignment, and quartz flattening of the banded and foliated host granite on Mouton Island (Unit 4). (see Maksaev, 1986)

b) The deformational episode that affected Unit 4 created variably preserved foliations parallel to the banding and regional deformation.

evidence: -the foliation in Unit 4 is defined by the planar orientation of biotite and muscovite

c) Unit 1 may not have been consolidated in the interior of the pluton prior to the emplacement of Unit 4.

evidence: -the inclusions of Unit 1 in 4 are more rounded and the contacts between the two units are diffuse and irregular although this may also be a function of the longer residence time of the xenoliths in the granite.

d) Consolidation of Unit 4 (along the peripheries of the pluton).

evidence: -see Stage 4 (a)

STAGE 4: a) Emplacement of Unit 5A dykes (near the periphery of the pluton). Units 1 and 4 were consolidated prior to the emplacement of the 5A dykes.

evidence: -a contact aureole is superimposed on the intruded granitoids of Units 1 and 4 (Forbes Point).

b) Local deformation of the MacLeods Cove lamprophyre dyke.

evidence: -a pronounced schistosity is evident in the hand specimens of the dyke and there is petrological evidence of recrystallization.

c) Emplacement of Unit 5B tonalite breccia along the PMP-Meguma contact.

evidence: -the high concentration and the angular shape of the clasts of Meguma Group, quartz and Unit 1 indicates explosive emplacement. The matrix of the breccia is similar in appearance to the hypidiomorphic granular textures of the average Unit 7 dykes.

d) Emplacement of Unit 6 leucomonzogranite and pegmatite dykes.

STAGE 5: a) Emplacement of Unit 7 dykes

b) Deformation event (at least locally on Port Mouton Island)

evidence: -sinistral shear stress parallel to the banding in Unit 4, forms zig-zag folds with 's' patterns in the banding and a weak foliation in the Unit 7 dyke.

STAGE 6: Emplacement of Units 8 and 9. These late phase dykes are characterized by sharp intrusive contacts with Units 1, 4 and 7. These rocks were probably emplaced along fractures in brittle, semi-cooled granitoids. Late, low-temperature deformation is recorded in microscopic features of monzogranite dykes of Units 8 and pegmatite veins of Unit 9.

evidence: -this deformation was observed on Port

Mouton Island (Maksaev, 1986)

-shear zones developed in granitoids

at the PMP/Meguma contact at Highway 103.

The banding and deformation in the PMP granite are believed to be the result of stresses imposed during the late stages of magma crystallization (i.e. Maksaev (1986)). It is unlikely that these are a product of the Acadian Orogeny that produced the isoclinal folds in the Meguma Group, but are a product of some later deformational event, because evidence suggests that the PMP was emplaced after the Acadian deformation. Elias (1986) postulated that the overprinting event affecting the Southern Satellite plutons occurred at about 300 Ma. He describes it as having had varying intensities but being sufficiently strong to partly or completely outgas biotite, and completely reset K-feldspar in the Southern Satellite plutons. It is not clear how resetting of these minerals could be possible since the PMP was probably consolidated at 300 Ma and no evidence of late-stage fluid alteration has been found.

5-2 Depth of Emplacement of the PMP

Only a few petrological and geochemical observations reflect on the depth of emplacement of the PMP. De Albuquerque (1977) concluded from Qz-Or-Ab normative plots that the emplacement pressures and temperatures of two biotite-muscovite granodiorite samples from the PMP were 3.5 to 4.5 kbar, 670 to 690° C. Two muscovite-biotite granites from the PMP show 4.5 to 5.5 kbar pressures and 675 to 705° C temperatures. These P-T conditions were derived by comparison of

whole-rock normative values with experimental data of Winkler (1974) (Fig. 5-1). Figure 5-2 shows the whole-rock CIPW normative Ab-Or-Qz plot of Units 1, 4 and 7 of the Port Mouton Pluton in relation to the ternary minima and eutectics (Tuttle and Bowen, 1958, Luth et al., 1964), and in relation to the trend of isobaric univariant points at varying Ab/An ratios (James and Hamilton, 1969). The position of the invariant points at 4 kbars is inferred from the suggestion of Winkler (1967) and James and Hamilton (1969) that these ternary minimum points shift towards the Ab apex with increasing pressure in a manner similar to that of the eutectics. It is apparent from this plot (Fig. 5-2) that Units 1 and 7 are displaced from 'normal' granitoid trends towards the Ab apex and fall outside the field of possible invariant points and that Unit 4 has a wide variation in its normative Qz, Ab and Or contents, making pressure estimates imprecise. Most of the Unit 4 whole-rock compositions fall between 0.5 and 5 kbar trends of piercing points. The average Ab/An normative ratios for the three Units (1, 4 and 7) are 3.2 ± 1.3 (N=10), 6.5 ± 4.3 (N=22) and 4.7 ± 1.9 (N=8) respectively. There is considerable variation in the Ab/An ratios in Unit 4. Experimental data show that the Ab-component of the melt increases with increased temperature of melting (i.e. Winkler, 1984). It can be inferred from the Qz-Or-Ab normative compositions of the Unit 4 granitoids (Fig. 5-2) that the emplacement pressures are higher than 2 kbar as there is a systematic shift towards the Ab corner for specific Ab/An ratios in contrast with the lower Ab values observed with experimental data at that pressure (e.g. Winkler, 1974; Brown and Fyfe, 1970).

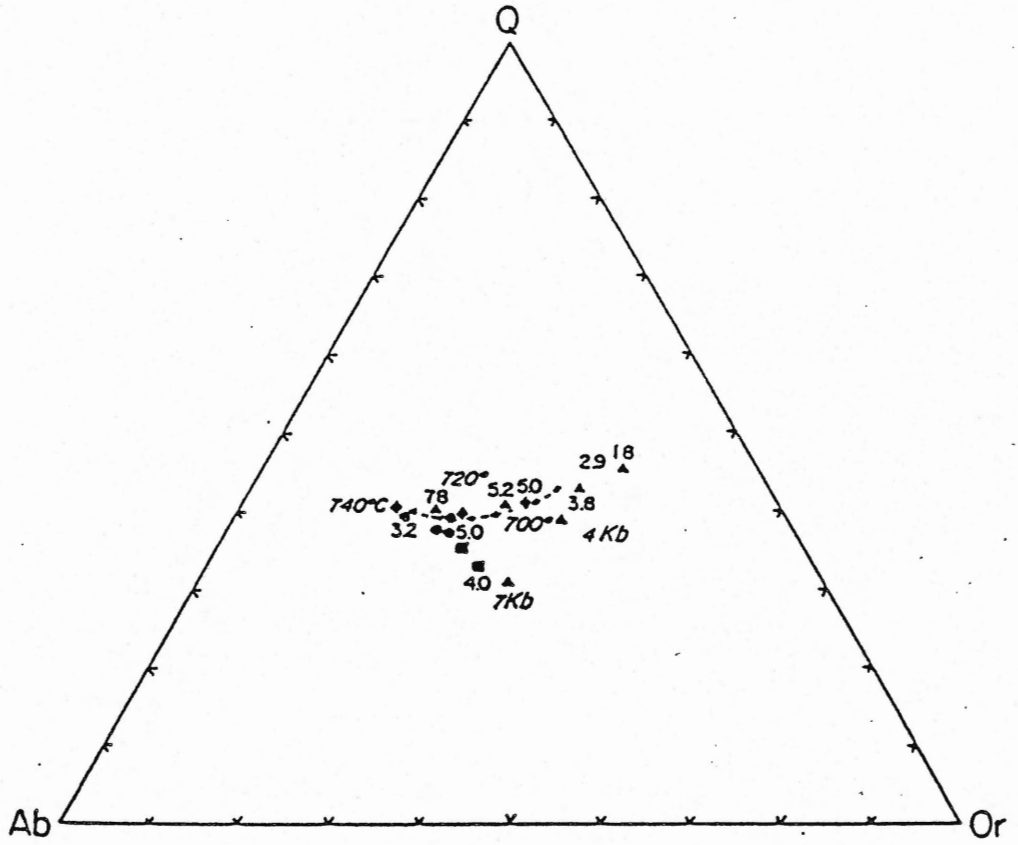

Figure 5-1: Normative Q-Ab-Or diagram. ●- Trondhjemite and muscovite-biotite granodiorite. ■-Muscovite-biotite granite (Port Mouton pluton). Data from Winkler (1974): ▲ 'minimum melt' compositions for various Ab/An ratios and for the Ab/An ratio of 2.9 in the pressure range 2-7 kbar. ▪ Melt compositions at various temperatures above the 'minimum melt' temperature (from de Albuquerque, 1977, Figure 3).

Muecke (1974) noted that the regional metamorphic grade in southwestern Nova Scotia attains a maximum of upper amphibolite facies near Shelburne. The contact aureole surrounding the PMP approaches melt-producing reactions (curve #5, Fig. 5-3) at 3.5 kbars and 650° C (Hope and Woodend, 1985). These P-T conditions are based on andalusite-cordierite-sillimanite-garnet-quartz assemblages (curve #4 of Fig. 5-3) in the contact aureole and on the presence of migmatites east of Summerville Beach and St. Catherines River Bay, which indicate melt-producing reactions (curve #5, Fig. 5-3). These were the minimum temperature and pressure conditions during emplacement of the PMP. Pitcher (1979) suggested that the mineral assemblages in the aureoles should provide a more reliable indication of the pressure and temperature at which a particular granitic magma came to rest in the crust (e.g. Kerrick, 1970). The PMP emplacement P-T values are similiar to the P-T values estimated for the South Mountain Batholith (4 kbars, 650° C to 0.5 kbars, 800° C, (McKenzie, 1974)) and the Musquodoboit Batholith (3-4 kbars and 645-725° C (MacDonald, 1981)).

Garnet is a constituent of some leucomonzogranites of Unit 8 and aplites of Unit 9 from the PMP. Green (1977) showed that low Ca and Mn garnet is stable in silicate liquids from 7-10 kbars. Garnets (similar to those in the PMP) with greater than 10 mol. % spessartine and 2-6 mol. % grossular are stable in silicic liquids at 5 kbars or less (similar to PMP garnets) (Green, 1977). The primary-looking garnets analysed from Unit 8 dykes of the PMP could, therefore, have been stable at pressures less than or equal to 5 kbars. This is in agreement with the P-T conditions obtained from the contact aureole.

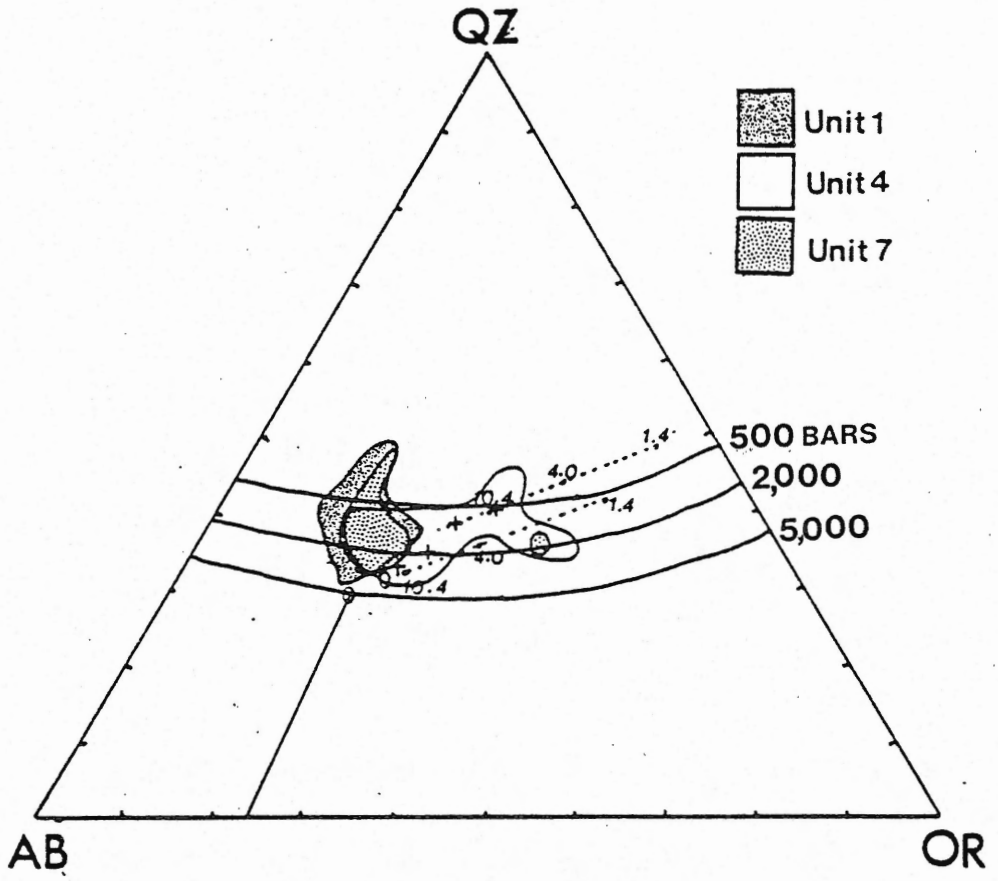

Figure 5-2: Plot of normative Ab-Qz-Or for the Port Mouton pluton. Minima, eutectics and cotectics from Tuttle and Bowen (1958) and Luth et al., (1964). Ab/An piercing points after James and Hamilton (1969).

LEGEND:

Unit 1 (N=10 samples)
Unit 4 (N=22 samples)
Unit 7 (N=8 samples)
\+ Ternary Minima
O Eutectics
4.0 Ab/An

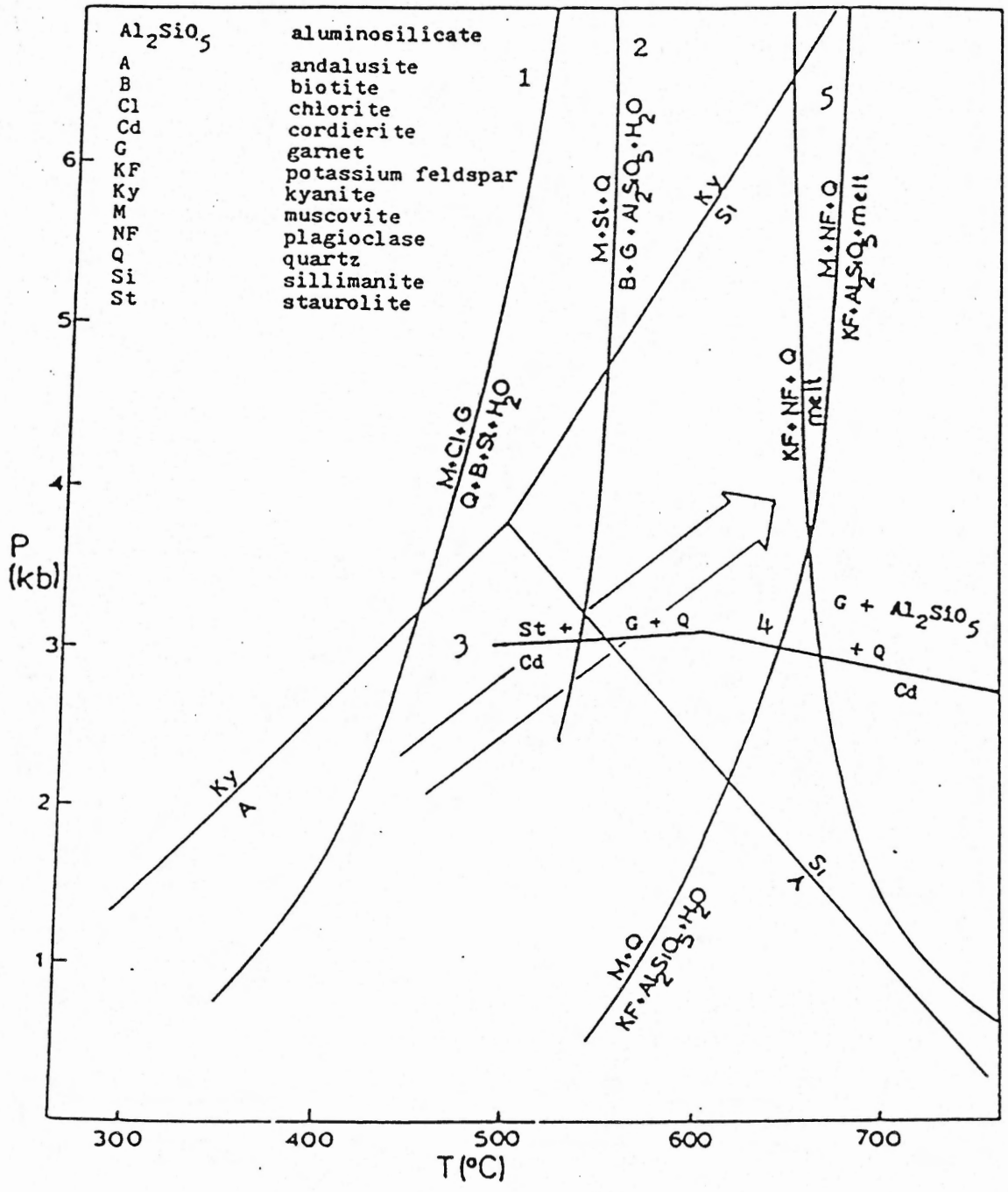

Figure 5-3: (from Hope and Woodend, 1985). Pressure-temperature diagram showing the path of metamorphism in the Port Mouton-Port Joli map area.

An attempt to determine P-T conditions using biotite-garnet geothermobarometers (Ferry and Spear, 1978; Indares and Martignole, 1985; Hoinkes, 1986) from Unit 8 leucomonozogranite dykes of the PMP was unsuccessful. The temperatures obtained (850°-990° C) were unrealistically high considering that the P-T conditions in these late-stage leucocratic granitoids are most likely lower than earlier melts which were 670°-705° C (de Albuquerque, 1977). Table 5-1 summarizes garnet-biotite geothermobarometry results for pressures from 1 to 5 kilobars. The P-T conditions of emplacement of the PMP are contradictory. The contact aureole, which does not reflect accurately the maximum temperature at the time of emplacement, indicates 3.5 kilobar pressure and 650° C temperature. Qz-Ab-Or normative plots indicate 2 to 5.5 kilobar pressures and 670 to 705 degree temperatures (this paper and de Albuquerque, 1977). Using the aureole conditions and assuming a pressure/depth relationship of 10 kilometers being equivalent to 2.6 kbars (after Miyashiro, 1973), the PMP was emplaced at depths of 13.5 kms or so. According to the definitions of Buddington (1959) the PMP appears to characterize a mesozonal complex. He defined the mesozone as extending from 6.5 km to 16 km (approx. 1.5 kbars to 4.0 kbars).

5-3 Origin of the PMP magma

The Port Mouton Pluton is a peraluminous complex ranging in composition from tonalite to trondhjemite, granodiorite and monzogranite. Shoshonitic and alkaline lamprophyres are associated with the pluton. The following is a review of the current theories on the

Table 5-1 Results of Garnet-Biotite Geothermometry Calculations for pressures ranging from 1 to 5 kbars.

Sample	Ferry +Spear (1978)	Indares + Martignole(1985)	Hoinkes(1986)
Unit 8			
NPM107	850°C	990°C	870C
NPM344	990°C	1150°C	1020°C
NPM611	905°C	970°C	920°C
NPM8A	970°C	1070°C	980°C
Unit 1			
NPM484	910°C	870°C	930°C
metasediment from aureole			
NPM108	860°C	920°C	910°C

The P-T garnet-biotite geothermobarometers used are only accurate if a significant quantity of Ca and Mn are contained in the garnet (according to Ferry and Spear (1978) the (Ca+Mn)/(Ca+Mn+Fe+Mg) content of garnets must be less than 0.2). In the PMP garnets analysed all but one sample (NPM484 satisfied this condition (ranging from 0.15 to 0.39). Low Ti contents in the biotites are also required. Ferry and Spear (1978) stipulated that the $(Al^{vi}+Ti)/(Al^{vi}+Ti+Mg+Fe)$ in biotite should be no more than 0.15. In the PMP biotites analysed for this study, all of the ratios are greater than 0.15 (ranging from 0.17-0.21).

origin of these rock types.

5-3-1 Origin of Peraluminous Granites- A general overview.

Peraluminous granites form in both stable cratons and in orogenic zones that were formerly parts of active and subducting plate margins (Zen, 1987). The granitoid rocks analysed from the PMP (48 samples) are peraluminous with A/CNK ratios ranging from 0.96 to 1.30. Clarke (1981) stated that peraluminous granite complexes can arise from the differentiation of parental magmas which are largely, but by no means exclusively, of crustal origin. Anatexis in the continental crust at reasonable pressures and temperatures (i.e. 8 kbars and 700° C) probably depends upon the presence of H_2O produced by the breakdown of a hydrous mineral such as muscovite (Huang and Wyllie, 1975). Water from other sources (such as deuteric) is considered generally insufficient for melting (Hyndman, 1981).

Four models, presented below, are proposed as possible mechanisms for the formation of peraluminous magmas:

1) fractional crystallization from originally subaluminous magmas, or partial melting of subaluminous rocks;

2) the result of interaction between late-stage magmas or subsolidus rocks and hydrothermal fluids in the form of alkali loss from end-stage volatile-bearing magmas;

3) partial melting of peraluminous source rocks;

4) the assimilation of host rock.

Model 1: Fractional crystallization of subaluminous minerals (e.g.

hornblende) from originally subaluminous magmas has been proposed as a mechanism for producing peraluminous magmas (Abbott, 1981; Conrad et al., 1986; Zen, 1986, 1987). Abbott (1981) used AFM liquidus projections to show that it is possible to evolve peraluminous melts from original metaluminous magmas by the fractionation of hornblende from a hornblende + biotite + quartz + alkali feldspar + plagioclase melt. Zen (1986) supports this theory but stipulates that only the origin of mildly peraluminous granites (A/CNK between 1.0 and 1.1) could occur as a result of fractional crystallization of subaluminous hornblende from subaluminous (A/CNK <1.0) magma. 'For hornblende to effectively cause a melt to evolve into a peraluminous composition it must be able to coexist with peraluminous magmas' (Zen, 1986). He concluded that the process is unlikely to give rise to peraluminous plutons of batholithic dimensions because of its inefficiency. Large amounts of subaluminous crystals must be subtracted before the magma can show significant change in its A/CNK. Zen (1986) suggests that peraluminous melts can also be derived by fractionation of grossular-rich garnet at high temperatures, presumably in the upper mantle or at the base of the crust. Section 5-6-1 contains more details of this model, pertaining specifically to the PMP.

Model 2: Peraluminous granites, at least in part, may be the result of interaction between late-stage magmas or subsolidus rocks and hydrothermal fluids (alkali-loss from end-stage volatile-bearing magmas)(Muecke and Clarke, 1981; Martin and Bowen, 1981; Goad and Cerny, 1981; Currie and Pajari, 1981).

Alkali transport depends heavily on a volatile-rich phase and it can be expected to be effective primarily during late magmatic stages (Zen, 1987). If the entire rock became peraluminous only through this process, then its earlier petrogenetic history and even chemical and mineralogical features should betray its origin (Halliday, et al., 1981). These features include evidence for high volatile content, especially halogens that facilitate alkali loss from the magma (Orville, 1963; Manning and Pichavant, 1984), in the pluton, and/or remnant or relict metaluminous mineral assemblages, especially in the cumulate fractions. The peraluminous assemblages might be concentrated in later, residual parts of the batholith (Zen, 1987).

If strongly peraluminous minerals (e.g. cordierite, muscovite, almandine or the aluminum silicates) can be shown, on textural evidence, to have been early, or if the magma can be shown to have been relatively dry, it is unlikely that late-stage, vapour-phase, alkali loss has taken place (Zen, 1987). Section 5-6-6 contains further details of this model as it pertains to the PMP.

Model 3: The derivation of peraluminous magmas from the partial melting of peraluminous source rocks has been suggested by Conrad et al., 1986; Phillips et al., 1981, Currie and Pajari, 1981; Strong and Hanmer, 1981; Halliday et al., 1981, Anderson and Rowley, 1981; Clemens and Wall, 1981; Spear, 1981; and Chappell and White, 1974.

'Magmas with broadly S-type chemical characteristics may be derived by partial fusion of strongly to weakly peraluminous source rocks ranging respectively from pelites or semi-pelites to relatively

immature, quartzofeldspathic sediments or even altered igneous materials' (Clemens and Wall (1981)).

Chappell and White (1974) believed that peraluminous batholiths with an S-type character are derived from the anatexis of sedimentary rocks. Characteristic features of S-type granites are as follows:

1) A/CNK > 1.1: CIPW norm yields >1% corundum;

2) relatively low Na_2O and low Na/K ratio;

3) restricted SiO_2 range for rocks within the series;

4) high initial Sr isotope ratios;

5) high $\delta^{18}O$;

6) inclusions are peraluminous metasedimentary material;

7) opaque mineral is ilmenite;

8) cordierite phenocrysts.

Model 4: The composition of the peraluminous granites may at least in part be the result of assimilation of the host rock (Goad and Cerny, 1981; Longstaffe et al., 1981). One model for the origin of the peraluminous pegmatite granites of the Winnipeg River district involves igneous differentiation from a juvenile source modified by interaction of the intruding melt with the host greenstone-belt rocks (contaminated I-type magma)(Goad and Cerny, 1981). In this model, variable contamination of a fractionated I-type melt by different supracrustal lithologies explains the regional distribution of accessory minerals and the deviations of subordinate and trace elements from ideal fractionation trends within the pluton (Goad and Cerny, 1981).

Bulk assimilation of clastic metasedimentary rocks has been suggested as a possible model in the contribution of the peraluminous character of the Tin Lake and Osis Lake plutons in southeastern Manitoba (Longstaffe et al., 1981). Both bodies are tourmaline-bearing, and the latter contains numerous partly digested metasedimentary inclusions. The clastic metasedimentary rocks would also contribute to the ^{18}O-rich character of the two plutons (Longstaffe et al., 1981). See section 5-6-4 for a discussion of this model with respect to the PMP.

5-3-2 Discussion

In discussing the possible origin of the peraluminous granites of the PMP, only the granodiorites and the peraluminous monozogranites will be considered. Further complications arise in explaining the origin of peraluminous tonalites and they will be evaluated in the following section. The A/CNK content of the granodiorites and monzogranites of the PMP ranges from 0.96 to 1.26. Combined evidence from whole-rock geochemistry and field relations is adequate to identify potential lineages in the derivation of these peraluminous magmas.

It is unlikely that all of the peraluminous granodiorites and monzogranites of the PMP are a result of interaction with hydrothermal fluids (alkali-loss from end-stage volatile-bearing magmas). If this were so, there should be an uneven alkali loss in the pluton and remnant or relict metaluminous mineral assemblages (Zen, 1987). The A/CNK ratio of the PMP granodiorites varies by no more than 25% (which

would mean a very improbable, uniform fluid alteration) and there is no evidence (either petrologically or chemically) to support a 'front' of fluid alteration. The high A/CNK ratio (1.29), low SUM7REE (e.g. Muecke and Clarke, 1981) and low K/Rb ratios of the highly evolved aplites of Unit 9 may reflect their involvement with volatile-bearing magmas (or fluids).

The whole-rock chemistry of the PMP granodiorite and monzogranites was probably not affected by contamination with the host rock because super-heated magmas would be required to melt and digest large quantities of the host rock. The granodiorite and monzogranite from the PMP may have been derived from a subaluminous source, however, there is no evidence of metaluminous fractionate phases (e.g. hornblende) in the granodiorites or monzogranites. Also, the success in modelling peraluminous melts from subaluminous sources applies only to evolved peraluminous granites with A/CNK values between 1.0 and 1.1 (Zen, 1986).

The peraluminous granodiorites and monzogranites of the PMP may also have been derived from the partial melting of a peraluminous source rock. This is supported by the apparent lack of 'exotic' metaluminous enclaves and the abundance of quartzofeldspathic enclaves and the high A/CNK ratio.

In conclusion the data do not conclusively show whether the peraluminous granodiorites and monzogranites of the PMP were derived from a metaluminous or a peraluminous source rock in the crust. On balance though, they probably were derived from a metasedimentary (peraluminous) source. Late aplites (Unit 9) may have been affected

by late-stage fluids. The PMP has assimilated Meguma Group material (based on the presence of abundant Meguma-like xenoliths in the PMP), the quantities of which are unknown.

5-3-3 Origin of Tonalites

Few studies have addressed the problem of the origin of peraluminous tonalites. Many of these models are still in the early stages of development.

The formation of a melt of tonalitic composition with 1-2% dissolved H_2O requires temperatures of 1100-1150° C (Wyllie, 1977). These temperatures are higher than those required for the formation of granodiorites and granites (Fig. 5-4). These are also unusually high temperatures for a normal crustal environments (Wyllie, 1983), implying one of several special conditions, as follows:

1) major perturbation in the geotherms of the lower crust e.g. subduction zone environment (Wyllie, 1983) increases the temperatures in the lower crust;

2) contamination of more mafic magmas (from below the continental crust) by the host crustal rocks (Wyllie, et al., 1976);

3) the tonalites are derived from a more mafic parental magma originating in the mantle (Piwiniskii and Wyllie, 1968, 1970);

4) the tonalites are not melts but rather a melt and restite (Chappell and White, 1974).

Little evidence is available to support the theory that the PMP tonalites are of mantle origin (except for the high temperatures required in order to produce a melt of tonalite composition). Like

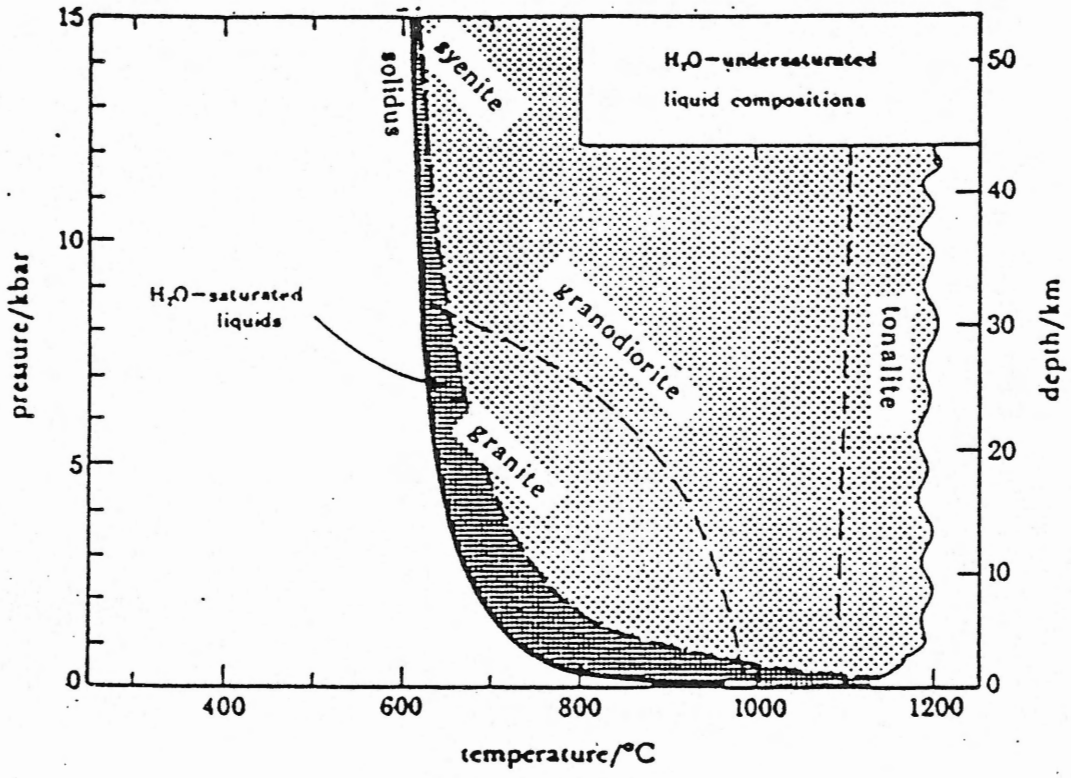

Figure 5-4: Composition of liquids generated within the melting interval of rocks of continental crust in the presence of H_2O (Wyllie, 1977).

the granodiorites and monzogranites of the PMP, no exotic mantle xenoliths (suggesting mantle derivation) are associated with the PMP tonalites.

The high A/CNK ration (1.09-1.23) of the tonalites may indicate that the source area was peraluminous (or crustal). Conrad (1986) has shown experimently that it is possible to derive peraluminous tonalites from metaluminous rocks with 65 wt. % SiO_2 but the high A/CNK ratios of the PMP tonalites suggest that this is an unlikely mechanism.

5-3-4 Discussion

Approximately 10-20% of the PMP granitoids are tonalitic in composition and have A/CNK ratios ranging from 1.09-1.23. The discussion above leads to the conclusion that the PMP peraluminous tonalites were derived from a peraluminous source probably in the lower crust, or mantle. If the peraluminous tonalites were derived from the lower crust, a large thermal perturbation was required to melt possible source rocks e.g. Wyllie, 1983. Elias (1986) offers a possible mechanism for the increase in the geothermal gradient. He proposes that the increase in elevation of the isotherms in the lower crust during the Devonian of southwestern Nova Scotia is caused by thermal doming influenced by a mantle hot spot.

5-3-5 Origin of Lamprophyres

Lamprophyres globally are interesting because of their hydrous nature and high mafic content, their apparent close spatial

relationship to more felsic granitoid rocks, and their strikingly different chemistry from their associated granitoid rocks.

Many theories have been suggested for the petrogenesis of these 'exotic' mafic dykes. Models involve one or more of these processes- hybridisation, contamination, metasomatism, metamorphism and differentiation. It is not clear whether lamprophyres are directly derived from the mantle (Bachinski and Scott, 1979; Ruddock and Hamilton, 1978) or the crust (Rock, 1980; Wimmenauer, 1973). This thesis will not attempt to resolve this issue but will simply note that the shoshonitic lamprophyres from the PMP are similar in chemical and mineralogical composition to the Caledonian kersantite lamprophyres of MacDonald et al., (1985). These may originate from a Mg- and alkali-rich mantle-derived parent magma. Complex fractional crystallization processes were accompanied and followed by late- and post-magmatic modification by hydrothermal processes and interactions with crustal material (MacDonald et al., 1985).

5-4 Modelling the Whole-Rock Chemistry of the PMP

5-4-1 Introduction

Some of the trace and major element analyses show distinct fields for Units 1, 4 and 7 such that Units 1 and 4 are separated by a Unit 7 field (Chapter 4). This section will attempt to explain the possible petrogenetic relationships among these three predominant units.

Any model proposed will have to explain the following:

1) Unit 1 and Unit 4 plot as distinct fields in some trace element, major element and REE plots;

2) Unit 7 plots between Units 1 and 4 on some of the trace and major plots;

3) the average SUM7REE of Unit 4 is higher than the average SUM7REE of Unit 1;

4) the Eu/Eu^* values of average Unit 4 have large negative values compared with the average Unit 1 value ($Eu/Eu^* = 1$);

5) the SUM7REE of the average Unit 7 is lower than the average of Unit 1;

6) two (of the four) Unit 7 analyses have distinct negative Eu/Eu^* values (samples NPM566 and NPM539) and two other samples (NPM583 and 560) have Eu/Eu^* values approximately equal to 1;

7) the average negative Eu/Eu^* values for Unit 4 (see Fig. 4-19) are larger than any of the negative Eu/Eu^* values of Unit 7;

The purpose of the whole-rock chemical analysis of the PMP is to provide further insight into the processes that controlled the chemical evolution of the pluton. Primary magmas are rare (Wyllie et al., 1981), and it is important to define the processes that have affected the evolution of the magmas within a pluton. The following models are considered in an attempt to determine their relative importance in the evolution of the PMP:

1) simple fractionation;

2) restite model;

3) batch melting;

4) assimilation of country rock;

5) contamination by earlier evolved granitoid phases;

6) role of fluids;

7) separate sources.

Table 5-2 is a summary of all the rocks from the PMP that have major, trace and REE analyses.

5-4-2 Fractional Crystallization

Units 1, 4 and 7 are the most abundant phases in the PMP and therefore will be tested in the following fractional crystallization model. The purpose of this modelling is to attempt to account for the between-unit variations by fractional crystallization. To demonstrate that fractional crystallization can be modelled in the PMP two rock samples from Unit 1 were used. This is the fractional crystallization Model A.

Having shown that fractional crystallization can account for the within-unit chemical variations the next step is to try to account for between unit variations by measuring/calibrating these between-unit models against Model A. Five between-unit fractional crystallization models are attempted. The assumption is made that, having demonstrated that fractional crystallization is viable for within-unit variations Model A, it is also true for other within-unit variations.

5-4-2-1 Methodology of the Fractional Crystallization Model:

Six major, trace and REE whole-rock analyses are used in this modelling (Table 5-2). The Unit 1 sample NPM533 was used as a parental magma because of its low DI values, high mg #, high anorthite compositions in its plagioclase, and lowest total whole-rock SUM7REE

Table 5-2
Table of ten whole geochemical samples and their mineral phases used in the crystal fractionation modelling.

LEGEND: trace element analyses in ppm
DI= differentiation index
BI= Mg/(Fe+Mg) content of average of three biotite grains
AN= average of three plagioclase grains (anorthite content)

UNIT SAMPLE#	WHOLE-ROCK ANALYSES								MINERAL ANALYSES	
	Sr	Zr	Y	DI	Mg+Fe	Mg/(Mg+Fe)	SUM7REE	Eu/Eu*	BI	AN
UNIT 1										
NPM584 -tonalite	385	156	11	74.3	5.3	0.27	105	1.3	*	*
NPM582 -tonalite	213	389	27	70.3	5.3	0.29	88	0.8	0.4	37
NPM 533 -tonalite	474	182	17	67.7	6.7	0.30	65	0.9	.40-.46	39
UNIT 4										
NPM558 -granodiorite	226	217	17	80.1	4.6	0.29	196	0.2	.43-.45	
NPM477 -monzogranite	113	113	16	90.1	2.3	0.21	129	0.3	.35-.39	12
NPM458 -granodiorite	139	139	22	84.4	2.9	0.28	96	0.4	.32-.36	19
UNIT 7										
NPM583 -tonalite	197	209	22	81.7	3.1	0.23	66	0.9	.35-.38	35
NPM566 -monzogranite	118	112	16	81.7	1.8	0.19	82	0.4	.36-.37	21
NPM539 -granodiorite	151	128	16	83.7	3.3	0.27	74	0.6	.44	18
NPM560 -tonalite	184	210	15	80.5	3.3	0.23	25	1.1	.38-.40	36

of the three Unit 1 whole-rock analyses. Two samples of Unit 7 were used in the modelling because of the extreme variation in the modal mineralogy of this unit. The mineral phases that were fractionated in this model are biotite, plagioclase (An40), apatite, and sphene (in Models 1, 2 and 4). Sphene was used in an attempt to model the variation in Ca content. Models were tested with labradorite (An60) fractionates instead of fractionating sphene with similar results (i.e. comparable sum of the residuum and similar fractional components of plagioclase, biotite and apatite).

The whole-rock chemical modelling is accomplished in two steps- modelling the fractional crystallization from parental magma to an evolved magma using major oxide XLFRAC Fortran program (Stormer and Nicholls, 1978), and testing the applicability of the above major oxide models to explain the observed trace element variations between the same parental and evolved magmas. The trace elements tested are REEs, Ba, and Rb. Both the Rayleigh fractionation model and the equilibrium fractionation model were used, calculated from the percentage of mineral phases fractionated as defined by the XLFRAC major oxide models. Results were compared to the actual variation in trace element concentrations between the parental magma and the evolved magma.

The six fractional models (see Table 5-4) tested are:

- Model A- This is a test model to determine the limitations of this type of modelling. The parental magma is a tonalite of Unit 1 (NPM533) and the evolved magma is also a tonalite of Unit 1 (NPM584). Theoretically the modelled evolved magma should compare favourably

with the actual evolved magma because both of these samples are from the same unit.

- Model 1- fractionation of parental magma (Unit 1, NPM533 = tonalite) evolving to average Unit 4 magma (N = 3). The fractionating phases are plagioclase (An 40), biotite (average chemical analyses from NPM533), sphene, and apatite.

Model 2- fractionation of parental magma (Unit 1, NPM533) evolving to Unit 7 (NPM566 = monzogranite). The fractionating phases are the same as Model 1.

- Model 3- fractionation of parental magma (average Unit 4 (N = 3)) evolving to Unit 7 (NPM566 = monzogranite). The fractionating phases are plagioclase (An 29) and biotite (average chemical analyses from average NPM558 (Unit 4)) and apatite.

- Model 4- fractionation of parental magma (Unit 1, NPM533) evolving to Unit 7(NPM558 = granodiorite). The fractionating phases are the same as Models 1 and 2.

- Model 5- fractionation of parental magma (average of Unit 4) evolving to Unit 7 (NPM539 = granodiorite). The fractionating phases are the same as Model 3.

5-4-2-2 The Major Oxide Fractionation Model-XLFRAC

The XLFRAC program (Stormer and Nicholls, 1978) is a simple program that solves linear least-squares mass-balance equations and can estimate the composition of the fractionate (given defined mineral phases to be removed) required to evolve the parental magma to the evolved magma. The results of the XLFRAC, major element modelling are

summarized on Table 5-3. Ten oxides were used in the modelling: SiO_2, TiO_2, Al_2O_3, FeO_t, MnO, MgO, CaO, Na_2O, K_2O and P_2O_5. The comparative 'validity' of each of the six models can be assessed by the value of the sum of the squares of the residuals. A large value indicates that the model is not a good comparison with the actual evolved magma. Model A has the lowest value for its sum of the residuals, 0.08, because both parent and evolved magma are from the same unit. Model 5 can immediately be removed as a possible model because plagioclase, sphene, and apatite cumulates must be added to the initial melt (average Unit 4) for it to evolve to the daughter magma, Unit 7 (NPM539). The model with the lowest sum of the squares of the residuals (other than the test Model A), is Model 4 (at 1.9). The second and third 'best-fit' models are 1 and 3 respectively with residuals of 3.3 and 4.2. Model 4 involves the fractionation of 11.7% biotite, 20.9% plagioclase, 0.4% sphene and 0.8% apatite from the total parental magma, a tonalite (NPM533), in order to evolve to the granodiorite of Unit 7 (NPM539). The difference in modal mineralogy in biotite and plagioclase content of Unit 1 (NPM533) and Unit 7 (NPM539) is 7% and 3%, respectively,- lower than projected by the model. For a complete summary of the five fractionation models tested see Tables 5-3 and 5-4.

5-4-2-3 Limitations of Fractional Crystallization Modelling.

The limitations of this method of modelling the fractionation history are as follows:

a) the assumption that NPM533 of Unit 1 and the average analyses of

Table 5-3
Database for the XLFRAC modelling of major elements. Major element chemistry of the inital magmas and the evolved magmas (recalculated to 100) and their fractionating mineral phases.

	1	2	3	4	5	6	7	8	9	10	11
	533	584	AVE4	539	566	BI-1	BI-4	PL-1	PL-4	SPH	AP
SIO2	64.26	68.63	71.5	71.2	73.33	37.44	35.60	59.07	61.49	31	0
TIO2	0.69	0.69	0.41	0.36	0.22	3.64	2.79	0.00	0.00	41	0
AL2O3	17.84	16.37	15.33	15.55	14.76	18.07	17.63	25.86	23.79	0	0
FEOT	4.68	3.89	2.4	1.48	20.78	20.02	0.05	0.16	0.0	0	0
MNO	0.09	0.07	0.04	0.06	0.03	0.48	0.34	0.00	0.0	0	0
MGO	2.04	1.47	0.90	0.89	0.34	9.70	9.06	0.01	0.0	0	0
CAO	4.06	3.14	1.68	2.14	0.87	0.0	0.01	7.78	6.22	29	56
NA2O	4.01	4.05	3.77	4.34	2.87	0.0	0.02	6.98	8.30	0	0
K2O	2.14	1.74	3.73	2.87	5.91	9.89	10.62	0.25	0.16	0	0
P2O5	0.19	0.13	0.22	0.19	0.18	0.0	0.0	0.0	0.0	0	44

LEGEND:
COLUMN
1= NPM533
2= NPM584, Unit 1 tonalite
3= Unit 4 samples, NPM558,477 and 458
4= Unit 7 sample NPM 539-granodiorite
5= Unit 7 sample NPM566- monzogranite
6= biotite from Unit 1 NPM533 (n=3)
7= biotite from Unit 4 NPM558 (n=3)
8= plagioclase from Unit 1 NPM533 (n=3)
9= plagioclase from Unit 4 NPM558 (n=3)
10= sphene
11= apatite

Table 5-4

Results of XLFRAC modelling of Major Oxides

Model A

initial magma=NPM533 (Unit 1)
evolved magma= NPM584 (Unit 1)

modelled fractionating component:

biotite=	8.3%
plagioclase=	15.4%
sphene=	0.14%
apatite=	0.53%
total % of fractionate=	24.36%

Observed difference between evolved magma (NPM533) and model evolved magma: (relative %)

none greater than 0.5

sum of the residuals 0.08

MODEL 1

inital magma=NPM533 (Unit 1)
evolved magma= average Unit 4 (n=3)

modelled fractionating component:

biotite =	10.9%
plagioclase=	24.4%
sphene=	0.52%
apatite=	0.79%
total % of fractionate	36.59%

Observed difference between evolved magma (average Unit 4) and model evolved magma: (relative %)

FEO_T	-0.87
CAO	-0.50
K_2O	-1.40

sum of the residuals 3.27

Table 5-4 continued...

MODEL 2
inital magma=NPM533 (Unit 1)
evolved magma=Unit 7, NPM566=monzogranite
modelled fractionating component: biotite=11.8%
plagioclase= 32%
sphene=0.95%
apatite= 0.57%

total % of fractionate = 45.14%

Observed difference between evolved magma (NPM566) and model evolved magma: (relative %)

SiO_2	-0.57
Al_2O_3	+0.65
FEO_T	-1.40
MGO	-0.70
CAO	-0.50
K_2O	+2.33
Sum of the residuals	9.03

MODEL 3
initial magma=average of Unit 4 (n=3)
evolved magama= Unit 7 (NPM566- monzogranite)
modelled fractionating component:
biotite=1.4%
plagioclase=12.9%
apatite=0.11%

total % of fractionate 13.41%

Observed difference between evolved magma (average Unit 4) and model evolved magma: (relative %)

Al_2O_3	+0.63
FEO_T	-0.84
K_2O	+1.5
sum of the residuals	3.75

Table 5-4 continued...

MODEL 4
initial magma=Unit 1 NPM533
evolved magma= Unit 7 (NPM539- granodiorite)
modelled fractionating component:

biotite	11.7%
plagioclase	20.9%
sphene	0.38%
apatite	0.76%
total % of fractionate	33.24%

Observed difference between evolved magma (Unit 7 NPM539) and model evolved magma:(relative %)

FEO_T	-0.65
K_2O	+0.97
sum of the residuals	1.94

MODEL 5
inital magma =average of Unit 4
final magma = Unit 7 (NPM539- granodiorite)

model failed because cannot fractionate from Unit 4 to Unit 7 without adding a cumulate component. This not to say that geologically this is impossible. This model may suggest that Unit 7 evolved from Unit 4 by a cumulate mineral mechanism. Because it no longer conforms to a simple fractionation model, accumulation may also have occurred.

Unit 4 (N=3) can be used as parental magmas;

b) the assumption that one can use the average chemical analyses from Unit 1 (NPM533) biotite and plagioclase for models 1, 2 and 4 and the average chemical analyses from biotites and plagioclase of Unit 4 (NPM558) as fractionating phases for models 3 and 5;

c) the assumption that all the minerals are removed during one step;

d) assuming a closed fractionation system (no input into the primary magma).

5-4-2-4 Testing the XLFRAC Models on the REE and Trace Element Analyses of the PMP.

The concentration of each trace and REE element (given the predicted mineral fractionate model) is determined by the following equations:

1) $[\ C_l/C_i\ ]_l = F'^{\,(Ds-1)}$

where: $[\ ]_l$= Rayleigh fractionation model

F'= the fraction of liquid remaining

C_i= the concentration of the element in the original melt

C_l= the concentration of the element in the differentiated liquid

D_s= the bulk distribution coefficient given by:

$D_s = W_aK_a + W_bK_b + \ldots$

where: K= solid-liquid partition coefficient between mineral and melt, and W = weight fraction of the element in the precipitating phase. This model is based on the quantitative description of the

distillation process developed by Rayleigh (1896)- (see Arth, 1976). This equation is for the simplified case of crystallization of phases of constant proportions with constant distribution coefficients (Greenland, 1970).

2) $[C_l/C_i]_2 = 1/ (F' + D_s (1-F'))$

where: $[ ]_2$= equilibrium fractionation model

This fractional model assumes equilibrium between the total crystallizing solid and melt, and may be more applicable to the plutonic conditions where the cooling of an intruded magma is extremely slow so that the crystallizing phases may be in total equilibrium with the melt (Rittman, 1973, p. 18).

The REE elements used in the modelling are Ce, Eu, Yb and Lu. Two trace elements are used, Ba and Rb. Kd values for plagioclase, biotite and apatite were obtained from Sultan et al., (1986). The Kd values for sphene are derived from dacite and rhyolite rocks (from Henderson, 1984, p27).

By solving the value of $[C_l/C_i]_1$ (Rayleigh fractionation model) or $[C_l/C_i]_2$ (equilibrium fractionation model) and using the F' values obtained from the major oxide XLFRAC model and calculated bulk distribution of the element (D_s) (based on the mineral proportions specified by the XLFRAC model) one can compare the modelled $[C_l/C_i]_{1 \text{ or } 2}$ value with the actual value $[C_l/C_i]^*$ obtained by the concentration of the element in the parent and evolved magma. The results are listed on Table 5-6.

5-4-2-5 Discussion of Trace Element Fractionation Model Results

Results from Model A indicate that the modelling of the trace elements is unsuccessful. Because of the obvious problems in the major oxide Model 1 (large sum of the residual value), it was not tested further using trace element fractionation. Models A, 1, 3 and 4 were tested and the results are listed in Tables 5-5 and 5-6. The wide and irregular variations between modelled trace element compositions and actual trace element compositions in the evolved magma and the initial magma (even in Model A), suggests that there is no simple model to explain the fractional crystallization between Units 1, 4 and 7 on the basis of trace elements alone . This may be a function of poor selection of initial and evolved magma, poor selection of mineral fractionates, poor selection of Kd values, inaccurate trace element whole-rock values, or failure of simple fractionation to explain the observed evolutionary patterns observed.

If one assumes that the trace element modelling was not succesful because of the Kd's, it may be possible to make some conclusions based on trace element behaviour and the XLFRAC major element models. With increasing fractionation of mineral phases, the SUM7REE (Ce, Eu, Yb, and Lu) decrease according to the Rayleigh and equilubrium models within each model tested. Using the values of the 'sum of the residual', the SUM7REE's and the Eu/Eu^* values as indicators of the validity of the models tested, the best-fit models (in descending order) are Model A, Model 4, Model 1, Model 3, Model 2 and Model 5. A large 'sum of the residuals' value excludes Model 2 (9.03) as a viable model. Model 5 is also excluded because it requires a cumulate

Table 5-5
REE and Ba, Rb concentrations (ppm) of inital magmas and evolved magmas and mineral Kd's

LEGEND:
column:
1= NPM533, Unit 1
2= NPM584, Unit 1
3= average of Unit 4 (NPM558,477 and 458)
4= NPM566, Unit 7=monzogranite
5= NPM539, Unit 7=granodiorite
6= precision of whole-rock trace element analyses -reproducibility of individual elements (deviations from repeat analyses)
7= Kd's of plagioclase from Bishop Tuff,Sultan et al., 1986
8= Kd's of biotite from Bishop Tuff, Sultan et al., 1986
9= Kd's of sphene from dacite and rhyolite rocks, Henderson (1984, p27)
10=Kd's of apatite from dacite and rhyolite rocks, Henderson (1984, p27)

	1 533	2 584	3 ave4	4 566	5 539	6 %	7 PL	8 BI	9 SPH	10 AP
Ce	38.51	67.96	80.85	48.70	43.41	5	0.35	3.49	53.3	29.6
Eu	1.21	1.34	0.86	0.64	0.75	3	6	0.87	101	9.22
Yb	1.38	0.87	1.43	0.60	1.70	2	0.18	0.69	37.4	232
Lu	0.20	0.10	0.18	0.07	0.23	1	0.18	0.8	26.9	199
Ba	601	475	654	963	399	9	1.7	7	-	-
Rb	71	71	128	157	128	1	0.19	5.3	-	-

Table 5-6
Trace element crystal fractionation modelling using equilibrium fractionation models and Rayleigh fractionation models.

Legend:

D_s= bulk distribution values calculated on the basis of published Kd values

$[C_l/C_i]$*= actual ratio of the element concentration in the evolved magma divided by the element concentration in the initial magma

$[C_l/C_i]_1$= the concentration of the trace element in the evolved magma divided by the concentration in the initial magma- based on equation # 1, Rayleigh fractionation model.

$[C_l/C_i]_2$= the concentration of the trace element in the evolved magma divided by the concentration in the initial magma - based on equation # 2, equilibrium fractionation.

MODEL A: Initial Magma= Unit 1 (NPM533)
Evolved Magma= Unit 1 (NPM584)

	Ds	$[C_l/C_i]$* actual	$[C_l/C_i]_1$ model 1	$\frac{[C_l/C_i]_1}{[C_l/C_i]^*}$ comparability	$[C_l/C_i]_2$ model 2	$\frac{[C_l/C_i]^2}{[C_l/C_i]^*}$ comparability
Ce	2.38	1.76	0.68	0.38	0.75	0.43
Eu	4.89	1.1	0.34	0.31	0.52	0.47
Yb	5.46	0.63	0.29	0.46	0.48	0.76
Lu	4.92	0.5	0.34	0.68	0.52	1.04
Ba	3.45	0.79	0.51	0.64	0.63	0.79
Rb	1.91	0.87	0.78	0.90	0.82	0.94

MODEL 1: Initial magma = Unit 1 (NPM533)
Evolved magma = average Unit 4

	D_s	[Cl/Ci]* actual	[Cl/Ci]1 model 1	$\frac{[C_l/C_i]1}{[Cl/Ci]^*}$ comparability	$[C_l/Ci]_2$ model 2	$\frac{[C_l/C_i]2}{[Cl/Ci]^*}$ comparability
Ce	2.40	2.10	0.52	0.25	0.66	0.31
Eu	5.47	0.71	0.12	0.17	0.38	0.54
Yb	5.34	1.04	0.13	0.13	0.38	0.37
Lu	4.61	0.90	0.19	0.21	0.42	0.47
Ba	3.23	1.08	0.3	0.33	0.55	0.51
Rb	1.73	1.8	0.7	0.39	0.79	0.44

Table 5-6 continued...

MODEL 3 : initial magma= average of Unit 4
evolved magma= Unit 7 (NPM566-monzogranite)

	D_s	[Cl/Ci]* actual	[Cl/Ci]1 model 1	$[C_l/C_i]_1$ [Cl/Ci]* comparability	$[C_l/Ci]_2$ model 2	$[C_l/C_i]_2$ [Cl/Ci]* comparability
Ce	0.90	0.60	1.0	1.7	1.01	1.68
Eu	5.50	0.74	0.51	0.69	0.61	0.82
Yb	2.09	0.42	0.85	2.02	0.87	2.07
Lu	1.84	0.39	0.88	2.26	0.89	2.28
Ba	2.20	1.47	0.83	0.56	0.86	0.59
Rb	0.70	1.22	1.05	0.86	1.04	0.85

MODEL 4 : initial magma= Unit 1 (NPM533)
evolved magma = Unit 7 (NPM539- granodiorite)

	Ds	$[C_l/C_i]$* actual	$[C_l/C_i]_1$ model 1	$[C_l/C_i]_1$ [Cl/Ci]* comparability	$[C_l/C_i]_2$ model 2	$[C_l/C_i]_2$ [Cl/Ci]* comparability
Ce	2.56	1.13	0.52	0.46	0.65	0.58
Eu	5.21	0.62	0.17	0.27	0.41	0.66
Yb	5.36	1.23	0.16	0.13	0.40	0.33
Lu	4.64	1.15	0.22	0.19	0.45	0.39
Ba	3.50	0.66	0.35	0.53	0.54	0.82
Rb	1.98	1.80	0.67	0.37	0.75	0.42

component.

Model A, as expected, shows the lowest 'sum of the residual value' (at 0.08). The best-fit model is Model 4. This model invokes the fractionation of biotite, plagioclase, sphene and apatite from a tonalite of Unit 1 (NPM533) to evolve to a granodiorite of Unit 7 (NPM539). The Eu/Eu^* ratios (Table 5-1) also support this model where Eu/Eu^* decreases from 0.9 (in the parental magma) to 0.6 in the evolved magma, as would be expected with the removal of plagioclase. The SUM7REE of the parental and evolved magma are comparable at 65 and 75 respectively. The next 'best-fit' model is Model 1 (parental magma is Unit 1 (NPM533) and the evolved magma is average Unit 4). Its 'sum of the residual' value is 3.27 (significantly higher than Model 4). The Eu/Eu^* ratio decreases from 0.9 in the parental magma to 0.3 in the evolved magma, as is expected with the removal of plagioclase. The SUM7REE of the parental magma is significantly lower (65) than the evolved magma (140) and it is questionable whether Model 1 represents a viable model or not. The third 'best-fit' model is Model 3 (parental magma = average Unit 4, evolved magma= monzogranite of Unit 7 (NPM566)). Its 'sum of the residual' value is 3.75, a relatively large value, and is questionable whether this is a viable model. The Eu/Eu^* ratio in the parental magma (0.3) is comparable to the evolved magma (0.4). This is unexpected considering the large quantity of fractionated plagioclase (13%) that is required in the modelling. The SUM7REE of the parental magma (82) is lower than the evolved magma (140), this being in direct contrast with the increase in value of the evolved magma in Model 4.

In conclusion, the major element modelling, in conjunction with Eu/Eu^* values, suggests that the mafic end-member of Unit 1 (NPM533) may be related to the granodiorite of Unit 7 (NPM539) by fractional crystallization of biotite, plagioclase, sphene and apatite (Model 4). It is not possible to evolve average Unit 4 to a granodiorite of Unit 7 (Model 5) and it is not possible to evolve the mafic end-member of Unit 1 (tonalite-NPM533) to Unit 7 (monzogranite (NPM566)) by simple fractional crystallization processes (Model 2). It is not clear whether Unit 1 tonalite can evolve to a Unit 4 (average) or whether Unit 4 (average) can evolve to a monzogranite of Unit 7 by the process of simple fractionation as specified in this modelling. In all discussions of between cycle crystal fractional models it is assumed that at depth a magma chamber (from which the PMP was derived) has remained a melt (or partial melt).

5-4-3 Restite Model

The restite model (White and Chappell, 1977) is an attempt to explain the geochemical and mineralogical characteristics of granitoids and their restites in terms of the separation of a melt from its source region. White and Chappell (1977) suggested that because of the high viscosity of the partially crystallized melt, wall and roof rocks are less likely to become incorporated into granitoid magma and that 99% of the xenoliths found in granitoids are pieces of relict source rock. Their restite model suggests that the biotite, aluminosilicates (mostly sillimanite), cordierite, and garnet in the

granitoid rock may be "restite" or residual minerals remaining after partial melting of the source rock. Milky quartz inclusions, mostly fist-sized, are common in the granitoids studied by White and Chappell (1977) and are interpreted as being a result of the segregation of vein quartz from the high-grade metamorphic source terranes. Near-linear chemical trends are thought to be the products of restite unmixing (White and Chappell, 1977).

Arguments against the restite theory are given by Clemens et al., (1983) and Wall et al., (1987). They pointed out the ambiguity of the evidence in support of the restite model. Clemens et al., (1983) suggested that less than 99% of the xenoliths in granitoids are remnants of the source rock. The textures of some xenoliths (cognate inclusions, or products of hybridisation) in many granitoids indicate their magmatic crystallization and even where xenoliths are demonstrably non-magmatic they may not be representative of the source rock (Clemens et al., 1983). Xenocrysts (i.e. plagioclases with corroded calcic cores, pyroxenes, garnets and cordierite) commonly regarded as restite have magmatic explanations compatible with their textural and phase relations. Near linear chemical trends purported by Chappell and White (1977) to be characteristic of unmixing, can also be exhibited by granitoid/volcanic suites which show no evidence for appreciable restite (Clemens et al., 1983).

In light of the ambiguity of the evidence in support of the restite model, little discussion will be made on the probability of the PMP conforming to this model. Two points should be made in regard to the PMP: very few of the whole-rock chemical plots show

well-defined linear plots, and there are no obvious 'exotic' xenoliths in the PMP, all could be from the country rock or are cognate enclaves. The variation in composition and the texture of the xenoliths of the SMB, ranging from quartzofeldspathic, potassic-feldspar porphyries, 'ghost' xenoliths (Jamieson, 1974), and biotite schlieren, may be a function of the degree and duration of alteration of the xenoliths by the surrounding granitoid melt.

5-4-4 Batch Melting Model

Batch melting involves the partial melting of a source rock under conditions of continuous equilibrium between the liquid phase and the residual solid until the removal of the liquid from the solid. It is unlikely that the PMP has evolved as a result of batch melting. In the simplest model, the inital batch melt should contain the highest concentration of LIL's and the most felsic melts (closest to minimum melt composition). During the petrogenesis of the PMP the first phase emplaced was the mafic tonalite of Unit 1. Three cycles derived from an initial mafic end-member evolve to more felsic end-members. The three cycles begin with Units 1, 4 and 7 and evolve to their felsic end-members Units 3, 6 and 9 respectively. The late-stage felsic end-members are enriched in LIL's compared with their corresponding mafic end-members.

The batch melting model does not effectively describe the evolutionary history of the PMP, either on the overall scale (from Unit 1 to Unit 9) or within Cycles I, II or III. A complex trapping system whereby the initial felsic melts (high LIL's) are held at a

lower level until later, more mafic melts formed, requires further evidence.

5-4-5 Assimilation of Meguma Rocks

Partially digested xenoliths of Meguma origin are abundant at the margins of the PMP, and less so in the interior of the pluton. Liew (1979) and Muecke (unpubl. data) have analysed the REE content of lithological subdivisions in the Meguma Group. Muecke and Clarke (1981) observed that the whole-rock REE patterns of the Meguma Group rocks bracket the range of the SMB (and therefore the PMP (Fig. 6-3)). Following this reasoning, the total assimilation of the Meguma Group rocks by the PMP will not have a large effect on the overall REE composition of the PMP. The average REE content of the PMP magma probably underwent little modification by the assimilation of the Meguma Group. Assimilation of the Meguma Group does not explain the REE evolution of Unit 1 to Unit 4 where the SUM7REE's increase. The rate of decrease in SUM7REE between Units 4, 7 and 9 and between Units 1 and 3 may have been retarded by the assimilation of the Meguma.

5-4-6 Assimilation of Earlier Plutonic Units

Extensive contamination of Unit 4 by Unit 1 is unlikely given the superheated conditions required by a granodiorite to melt a tonalite. The presence of xenoliths of Unit 1 in Unit 4 suggests that at least minor local contamination may have occurred. The major and trace element contents of whole-rocks of Unit 1 and 4 become more similar in composition toward the interior of the pluton. Magma mixing may have

occurred in the interior of the pluton in locations where Unit 1 was probably semi-liquid during the emplacement of Unit 4.

Unit 7 may have been contaminated by earlier Unit 1 or Unit 4 magmas. The similarities in modal mineralogy of Unit 7 (tonalite) and Unit 1 (tonalites), may suggest that Unit 7 has been contaminated by Unit 1 (or is a retapped magma from the Unit 1 source reservoir). The similarities in modal mineralogy of the Unit 4 monzogranites with the more felsic end-members of Unit 7 (monzogranites) may indicate that Unit 7 was contaminated by Unit 4 magmas during the later phases of emplacement. The degree of contamination by earlier granitoids is difficult to model and will not be attempted in this thesis.

5-4-7 Role of Fluids

Products of the late stages of each cycle within the PMP show evidence of aqueous fluids (i.e. pegmatite and aplite dykes). Greisenization and polymetallic mineralization are not evident in the late phases of any of these cycles. The lamprophyre dykes of Unit 5A were emplaced with an abundance of hydrous fluids, shown by the abundance of hydrous mineral phases. The brecciated texture of Unit 5B may have been produced by the contact of hot magma with hydrous fluids. The biotites from this unit have minor chlorite alteration and the feldspars are cloudy, showing minor fluid interaction. There is no evidence to support the hypothesis that the petrogenesis of the PMP was controlled by fluid alteration (i.e. no evidence of the effects of 'fluid alteration fronts' in the main phase granitoids of Units 1, 4 and 7 exists).

5-4-8 Different Sources

The XLFRAC major element modelling, the SUM7REE contents and the Eu/Eu^* values support the hypothesis that Unit 4 and the mafic end-members of Unit 7 (tonalite and granodiorite) may have different sources and that Unit 1 (tonalite) and the mafic end-member of Unit 7 (tonalite and granodiorite) may have the same source. Normative Qz-Ab-Or plots (Fig. 5-1), indicate that Units 1 and 7 samples plot in the same field supporting the hypothesis that Unit 1 and Unit 7 may have similar sources and Unit 4, having a different source plots further towards the Or apex than Unit 1 and 7. Units 1 and 7 do not plot in the granitic field as defined 'sensu stricto', whereas Unit 4 does. The source of Unit 4 was probably in the crust. Because of the higher temperatures required to produce tonalites compared to granites and granodiorites of Unit 4, the source rock of Unit 1 was probably deeper in the crust than Unit 4 or in the upper mantle. The mafic dykes of Unit 5A (lamprophyres) have exotic whole-rock, major and trace compositions which indicate that they may be of mantle origin.

5-5 Proposed three-stage model of the evolutionary history of the PMP.

The key observations that this model seeks to explain are:
1) the apparent lack of whole-rock chemical evidence to support a simple fractional crystallization history relating Units 1, 4 and 7;
2) the apparent relationship between Unit 1 and the tonalites and granodiorites of Unit 7, and the lack of conclusive evidence that

would indicate a relationship between Unit 1 and Unit 4, or Unit 4 and the tonalites and granodiorites of Unit 7;

3) the apparent different source regions of Units 1, 4 and 5A;

4) the apparent mantle source region for the Unit 5A lamprophyres and possibly Unit 1;

5) the emplacement history of the ten units observed in the PMP;

6) the apparent perturbation in the crustal isotherms to attain P-T conditions required to produce tonalites in the crust (see Wyllie, 1983).

The model is summarized in three stages (Fig. 5-5):

Stage 1: A hot spot in the upper mantle (elevation of the isotherms) facilitated the generation of Unit 1 tonalite. The melt of Unit 1 probably evolved from the metaluminous lower crust or upper mantle material (tonalite requires high T conditions). Heat from the Unit 1 source area caused melting above it, and produced a Unit 4 melt chamber at higher levels in the crust. Migration of Unit 1 to its level of emplacement involves some contamination by Unit 4 during its ascent through the Unit 4 melt zone and country rock contamination. Unit 4 was emplaced after the emplacement of Unit 1. Unit 2 is a segregate of Unit 1 enriched in plagioclase and quartz and depleted in biotite. Unit 3 evolved from Unit 1 by crystal-liquid fractionation.

Stage 2: An ultramafic magma from the upper mantle (Unit 5A-lamprophyres) was emplaced after the consolidation of Units 1 and 4. The tonalite breccia of Unit 5B was emplaced close, spatially and temporally, to the Unit 5A lamprophyre dykes. Unit 5B may be a

remnant from the Unit 1 chamber. Its matrix has similar modal mineralogy to that of the mafic Unit 1. Unit 6 (a leucomonzogranite) may be an evolved felsic end-member of Unit 4 that was emplaced late in the emplacement history of Cycle II.

Stage 3: The initial magmas of Unit 7 were probably the most mafic phases (tonalite of Unit 7). They may have evolved from the same lower crustal areas as Unit 1 by a reheating event because a high T is required to produce a tonalitic composition. During the upward migration of Unit 7 past the semi-consolidated source chamber of Unit 4, Unit 7 underwent considerable contamination, shown particularly in the more felsic phases of the unit. Units 8 and 9 are felsic magmas that probably evolved from Units 4 and 7. Continual fractionation of plagioclase, and biotite and subsequent enrichment of residual water may have evolved the late-stage massive pegmatite complexes of Unit 9.

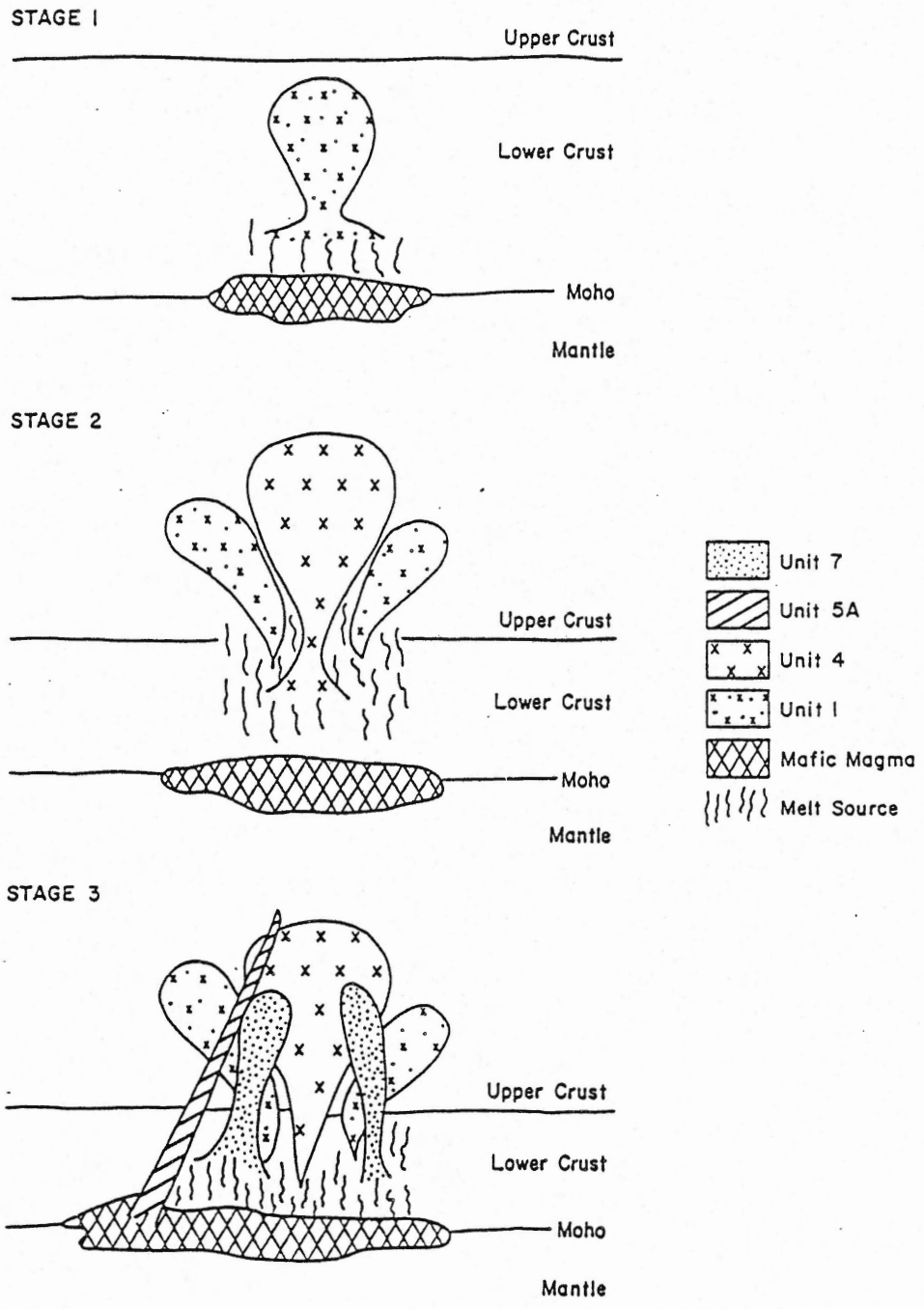

Figure 5-5: Cross-sections showing the proposed petrogenetic model for the PMP. The felsic end-members of Cycles I, II and III (including Units 3,6,8 and 9) are not illustrated in order to simplify the diagram.

Chapter 6 THE PORT MOUTON PLUTON IN RELATION TO SOUTHERN AND NORTHERN PERALUMINOUS GRANITOID BODIES IN SOUTHWESTERN NOVA SCOTIA.

6-1 Introduction

Studies of peraluminous granitoid rocks of the Meguma Zone have recorded distinct differences in the age, composition and mode of emplacement of the granitoid bodies in the northern and southern zones. This section reviews the differences between the northern and southern plutons (and batholiths) and attempts to determine whether the PMP is similar to either the northern or southern plutons. The dividing line separating the northern and southern plutons was placed on the basis of differences in granitoid rock types, metamorphic grade in the regional country rock and preliminary age dates of the plutons. The SMB is considered to be a northern batholith and, as such, the line separating northern and southern plutons had to run south of the SMB. The northern plutons (as defined in this thesis) include the South Mountain Batholith, Musquodoboit Batholith, Liscomb Pluton, Canso Pluton, Bull Ridge Pluton, Sherbrooke Pluton and the Ellison Lake Pluton. The southern plutons include Bald Mountain, Moose Point, Strawberry Point, Shelburne, Quinan, Barrington Passage, Wedgeport, Breton, Seal Island, Beach Hill, Deception Lake, Lyons Bay and Western Granite Plutons (Fig. 2-2). The Port Mouton Pluton is located in the southern Meguma Terrane in the zone occupied by southern plutons.

6-2 Petrographic Variations between the Northern and Southern Plutons

The SMB is the largest northern pluton and is a post-Acadian, epizonal, peraluminous, granitoid batholith (McKenzie, 1974) with three dominant intrusive units; biotite granodiorite, two mica-monzogranite, and late-stage leucomonzogranites. Many other smaller granitoid plutons outcrop northeast of the boundary which delimits southern and northern plutons. They are peraluminous and similar in composition to the SMB. These plutons include the the main complex of the Liscomb Pluton (King et al., 1975: Giles and Chatterjee, 1986, pers. comm.), the Musquodoboit Batholith (MacDonald, 1981; MacDonald and Clarke, 1985), the Halfway Cove and Queensport Plutons (Ham, 1988, pers.comm.), the Sangster Lake and the Larrys River Pluton (O'Reilly, 1986, pers. comm.), and the Canso Pluton (Hill, 1986). In general, the compositions of the northern plutons range from granodiorites to monzogranites with no associated early melanocratic intrusions (e.g. tonalites). Two granitoid bodies have early melanocratic intrusions associated with them. They are the tonalites of the peraluminous Canso Pluton (Hill, 1986) and early the gabbros associated with the Liscomb Complex (Giles and Chatterjee, 1986).

In southwestern Nova Scotia, predominantly peraluminous plutons include the Brenton Pluton (O'Reilly, 1976; Clarke et al., 1979; Longstaffe et al., 1979), the Wedgeport Pluton (Taylor, 1967; Longstaffe et al., 1979; Reynolds et al., 1981; Keppie and Cormier, 1983; Chatterjee et al., 1985), the Barrington Passage Pluton (Taylor, 1967; Smith, 1979; Longstaffe et al., 1979; Kubilius, 1983; Rogers,

1985; Elias, 1986 pers.comm.), the Lyons Bay Pluton (de Albuquerque, 1979; Rogers, 1986 pers.comm.), the Moose Harbour Pluton (Weagle, 1983), and the Port Mouton Pluton (Elias, 1986; Kubilius, 1983; Reynolds et al., 1981; Longstaffe et al., 1979; Smith, 1979; de Albuquerque,1977).

These southern plutons are more varied in composition than the northern plutons and often contain early mafic material. Collectively, their compositions range from lamprophyre, high K-diorite, norite, hornblende biotite tonalite, biotite tonalite trondhjemite, granodiorite, monzogranite, and leucomonzogranite. The PMP includes lamprophyre, biotite tonalite, granodiorite, monzogranite and leucomonzogranite and, in this respect, it is like the other southern plutons.

6-3 A Comparison of $^{40}Ar/^{39}Ar$ Ages and Emplacement Histories.

Five samples from three northern plutons (Musquodoboit, Liscomb and Canso), yield an average $^{40}Ar/^{39}Ar$ radiometric age of 365.5 $\pm$ 4.3 Ma in agreement with the those from SMB (at 366.7 $\pm$ 11 Ma) (Reynolds et al., 1981). The Canso Pluton has a similar age of 368 $\pm$ 8 Ma (Reynolds et al., 1981) although it is unlike other northern plutons because of its tonalite association. The SMB, the Musquodoboit Batholith (MacDonald, 1981), the Liscomb Pluton (Giles and Chatterjee pers. comm., 1986), Canso Pluton (Hill, 1986), the Halfway Cove and Queensport Plutons (Ham, 1986 pers. comm.) all post-date the Acadian deformation and regional metamorphism of the Meguma Group. The Liscomb Pluton, Halfway Cove Pluton, Queensport Pluton, and the

Canso Pluton have been variably deformed by the Glooscap Fault and therefore predate the fault.

Apparent $^{40}Ar/^{39}Ar$ ages from biotite and muscovite spectra of samples from the Barrington Passage, Bald Mountain, Shelburne, Port Mouton, Quinan and the Upper Clyde River pegmatite, all southern plutons, yield an average age of 337 $\pm$ 16 Ma, younger than the SMB (Elias, 1986). Biotite and muscovites from the Bald Mountain monzogranites yield $^{40}Ar/^{39}Ar$ ages of 340-370 Ma. Dallmeyer and Keppie (1987) recorded $^{40}Ar/^{39}Ar$ muscovite and biotite plateau ages from the Shelburne Pluton yield ages of 234.4 $\pm$ 0.9 and 308.6 $\pm$ 0.5 Ma, respectively . A high K-diorite yield ages from 310 to 382 Ma (Reynolds et al., 1987) associated with the Shelburne Pluton. The oldest ages obtained from the southern plutons come from Bald Mountain and Barrington Passage Plutons, ranging from 386 to 370 Ma (Elias, 1986). $^{40}Ar/^{39}Ar$ biotite plateau age of 312.7 $\pm$ 0.4 Ma was recorded from the Barrington Passage Pluton. Biotite and muscovite $^{40}Ar/^{39}Ar$ ages from a shear zone developed in the Brenton granite yield plateau ages from 325 $\pm$ 0.8 and 321.6 $\pm$ 1.3 Ma, respectively (Dallmeyer and Keppie, 1976). Biotite and muscovite spectra of PMP samples analysed by Elias (1986) and this study (see Appendix E) yield plateau ages ranging from 309 to 343. These ages are significantly younger than the average ages derived for samples from the northern plutons.

Elias (1986) suggested that the intrusion ages of all of the granitoid plutons in southwestern Nova Scotia, including the SMB, have been reset, and that the original cooling ages of the southern plutons have been obliterated from most domains by overprinting (Elias, 1986).

The overprinting associated with shearing is reflected by the varying degrees of discordance in the age spectra from the southern plutons. This discordance is readily apparent in the $^{40}Ar/^{39}Ar$ samples analysed for the PMP (Elias, 1986; and this thesis, Appendix E) where relative ages of the samples are not in agreement with field relations.

There is evidence that some of the southern plutons were emplaced before or during the Acadian Orogeny, compared with the apparent post-tectonic emplacement of the northern plutons. The Brenton Pluton was emplaced prior to the regional foliation (O'Reilly, 1975). Rogers (1986 pers. comm.) argues that the foliations in the Barrington Passage and Shelburne Plutons are evidence of pre- or syn-tectonic (Acadian) emplacement of the plutons. Field relationships show that the Port Mouton Pluton was emplaced after the regional deformation that produced folding in the surrounding country rock (see Chapter 2).

6-4 Metamorphic grade comparisons.

The metamorphic grade in the Meguma Group ranges from greenschist to amphibolite facies in both the northern and southern Meguma Zone. The northern zone is dominated by metamorphism of greenschist facies and no granitoid bodies in the northern zone have migmatized contacts. A linear, regional, amphibolite-grade zone is located in northeastern Nova Scotia subparallel to the Glooscap Shear Zone (Muecke, 1984). This high grade metamorphic zone encompasses the Canso, Halfway Cove, Queensport, Larrys River and Sangster Lake Plutons (Keppie and Muecke, 1979), (Fig. 6-1). The southern zone contains few greenschist facies areas and is dominated by the amphibolite to upper amphibolite facies.

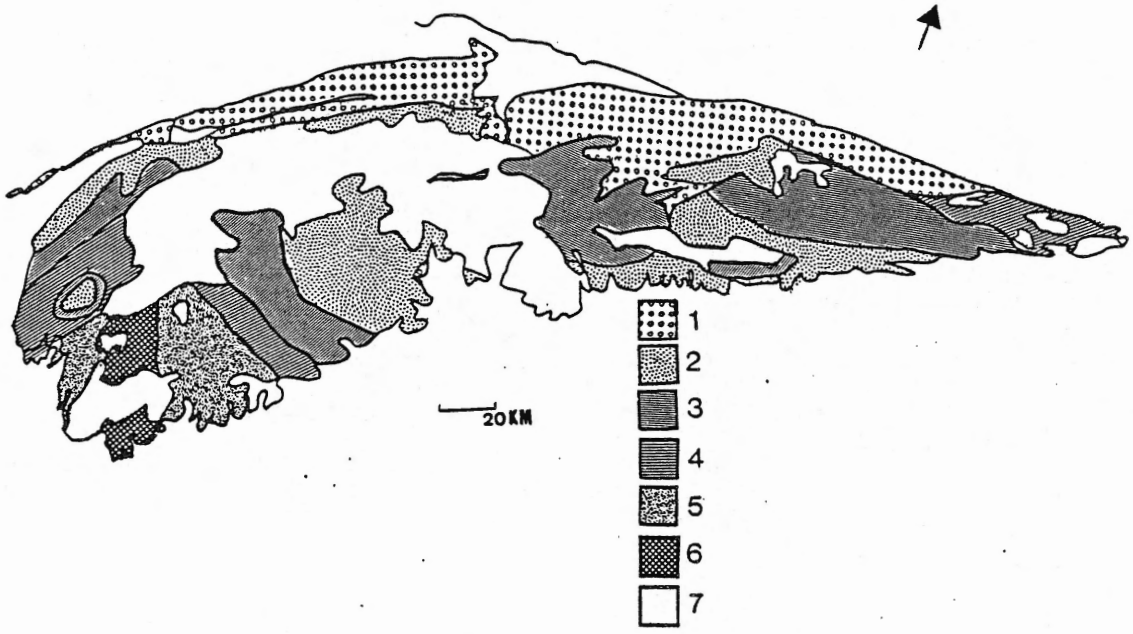

Figure 6-1: Regional metamorphic map of southern Nova Scotia (compiled by Keppie and Muecke, 1979).

Legend:			
	Subgreenschist Facies	1	
	Greenschist Facies	2	-chlorite zone
		3	-biotite zone
	Amphibolite Facies	4	-garnet zone
		5	-andalusite-staurolite cordierite zone
		6	-sillimanite zone
	Granitoids	7	

Extensive migmatization parallels the margin of the Barrington Passage Pluton. Minor migmatization occurs along the northeastern contact of the Port Mouton Pluton. It is significant to note that the amphibolite zone in northeastern Nova Scotia may reflect a different tectonic setting from that of southwestern Nova Scotia, a setting in which the Glooscap Shear Zone may have controlled the thermal pattern and granite generation (Muecke, 1984).

Assuming that Elias (1986) is correct in postulating that all the Meguma Zone granitoids were emplaced during the same time period, the predominance of amphibolite facies in the south may reflect a corresponding increase in the depth of emplacement of granitoids.

6-5 A Comparison of Oxygen and Sulfur isotopes in granites.

On the basis of $\delta^{18}O$ whole-rock data, Longstaffe et al., (1979) were able to distinguish SMB samples (Northern Zone) from the southern pluton samples (Port Mouton, Shelburne, Barrington Passage, Wedgeport and Brenton Plutons) on the basis of $\delta^{18}O$. The SMB whole rock $\delta^{18}O$ range from 10.1 to 12.0 ppm, whereas the southern satellite plutons have lower $\delta^{18}O$ (7.8-10.4 ppm). The Brenton Pluton (northwest of Yarmouth) is much lower, at 5.0 ppm, than any of the other southern plutons analysed. Longstaffe et al., (1979) suggested that this is the result of exchange with low $\delta^{18}O$ fluids during the shearing of the pluton.

The granite and granodiorite samples from the Port Mouton Pluton contain 8.9-10.4 ppm of $\delta^{18}O$, within the upper range of the other southern plutons. The relatively high $\delta^{18}O$ of the peraluminous SMB

indicates that it formed by anatexis of ^{18}O-rich metasedimentary rocks. The southern plutons were also derived by partial melting of clastic metasedimentary rocks, but their lower $\delta^{18}O$ values reflect exchange of the source material with a low ^{18}O reservoir (mafic magmas?) prior to, or during, anatexis (Longstaffe et al., 1981). Kubilius (1983) distinguished the SMB from the southern satellite plutons (Barrington Passage, Shelburne and Port Mouton Plutons) on the basis of $\delta^{34}S$ whole-rock values. Fifteen SMB samples of granodioritic composition range in whole-rock $\delta^{34}S$ values from +5.4 to 10.1 per mil, with an average of 7.3 and a standard deviation of 1.2 per mil. These same southern plutons show distinctly different sulfur isotopic signature compared with the SMB. Eleven of the twelve samples of various rock types range from 0.1 to 6.0 per mil (average 3.0). A PMP sample containing xenoliths of the isotopically heavy Goldenville greywacke, yielded a $\delta^{34}S$ value of 14.6 per mil. Two other PMP samples (devoid of xenoliths) are within range of the southern plutons (at 1.0 and 4.0 per mil). Kubilius (1983) suggested that the marked variation in $\delta^{34}S$ whole-rock contents of SMB and southern pluton samples indicates distinct histories for the two groups of granitoids. Although the southern plutons are closer to the $\delta^{34}S$ mantle value of 0 $\pm$ 1 per mil than the SMB, all are displaced somewhat from that value.

6-6 A Comparison of Granite Whole Rock Chemistry

6-6-1 Brief Description of the Nova Scotia Database

The Nova Scotia database was compiled by Richard (in progress, 1988) and consists of selected major and trace elements of 413

published and unpublished samples from granitic plutons and batholiths in southern Nova Scotia (Fig. 2-2). It includes samples from the following plutons and batholiths of the Meguma Zone: the SMB, the Musquodoboit Batholith, the Liscomb Pluton, the Halfway Cove and the Queensport Pluton, the Sherbrooke Pluton, the Bull Ridge Pluton, the Sangster Lake and Larrys River Pluton, the Ellison Lake Pluton, the Moose Point Pluton, the Barrington Passage Pluton, the Bald Mountain Pluton, the Seal Island Pluton, the Shelburne Pluton and the Port Mouton Pluton.

The REE database is considerably smaller than the major and trace element database and contains analyses of 36 samples from published studies of northern plutons. It includes samples from the South Mountain Batholith and the Musquodoboit Batholith. All samples in both the major/trace database and the REE database were the least altered samples from the plutons or batholiths. Hydrothermal alteration zones (i.e. greisens) were excluded. The samples in both databases span a wide range of rock types from amphibole tonalites and biotite tonalites to granodiorites and monzogranites. It is important to note that the southern plutons have a larger volume of more mafic granitoids (e.g. tonalites and granodiorites) than do the northern plutons and, therefore, the whole-rock chemical variations observed between these two populations may reflect only a difference in rock types. In the northern pluton database there are no tonalite samples. All analyses cited in both the whole-rock trace/major database and the REE database are referenced in Richard (1988).

6-6-2 Separation of Northern and Southern Plutons by Multivariate Analysis

Richard (1988) was able to subdivide the Nova Scotia database into two distinct chemical zones on the basis of whole-rock, major and trace element chemistry. Multivariate analysis showed that certain elements were distinct in their abundance and were diagnostic of either northern or southern plutons (Richard, 1988). The elements used in the most statistically valid model were: SiO_2, TiO_2, Al_2O_3, Fe_2O_3, MgO, CaO, Na_2O, K_2O, P_2O_5, Ba, Rb and Sr. Coefficients in the multivariate equation are listed in Table 6-1. The validity of the model is assessed by a high percentage of correctly classified analyses (93.5%, Table 6-1).

Figure 6-2 shows histograms of the discriminant scores of each of the plutons tested using this model. The northern plutons have values greater than -0.2 and the southern plutons have values of less than -0.2. Analyses from the PMP were 96.1% correctly classified and their discriminant scores are within the range of the southern plutons.

6-6-3 Rare earth elements

The REE database consists of northern pluton analyses only with 36 REE samples from the South Mountain Batholith and the Musquodoboit batholith.

Figure 6-3 is a chondrite-normalized (Haskin et al., 1966) plot of the samples from the SMB and the Musquodoboit Batholith. They possess a similar range of values as the 13 analyses of the PMP samples (Figs. 4-19 and 4-20). Most of the samples from the northern

Table 6-1 MODEL 1 Discriminating northern and southern plutons (batholiths) on the basis of whole-rock chemistry (Richard, 1988).

GRANITE	CORRECTLY CLASSIFIED		MISCLASSIFIED	
	#	%	#	%
-NORTHERN-				
SMB -Charest	17	100	0	0
-McKenzie	16	88.9	2	11.1
-Smith	32	100	0	0
-Richardson	8	100	0	0
Musquodoboit	9	90	1	10.0
Liscomb	8	88.9	1	11.1
Sherbrooke	17	94.4	1	5.6
Bull Ridge	10	83.3	2	16.7
Sangster Lake and Larry River	29	96.7	1	3.3
Halfway Cove and Queensport	36	100	0	0
Ellison Lake	13	92.9	1	7.1
-Southern-				
Barrington Passage	31	100	0	0
Shelburne	22	81.5	5	18.5
Bald Mountain	4	100	0	0
Port Mouton	50	96.1	2	3.9
Moose Point	6	75.0	2	25.0
Lyons Bay Seal Island Western Granite	6	60.0	4	40.0

DESCRIMINANT FUNCTION USING THE FOLLOWING ELEMENTS:
SiO_2-TIO_2-Al_2O_3-Fe_2O_{3T}-MgO-CaO-Na_O-K_2O-P_2O_5-Ba-Rb-Sr
Coefficients:

Rb	+0.9477
Ba	-0.6998
CaO	-0.6205
Sr	+0.5033
TiO_2	+0.5025
K_2O	+0.3966
Fe_2O_3	+0.3148
P_2O_5	-0.3012
MgO	+0.1196
Na_2O	+0.0335

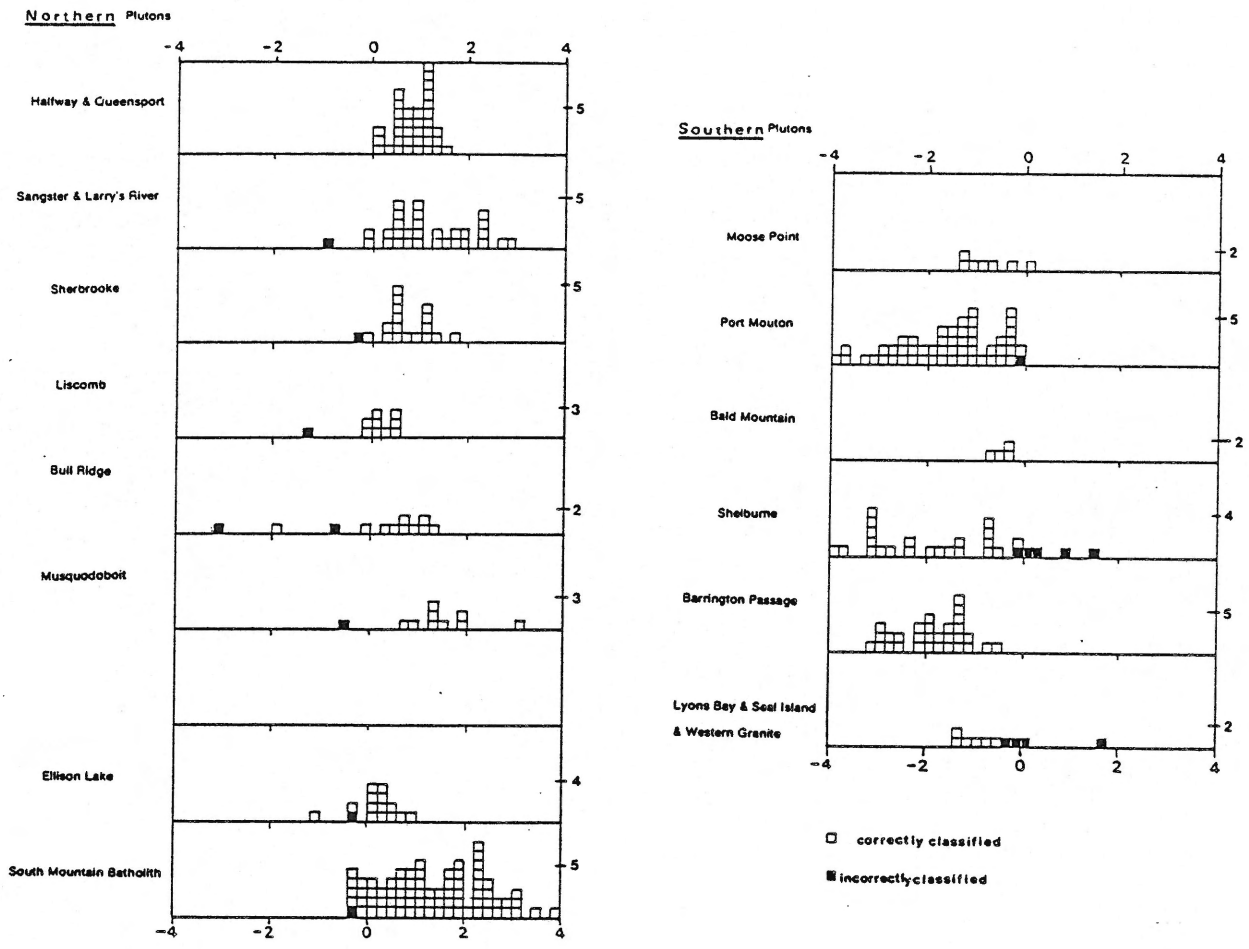

□ = correctly classified
■ = incorrectly classified

Figure 6-2: Model 1. Discriminant scores of northern and southern plutons in Nova Scotia, based on the discriminant function of Model 1. (after Richard, 1988). See Table 6-1.

database have significant negative europium anomalies. Only Units 4 and 9 have significant negative europium anomalies in the PMP samples. There is a progressive decrease in the SUM7REE values corresponding with increasing differentiation of samples from the SMB and Musquodoboit Batholith (see Muecke and Clarke, 1981; MacDonald, 1981). This pattern is not reflected in the PMP samples where the decrease in SUM7REE fall in this order; average Unit 4, Unit 5A, average Unit 1, average Unit 7, Unit 3, Unit 9. The PMP appears to have undergone a more complex history than the two northern batholiths for which REE data exist.

6-7 Conclusions:

The southern plutons differ from the northern plutons in that:

1) the $^{40}Ar/^{39}Ar$ biotite and muscovite ages in the south generally are younger than the northern pluton ages;

2) the southern plutons have a wider variation in composition than the northern plutons;

3) some of the southern plutons may have been emplaced syntectonically during the Acadian Orogeny, whereas the northern plutons are post-tectonic (post Acadian deformation);

4) the regional metamorphic grade and style differ between the south and the north (Fig. 6-1);

5) migmatization often occurs in association with the southern plutons but does not occur in the northern plutons;

6) whole-rock oxygen isotope values indicate that the southern plutons are isotopically different from the northern plutons

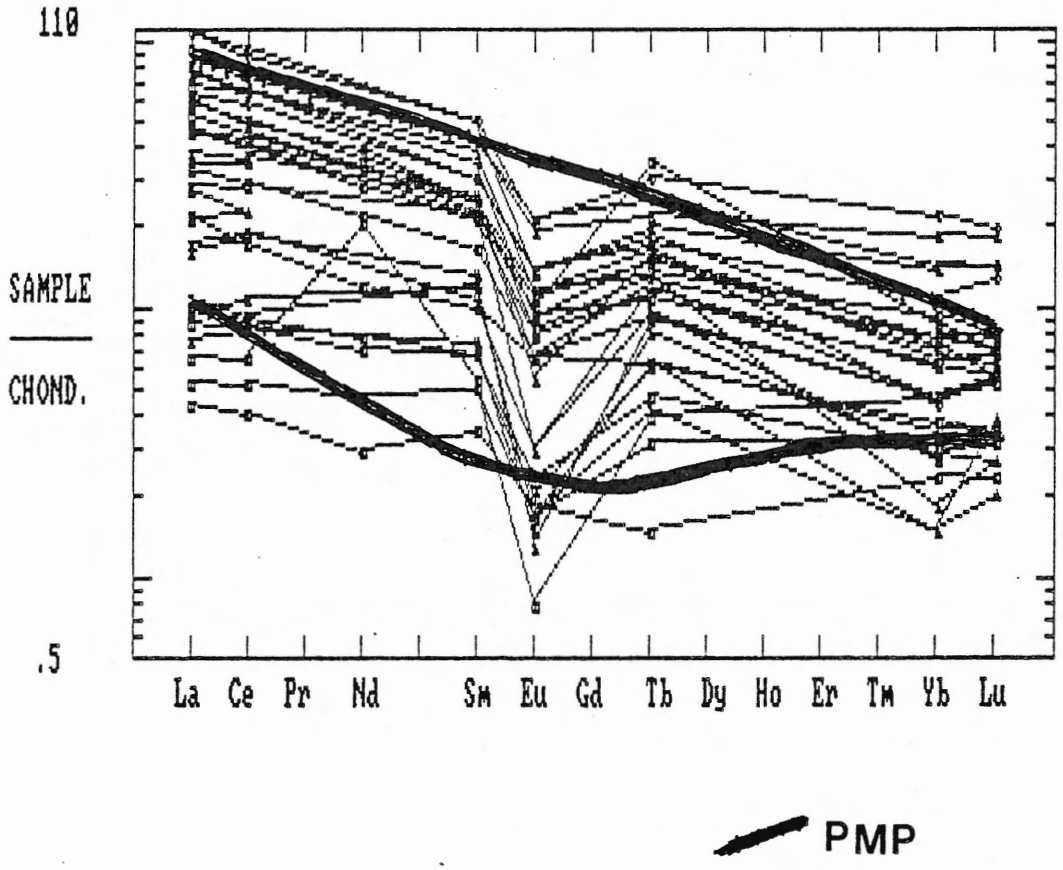

Figure 6-3: Whole-rock REE chemical analyses of selected samples from the South Mountain Batholith and the Musquodoboit Batholith compared with the Port Mouton Pluton. All samples are normalized to chondrite values of (Haskin et al., 1966).

(Longstaffe et al., 1981);

7) whole-rock sulphur isotope values indicate that the southern plutons are isotopically different from the northern plutons (Kubilius, 1983);

8) the northern and southern plutons can be distinguished on the basis of their whole-rock, geochemical analyses by a multivariant equation (Richard,1988);

9) whole-rock available REE data indicate that the southern plutons are not distinct in their REE abundances compared with the northern plutons, but their distribution within individual plutons is variable.

The Port Mouton Pluton is similar to the southern plutons in that it:

1) has similar $^{40}Ar/^{39}Ar$ biotite and muscovite ages to most southern plutons;

2) shows similar, wide, variations in composition (i.e. the PMP varies from a tonalite to a monzogranite);

3) is located in the southern zone;

4) possesses local migmitization;

5) has whole-rock $\delta^{18}O$ values similar to those of the southern plutons;

6) shows whole-rock $\delta^{34}S$ values similar to the southern plutons;

7) has whole-rock chemistry is comparable to the southern plutons (Richard, 1988).

In conclusion the Port Mouton Pluton has many features similar to the southern plutons suggesting that they are of similar origin. The southern plutons may have been derived from lower in the crust than

the northern plutons (based on the metamorphic grade of the surrounding country rock, sulphur and oxygen isotopes, and the presence of more melanocratic rock types, like tonalite).

CHAPTER 7 CONCLUSIONS AND RECOMMENDATIONS

7-1 Conclusions

The following are the more significant conclusions from this study of the PMP.

1. The Port Mouton Pluton is a complex, peraluminous, post-tectonic body that is distinct from the northern plutons and batholiths of the northeastern Meguma Terrane. One of its distinctive characteristics is that it contains two mafic phases, tonalites and lamprophyres, not observed in the northern plutons. These mafic phases may have an important bearing on the evolution of the PMP. The whole-rock geochemistry of the PMP is distinct from the northern plutons (batholiths) and is similar to the whole-rock chemistry of the southern plutons.

2. The PMP contains at least ten distinctive lithologies.

3. The PMP is a post-tectonic intrusive body that deflects the regional foliation in the country rock.

4. The PMP was emplaced at a pressure of approximately 3.5 kilobars and temperatures of at least 650^{o} C. These conditions were estimated by the andalusite-cordierite-sillimanite-garnet assemblage in the contact aureole of the PMP and by Qz-Or-Ab normative plots of whole-rock chemical analyses.

Minor migmatization occurs in some portions of the margins of the PMP (Merrett, 1987). Other contacts between the pluton and the country rock are sharp.

5. The foliation of Unit 1 tonalite is perpendicular to the foliation

of the country rock and is believed to be of igneous origin. The foliation in Unit 4 is local and perpendicular to Unit 1, and its origin is unknown. The banding may have been produced as a function of emplacement (flow banding) or as a result of regional deformation when the magma was still ductile. The orientation of the Unit 4 foliation and its coarse and fine banding is parallel to the regional foliation in the surrounding country rock.

6. The petrology of the PMP granitoid rocks are relatively simple involving varying proportions of quartz, plagioclase, potassic feldspar (predominantly microcline), muscovite, biotite and traces of garnet, and very rarely rutile. Apatite and zircon are ubiqitous. The shoshonitic lamprophyres that intruded the pluton mid-way through its emplacement history have a distinctive mineralogy compared with the granitoids of the PMP. This mineralogy includes phlogopite, amphibole and sphene.

7. The PMP evolved in three mafic-to-felsic cycles, defined by the initial mafic end-members for each cycle (Units 1, 4 and 7). These intrusive cycles may not be genetically unrelated. Both mineral-chemistry (biotite and plagioclase) and whole-rock chemical analyses (trace elements, rare earth elements and Qz-Ab-Or normative plots) suggest that the chemistry of Unit 1 is distinct from Unit 4.

8. Simple, fractional crystallization cannot explain the major and trace element variations observed between Unit 1 and Unit 4 (see XLFRAC Model 1).

9. Unit 1 and the tonalites and granodiorites of Unit 7 may be related by the fractionation of plagioclase, biotite, sphene and apatite from

the 'parental', Unit 1 magma. This hypothesis is supported by major element fractional crystallization modelling (see XLFRAC Model 3), Eu/Eu* values compatible with this modelling and similar Qz-Or-Ab normative values.

10. Unit 7 has the largest variation in its mineralogical composition, ranging from tonalite to granodiorite to monzogranite. Unit 7 was probably derived by crystal fractionation of Unit 1 and by contamination by Unit 4 which is particularly evident in the more felsic rocks. Trace and REE plots of Unit 7 have whole-rock elemental abundances intermediate between Unit 1 and Unit 4, supporting the crystal fractionation hypothesis for the origin of Unit 7.

11. Simple batch-melting models cannot adequately explain the evolution of the PMP Units from a biotite tonalite of the initial phase (Unit 1) to the leucomonzogranite phases of the late phases (Units 8 and 9) because the initial melts are more mafic than the evolved melts, a situation which is difficult to model in a simple first-melt-low-mafic-composition batch-melting model.

12. As a result of not being able to demonstrate co-genetic relationships between Unit 1, Unit 4 and Unit 5A, it is concluded that there may be three distinctly separate sources for the PMP granitoids- Unit 1 (lower crust), Unit 4 (lower to intermediate level in crust), and Unit 5A (mantle).

13. $^{40}Ar/^{39}Ar$ mineral-separate plateau ages of some Units within the PMP indicate that they are at least 352 million years old (the oldest 'preserved' age in the PMP) but clearly are younger that the regional metamorphic age of 395 Ma (Elias, 1986). The lamprophrye dykes have

similar $^{40}Ar/^{39}Ar$ ages as the PMP granitoid phases, at 328 ± 0.9 Ma (based on phlogopite mineral separate analyses) (Appendix E).

14. The PMP is similar to other southern plutons in the Meguma Terrane with respect to:

- $^{40}Ar/^{39}Ar$ biotite and muscovite ages
- whole-rock composition, $\delta^{18}O$, $\delta^{34}S$
- local migmatization.

7-2 Recommendations For Future Work

The primary purpose of this thesis was to map the PMP and describe the mineralogy, petrology and geochemistry of the pluton and its relationship with other granitoid units in the Meguma Terrane. Many possibilities for further studies became apparent in the course of the investigation.

Because of inadequate opportunity to observe the following features in detail it is recommended that:

1. a detailed investigation be made of the migmatite contacts in select areas of the PMP (e.g. Merrett, 1987). These areas may give better insight into the emplacement P-T conditions of the PMP.
2. a more detailed investigation of the leucomonzogranite phases in the pluton (i.e. Units 3, 6, 8 and 9) in order to determine their relative chemical variation and their origin.
3. detailed mapping, and mineral and whole-rock analysis of the extensive pegmatite dyke complexes of Unit 9. These pegmatites contain rare, large crystals of beryl. The dykes are commonly complexly zoned. Using the report by Oldale (1959), it is recommended

that selected pegmatite areas be remapped to determine the evolutionary history of the pegmatite dykes.

4. the economic potential of the PMP be investigated. Preliminary investigation for beryl, tin and uranium have been undertaken by various private companies and the provincial government.

5. a detailed study of the internal structure of the PMP be conducted addressing the two different foliations developed in the PMP granitoid units (Unit 1 and Unit 4) and origin of the coarse and fine-banding within Unit 4 (observed on the mainland and on Mouton Island). Preliminary work was completed (Maksaev, 1986) on the fine-banding on Mouton Island.

Because of inconclusive results obtained from samples and techniques available for this study, further studies to advance the understanding of the PMP are suggested.

- Determine by radiometric methods (i.e. Rb^{87}/Sr^{86} dating methods), the relatives age of Units 1, 4 and 7:
- Use Nd and Sm isotopes to determine the genetic relationship between Units 1, 4 and 7.
- Continue to attempt to model, by fractional crystallization, the petrogenesis of the PMP.
- Compare the lamprophyre dykes of the PMP with all mafic dykes of similar age (approximately 340 to 320 Ma) in the Meguma Terrane to determine if they are genetically related.
- Compare the tonalites of Unit 1 from those associated with other southern satellite plutons (i.e. Barrington Passage and Shelburne plutons).

APPENDIX A

Petrographic Descriptions of Chemically Analyzed Samples

B-1 Definitions of Terms Used in the Petrographic Descriptions

1. Quality of Outcrop

excellent- large outcrop with abundant fresh surfaces

good- large to intermediate-sized outcrop with some fresh surfaces

fair- intermediate to small outcrop with few fresh surfaces

poor- glacial pavement or ocean shoreline, weathered outcrop with rare fresh surfaces

2. Degree of Alteration (by thin section analyses)

5 = no obvious alteration of minerals, no brittle deformation

4 = minor feldspar kaolinisation and muscovite alteration

3 = moderate feldspar kalinisation and muscovite alteration, minor brittle deformation

2 = extensive feldspar kaolinisation and muscovite alteration and moderate brittle deformation

1 = extensive secondary alteration of minerals and/or brittle deformation

3. Grain Size

Coarse > 4 mm

Medium 1-4 mm

Fine < than 1 mm

4. % of Mafics (biotite and amphibole)

Melanocratic > 20%

Mesocratic 10-20%

Leucocratic < 5%

Petrographic Descriptions of Chemically Analyzed Samples

UNIT 1

NPM11 m.g. subporphyritic mafic tonalite, 0.8 km south of Forbes Point

Quality of Outcrop:fair, shoreline
Degree of Alteration:3+
Mafic Content: 23%
Grain Size: matric 1-1.5mm, plagioclase=3.5-5 mm

Groundmass comprised of medium grained assemblage of quartz, (exhibiting undulose (mosaic) extinction), well zoned, normally zoned plagioclase, biotite (containing inclusions of zircon and apatite) and muscovite (matrix and often overgrowing biotite). Accessory minerals include apatite (0.03-0.15mm) associated with biotite and rare anhedral opaque minerals associated with biotite. The overall texture is subporphyritic with occasional 3.5-4mm phenocrysts of zoned plagioclase. The plagioclase (An36) contains rare inclusions of biotite. The centres of the zoned plagioclase are kaolinised. Moderate sericitization is common in the plagioclase. Muscovite occurs only as alteration products of biotite and plagioclase.

NPM 2 m.g. subporphyritic mesocratic tonalite, 2.5 km S.E. of Summerville Beach

Quality of Outcrop:good, shoreline
Degree of Alteration:4+
Mafic Content: 10%
Grain Size: matric 1-1.5 mm, plagioclase porphyries 3-5 mm

Groundmass comprised of m.g.-c.g. assemblage of undulose quartz, biotite (minor chloritization and often kinked) muscovite (often kinked) and normally zoned plagioclase (An24). The overall texture of the groundmass is hypidiomorphic granular. Biotite often contains zircons, and are altered by muscovite. The muscovite is found in two modes 1) overgrowths of biotite 2) distinct grains (0.3-3mm) in the groundmass. Plagioclase often kaolinised along its twin planes and in the centres of the grains. Seritiziation is common. Accessory minerals include apatite (associated with biotite).

NPM 484 m.g.mesocratic granodiorite, MacLeod's Cove
Quality of Outcrop:good,shoreline
Degree of Alteration:3-
Mafic Content: 11%
Grain Size: 2-3mm

The groundmass has undergone ductile deformation. The groundmass is composed of undulose, mortar textured quartz, normally zoned plagioclase, anhedral, ragged, chloritized biotite, muscovite and microcline. The plagioclase is kaolinised along twin planes and in the centre of the grains. Minor epidote is associated with the altered plagioclase. Rare inclusions of biotite are found in the plagioclase. Muscovite occurs as both secondary and possibly primary origin. The secondary muscovite alters plagioclase and biotite. The primary looking muscovite occurs as 1-1.5 mm grains in the matrix. Microcline occurs in the groundmass and in one case as a 0.2mm outer rind on a 2mm subhedral plagioclase grain. Garnet occurs as a secondary mineral. The garnets have minor chorite alteration and are fractured and are intimately associated with the biotite. The garnets are often found as 'inclusions' in plagioclase.

NPM 487 c.g. mesocratic tonalite, 0.5 km north of Isaac Harbour
Quality of Outcrop:good,shoreline
Degree of Alteration:4
Mafic Content: 12%
Grain Size:1-6 mm

Groundmass has a hypidiomorphic granular texture. Groundmass consists of oscillatory quartz with minor mortar texture, minor chloritized biotite, muscovite and normally zoned plagioclase. The bioite grains contain inclusions of zircon and are often overgrown by secondary muscovite. The long axes of the biotites are subparallel to parallel to the long axes of the plagioclase. Secondary muscovite overgrown biotite and alters plagioclase. Possible primary muscovite found in the matrix. The plagioclase are moderately altered by kaolin and contains inclusions of earlier crystallized, zoned plagioclase, biotite and muscovite. Zircon is an accessory mineral.

NPM 533 c.g. foliated mafic tonalite, Forbes Cove
Quality of Outcrop:fair to good (weathered),shoreline

Degree of Alteration: 4
Mafic Content: 23%
Grain Size: 2-5mm

The groundmass includes planar oriented biotite,quartz, secondary muscovite, and normally zoned plagioclase (core An 39). The biotite commonly are 2 mm in size and contain a few inclusions of apatite, rutile (alteration?) and zircons. The biotite grains are well developed. Quartz occurs as small interstitial grains and as inclusions in plagioclase and as larger grains (1.5-3 mm) with occasional inclusions of biotite. The plagioclase is well zoned and contains inclusions of quartz and earlier crystallized zoned plagioclase. Minor epidote and kaolinization occurs preferentially in the cores of the plagioclase. One plagioclase grain has a distinct red coloured, altered core. Muscovite only occurs as a secondary mineral altering biotite and plagioclase. Accessory minerals include epidote, negligible anhedral opaques associated with the biotite. One 2.5 mm subhedral grain of microcline observed, and it contained no inclusions.

NPM 544 c.g. mesocratic tonalite, west of Black Point
Quality of Outcrop:fair,shoreline
Degree of Alteration:3
Mafic Content: 16%
Grain Size:0.5-6mm, ave=2.5mm

The hypidiomorphic granular groundmass includes, subhedral biotite with minor chlorite alteration, two forms of quartz (matric and porphyries (or xenocrysts)), normally zoned, plagioclase and secondary muscovite. The biotite is subhedral and contains inclusions of apatite, zircon and is often overgrown by muscovite. Plagioclase occurs in two forms a)minor, as inclusions in large quartz grains b) subhedral grains 1 to 4 mm grains which contain inclusions of plagioclase, quartz,biotite and minor mymerkite. Minor kaolinization and seritization of the plagioclase is frequent. Quartz has two forms a) as small 0.5mm grains in the matrix b) large 4-6 mm grains which contain inclusions of biotite and feldspars. Accessory minerals include microcline (with minor sericite alteration) and minor epidote needles as inclusions in the plagioclase.

NPM 582 f.g. subporphyritic mafic tonalite, Port Joli Head
Quality of Outcrop:fair to good,shoreline
Degree of Alteration:3+
Mafic Content: 21%
Grain Size: 0.2-1mm=matrix,plag. porphyries=4.5mm

Texture ductile deformation, subporphyritic hypidiomorphic granular. Groundmass consists of quartz with undulose extinction and significant subgrain developement, normally zoned plagioclase (core An36), subhedral to anhedral biotite with minor chlorite alteration and rare secondary muscovite (altering the biotite). The plagioclase occurs in two forms a) in the groundmass (0.3-0.7mm) normally zoned, with rare inclusions of biotite b) as normally zoned porphyries ranging up to 4.5 mm in size containing inclusions of plagioclase, quartz, with minor muscovite alteration. Biotite is subhedral to

anhedral and have ragged crystal boundaries. The biotite contains rare inclusions of anhedral opaques, zircons and apatite. Muscovite appears to only be secondary in origin and is intimately associated with biotite. Accessory minerals include; epidote (associated with biotite) and anhedral opaque minerals (associated with biotite), zircons and apatite.

NPM 593 c.g. mesocratic granodiorite, Mitchell Point
Quality of Outcrop:poor
Degree of Alteration:3+
Mafic Content: 12%
Grain Size:1-6.5 mm, ave=3 mm

The hypidiomophic granular groundmass consists of subhedral biotite (occasionally kinked), normally zoned plagioclase (moderately kaolinised particularly in the core), microcline, and string perthite. Biotite contains occasional inclusions of apatite and zircons and has minor overgrowths of muscovite. Plagioclase contains inclusions of quartz. Microcline occurs as large matrix grains up to 5 mm long and contains inclusions of plagioclase and biotite. Perthite(rare) is similar in size to the microcline and contains inclusions of biotite. Minor mymerkite is present. Apatite and zircon are accessory minerals.

NPM 565 m.g.-c.g.mesocratic granodiorite to tonalite, Port Mouton Head
Quality of Outcrop: fair-good,shoreline
Degree of Alteration: 4
Mafic Content: 12%
Grain Size: 1.5-3.5mm (ave), quartz up to 11mm

The texture is predominantly hypidiomorphic granular. Large quartz grains (up to 11 mm) occur in the matrix and contain inclusions of biotite. The groundmass consists of subhedral, mildly chloritized biotite (with inclusions of zircon, and apatite), normally zoned, moderately kaolinized plagioclase (contains inclusions of biotite), minor string perthite(with inclusions of biotite),traces of microcline and multiple extinction quartz. Secondary muscovite overgrown biotite and plagioclase. The large quartz grains may represent late stage quartz veining. The quartz in the 'veins' are deformed.

UNIT 2

NPM 546 c.g. subporphyritic trondhjemite, East of Black Point
Quality of Outcrop:good
Degree of Alteration:3+
Mafic Content:0-10%
Grain Size:matrix=0.5-1mm,plagioclase=3-6 mm

The groundmass has a hypidiomorphic granular texture with subporphyries of zoned subhedral plagioclase. The groundmass consists of ragged, chloritized biotite (with inclusions of zircon and apatite), plagioclase with normal zoning core (An25) and patchy zoning and quartz, minor secondary muscovite overgrows the biotite. Plagioclase contains inclusions of biotite and plagioclase, and is preferentially altered by kaolin and sericite in the core. The quartz

has multiple extinction. The muscovite appears to be secondary in origin and is imtimately associated with biotite.

UNIT 3

NPM 542 m.g.leucomonzogranite, Hwy 103, north of Robertson Lake
Quality of Outcrop:Good
Degree of Alteration:1
Mafic Content:1%
Grain Size:0.5-3mm

The texture of the groundmass is subcataclastic hypidiomorphic granular. Shear planes are prevalent are are enriched in sericite. The groundmass consists of normally zoned plagioclase (moderately kaolinised), microcline (with inclusions of quartz and plagioclase), perthite,multiple extinction quartz and minor muscovite. Muscovite is association with the biotite and plagioclase is probably secondary in origin. The subhedral muscovite grains in the matrix may be primary. Minor perthitic feldspar is common.

UNIT 4

NPM 17 m.g.mesocratic granodiorite, approx. 2 km south along Port Joli Road from Hwy 103.
Quality of Outcrop:Good
Degree of Alteration: 4
Mafic Content: 13%
Grain Size:0.5-5.5mm, ave 2mm

The groundmass has a hypidiomorphic granular texture, with occasional porphyries of quartz (up to 5.5 mm) and plagioclase (3.5mm). The groundmass consists of randomly oriented, well developed grains of biotite, normally zoned plagioclase (with inclusions of biotite and plagioclase), microcline (with inclusions of quartz and biotite) and quartz (up to 5.5 mm). The large quartz grains may be xenocrysts. Traces of secondary muscovite overgrow biotite and the cores of plagioclase. Minor kaolinisation alters the plagioclase. Accessory minerals include apatite and zircon. Rounded apatite grains (0.2mm) occur in the matrix.

NPM 32 m.g. subcataclastic mesocratic, monzogranite, Hunts Point Wharf
Quality of Outcrop:Good
Degree of Alteration: 2
Mafic Content: 5%
Grain Size: ave.=0.2-3.5mm, Plagioclase up to 5.5 mm

The groundmass has a subcataclastic texture. Quartz have moderate subgrain growth. The groundmass consists of minor chloritized biotite (with ragged grain boundaries), normally zoned plagioclase (moderately kaolinised and sericitized), microcline (with inclusions of quartz) and multiple extinction quartz (with shear planes and subgrain growth). Secondary muscovite overgrows biotite and plagioclase. Primary looking subhedral grains of muscovite (up to

1.5mm) are found in the matrix. Accessory minerals include apatite and zircons.

NPM 368B m.g.mesocratic granodiorite, West Mouton Island
Quality of Outcrop: Good
Degree of Alteration: 4
Mafic Content: 9%
Grain Size:1-3mm

The groundmass has a hypidiomorphic granular texture. The quartz appears strained and has minor subgrain growth. The mineralogy of the groundmass includes, subhedral to anhedral biotite (with ragged grain boudaries), normally zoned, moderately kaolinised plagioclase (with inclusions of quartz and biotite), microcline (with inclusions of plagioclase and quartz) and quartz. Occasional string perthites are found in the groundmass. Biotite contains inclusions of zircon and apatite and is overgrown by secondary muscovite. Traces of secondary muscovite alter biotite and plagioclase.

NPM 371 c.g.mesocratic monzogranite,N.W. Mouton Island
Quality of Outcrop:fair
Degree of Alteration:2+
Mafic Content: 6%
Grain Size: 1.5-6 mm ave.=3 mm

The groundmass has a hypidiomorphic granular texture. The groundmass consists of anhedral ragged grains of biotite (with inclusions of zircon), kaolinised, zoned plagioclase (inclusions of biotite), microcline (inclusions of biotite), and multiple extinction quartz (with inclusions of biotite). The biotite is overgrown by muscovite. Muscovite also alters the plagioclase.

NPM 440 m.g. mesocratic granodiorite, 2.5 km S.E. of Summerville Beach
Quality of Outcrop:fair to good, shoreline
Degree of Alteration: 4
Mafic Content: 16%
Grain Size:0.5-3.5 mm, ave. = 1.5 mm

The groundmass has a poorly developed foliation defined by the alignment of biotite. The texture is hypidiomorphic granular. Mineralogy of the groundmass consists of subhedral grains of biotite (wtih inclusions of zircon and apatite), minor kaolinised and sericitized normally zoned plagioclase (with minor inclusions of biotite), microcline and quartz. Traces of secondary muscovite overgrow biotite and plagioclase and primary-looking muscovite (subhedral) occur in the groundmass. Accessory minerals include zircon and apatite.

NPM 441 m.g. mesocratic monzogranite, Hunts Point Wharf
Quality of Outcrop: Good, shoreline outcrop
Degree of Alteration: 3-
Mafic Content: 7%
Grain Size: 1-3.5 mm, ave=2 mm

The groundmass has undergone ductile deformation and has a subporphyritic hypidiomorphic granular texture. The groundmass

consists of chloritized, ragged grains of biotite (with inclusions of zircon), extensively kaolinised and sericitized normally zoned plagioclase (An7), large (3.5 mm) perthites (containing inclusions of biotite, plagioclase and quartz) and moderately sericitized microcline (with inclusions of plagioclase) and multipe extinction quartz. Secondary muscovite (up to 1 mm) overgrow biotite and plagioclase. Primary looking (subhedral) muscovite overgrow the matrix. Rounded apatites (up tp 0.4 mm) occur as inclusions in biotite and in the matrix.

NPM 477 m.g. mesocratic monzogranite, 3 km south of Hwy 103 on LeHebert Rd.
Quality of Outcrop: poor to fair, road outcrop
Degree of Alteration: 3
Mafic Content: 6%
Grain Size: 1-3.5 mm, ave=2 mm

The groundmass has a hypidiomorphic granular texture. The mineralogy of the groundmass consists of chloritized, ragged grains of biotite (with inclusions of zircon), moderately kaolinized normally zoned inclusion-rich plagioclase (core=An12), (inclusions of quartz,biotite, plagioclase), microcline and quartz with minor subgrain growth and containing occasional inclusions of biotite). Trace epidote is associated with a few of the biotites. Apatites up to 2.5 mm are associated with the biotite. Traces of muscovite (grains up to 3.5 mm) occur in the matrix and contain inclusions of quartz, plagioclase and biotite. Secondary muscovite preferentially alters the cores of the plagioclase.

NPM 458 f.g-m.g. mesocratic granodiorite, 3 kms of Hwy 103 on Port Joli Road
Quality of Outcrop: fairto good, road outcrop
Degree of Alteration: 3-
Mafic Content: 10%
Grain Size: 0.5-1.5 mm

Texture is hypidiomorphic granular. The groundmass consists of ragged grains of biotite (with inclusions of zircon and minor apatite), mildly kaolinised normally zoned plagioclase (core=An22) (with rare inclusions of quartz and biotite), minor string perthite, microcline (contains inclusions of biotite and quartz) and quartz. Traces of secondary muscovite alter biotite and plagioclase. Apatite is an accessory mineral and is associated with plagioclase and biotite. A poorly developed foliation is defined by the biotite.

NPM 469 m.g.mesocratic granodiorite, 2 km S. of Hwy103 on Port LeHebert Road
Quality of outcrop: poor, road outcrop
Degree of Alteration: 3-
Mafic Content: 10%
Grain Size: 0.3-2.5 mm, ave=2 mm

Texture is hypidiomorphic granular. The groundmass consists of subhedral biotite (with inclusions of zircon and apatite), normally zoned, mildly kaolinised plagioclase (with inclusions of biotite),

large icroclines (up to 5.5 mm) with inclusions of quartz, biotite and plagioclase. Quartz also occurs in the groundmass. Secondary muscovite alters biotite and plagioclase. Primary-looking muscovite (subhedral, up to 2.5mm) overgrow the matrix and contain occasional quartz inclusions.

NPM 472 f.g.-m.g. mesocratic monzogranite, Junction of Hwy 103 and Port LeHebert Road
Quality of Outcrop: good, road outcrop
Degree of Alteration: 1
Mafic Content: 7%
Grain Size:0.2-2 mm

The groundmass has undergone ductile deformation and has hypidiomorphic granular texture. The groundmass consists of anhedral ragged moderately chloritized grains of biotite (with inclusions of zircon), kaolinized and often kinked normally zoned plagioclase, sericitzied microcline and quartz. Secondary muscovite up to 2 mm alters biotite, plagioclase and microcline. Primary-looking subhedral grains (up to 2 mm) overgrow matrix.

NPM 511 m.g. mesocratic monzogranite, South Spectacle Island
Quality of Outcrop: fair to good, shoreline
Degree of Alteration: 2-
Mafic Content: 5%
Grain Size 0.1-4.5 mm, ave=2mm

This sample has been deformed as is evident by the many slippage planes observed in thin section. The overall texture is hypidiomorphic granular. The quartz grains exhibit undulose extinction and are stretched parallel to the slippage planes. The groundmass consists of minor chloritized, ragged, anhedral grains of biotite (with inclusions of zircon), normally zoned, moderately kaolinised plagioclase (with rare biotite inclusions), rare string perthite (with inclusions of plagioclase and biotite), microcline and quartz with extensive subgrain growth. Secondary muscovite overgrows biotite and plagioclase and large (up to 1.5 mm) grains (often kinked) overgrow the matrix. The matrix muscovite is possibly of primary origin.

NPM 535 m.g.-c.g. subporphyritic mesocratic granodiorite, 0.5 km north of Forbes Cove
Quality of Outcrop: good,shoreline
Degree of Alteration: 3+
Mafic Content: 9%
Grain Size: 1-6 mm, ave=2.5mm

The texture is subporphyritic hypidiomorphic granular. The groundmass consists of ragged biotite grains (with inclusions of apatite and zircon), kaolinized, normally zoned plagioclase (containing inclusions of string perthite, quartz and biotite), microline (with inclusions of quartz), quartz (with minor subgrain growth). The perthite grains are overgrown by secondary muscovite. The grains of perthite and microcline are up to 4.5 mm in length giving the rock a subporphyritic texture. Secondary muscovite alters

the perthite, plagioclase and biotite. Primary looking muscovite (euhedral grains in matrix up to 1.5 mm) in the matrix.

NPM 536 m.g. mesocratic granodiorite, 0.5 km north of Forbes Cove
Quality of Outcrop: good, shoreline
Degree of Alteration: 3-
Mafic Content: 8%
Grain Size: 0.5-6 m, ave= 2mm, occasional 6 mm porphyries of microline.

The groundmass is predominantly hypidiomorphic granular. Minor shearing (characterized by elongation of quartz) is prevalent. The groundmass consists of subhedral, poorly chloritized biotite (with inclusions of zircon and apatite), normally zoned subhedral, poorly kaolinised plagioclase (with inclusions of biotite and quartz), anhedral and embayed grains of microcline (with abundant inclusions of quartz, plagioclase, biotite and muscovite) and multiple extinction, elongated quartz grains. Microcline grains occasionally are 6 mm in length. Secondary muscovite alters plagioclase,biotite and microcline and 0.5 mm grains (possibly of primary origin) are located in the matrix.

NPM 543 m.g. mafic granodiorite, West of Black Point
Quality of Outcrop:fair, shoreline
Degree of Alteration: 3+
Mafic Content: 26%
Grain Size:0.5-3 mm

The texture is hypidiomorphic granular. The groundmass consists of subhedral grains of biotite (with inclusions of zircon and apatite), subhedral moderately kaolinised and sericitized plagioclase (with occasional inclusions of biotite), quartz and minor interstitial plagioclase. Accessory minerals include apatite, zircon and rutile. The rutile occurs as inclusions in biotite. The groundmass contains minor mymerkite.

NPM 548 m.g. mesocratic monzogranite, Black Point
Quality of Outcrop: fair to good, shoreline
Degree of Alteration: 3-
Mafic Content: 8%
Grain Size: 0.5-5.5 mm, ave=3-4 mm

The groundmass has a hypidiomorphic granular texture. Deformation is evident by the elongation of the quartz and kinking of some of the muscovite. The groundmass consists of ragged grains (reddish-brown) of mildly chloritized biotite (contains inclusions of zircon), moderately kaolinised normally zoned plagioclase (contains inclusions of biotite) occasional string perthite (large grains up to 5 mm), moderately kaolinised microcline (contains inclusions of zoned plagioclase, strained quartz with moderate subgrain growth). Muscovite occurs as an alteration of plagioclase and biotite and as large interstial grains in the matrix. The muscovite is occasionally kinked. The larger quartz appear to be quartz veining in sample. The width of the vein is approximately 1 mm wide.

NPM 549 m.g. mesocratic granodiorite, East of Black Point
Quality of Outcrop: fair to good, shoreline
Degree of Alteration:3-
Mafic Content: 15%
Grain Size: 1.5-4 mm

The groundmass has a hypidiomorphic granular texture. The mineralogy consists of subhedral, mildly chloritized biotite (with inclusions of zircon and apatite), patchy and normally zoned moderately kaolinised and sericitized plagioclase, microcline (with inclusions of biotite), rare string perthite, and quartz (up to 4.5 mm). Secondary muscovite alters biotite and plagioclase. Occasional large matrix grains of muscovite (3.5 mm) may be primary in origin.

NPM 551 m.g.-c.g. subporphyritic mesocratic monzogranite, House Cove
Quality of Outcrop: fair to good, shoreline
Degree of Alteration: 3
Mafic Content: 13%
Grain Size: ave 2-4 mm, some quartz and microcline up to 11mm

The texture is subporphyritic, hypidiomorphic granular. The groundmass consists of subhedral to anhedral biotite (with inclusionsof zircon and apatite), large subhedral (up to 5 mm) of moderately kaolinised normally zoned plagioclase, large up to 11mm inclusion-rich microclines (inclusions of plagioclase, quartz and biotite), a few grains of perthite (inclusions of plagioclase, muscovite and quartz), and multiple extinction quartz (up to 7 mm long)(contains inclusions of apatite, biotite and minor mymerkite). Secondary muscovite (up to 3 mm) alters biotite, plagioclase and microcline. There are a few primary looking muscovite (subhedral, inclusion-free) in the matrix. Traces of anhedral opaques occur as inclusions in muscovite. The large quartz grains may be quartz veining in sample. Width of the vein is 2 mm. The quartz is strained within this 'vein'.

NPM 556 c.g. mesocratic monzogranite, West of Port Mouton Head
Quality of Outcrop: poor
Degree of Alteration: 3
Mafic Content: 9%
Grain Size: 0.5-7 mm, ave= 4.5 mm

The texture is hypidiomorphic granular. The quartz grains are elongated and show moderate subgrain growth. The groundmass consists of anhedral, ragged grains of mildly chloritized biotite (contains inclusions of zircon and apatite), moderately kaolinised normally zoned plagioclase (with inclusions of biotite), microcline (with inclusions of plagioclase), string perthite (up to 5.5 mm)(with inclusions of biotite), and multiple extinction, elongated quartz. Secondary muscovite alters biotite and plagioclase. Primary-looking muscovite (subhedral) up to 0.75 mm is found in the matrix.

NPM 558 m.g. mesocratic granodiorite, Port Mouton Head
Quality of Outcrop: fair, shoreline
Degree of Alteration: 3
Mafic Content: 16%

Grain Size: 0.5-3.5 mm, ave=1.5 mm, plgioclase up to 3.5 mm

The texture is predominantly subporphyritic hypidiomorphic granular with minor brittle deformation (quartz subgrain growth). The groundmass consists of anhedral, moderately chloritized biotite (with inclusions of zircon and apatite), moderately kaolinized normally zoned plagioclase (Core= An29) (contains inclusions of biotite, plagioclase and quartz), microcline, multiple extinction quartz and minor string perthite. The plagioclase grains are up to 3.5 mm long. Apatite occurs as an accessory mineral and is found as inclusions in biotite and in the groundmass.

NPM 578 m.g. mesocratic monzogranite, New House Cove
Quality of Outcrop: fair to good, shoreline
Degree of Alteration: 3
Mafic Content: 10%
Grain Size: 1.5 to 4.5 mm, ave= 2mm

The texture is hypidiomorphic granular. The groundmass consists of subhedral grains of biotite (with inclusions of zircon and apatite), normal and patchy zoned minor kaoinized and sericitized plagioclase (with inclusions of biotite), microcline (inclusions of plagioclase, biotite and quartz), minor string perthite (with inclusions of quartz and plagioclase) and multiple extinction quartz. Occasional quartz grains up to 3.5 mm in diameter. The microcline has embayed grain boundaries. Traces of secondary muscovite alter biotite and plagioclase and primary looking muscovite occurs in the matrix.

NPM 580 m.g. leucocratic monzogranite, Bull Point
Quality of Outcrop: fair to good, shoreline
Degree of Alteration: 3-
Mafic Content: 4%
Grain Size: 1-4.5 mm, ave=1.5mm

Texture is subpophyritic hypidiomorphic granular. The groundmass consists of ragged chloritized biotite, normally zoned (core = An18)moderately kaolinized plagioclase (contains inclusions of quartz), kaolinised string perthite (up to 3 mm) (inclusions of quartz,plagioclase and biotite), sericitized microcline, and quartz. Muscovite occurs as subhedral (up to 2 mm) grains in the matrix (inclusions of quartz and feldspar) and as secondary overgrowths of biotite.

NPM 581 m.g. mesocratic granodiorite, Bull Point
Quality of Outcrop: fair to good, shoreline
Degree of Alteration: 3+
Mafic Content: 12%
Grain Size: 0.5-4.5 mm, ave=2.5 mm

The texture is hypidiomorphic granular. The groundmass consists of subhedral biotite (with inclusions of zircon and apatite (up to 0.5mm)), normally zoned plagioclase (with rare inclusions of biotite), large microcline (up to 4.5 mm) (inclusions of plagioclase, biotite and quartz), string perthite (up to 3.5 mm)(with inclusions of biotite and plagioclase), and quartz. Traces of secondary muscovite alter the plagioclase and biotite. Primary looking muscovite with biotite

inclusions overgrow the matrix (up to 2mm).

UNIT 5A

NPM 485 f.g. mafic phlogopite-actinolite shoshonitic lamprophyre, MacLeod's Cove
Quality of Outcrop:poor, shoreline
Degree of Alteration: 3
Mafic Content: 55%
Grain Size: 0.03-0.6 mm

The texture is hypidiomorphic granular with extensive recrystallization of the phlogopite and actinolite. The groundmass consists of subhedral, randomly oriented phlogopite intimately associated with actinolite (the phlogopite contains inclusions of sphene, anhedral opaques and apatite), ragged, anhedral grains of actinolite contain inclusions of sphene and apatite and normally zoned (core=An24) plagioclase contain inclusions of apatite, actinolite and phlogopite. Phlogopite occurs in two modes 1) dessiminated, descrete grains in matrix 2) as compact clusters up to 2.5 mm radius. The actinolite occurs in mat-like clusters. Accessory minerals include apatite and sphene. Sphene is subhedral and anhedral (size 0.1-0.6 mm) and is intimately associated with phlogopite and actinolite.

NPM 612 (NPM 405 recollected) m.g.-c.g. mafic phlogopite- actinolite-porphyry
Quality of Outcrop: poor to fair, shoreline
Degree of Alteration: 5
Mafic Content: 82%
Grain Size: 0.2-4.5 mm

The texture is panidiomorphic. Large (up to 4.5 mm) actinolites, phlogopites define the porphyritic texture. The groundmass consists of normally zoned (core=An54) severely kaolinised plagioclase with inclusions of phlogopite, small actinolite and anhedral apatite. Phlogopite occurs as subhedral to euhedral grains and occurs in two forms 1) separate grains with actinolite inclusions 2) large phlogopite clusters (up to 4 mm in diameter). Phlogopite contains inclusions of apatite and anhedral opaques. Actinolite is euhedral to subhedral and is altered by phlogopite. Phlogopite contains rare apatites. The opaques are anhedral and occur as inclusions in phlogopite and actinolite and as interstitital minerals.

NPM 615 (recollected NPM 406) f.g. porphyritic actinolitic-hornblende-plagioclase alkali lamprophyre, Forbes Cove
Quality of Outcrop: poor to fair, shoreline
Degree of Alteration: 5
Mafic Content: 65%
Grain Size: 0.2-0.75 mm, plagioclase porphyries 0.75-2.5 mm

The texture is porphyritic with a groundmass of glomeroporphyritic phlogopite and amphibole in a hypidiomorphic granular groundmass. The groundmass consists of clusters of subhedral actinolitic hornblende grains (with inclusions of sphene and anhedral opaques, in close spatial relationship to the phlogopite), rare quartz

(up to 0.3-0.75 mm), (contains occasional inclusions of amphibole, and subordinate phlogopite). The porphyries of plagioclase are kaolinised and normally zoned (core=An 47) (with inclusions of actinolitic hornblende, apatite and sphene). Accessory minerals include subhedral sphene (0.15-3.5 mm)as inclusions in amphibole, needle-like grains (up to 1.5 mm) of apatite (often as inclusions in plagioclase) and anhedral opaques (less than 0.03 mm) as inclusions in amphibole.

UNIT 7

NPM 464 f.g. mesocratic monzodiorite and monzogabbro, approx. 3 km south of Hwy 103 on Port Joli Road
Quality of Outcrop: good, roadside
Degree of Alteration: 1
Mafic Content: 16%
Grain Size: 0.5-5 mm, ave=1mm

Texture looks granoblastic, probably a recrystallized hypidiomorphic granular texture. Groundmass consists of subhedral biotite (with inclusions of zircon and apatite), normally zoned mildly sericitized plgioclase (with inclusions of biotite), microline (orthoclase) and quartz. A few of the plagioclase grains are 5 mm long. Quartz occurs as small interstitial grains and as large 3.5 mm grains. Minor secondary muscovite alters biotite and plagioclase. Occasional 0.5 mm muscovite grains overgrow matrix minerals.

NPM 539 m.g. mesocratic grnodiorite,Port Joli Shoreline
Quality of Outcrop: fair, shoreline
Degree of Alteration: 4
Mafic Content: 16%
Grain Size:0.3-2.5 mm, plgioclase and some quartz=2-2.5 mm

The texture is hypidiomorphic granular. The groundmass consists of subhedral grains of biotite (with inclusions of zircon and apatite), mildly kaolinized, normally zoned plagioclase (core=An18) (with inclusions of biotite and quartz), quartz occurs as groundmass minerals and as large grains with inclusions of biotite and plagioclase. The large quartz grains may be xenocrysts. Trace secondary muscovite alters biotite and plagioclase.

NPM 545 f.g. mesocratic granodiorite, Black Point
Quality of Outcrop: poor,shoreline
Degree of Alteration: 3+
Mafic Content: 13%
Grain Size: 0.2-1.5 mm, occasional 2.5 mm grains of plagioclase.

Texture is partially recrystallized hypidiomorphic granular. The groundmass consists of subhedral bioatite (with inclusions of zircon and apatite), normally zoned, mildly kaolinised and sericitized plagioclase (with inclusions of quartz and biotite),microcline and quartz. Secondary muscovite alters biotite and primary looking muscovite is interstitial in the matrix.

NPM 560 f.g.mesocratic tonalite, East of Port Mouton Head
Quality of Outcrop: poor, shoreline

Degree of Alteration: 3-
Mafic Content: 13%
Grain Size: 1 mm

Texture is hypidiomorphic granular. The grains are equigranular. The groundmass consists of well developed mildly chloritized biotite (with inclusions of zircon and apatite), normally zoned (core=An36) moderately kaolinised plagioclase (with inclusions of biotite, anhedral opaques and quartz), microcline (with inclusions of plagioclase and biotite), and quartz. Traces of secondary muscovite alters plagioclase and biotite. Trace anhedral opaques are associated with the biotite and rarely with the plagioclase.

NPM 563 m.g. mesocratic granodiorite, East Port Mouton Head
Quality of Outcrop: poor, shoreline
Degree of Alteration: 3+
Mafic Content: 10%
Grain Size: 0.75-4 mm, ave=2 mm

Texture is hypidiomorphic granular. The groundmass consists of ragged anhedral grains of biotite (with inclusions of zircon and apatite), normally zoned, moderately kaolinised and sericitized plagioclase, microcline (with inclusions quartz and biotite), quartz with moderately developed subgrain growth. Traces of secondary muscovite alters biotite and plagioclase. Primary looking muscovite is subhedral and is found in the interstices (0.75 mm).

NPM 566 f.g. mesocratic monzogranite, Port Mouton Head
Quality of Outcrop: good, shoreline
Degree of Alteration: 2
Mafic Content: 8%
Grain Size: 0.5-1 mm

The texture is hypidiomorphic granular. Minor porphyries of quartz, plagioclase and kspar are desseminated throughout the speciman. The groundmass consists of ragged grains of biotite (with inclusions of zircon), moderately kaolinised, normally zoned (core=An21) plagioclase (with inclusions of biotite, quartz and plagioclase), microcline (with inclusions of quartz and rarely biotite), minor mermykite and quartz. Traces of secondary muscovite overgrow plagioclase and biotite. Primary looking muscovite (subhedral) contains inclusions of quartz, biotite and plagioclase.

NPM 579 m.g. mesocratic granodiorite, New House Cove
Quality of Outcrop: good, shoreline
Mafic Content: 5%
Grain Size: 0.5-4 mm, ave=1.5 mm

The texture is hypidiomorphic granular. The groundmass consists of anhedral, ragged biotite (with inclusions of zircon and apatite), normally zoned, moderately kaolinsed plagioclase (contains inclusions of biotite), microcline (with inclusions of plagioclase), and multiple extinction quartz. Traces of secondary muscovite overgrows biotite and plagioclase. Primary looking muscovite (wubhedral) up to 0.75 mm occur in the interstices of the matrix.

NPM 583 f.g. mesocratic tonalite, East of Port Joli Head
Quality of Outcrop: fair to good, shoreline
Degree of Alteration: 2
Mafic Content: 5 %
Grain Size: 0.2-.75 mm, occasional 1.5-3 mm porphyries of plagioclase, muscovite and quartz

Texture predominantly hypidiomorphic granular with minor cataclastic deformation. Quartz grains are lenticular in shape. The groundmass consists of ragged chloritized biotite with inclusions of zircon), normally zoned (core= An35) kaolinised plagioclase (with inclusions of quartz, plagioclase and biotite), microcline and lenticular quartz (with inclusions of biotite). Occasional plgioclase porphyries up to 1.5-3 mm in size occur with abundant inclusions of plagioclase, quartz and biotite. The zoning in these porphyries are often patchy. Secondary-looking muscovite overgrows matrix and biotite. The minor cataclastic texture observed in this sample is also manifested by planes of slippage which are infilled by fine grained muscovite.

UNIT 8

NPM 10 m.g. mesocratic monzogranite, at wharf south of Forbes Cove
Quality of Outcrop: fair, shoreline
Degree of Alteration: 3
Mafic Content: 6%
Grain Size: 1.5-4.5 mm, ave=3.5 mm

The texture is hypidiomorphic granular. The groundmass consists of ragged, anhedral, mildly chloritized biotite(with inclusions of zircon), normally zoned moderately kaolinized and sericitized plagioclase, microcline (with large grains up to 2 mm) (with inclusions of plagioclase), and quartz (large matrix grains up to 3.5 mm). Trace secondary muscovite alters biotite and plagioclase, large muscovite grains in the interstices (up to 2.5 mm) may be primary. Muscovite contains inclusions of quartz. Occasionally muscovite grows in 'clumps'.

NPM 361 m.g. leucocratic monzogranite, north-east Mouton Island
Quality of Outcrop: good, shoreline
Degree of Alteration: 4
Mafic Content: 1%
Grain Size: 0.5-3.5 mm

The texture is hypidiomorphic seriate. The groundmass consists of ragged moderately chloritized biotite, normally zoned, moderately kaolinised plagioclase (with inclusions of quartz, plagioclase and minor biotite), large well developed microclines (with abundant inclusions of quartz, biotite and plagioclase) and multiple extinction quartz. Plagioclase occurs as matrix minerals and occasionally as large grains (2.5-3.5 mm) with inclusions of anhedral small opaques and quartz.

NPM 537 m.g. leucocratic monzogranite, 0.5 km north of Forbes Cove

Quality of Outcrop: fair to good, shoreline
Degree of Alteration: 3-
Mafic Content: 3 %
Grain Size: 0.5-2.5 mm

The groundmass has undergone ductile deformation and has a hypidiomorphic granular texture. The groundmass consists of ragged, anhedral grains of biotite (with inclusions of zircon), normal and patchy zoned (core=An13) moderately kaolinized plagioclase (with inclusions of quartz and biotite), rare string perthite (with inclusions of quartz), microcline (with inclusions of quartz), and multiple extinction extensive subgrain growth of quartz. Muscovite appears to be secondary in origin and alters biotite. It appears as clusters when altering plagioclase.

UNIT 9

NPM 491 f.g. leucotonalitic aplite, Sandy Bay Cove
Quality of Outcrop: good, shoreline
Degree of Alteration: 2+
Mafic Content: less than 1%
Grain Size: 0.1-1 mm

The texture is saccharoidal. The groundmass consists of moderately kaolinised and sericitized, anhedral, normally zoned (core=An8) plagioclase (with inclusions of quartz, apatite needles and plagioclase), mildly sericitized microcline, and embayed quartz. Muscovite occurs as subhedral grains in the matrix. Trace biotite is chloritized and occurs as anhedral 'slivers'.

NPM 8B f.g. leucomonzogranite, north of Robertson Lake on Hwy 103
Quality of Outcrop: excellent, roadside
Degree of Alteration: 1
Mafic Content: trace
Grain Size: 0.1-1.5 mm

The texture is cataclastic and saccharoidal. Quartz has undergone extensive subgrain growth. The groundmass consists of chloritized, ragged anhedral traces of biotite, normally zoned (core =An11) severely kaolinised plagioclase, sericitized microcline (with inclusions of quartz and plagioclase), multiple extinction fracture quartz and rounded, mildly chloritized euhedral to subhedral garnets. Secondary muscovite alters the feldspars and muscovite (0.2-0.5 mm) grains overgrow the matrix.

TABLE A-1

Modal Analyses of point counted samples illustrated on Q-A-P plots of chapter 2 (field relations).
Point counts were counted on a 2 mm grid.

SAMPLE	UNIT	QU %	KF %	PL %	MU %	BI %	TOTAL COUNT	GRAIN SIZE
NPM533	1	21	0	54	2	23	1030	M.G.
NPM582	1	25	0	50	4	21	1020	F.G.-M.G.
NPM584	1	32	0	48	4	16	1008	C.G.
NPM544	1	30	3	47	4	16	1100	M.G.-C.G.
NPM557	1	26	20	42	3	9	1044	C.G.
NPM58	1	24	0	53	11	11	811	C.G.
NPM252	1	41	13	33	7	7	923	C.G.
NPM461	1	22	0	57	3	18	1036	M.G.-C.G.
NPM593	1	31	12	40	5	12	1017	C.G.
NPM456	1	20	0	56	8	16	1075	M.G.-C.G.
NPM487	1	33	0	49	6	12	1014	M.G.-C.G.
NPM484	1	29	12	40	8	11	1007	M.G.
NPM11	1	22	2	52	2	23	1024	M.G.
NPM148	1	33	0	52	4	11	1003	M.G.
NPM2	1	24	0	51	4	22	1021	M.G.
NPM168	1	18	0	58	6	18	1036	C.G.
NPM346	1	20	5	57	1	16	1042	M.G.
NPM447	1	28	0	47	2	22	1047	M.G.-C.G.
NPM177	1	25	3	53	2	18	1019	M.G.-C.G.
NPM217	1	26	16	45	1	13	1021	M.G.
NPM565	1	33	5	48	2	12	1004	M.G.-C.G.
NPM546	2	19	0	68	3	10	1050	C.G.
NPM468	3	28	25	38	5	4	1023	F.G.
NPM542	3	27	26	43	3	1	1061	M.G.
NPM469	4	32	15	38	5	10	1013	M.G.
NPM535	4	30	13	45	3	9	1016	M.G.
NPM553	4	26	30	35	7	2	1013	M.G.
NPM549	4	28	13	38	6	15	1043	C.G.
NPM371	4	40	28	24	2	6	1024	M.G.
NPM567	4	26	9	42	8	15	1023	M.G.
NPM543	4	20	5	45	4	26	1005	M.G.
NPM214	4	28	23	42	3	3	818	M.G.
NPM234	4	37	20	32	5	4	835	M.G.
NPM269	4	21	24	38	7	8	843	M.G.
NPM52	4	40	13	37	5	5	1500	M.G.
NPM551	4	27	19	34	5	15	1013	M.G.-C.G.
NPM548	4	38	19	30	5	8	1053	M.G.
NPM477	4	37	30	25	2	6	1013	M.G.
NPM536	4	28	12	45	4	8	1112	M.G.-C.G.
NPM511	4	32	21	38	4	5	1017	M.G.
NPM580	4	33	36	23	4	4	1030	M.G.
NPM555	4	31	22	40	0	6	1013	M.G.
NPM581	4	26	13	46	3	12	1061	M.G.
NPM578	4	28	22	39	1	10	1023	M.G.

SAMPLE	UNIT	QU %	KF %	PL %	MU %	BI %	TOTAL COUNT	GRAIN SIZE
NPM532	4	30	16	43	4	7	1080	M.G.
NPM368B	4	28	10	50	3	9	1019	M.G.
NPM556	4	25	23	41	2	9	1010	M.G.
NPM458	4	18	9	59	4	10	1069	F.G.-M.G
NPM379	4	16	33	34	4	13	1027	F.G.
NPM494	4	21	21	45	8	5	1091	M.G.
NPM590	4	27	11	45	10	7	1075	M.G.
NPM348	4	27	11	45	10	7	1075	M.G.
NPM558	4	22	14	43	5	16	1145	M.G.
NPM540	4	24	29	31	11	5	1085	M.G.
NPM440	4	23	7	51	4	16	1016	M.G.
NPM505	4	20	30	33	11	6	1021	F.G.
NPM526	4	17	27	39	14	3	1028	M.G.
NPM391	4	29	18	44	8	7	1011	M.G.
NPM467	4	22	29	39	3	6	1291	F.G.
NPM470	4	28	14	42	4	12	1078	M.G.
NPM3	4	35	20	38	2	9	1041	M.G.
NPM240	4	22	28	38	2	9	1041	M.G.
NPM473	4	30	21	49	2	11	1052	M.G.
NPM273	4	18	6	55	1	20	1165	M.G.
NPM239	4	24	14	48	<1	13	1039	M.G.
NPM442	4	23	39	32	3	3	1048	M.G.
NPM441	4	30	22	38	3	7	1010	M.G.
NPM509	4	27	32	31	1	9	1028	M.G.
NPM472	4	22	26	42	3	6	1036	M.G.
NPM175	4	18	8	49	<1	23	1046	M.G.
NPM188	4	26	27	37	<1	9	1045	M.G.
NPM259	4	38	30	22	4	6	1014	M.G.
NPM502	4	31	32	30	2	5	1109	M.G.
NPM17	4	20	15	52	1	13	1043	M.G.
NPM32	4	33	25	35	2	5	1080	C.G.
NPM486	5B	23	0	46	4	26	1010	F.G.-C.G.
NPM538	6	29	31	35	2	3	1029	F.G.
NPM568	7	17	0	52	7	24	1017	M.G.
NPM482	7	37	34	18	5	6	1069	F.G.
NPM545	7	27	9	45	6	13	1033	F.G.
NPM508	7	34	26	29	4	7	1007	F.G.
NPM579	7	21	19	52	3	5	1033	F.G.
NPM583	7	24	3	64	3	6	1006	F.G.
NPM563	7	28	19	39	4	10	1049	F.G.
NPM566	7	20	44	24	4	8	1031	F.G.-M.G.
NPM550	7	19	15	52	3	11	1049	F.G.
NPM397	7	15	4	48	6	27	1220	F.G.
NPM436	7	20	3	47	6	24	1070	F.G.
NPM560	7	26	4	53	4	13	1043	F.G.
NPM539	7	18	12	51	3	16	1020	F.G.-M.G.
PM457	7	23	4	55	2	15	1013	F.G.
PM464	7	16	15	51	2	16	1019	F.G.

SAMPLE	UNIT	QU %	KF %	PL %	MU %	BI %	TOTAL COUNT	GRAIN SIZE
PM576	7	23	6	50	4	17	1110	M.G.
PM573	7	17	0	62	2	19	1014	M.G.
PM365	7	16	0	54	6	24	1005	F.G.
PM570	7	22	11	52	5	10	1049	F.G.
PM574	7	26	11	48	<1	15	1091	F.G.
PM298	7	19	27	43	1	11	1035	F.G.
PM479	7	23	6	49	8	15	1014	F.G.
PM185	7	27	19	42	1	11	1041	F.G.
PM183	7	29	14	45	3	10	1056	F.G.
PM300	7	22	3	53	<1	22	1007	F.G.
PM534	8	29	37	30	4	0	1015	M.G.-C.G.
PM547	8	17	25	52	3	4	1043	M.G.
PM537	8	26	30	38	3	3	1103	F.G.-M.G.
PM361	8	27	25	44	3	1	1011	F.G.-M.G.
PM10	8	29	27	36	2	6	1010	M.G.
PM575	9	25	36	31	3	5	1020	F.G.
PM491	9	27	3	59	10	1	1066	F.G.
PM541	9	18	26	47	8	1	1003	F.G.

APPENDIX B

Microprobe Analyses

B-1: Biotite Analyses (recalculations based on 24 oxygens).

LEGEND for all microprobe analyses:

line # 1= sample number
line # 2= last number is the grain number within the sample = numbers (or letters) preceding the last number are the Unit numbers ie. 11- Unit 1, grain 1 or GB= analysed uses for garnet-biotite geothermometry experiment line # 3= mineral analysed ie. Bi=biotite line # 4= microprobe analyses location (core or rim)

	NPM11	NPM11	NPM2	NPM533	NPM582	NPM11	NPM11	NPM2	NPM533
	11 BI RIM	11 BI CORE	11 BI CORE	11 BI CORE	11 BI CORE	12 BI RIM	12 BI CORE	12 BI CORE	12 BI RIM
SIO2	35.17	35.19	34.88	35.51	35.17	36.01	34.61	35.34	35.35
TIO2	2.70	3.36	2.82	3.42	3.23	2.93	3.13	2.81	3.44
AL2O3	17.89	17.81	19.09	17.30	18.01	18.33	17.85	19.72	17.42
CR2O3	0.00	0.00	0.00	0.00	0.00	0.00	0.00	0.00	0.00
FEO	21.12	21.09	19.64	19.38	21.03	19.18	20.11	19.34	19.81
MNO	0.51	0.50	0.48	0.44	0.36	0.52	0.49	0.49	0.49
MGO	8.57	8.51	8.10	9.43	7.86	9.02	8.69	8.68	9.15
CAO	0.00	0.00	0.00	0.00	0.00	0.00	0.01	0.18	0.00
NA2O	0.01	0.05	0.12	0.00	0.01	0.00	0.13	0.18	0.08
K2O	9.43	9.48	9.92	9.71	9.97	8.61	9.75	9.75	8.98
P2O5	0.00	0.00	0.00	0.00	0.00	0.00	0.00	0.00	0.00
H2O	3.89	3.92	3.90	3.91	3.89	3.93	3.87	3.97	3.90
TOTAL	99.29	99.91	98.95	99.10	99.53	98.53	98.64	100.46	98.62
SI	5.413	5.385	5.362	5.441	5.410	5.492	5.361	5.329	5.434
TI	0.313	0.387	0.326	0.394	0.374	0.336	0.365	0.319	0.398
AL	3.246	3.213	3.460	3.125	3.266	3.296	3.260	3.506	3.157
CR	0.000	0.000	0.000	0.000	0.000	0.000	0.000	0.000	0.000
FE2	2.719	2.699	2.525	2.483	2.705	2.446	2.605	2.439	2.547
MN	0.066	0.065	0.063	0.057	0.047	0.067	0.064	0.063	0.064
MG	1.966	1.941	1.856	2.153	1.802	2.050	2.006	1.951	2.096
CA	0.000	0.000	0.000	0.000	0.000	0.000	0.002	0.029	0.000
NA	0.003	0.015	0.036	0.000	0.003	0.000	0.039	0.053	0.024
K	1.852	1.851	1.946	1.898	1.957	1.675	1.927	1.876	1.761
P	0.000	0.000	0.000	0.000	0.000	0.000	0.000	0.000	0.000
OH	4.000	4.000	4.000	4.000	4.000	4.000	4.000	4.000	4.000

	NPM582	NPM11	NPM11	NPM2	NPM533	NPM533	NPM582	NPM546	NPM546
	12 BI CORE	13 BI RIM	13 BI CORE	13 BI CORE	13 BI CORE	13 BI RIM	13 BI CORE	21 BI RIM	21 BI CORE
SIO2	35.24	35.41	35.36	35.36	35.85	36.19	35.46	36.34	36.28
TIO2	1.91	3.41	2.87	2.39	3.51	3.07	2.49	3.14	3.38
AL2O3	18.57	17.81	17.52	19.59	17.15	17.35	18.29	16.91	17.42
CR2O3	0.00	0.00	0.00	0.00	0.00	0.00	0.00	0.00	0.00
FEO	20.21	21.29	21.13	18.38	20.22	19.65	21.35	18.92	18.86
MNO	0.38	0.49	0.43	0.47	0.48	0.39	0.38	0.46	0.39
MGO	8.60	8.50	8.78	8.45	9.04	9.42	8.25	10.24	9.65
CAO	0.00	0.00	0.00	0.03	0.00	0.00	0.03	0.00	0.00
NA2O	0.00	0.00	0.07	0.22	0.00	0.04	0.16	0.00	0.09
K2O	9.44	9.45	9.39	10.03	9.13	8.98	9.84	9.92	10.05
P2O5	0.00	0.00	0.00	0.00	0.00	0.00	0.00	0.00	0.00
H2O	3.87	3.93	3.90	3.92	3.92	3.93	3.92	3.95	3.96
TOTAL	98.22	100.29	99.45	98.84	99.30	99.02	100.17	99.88	100.08
SI	5.450	5.396	5.432	5.404	5.480	5.519	5.420	5.510	5.488
TI	0.222	0.391	0.332	0.275	0.404	0.352	0.286	0.358	0.385
AL	3.386	3.200	3.173	3.529	3.091	3.120	3.296	3.022	3.107
CR	0.000	0.000	0.000	0.000	0.000	0.000	0.000	0.000	0.000
FE2	2.614	2.713	2.715	2.349	2.585	2.506	2.729	2.399	2.386
MN	0.050	0.063	0.056	0.061	0.062	0.050	0.049	0.059	0.050
MG	1.982	1.931	2.010	1.924	2.059	2.141	1.879	2.314	2.176
CA	0.000	0.000	0.000	0.005	0.000	0.000	0.005	0.000	0.000
NA	0.000	0.000	0.021	0.065	0.000	0.012	0.047	0.000	0.026
K	1.863	1.837	1.840	1.955	1.781	1.747	1.919	1.919	1.940
P	0.000	0.000	0.000	0.000	0.000	0.000	0.000	0.000	0.000
OH	4.000	4.000	4.000	4.000	4.000	4.000	4.000	4.000	4.000

	NPM546	NPM546	NPM546	NPM441	NPM458	NPM468	NPM477	NPM542	NPM542
	22 BI RIM	22 BI CORE	23 BI CORE	41 BI CORE	41 BI CORE	41 BI CORE	41 BI CORE	31 BI CORE	31 BI RIM
SIO2	35.54	35.58	35.41	34.43	34.85	35.35	35.26	34.94	35.06
TIO2	2.96	2.81	3.09	2.79	2.61	2.93	2.07	2.65	2.51
AL2O3	17.37	17.75	18.23	18.07	17.90	18.52	17.42	18.44	17.87
CR2O3	0.00	0.00	0.00	0.00	0.00	0.00	0.00	0.00	0.00
FEO	19.53	19.64	18.12	22.34	22.78	22.23	22.04	22.47	23.22
MNO	0.45	0.58	0.47	0.52	0.44	0.72	0.58	0.53	0.48
MGO	9.50	9.60	9.19	7.38	6.94	5.80	7.97	6.18	6.14
CAO	0.00	0.00	0.00	0.00	0.00	0.00	0.00	0.00	0.01
NA2O	0.04	0.03	0.14	0.07	0.03	0.11	0.00	0.00	0.02
K2O	9.73	10.00	10.09	9.96	10.42	9.69	10.16	10.12	10.57
P2O5	0.00	0.00	0.00	0.00	0.00	0.00	0.00	0.00	0.00
H2O	3.90	3.93	3.91	3.85	3.86	3.87	3.86	3.85	3.85
TOTAL	99.02	99.92	98.65	99.41	99.83	99.22	99.36	99.18	99.73
SI	5.454	5.420	5.428	5.351	5.410	5.477	5.474	5.437	5.461
TI	0.342	0.322	0.356	0.326	0.305	0.341	0.242	0.310	0.294
AL	3.142	3.188	3.294	3.311	3.276	3.383	3.188	3.383	3.281
CR	0.000	0.000	0.000	0.000	0.000	0.000	0.000	0.000	0.000
FE2	2.506	2.502	2.323	2.904	2.957	2.881	2.861	2.924	3.025
MN	0.058	0.075	0.061	0.068	0.058	0.094	0.076	0.070	0.063
MG	2.173	2.180	2.099	1.709	1.606	1.339	1.844	1.433	1.425
CA	0.000	0.000	0.000	0.000	0.000	0.000	0.000	0.000	0.002
NA	0.012	0.009	0.042	0.021	0.009	0.033	0.000	0.000	0.006
K	1.905	1.944	1.973	1.975	2.064	1.915	2.012	2.009	2.100
P	0.000	0.000	0.000	0.000	0.000	0.000	0.000	0.000	0.000
OH	4.000	4.000	4.000	4.000	4.000	4.000	4.000	4.000	4.000

	NPM558	NPM580	NPM441	NPM458	NPM468	NPM477	NPM542	NPM558	NPM580
	41 BI CORE	41 BI CORE	42 BI CORE	42 BI CORE	42 BI CORE	42 BI CORE	32 BI CORE	42 BI CORE	42 BI CORE
SIO2	35.43	35.62	34.85	34.89	34.71	35.22	35.00	36.04	35.09
TIO2	3.01	2.36	2.05	2.23	3.08	2.04	2.53	2.65	2.31
AL2O3	17.92	18.76	18.20	18.92	18.01	16.15	16.70	17.76	18.71
CR2O3	0.00	0.00	0.00	0.00	0.00	0.00	0.00	0.00	0.00
FEO	19.37	20.74	23.77	21.80	22.75	23.51	24.10	20.23	21.20
MNO	0.35	0.63	0.92	0.89	0.69	0.56	0.47	0.31	0.65
MGO	9.14	6.81	5.42	5.63	5.73	8.29	5.93	9.25	6.87
CAO	0.00	0.00	0.00	0.06	0.00	0.00	0.02	0.02	0.00
NA2O	0.05	0.00	0.00	0.12	0.02	0.00	0.04	0.01	0.00
K2O	10.53	10.65	10.11	9.62	9.87	9.90	10.35	10.69	10.17
P2O5	0.00	0.00	0.00	0.00	0.00	0.00	0.00	0.00	0.00
H2O	3.92	3.89	3.82	3.82	3.82	3.84	3.80	3.96	3.86
TOTAL	99.72	99.46	99.14	97.98	98.68	99.51	98.94	100.92	98.86
SI	5.414	5.488	5.470	5.472	5.440	5.500	5.524	5.457	5.446
TI	0.346	0.273	0.242	0.263	0.363	0.240	0.300	0.302	0.270
AL	3.229	3.408	3.368	3.498	3.328	2.973	3.107	3.170	3.423
CR	0.000	0.000	0.000	0.000	0.000	0.000	0.000	0.000	0.000
FE2	2.476	2.673	3.120	2.859	2.982	3.071	3.181	2.562	2.752
MN	0.045	0.082	0.122	0.118	0.092	0.074	0.063	0.040	0.085
MG	2.082	1.564	1.268	1.316	1.338	1.929	1.395	2.087	1.589
CA	0.000	0.000	0.000	0.010	0.000	0.000	0.003	0.003	0.000
NA	0.015	0.000	0.000	0.036	0.006	0.000	0.012	0.003	0.000
K	2.053	2.093	2.025	1.925	1.974	1.972	2.084	2.065	2.014
P	0.000	0.000	0.000	0.000	0.000	0.000	0.000	0.000	0.000
OH	4.000	4.000	4.000	4.000	4.000	4.000	4.000	4.000	4.000

	NPM580	NPM441	NPM458	NPM468	NPM542	NPM542	NPM558	NPM580	NPM580
	42 BI RIM	43 BI CORE	43 BI CORE	43 BI CORE	43 BI CORE	43 BI RIM	43 BI CORE	43 BI RIM	43 BI CORE
SIO2	35.19	34.98	35.81	35.09	34.86	35.14	35.33	35.17	34.91
TIO2	2.23	3.38	2.59	2.84	2.74	2.75	2.71	2.54	2.36
AL2O3	18.56	17.73	17.12	18.32	18.26	18.09	17.21	17.64	17.52
CR2O3	0.00	0.00	0.00	0.00	0.00	0.00	0.00	0.00	0.00
FEO	20.95	22.12	22.04	21.99	23.35	22.35	20.46	22.11	21.50
MNO	0.56	0.53	0.48	0.63	0.51	0.56	0.37	0.69	0.65
MGO	7.04	7.08	7.09	5.53	6.20	5.95	8.79	7.35	7.14
CAO	0.00	0.00	0.03	0.04	0.00	0.00	0.00	0.00	0.00
NA2O	0.12	0.12	0.04	0.12	0.08	0.02	0.00	0.00	0.00
K2O	10.34	9.65	9.85	9.43	10.09	10.25	10.63	10.05	10.39
P2O5	0.00	0.00	0.00	0.00	0.00	0.00	0.00	0.00	0.00
H2O	3.86	3.87	3.85	3.82	3.86	3.84	3.88	3.86	3.82
TOTAL	98.85	99.46	98.90	97.81	99.95	98.95	99.38	99.41	98.29
SI	5.461	5.413	5.566	5.507	5.407	5.483	5.455	5.457	5.480
TI	0.260	0.393	0.303	0.335	0.320	0.323	0.315	0.296	0.279
AL	3.396	3.235	3.137	3.389	3.339	3.328	3.133	3.227	3.242
CR	0.000	0.000	0.000	0.000	0.000	0.000	0.000	0.000	0.000
FE2	2.719	2.863	2.865	2.886	3.029	2.917	2.642	2.869	2.823
MN	0.074	0.069	0.063	0.084	0.067	0.074	0.048	0.091	0.086
MG	1.628	1.633	1.642	1.293	1.433	1.384	2.023	1.700	1.670
CA	0.000	0.000	0.005	0.007	0.000	0.000	0.000	0.000	0.000
NA	0.036	0.036	0.012	0.037	0.024	0.006	0.000	0.000	0.000
K	2.047	1.905	1.953	1.888	1.997	2.040	2.094	1.989	2.081
P	0.000	0.000	0.000	0.000	0.000	0.000	0.000	0.000	0.000
OH	4.000	4.000	4.000	4.000	4.000	4.000	4.000	4.000	4.000

	NPM477	NPM405	NPM407	NPM407	NPM485	NPM405	NPM405	NPM407	NPM485
	44 BI CORE	5A1 BI CORE	5A1 BI RIM	5A1 BI CORE	5A1 BI CORE	5A2 BI CORE	5A2 BI RIM	5A2 BI CORE	5A2 BI CORE
SIO2	34.82	39.55	38.27	38.11	38.55	39.34	38.16	38.40	38.86
TIO2	2.34	2.12	1.62	1.77	2.18	2.13	1.90	1.78	1.81
AL2O3	16.78	15.12	17.53	16.86	16.26	15.34	15.53	15.84	16.63
CR2O3	0.00	0.00	0.00	0.00	0.00	0.00	0.00	0.00	0.00
FEO	22.71	10.70	14.56	15.19	11.73	10.83	11.38	15.62	11.85
MNO	0.60	0.10	0.21	0.25	0.18	0.16	0.12	0.32	0.13
MGO	7.56	17.99	13.64	13.71	16.32	18.20	18.41	14.35	16.23
CAO	0.00	0.00	0.00	0.00	0.00	0.00	0.01	0.00	0.00
NA2O	0.00	0.65	0.12	0.09	0.07	0.44	0.54	0.14	0.12
K2O	9.78	8.22	9.48	9.78	9.57	8.90	8.18	10.10	9.76
P2O5	0.00	0.00	0.00	0.00	0.00	0.00	0.00	0.00	0.00
H2O	3.81	4.11	4.05	4.04	4.07	4.12	4.07	4.05	4.10
TOTAL	98.40	98.56	99.48	99.80	98.93	99.46	98.30	100.60	99.49
SI	5.478	5.772	5.657	5.651	5.669	5.715	5.617	5.678	5.684
TI	0.277	0.233	0.180	0.197	0.241	0.233	0.210	0.198	0.199
AL	3.112	2.601	3.055	2.947	2.819	2.627	2.695	2.761	2.868
CR	0.000	0.000	0.000	0.000	0.000	0.000	0.000	0.000	0.000
FE2	2.988	1.306	1.800	1.884	1.443	1.316	1.401	1.932	1.450
MN	0.080	0.012	0.026	0.031	0.022	0.020	0.015	0.040	0.016
MG	1.773	3.913	3.005	3.030	3.577	3.941	4.039	3.162	3.538
CA	0.000	0.000	0.000	0.000	0.000	0.000	0.002	0.000	0.000
NA	0.000	0.184	0.034	0.026	0.020	0.124	0.154	0.040	0.034
K	1.963	1.530	1.788	1.850	1.796	1.650	1.536	1.905	1.821
P	0.000	0.000	0.000	0.000	0.000	0.000	0.000	0.000	0.000
OH	4.000	4.000	4.000	4.000	4.000	4.000	4.000	4.000	4.000

	NPM405	NPM405	NPM407	NPM485	NPM538	NPM538	NPM538	NPM539	NPM539
	5A3 BI RIM	5A3 BI CORE	5A3 BI CORE	5A4 BI CORE	61 BI CORE	62 BI CORE	63 BI CORE	71 BI RIM	71 BI CORE
SIO2	39.24	40.08	37.83	39.55	34.94	34.85	34.79	35.92	35.67
TIO2	2.01	2.00	1.15	1.92	1.83	2.04	1.84	3.59	3.31
AL2O3	15.26	15.33	16.60	16.69	18.87	18.06	18.91	18.30	18.51
CR2O3	0.00	0.00	0.00	0.00	0.00	0.00	0.00	0.00	0.00
FEO	10.70	10.68	14.45	11.29	23.17	23.76	22.78	19.27	19.84
MNO	0.14	0.18	0.28	0.17	0.70	0.74	0.71	0.61	0.55
MGO	17.90	18.16	13.79	16.59	6.40	6.76	6.59	8.79	8.70
CAO	0.05	0.02	0.00	0.00	0.00	0.00	0.00	0.00	0.00
NA2O	0.40	0.45	0.37	0.11	0.00	0.05	0.05	0.00	0.12
K2O	8.63	8.49	9.79	9.42	9.91	10.16	10.36	10.09	9.92
P2O5	0.00	0.00	0.00	0.00	0.00	0.00	0.00	0.00	0.00
H2O	4.09	4.15	3.98	4.14	3.86	3.86	3.86	3.97	3.96
TOTAL	98.42	99.54	98.24	99.88	99.68	100.28	99.89	100.54	100.58
SI	5.748	5.790	5.692	5.727	5.420	5.407	5.393	5.421	5.393
TI	0.221	0.217	0.130	0.209	0.213	0.238	0.215	0.407	0.376
AL	2.635	2.611	2.944	2.849	3.451	3.303	3.456	3.256	3.299
CR	0.000	0.000	0.000	0.000	0.000	0.000	0.000	0.000	0.000
FE2	1.311	1.290	1.818	1.367	3.006	3.083	2.953	2.432	2.509
MN	0.017	0.022	0.036	0.021	0.092	0.097	0.093	0.078	0.070
MG	3.908	3.909	3.092	3.580	1.479	1.563	1.522	1.977	1.960
CA	0.008	0.003	0.000	0.000	0.000	0.000	0.000	0.000	0.000
NA	0.114	0.126	0.108	0.031	0.000	0.015	0.015	0.000	0.035
K	1.613	1.565	1.879	1.740	1.961	2.011	2.049	1.943	1.913
P	0.000	0.000	0.000	0.000	0.000	0.000	0.000	0.000	0.000
OH	4.000	4.000	4.000	4.000	4.000	4.000	4.000	4.000	4.000

	NPM560	NPM566	NPM583	NPM539	NPM539	NPM560	NPM566	NPM583	NPM583
	71 BI CORE	71 BI CORE	71 BI CORE	72 BI CORE	72 BI RIM	72 BI CORE	72 BI CORE	72 BI CORE	72 BI RIM
SIO2	35.58	34.93	34.85	35.19	35.63	35.34	35.32	34.26	34.46
TIO2	3.41	3.58	3.17	3.28	3.31	2.89	3.60	2.24	2.30
AL2O3	17.81	18.67	18.34	18.89	19.00	17.13	18.96	17.59	18.17
CR2O3	0.00	0.00	0.00	0.00	0.00	0.00	0.00	0.00	0.00
FEO	21.68	22.09	22.19	19.31	19.95	21.38	21.43	23.47	22.37
MNO	0.74	0.46	0.59	0.50	0.50	0.75	0.45	0.58	0.44
MGO	7.47	7.31	7.39	8.56	8.69	7.72	6.83	7.04	7.07
CAO	0.00	0.00	0.00	0.00	0.00	0.04	0.00	0.04	0.00
NA2O	0.10	0.00	0.01	0.12	0.00	0.00	0.00	0.00	0.03
K2O	8.67	8.00	9.54	10.50	10.00	9.20	7.76	9.97	9.93
P2O5	0.00	0.00	0.00	0.00	0.00	0.00	0.00	0.00	0.00
H2O	3.90	3.90	3.90	3.94	3.98	3.85	3.89	3.81	3.83
TOTAL	99.36	98.94	99.98	100.29	101.06	98.30	98.24	99.00	98.60
SI	5.462	5.369	5.359	5.344	5.359	5.504	5.433	5.383	5.396
TI	0.394	0.414	0.367	0.375	0.374	0.339	0.416	0.265	0.271
AL	3.223	3.383	3.325	3.382	3.369	3.145	3.438	3.259	3.354
CR	0.000	0.000	0.000	0.000	0.000	0.000	0.000	0.000	0.000
FE2	2.784	2.840	2.854	2.453	2.509	2.785	2.757	3.084	2.930
MN	0.096	0.060	0.077	0.064	0.064	0.099	0.059	0.077	0.058
MG	1.709	1.675	1.694	1.937	1.948	1.792	1.566	1.649	1.650
CA	0.000	0.000	0.000	0.000	0.000	0.007	0.000	0.007	0.000
NA	0.030	0.000	0.003	0.035	0.000	0.000	0.000	0.000	0.009
K	1.698	1.569	1.872	2.034	1.919	1.828	1.523	1.999	1.984
P	0.000	0.000	0.000	0.000	0.000	0.000	0.000	0.000	0.000
OH	4.000	4.000	4.000	4.000	4.000	4.000	4.000	4.000	4.000

	NPM539	NPM539	NPM560	NPM566	NPM583	NPM361	NPM537	NPM537	NPM361
	73 BI RIM	73 BI CORE	73 BI CORE	73 BI CORE	73 BI CORE	81 BI CORE	81 BI RIM	81 BI CORE	82 BI CORE
SIO2	35.91	36.11	35.92	35.69	34.86	35.22	35.96	34.61	35.01
TIO2	3.19	3.41	3.12	3.79	3.39	2.86	2.46	2.60	2.25
AL2O3	17.85	18.11	17.40	18.75	18.60	18.63	17.59	17.98	18.00
CR2O3	0.00	0.00	0.00	0.00	0.00	0.00	0.00	0.00	0.00
FEO	19.93	19.61	21.63	21.52	21.80	22.76	22.99	23.07	22.40
MNO	0.63	0.57	0.79	0.46	0.36	0.68	0.78	0.89	0.67
MGO	8.85	8.50	8.12	7.10	7.62	6.47	7.36	6.85	6.78
CAO	0.00	0.00	0.00	0.00	0.00	0.00	0.00	0.00	0.02
NA2O	0.08	0.00	0.00	0.12	0.03	0.06	0.00	0.00	0.02
K2O	9.66	9.81	8.96	8.41	8.87	7.96	10.03	9.87	9.39
P2O5	0.00	0.00	0.00	0.00	0.00	0.00	0.00	0.00	0.00
H2O	3.94	3.95	3.92	3.94	3.90	3.87	3.92	3.85	3.83
TOTAL	100.04	100.07	99.86	99.78	99.43	98.51	101.09	99.72	98.37
SI	5.455	5.472	5.492	5.427	5.352	5.454	5.495	5.382	5.475
TI	0.364	0.389	0.359	0.433	0.391	0.333	0.283	0.304	0.265
AL	3.197	3.235	3.137	3.361	3.367	3.401	3.169	3.296	3.319
CR	0.000	0.000	0.000	0.000	0.000	0.000	0.000	0.000	0.000
FE2	2.532	2.485	2.766	2.737	2.799	2.947	2.938	3.000	2.930
MN	0.081	0.073	0.102	0.059	0.047	0.089	0.101	0.117	0.089
MG	2.004	1.920	1.850	1.609	1.744	1.493	1.676	1.587	1.580
CA	0.000	0.000	0.000	0.000	0.000	0.000	0.000	0.000	0.003
NA	0.024	0.000	0.000	0.035	0.009	0.018	0.000	0.000	0.006
K	1.872	1.897	1.748	1.631	1.737	1.573	1.955	1.958	1.874
P	0.000	0.000	0.000	0.000	0.000	0.000	0.000	0.000	0.000
OH	4.000	4.000	4.000	4.000	4.000	4.000	4.000	4.000	4.000

	NPM537	NPM537	NPM361	NPM537	NPM107	NPM108	NPM108	NPM344	NPM344
	82 BI CORE	82 BI RIM	83 BI CORE	83 BI CORE	GB1 BI CORE	GB1 BI RIM	GB1 BI CORE	GB1 BI RIM	GB1 BI CORE
SIO2	34.97	34.52	34.86	35.41	35.46	35.26	34.90	34.23	34.26
TIO2	2.67	2.57	2.95	2.96	1.54	1.82	1.93	1.59	1.57
AL2O3	18.25	17.28	17.34	18.40	19.10	19.86	19.83	19.09	18.49
CR2O3	0.00	0.00	0.00	0.00	0.00	0.00	0.00	0.00	0.00
FEO	22.72	22.30	24.09	22.12	22.73	19.81	20.95	23.34	24.10
MNO	0.71	0.74	0.66	0.75	0.00	0.28	0.27	0.78	0.79
MGO	7.13	7.30	6.77	7.21	5.58	9.01	8.46	6.08	6.42
CAO	0.00	0.00	0.00	0.00	0.02	0.00	0.01	0.00	0.00
NA2O	0.01	0.00	0.00	0.00	0.09	0.09	0.11	0.00	0.00
K2O	9.81	9.97	8.21	9.79	9.52	9.81	9.83	9.59	9.88
P2O5	0.00	0.00	0.00	0.00	0.00	0.00	0.00	0.00	0.00
H2O	3.89	3.81	3.84	3.92	3.83	3.95	3.94	3.81	3.82
TOTAL	100.16	98.49	98.72	100.56	97.87	99.89	100.23	98.51	99.33
SI	5.390	5.425	5.445	5.412	5.552	5.351	5.313	5.380	5.373
TI	0.310	0.304	0.347	0.340	0.181	0.208	0.221	0.188	0.185
AL	3.316	3.202	3.193	3.316	3.525	3.553	3.559	3.537	3.419
CR	0.000	0.000	0.000	0.000	0.000	0.000	0.000	0.000	0.000
FE2	2.929	2.931	3.147	2.828	2.976	2.514	2.667	3.068	3.161
MN	0.093	0.099	0.087	0.097	0.000	0.036	0.035	0.104	0.105
MG	1.638	1.710	1.576	1.642	1.302	2.038	1.919	1.424	1.501
CA	0.000	0.000	0.000	0.000	0.003	0.000	0.002	0.000	0.000
NA	0.003	0.000	0.000	0.000	0.027	0.026	0.032	0.000	0.000
K	1.929	1.999	1.636	1.909	1.902	1.899	1.909	1.923	1.977
P	0.000	0.000	0.000	0.000	0.000	0.000	0.000	0.000	0.000
OH	4.000	4.000	4.000	4.000	4.000	4.000	4.000	4.000	4.000

	NPM484	NPM484	NPM611	NPM611	NPM8A	NPM8A	NPM107	NPM108	NPM344
	GB1 BI CORE	GB1 BI RIM	GB1 BI RIM	GB1 BI CORE	GB1 BI RIM	GB1 BI CORE	GB2 BI CORE	GB2 BI CORE	GB2 BI CORE
SIO2	33.22	34.42	34.66	34.97	34.94	34.21	34.22	34.90	34.42
TIO2	1.97	2.53	2.35	1.98	2.29	2.22	1.79	1.64	2.03
AL2O3	17.84	17.49	18.13	18.48	17.37	18.05	18.16	18.93	18.45
CR2O3	0.00	0.00	0.00	0.00	0.00	0.00	0.00	0.00	0.00
FEO	27.68	26.58	22.73	22.36	24.54	25.06	24.29	20.79	23.29
MNO	0.41	0.43	0.75	0.71	0.68	0.73	0.82	0.27	0.75
MGO	3.84	3.87	6.61	6.84	5.72	5.44	5.42	8.72	6.57
CAO	0.00	0.02	0.00	0.00	0.01	0.00	0.00	0.02	0.00
NA2O	0.08	0.00	0.01	0.00	0.04	0.06	0.00	0.20	0.00
K2O	9.44	9.06	10.04	10.28	10.01	9.80	9.69	9.89	10.12
P2O5	0.00	0.00	0.00	0.00	0.00	0.00	0.00	0.00	0.00
H2O	3.71	3.75	3.83	3.86	3.82	3.80	3.77	3.89	3.84
TOTAL	98.19	98.15	99.11	99.48	99.42	99.37	98.16	99.25	99.47
SI	5.363	5.498	5.415	5.431	5.487	5.388	5.435	5.374	5.375
TI	0.239	0.304	0.276	0.231	0.270	0.263	0.214	0.190	0.238
AL	3.396	3.293	3.339	3.384	3.216	3.352	3.400	3.436	3.397
CR	0.000	0.000	0.000	0.000	0.000	0.000	0.000	0.000	0.000
FE2	3.737	3.551	2.970	2.904	3.223	3.301	3.226	2.677	3.042
MN	0.056	0.058	0.099	0.093	0.090	0.097	0.110	0.035	0.099
MG	0.924	0.921	1.539	1.583	1.339	1.277	1.283	2.001	1.529
CA	0.000	0.003	0.000	0.000	0.002	0.000	0.000	0.003	0.000
NA	0.025	0.000	0.003	0.000	0.012	0.018	0.000	0.060	0.000
K	1.944	1.846	2.001	2.037	2.005	1.969	1.964	1.943	2.016
P	0.000	0.000	0.000	0.000	0.000	0.000	0.000	0.000	0.000
OH	4.000	4.000	4.000	4.000	4.000	4.000	4.000	4.000	4.000

	NPM611	NPM611	NPM8A	NPM107	NPM108	NPM108	NPM484	NPM484	NPM611
	GB2 BI RIM	GB2 BI CORE	GB2 BI CORE	GB3 BI CORE	GB3 BI CORE	GB3 BI RIM	GB3 BI RIM	GB3 BI CORE	GB3 BI CORE
SIO2	35.36	34.92	34.39	34.31	35.51	35.34	34.05	33.79	35.17
TIO2	2.29	2.26	2.09	1.69	1.74	1.83	2.19	2.27	2.35
AL2O3	18.62	18.67	18.17	18.76	19.87	19.55	17.49	17.56	19.35
CR2O3	0.00	0.00	0.00	0.00	0.00	0.00	0.00	0.00	0.00
FEO	22.16	22.89	24.18	23.94	19.63	20.29	28.52	28.93	22.14
MNO	0.59	0.73	0.86	0.80	0.23	0.31	0.42	0.48	0.58
MGO	6.21	6.47	5.21	5.71	9.24	8.82	3.94	3.85	6.72
CAO	0.00	0.02	0.07	0.00	0.00	0.00	0.00	0.00	0.00
NA2O	0.01	0.00	0.00	0.03	0.20	0.09	0.02	0.04	0.01
K2O	10.49	10.20	10.29	9.78	9.68	10.04	9.84	9.96	10.50
P2O5	0.00	0.00	0.00	0.00	0.00	0.00	0.00	0.00	0.00
H2O	3.87	3.87	3.80	3.81	3.96	3.95	3.78	3.78	3.92
TOTAL	99.60	100.03	99.06	98.83	100.06	100.22	100.25	100.66	100.74
SI	5.475	5.403	5.427	5.399	5.368	5.367	5.401	5.357	5.380
TI	0.267	0.263	0.248	0.200	0.198	0.209	0.261	0.271	0.270
AL	3.399	3.406	3.380	3.480	3.541	3.500	3.271	3.282	3.489
CR	0.000	0.000	0.000	0.000	0.000	0.000	0.000	0.000	0.000
FE2	2.870	2.962	3.191	3.150	2.482	2.577	3.783	3.836	2.832
MN	0.077	0.096	0.115	0.107	0.029	0.040	0.056	0.064	0.075
MG	1.433	1.492	1.225	1.339	2.082	1.996	0.931	0.910	1.532
CA	0.000	0.003	0.012	0.000	0.000	0.000	0.000	0.000	0.000
NA	0.003	0.000	0.000	0.009	0.059	0.026	0.006	0.012	0.003
K	2.072	2.013	2.072	1.963	1.867	1.945	1.991	2.014	2.049
P	0.000	0.000	0.000	0.000	0.000	0.000	0.000	0.000	0.000
OH	4.000	4.000	4.000	4.000	4.000	4.000	4.000	4.000	4.000

	NPM611	NPM8A	NPM344	NPM484	NPM484
	GB3 BI RIM	GB3 BI CORE	GB4 BI CORE	GB4 BI CORE	GB4 BI RIM
SIO2	34.74	34.59	34.37	33.58	33.44
TIO2	2.38	1.99	1.94	2.23	2.32
AL2O3	19.28	18.24	19.19	18.09	17.91
CR2O3	0.00	0.00	0.00	0.00	0.00
FEO	22.47	25.41	22.07	28.04	27.43
MNO	0.59	0.71	0.61	0.43	0.39
MGO	6.42	5.24	6.59	3.85	3.78
CAO	0.00	0.00	0.00	0.00	0.00
NA2O	0.00	0.06	0.02	0.01	0.01
K2O	10.49	9.60	10.16	9.84	10.09
P2O5	0.00	0.00	0.00	0.00	0.00
H2O	3.89	3.82	3.84	3.77	3.74
TOTAL	100.26	99.66	98.79	99.84	99.11
SI	5.356	5.425	5.367	5.340	5.355
TI	0.276	0.235	0.228	0.267	0.279
AL	3.504	3.373	3.533	3.391	3.381
CR	0.000	0.000	0.000	0.000	0.000
FE2	2.897	3.333	2.882	3.729	3.673
MN	0.077	0.094	0.081	0.058	0.053
MG	1.475	1.225	1.534	0.912	0.902
CA	0.000	0.000	0.000	0.000	0.000
NA	0.000	0.018	0.006	0.003	0.003
K	2.063	1.921	2.024	1.996	2.061
P	0.000	0.000	0.000	0.000	0.000
OH	4.000	4.000	4.000	4.000	4.000

B-2: Microprobe analyses of Amphiboles based on 23 oxygens

	612 NPM405	612 NPM405	612 NPM405	612 NPM405	612 NPM405	612 NPM405	615 NPM406	615 NPM406	615 NPM406
	5A3 HB RIM	5A1 HB CORE	5A3 HB CORE	5A2 HB RIM	5A2 HB CORE	5A1 HB RIM	5A1 HB CORE	5A1 HB RIM	5A2 HB CORE
SIO2	53.34	52.41	53.01	52.81	52.93	53.54	51.87	49.16	48.96
TIO2	0.08	0.24	0.18	0.20	0.19	0.19	0.32	0.50	0.57
AL2O3	4.23	4.55	4.25	4.87	4.02	3.98	5.10	7.33	7.91
CR2O3	0.07	0.07	0.07	0.07	0.07	0.07	0.07	0.07	0.07
FEO	7.78	7.62	7.41	7.97	7.43	7.56	9.67	10.94	10.70
MNO	0.26	0.22	0.18	0.20	0.22	0.15	0.31	0.24	0.36
MGO	18.59	18.25	18.63	18.11	18.64	18.42	6.63	15.05	14.83
CAO	12.23	12.70	12.62	12.37	12.43	12.91	12.49	12.34	12.54
NA2O	0.63	0.71	0.57	0.66	0.51	0.58	0.74	0.87	0.83
K2O	0.00	0.00	0.00	0.00	0.00	0.00	0.00	0.00	0.00
P2O5	0.00	0.00	0.00	0.00	0.00	0.00	0.00	0.00	0.00
H2O	0.00	0.00	0.00	0.00	0.00	0.00	0.00	0.00	0.00
TOTAL	97.21	96.77	96.92	97.26	96.44	97.40	87.20	96.50	96.77
SI	7.544	7.465	7.518	7.478	7.541	7.560	8.185	7.153	7.102
TI	0.009	0.026	0.019	0.021	0.020	0.020	0.038	0.055	0.062
AL	0.705	0.764	0.711	0.813	0.675	0.663	0.949	1.257	1.353
CR	0.018	0.018	0.018	0.018	0.018	0.017	0.020	0.018	0.018
FE2	0.920	0.908	0.879	0.944	0.885	0.893	1.276	1.331	1.298
MN	0.031	0.027	0.022	0.024	0.027	0.018	0.041	0.030	0.044
MG	3.919	3.874	3.938	3.822	3.958	3.876	1.559	3.264	3.206
CA	1.853	1.938	1.918	1.877	1.898	1.953	2.112	1.924	1.949
NA	0.173	0.196	0.157	0.181	0.141	0.159	0.226	0.245	0.233
K	0.000	0.000	0.000	0.000	0.000	0.000	0.000	0.000	0.000
P	0.000	0.000	0.000	0.000	0.000	0.000	0.000	0.000	0.000
OH	0.000	0.000	0.000	0.000	0.000	0.000	0.000	0.000	0.000

	615 NPM406	615 NPM406	615 NPM406	NPM407	NPM407	NPM407	NPM407	NPM407	NPM485
	5A2 HB RIM	5A3 HB RIM	5A3 HB CORE	5A2 HB RIM	5A2 HB CORE	5A3 HB RIM	5A1 HB CORE	5A3 HB CORE	5A2 HB CORE
SIO2	49.36	49.61	49.59	47.41	46.16	47.81	48.89	50.11	54.44
TIO2	0.46	0.46	0.39	0.43	0.43	0.36	0.26	0.18	0.13
AL2O3	7.22	6.81	7.24	7.97	9.47	8.16	6.95	5.93	3.50
CR2O3	0.07	0.00	0.00	0.00	0.00	0.00	0.00	0.00	0.07
FEO	10.91	10.53	10.40	12.95	13.92	12.68	12.51	12.11	7.04
MNO	0.38	0.27	0.26	0.00	0.13	0.21	0.11	0.11	0.00
MGO	15.41	15.95	15.81	14.07	12.87	14.36	14.52	15.08	18.74
CAO	12.61	12.59	12.33	12.81	12.75	12.87	12.79	12.80	13.06
NA2O	0.76	0.85	0.97	0.77	0.98	0.71	0.74	0.69	0.33
K2O	0.00	0.09	0.00	0.70	0.77	0.58	0.42	0.31	0.00
P2O5	0.00	0.00	0.00	0.00	0.00	0.00	0.00	0.00	0.00
H2O	0.00	0.00	0.00	0.00	0.00	0.00	0.00	0.00	0.00
TOTAL	97.18	97.16	96.99	97.11	97.48	97.74	97.19	97.32	97.31
SI	7.139	7.170	7.164	6.977	6.817	6.976	7.146	7.283	7.654
TI	0.050	0.050	0.042	0.048	0.048	0.040	0.029	0.020	0.014
AL	1.231	1.160	1.233	1.383	1.649	1.404	1.198	1.016	0.580
CR	0.018	0.000	0.000	0.000	0.000	0.000	0.000	0.000	0.017
FE2	1.320	1.273	1.257	1.594	1.719	1.547	1.529	1.472	0.828
MN	0.047	0.033	0.032	0.000	0.016	0.026	0.014	0.014	0.000
MG	3.322	3.436	3.404	3.086	2.832	3.123	3.163	3.266	3.927
CA	1.954	1.950	1.909	2.020	2.017	2.012	2.003	1.993	1.968
NA	0.213	0.238	0.272	0.220	0.281	0.201	0.210	0.194	0.090
K	0.000	0.017	0.000	0.131	0.145	0.108	0.078	0.057	0.000
P	0.000	0.000	0.000	0.000	0.000	0.000	0.000	0.000	0.000
OH	0.000	0.000	0.000	0.000	0.000	0.000	0.000	0.000	0.000

	NPM485	NPM485	NPM485	NPM485	NPM485	NPM485
	5A3 HB CORE	5A3 HB RIM	5A4 HB RIM	5A4 HB CORE	5A5 HB RIM	5A5 HB CORE
SIO2	51.96	56.08	55.64	53.65	40.23	53.73
TIO2	0.35	0.09	0.00	0.17	4.91	0.10
AL2O3	5.39	0.95	1.63	3.87	14.75	3.21
CR2O3	0.00	0.00	0.07	0.07	0.00	0.00
FEO	7.61	6.55	6.38	7.03	10.34	6.94
MNO	0.00	0.16	0.20	0.03	0.00	0.08
MGO	18.31	20.31	19.77	18.36	12.86	18.92
CAO	13.12	13.03	13.61	13.16	10.49	12.84
NA2O	0.54	0.03	0.13	0.30	2.51	0.24
K2O	0.21	0.00	0.00	0.00	2.17	0.02
P2O5	0.00	0.00	0.00	0.00	0.00	0.00
H2O	0.00	0.00	0.00	0.00	0.00	0.00
TOTAL	97.49	97.20	97.43	96.64	98.26	96.08
SI	7.361	7.872	7.802	7.606	5.901	7.659
TI	0.037	0.010	0.000	0.018	0.542	0.011
AL	0.900	0.157	0.269	0.647	2.551	0.539
CR	0.000	0.000	0.017	0.018	0.000	0.000
FE2	0.902	0.769	0.748	0.833	1.268	0.827
MN	0.000	0.019	0.024	0.004	0.000	0.010
MG	3.866	4.249	4.131	3.879	2.811	4.019
CA	1.992	1.960	2.045	1.999	1.649	1.961
NA	0.148	0.008	0.035	0.082	0.714	0.066
K	0.038	0.000	0.000	0.000	0.406	0.004
P	0.000	0.000	0.000	0.000	0.000	0.000
OH	0.000	0.000	0.000	0.000	0.000	0.000

B-3: Microprobe analyses of muscovite (based on 24 oxygens)

	NPM2	NPM533	NPM582	NPM533	NPM546	NPM582	NPM533	NPM582	NPM11
	11 MU CORE	11 MU CORE	11 MU CORE	12 MU CORE	12 MU CORE	12 MU CORE	13 MU CORE	13 MU CORE	14 MU CORE
SIO2	47.66	45.94	48.12	47.08	47.55	47.84	46.78	46.26	47.32
TIO2	0.74	0.26	0.94	2.21	0.93	0.56	0.32	1.20	1.16
AL2O3	35.93	30.93	33.65	29.82	33.35	34.89	31.44	33.64	32.52
CR2O3	0.00	0.00	0.00	0.00	0.00	0.00	0.00	0.00	0.00
FEO	1.44	5.36	1.95	4.16	2.35	1.99	5.48	2.09	1.90
MNO	0.07	0.12	0.00	0.09	0.08	0.07	0.05	0.05	0.12
MGO	0.67	1.47	1.24	1.41	1.10	0.85	1.39	1.06	1.06
CAO	0.01	0.00	0.00	0.00	0.03	0.00	0.02	0.00	0.00
NA2O	0.62	0.23	0.22	0.19	0.27	0.21	0.18	0.17	0.22
K2O	7.93	11.43	10.53	11.34	11.44	10.24	10.70	10.72	11.49
P2O5	0.00	0.00	0.00	0.00	0.00	0.00	0.00	0.00	0.00
H2O	4.57	4.39	4.56	4.45	4.54	4.57	4.45	4.47	4.49
TOTAL	99.64	100.13	101.21	100.75	101.64	101.22	100.81	99.66	100.28
SI	6.245	6.268	6.318	6.343	6.274	6.267	6.300	6.199	6.321
TI	0.073	0.027	0.093	0.224	0.092	0.055	0.032	0.121	0.117
AL	5.550	4.975	5.208	4.736	5.188	5.388	4.992	5.314	5.121
CR	0.000	0.000	0.000	0.000	0.000	0.000	0.000	0.000	0.000
FE2	0.158	0.612	0.214	0.469	0.259	0.218	0.617	0.234	0.212
MN	0.008	0.014	0.000	0.010	0.009	0.008	0.006	0.006	0.014
MG	0.131	0.299	0.243	0.283	0.216	0.166	0.279	0.212	0.211
CA	0.001	0.000	0.000	0.000	0.004	0.000	0.003	0.000	0.000
NA	0.158	0.061	0.056	0.050	0.069	0.053	0.047	0.044	0.057
K	1.326	1.989	1.764	1.949	1.926	1.711	1.838	1.833	1.958
P	0.000	0.000	0.000	0.000	0.000	0.000	0.000	0.000	0.000
OH	4.000	4.000	4.000	4.000	4.000	4.000	4.000	4.000	4.000

	NPM2	NPM546	NPM546	NPM2	NPM468	NPM468	NPM468	NPM441	NPM477
	14 MU CORE	22 MU CORE	23 MU CORE	31 MU CORE	31 MU CORE	32 MU CORE	33 MU CORE	41 MU CORE	41 MU RIM
SIO2	47.77	47.19	47.20	45.58	46.54	47.04	48.74	46.96	46.62
TIO2	0.70	1.41	1.30	0.80	0.92	0.79	0.56	0.45	1.32
AL2O3	36.16	33.73	33.65	34.99	34.59	33.91	34.64	35.05	34.27
CR2O3	0.00	0.00	0.00	0.00	0.00	0.00	0.00	0.00	0.00
FEO	1.06	2.41	2.50	1.16	1.46	1.64	1.27	1.19	2.77
MNO	0.00	0.14	0.00	0.00	0.07	0.04	0.05	0.03	0.08
MGO	0.61	0.94	0.87	0.67	0.75	0.77	0.81	0.65	0.69
CAO	0.02	0.03	0.00	0.02	0.00	0.00	0.08	0.00	0.00
NA2O	0.71	0.40	0.27	0.67	0.55	0.42	0.31	0.55	0.41
K2O	9.90	10.31	10.83	10.68	10.94	10.78	9.24	9.91	10.13
P2O5	0.00	0.00	0.00	0.00	0.00	0.00	0.00	0.00	0.00
H2O	4.61	4.54	4.53	4.46	4.51	4.50	4.58	4.50	4.52
TOTAL	101.54	101.10	101.15	99.03	100.33	99.89	100.28	99.29	100.81
SI	6.205	6.229	6.240	6.126	6.185	6.269	6.376	6.245	6.175
TI	0.068	0.140	0.129	0.081	0.092	0.079	0.055	0.045	0.131
AL	5.538	5.249	5.244	5.544	5.419	5.328	5.342	5.495	5.351
CR	0.000	0.000	0.000	0.000	0.000	0.000	0.000	0.000	0.000
FE2	0.115	0.266	0.276	0.130	0.162	0.183	0.139	0.132	0.307
MN	0.000	0.016	0.000	0.000	0.008	0.005	0.006	0.003	0.009
MG	0.118	0.185	0.171	0.134	0.149	0.153	0.158	0.129	0.136
CA	0.003	0.004	0.000	0.003	0.000	0.000	0.011	0.000	0.000
NA	0.179	0.102	0.069	0.175	0.142	0.109	0.079	0.142	0.105
K	1.641	1.736	1.827	1.831	1.855	1.833	1.542	1.681	1.712
P	0.000	0.000	0.000	0.000	0.000	0.000	0.000	0.000	0.000
OH	4.000	4.000	4.000	4.000	4.000	4.000	4.000	4.000	4.000

	NPM477	NPM542	NPM558	NPM580	NPM441	NPM477	NPM477	NPM542	NPM558
	41 MU CORE	31 MU CORE	41 MU CORE	41 MU CORE	42 MU CORE	42 MU RIM	42 MU CORE	32 MU CORE	42 MU CORE
SIO2	47.15	46.91	47.47	47.97	47.23	47.36	46.63	46.90	46.96
TIO2	1.33	0.55	1.32	0.46	0.48	1.01	1.10	0.72	0.82
AL2O3	34.25	34.50	34.29	35.08	35.69	33.87	33.90	34.56	33.62
CR2O3	0.00	0.00	0.00	0.00	0.00	0.00	0.00	0.00	0.00
FEO	2.65	1.53	1.72	1.40	1.46	2.89	2.88	1.63	1.79
MNO	0.00	0.11	0.00	0.02	0.15	0.04	0.04	0.05	0.13
MGO	0.64	0.70	0.88	0.69	0.62	0.74	0.74	0.76	0.84
CAO	0.00	0.00	0.02	0.00	0.00	0.00	0.00	0.00	0.00
NA2O	0.45	0.30	0.34	0.43	0.67	0.33	0.41	0.33	0.32
K2O	9.82	10.64	10.18	10.74	11.03	10.50	10.10	10.57	10.48
P2O5	0.00	0.00	0.00	0.00	0.00	0.00	0.00	0.00	0.00
H2O	4.54	4.50	4.55	4.58	4.58	4.54	4.50	4.51	4.48
TOTAL	100.83	99.74	100.77	101.37	101.91	101.28	100.30	100.03	99.44
SI	6.221	6.249	6.248	6.276	6.176	6.250	6.208	6.231	6.282
TI	0.132	0.055	0.131	0.045	0.047	0.100	0.110	0.072	0.082
AL	5.328	5.418	5.320	5.411	5.502	5.270	5.321	5.413	5.302
CR	0.000	0.000	0.000	0.000	0.000	0.000	0.000	0.000	0.000
FE2	0.292	0.170	0.189	0.153	0.160	0.319	0.321	0.181	0.200
MN	0.000	0.012	0.000	0.002	0.017	0.004	0.005	0.006	0.015
MG	0.126	0.139	0.173	0.135	0.121	0.146	0.147	0.150	0.167
CA	0.000	0.000	0.003	0.000	0.000	0.000	0.000	0.000	0.000
NA	0.115	0.077	0.087	0.109	0.170	0.084	0.106	0.085	0.083
K	1.653	1.808	1.709	1.793	1.840	1.768	1.715	1.792	1.789
P	0.000	0.000	0.000	0.000	0.000	0.000	0.000	0.000	0.000
OH	4.000	4.000	4.000	4.000	4.000	4.000	4.000	4.000	4.000

	NPM580	NPM580	NPM441	NPM477	NPM477	NPM542	NPM558	NPM538	NPM538
	42 MU CORE	42 MU CORE	43 MU CORE	43 MU RIM	43 MU CORE	33 MU CORE	43 MU CORE	61 MU CORE	62 MU CORE
SIO2	47.19	47.70	47.09	46.66	45.52	46.34	47.60	47.12	47.09
TIO2	0.62	0.82	0.53	1.14	1.19	0.68	1.15	0.45	0.32
AL2O3	34.79	35.11	35.56	34.22	33.36	34.30	33.75	35.13	35.59
CR2O3	0.00	0.00	0.00	0.00	0.00	0.00	0.00	0.00	0.00
FEO	1.44	1.31	1.13	2.88	2.94	1.39	1.74	1.49	1.71
MNO	0.05	0.68	0.00	0.00	0.00	0.06	0.11	0.05	0.00
MGO	0.74	0.68	0.62	0.69	0.65	0.68	0.80	0.61	0.63
CAO	0.00	0.01	0.00	0.00	0.00	0.01	0.00	0.03	0.00
NA2O	0.47	0.47	0.53	0.41	0.31	0.49	0.34	0.63	0.42
K2O	10.22	10.16	9.42	10.55	10.46	10.19	10.70	11.14	11.44
P2O5	0.00	0.00	0.00	0.00	0.00	0.00	0.00	0.00	0.00
H2O	4.52	4.58	4.53	4.52	4.42	4.45	4.53	4.55	4.57
TOTAL	100.04	101.52	99.41	101.07	98.85	98.59	100.72	101.20	101.77
SI	6.248	6.233	6.231	6.180	6.173	6.233	6.289	6.208	6.179
TI	0.062	0.081	0.053	0.114	0.121	0.069	0.114	0.045	0.032
AL	5.430	5.409	5.548	5.343	5.334	5.439	5.257	5.456	5.505
CR	0.000	0.000	0.000	0.000	0.000	0.000	0.000	0.000	0.000
FE2	0.159	0.143	0.125	0.319	0.333	0.156	0.192	0.164	0.188
MN	0.006	0.075	0.000	0.000	0.000	0.007	0.012	0.006	0.000
MG	0.146	0.132	0.122	0.136	0.131	0.136	0.158	0.120	0.123
CA	0.000	0.001	0.000	0.000	0.000	0.001	0.000	0.004	0.000
NA	0.121	0.119	0.136	0.105	0.082	0.128	0.087	0.161	0.107
K	1.726	1.694	1.590	1.783	1.810	1.749	1.804	1.872	1.915
P	0.000	0.000	0.000	0.000	0.000	0.000	0.000	0.000	0.000
OH	4.000	4.000	4.000	4.000	4.000	4.000	4.000	4.000	4.000

	NPM538	NPM539	NPM566	NPM583	NPM539	NPM566	NPM583	NPM539	NPM566
	63 MU CORE	71 MU CORE	71 MU CORE	71 MU CORE	72 MU CORE	72 MUN CORE	72 MU CORE	73 MU CORE	73 MU CORE
SIO2	47.04	46.51	46.18	45.64	45.23	47.23	46.45	46.91	46.69
TIO2	0.40	1.15	0.67	0.89	1.10	0.19	0.95	1.07	0.90
AL2O3	35.42	34.67	35.72	34.47	34.00	36.03	34.72	34.31	34.51
CR2O3	0.00	0.00	0.00	0.00	0.00	0.00	0.00	0.00	0.00
FEO	1.67	1.68	1.60	1.44	1.46	1.18	1.29	1.43	1.63
MNO	0.07	0.19	0.11	0.11	0.06	0.12	0.00	0.01	0.23
MGO	0.63	0.78	0.54	0.67	0.80	0.45	0.61	0.81	0.64
CAO	0.00	0.02	0.02	0.00	0.06	0.01	0.00	0.03	0.00
NA2O	0.57	0.41	0.53	0.45	0.45	0.34	0.34	0.41	0.45
K2O	11.38	11.32	11.40	11.08	11.47	11.52	11.42	11.30	10.82
P2O5	0.00	0.00	0.00	0.00	0.00	0.00	0.00	0.00	0.00
H2O	4.56	4.53	4.54	4.45	4.43	4.57	4.50	4.52	4.51
TOTAL	101.74	101.26	101.31	99.20	99.06	101.64	100.28	100.80	100.38
SI	6.177	6.148	6.099	6.146	6.123	6.188	6.181	6.211	6.202
TI	0.040	0.114	0.067	0.090	0.112	0.019	0.095	0.107	0.090
AL	5.484	5.403	5.562	5.472	5.426	5.565	5.447	5.356	5.405
CR	0.000	0.000	0.000	0.000	0.000	0.000	0.000	0.000	0.000
FE2	0.183	0.186	0.177	0.162	0.165	0.129	0.144	0.158	0.181
MN	0.008	0.021	0.012	0.013	0.007	0.013	0.000	0.001	0.026
MG	0.123	0.154	0.106	0.134	0.161	0.088	0.121	0.160	0.127
CA	0.000	0.003	0.003	0.000	0.009	0.001	0.000	0.004	0.000
NA	0.145	0.105	0.136	0.117	0.118	0.086	0.088	0.105	0.116
K	1.907	1.909	1.921	1.904	1.981	1.926	1.939	1.909	1.834
P	0.000	0.000	0.000	0.000	0.000	0.000	0.000	0.000	0.000
OH	4.000	4.000	4.000	4.000	4.000	4.000	4.000	4.000	4.000

	NPM583	NPM361	NPM537	NPM537	NPM361	NPM361	NPM537	NPM491	NPM8B
	73 MU CORE	81 MU CORE	81 MU CORE	81 MU CORE	82 MU CORE	83 MU CORE	83 MU] CORE	91 MU CORE	91 MU CORE
SIO2	46.69	47.32	46.65	48.79	46.65	46.82	46.23	47.53	47.80
TIO2	0.89	0.60	0.50	0.73	0.45	0.71	0.58	0.03	0.10
AL2O3	35.47	35.45	33.86	36.18	34.91	35.19	34.21	36.01	35.50
CR2O3	0.00	0.00	0.00	0.00	0.00	0.00	0.00	0.00	0.00
FEO	1.52	1.47	1.87	1.75	1.50	1.47	1.68	1.70	1.47
MNO	0.11	0.08	0.10	0.01	0.25	0.11	0.02	0.09	0.05
MGO	0.63	0.62	0.91	0.68	0.66	0.62	0.77	0.50	0.72
CAO	0.00	0.00	0.00	0.00	0.00	0.00	0.00	0.00	0.00
NA2O	0.41	0.50	0.33	0.24	0.47	0.60	0.48	0.38	0.33
K2O	10.96	11.14	10.99	5.81	11.06	11.55	11.08	11.48	11.82
P2O5	0.00	0.00	0.00	0.00	0.00	0.00	0.00	0.00	0.00
H2O	4.55	4.58	4.47	4.60	4.51	4.55	4.46	4.59	4.59
TOTAL	101.23	101.76	99.68	98.79	100.46	101.62	99.51	102.31	102.38
SI	6.146	6.195	6.248	6.348	6.195	6.163	6.204	6.198	6.232
TI	0.088	0.059	0.050	0.071	0.045	0.070	0.059	0.003	0.010
AL	5.504	5.471	5.346	5.550	5.465	5.461	5.413	5.536	5.457
CR	0.000	0.000	0.000	0.000	0.000	0.000	0.000	0.000	0.000
FE2	0.167	0.161	0.209	0.190	0.167	0.162	0.189	0.185	0.160
MN	0.012	0.009	0.011	0.001	0.028	0.012	0.002	0.010	0.006
MG	0.124	0.121	0.182	0.132	0.131	0.122	0.154	0.097	0.140
CA	0.000	0.000	0.000	0.000	0.000	0.000	0.000	0.000	0.000
NA	0.105	0.127	0.086	0.061	0.121	0.153	0.125	0.096	0.083
K	1.841	1.861	1.878	0.964	1.874	1.940	1.897	1.910	1.966
P	0.000	0.000	0.000	0.000	0.000	0.000	0.000	0.000	0.000
OH	4.000	4.000	4.000	4.000	4.000	4.000	4.000	4.000	4.000

	NPM491 92 MU CORE	NPM8B 92 MU CORE	NPM491 93 MU CORE	NPM8B 93 MU CORE
SIO2	46.14	47.04	44.95	46.86
TIO2	0.00	0.22	0.03	0.18
AL2O3	34.80	36.49	35.90	36.35
CR2O3	0.00	0.00	0.00	0.00
FEO	1.70	1.26	1.66	0.94
MNO	0.03	0.07	0.07	0.05
MGO	0.46	0.50	0.41	0.39
CAO	0.00	0.01	0.00	0.05
NA2O	0.36	0.31	0.53	0.34
K2O	12.08	11.44	11.68	12.07
P2O5	0.00	0.00	0.00	0.00
H2O	4.47	4.59	4.45	4.57
TOTAL	100.04	101.93	99.68	101.80
SI	6.189	6.145	6.050	6.145
TI	0.000	0.022	0.003	0.018
AL	5.503	5.620	5.697	5.620
CR	0.000	0.000	0.000	0.000
FE2	0.191	0.138	0.187	0.103
MN	0.003	0.008	0.008	0.006
MG	0.092	0.097	0.082	0.076
CA	0.000	0.001	0.000	0.007
NA	0.094	0.079	0.138	0.086
K	2.067	1.907	2.006	2.019
P	0.000	0.000	0.000	0.000
OH	4.000	4.000	4.000	4.000

B-4: Microprobe analyses of garnet (recalculations based on 24 oxygens)

	NPM484	NPM484	NPM484	NPM484	NPM484	NPM484	NPM107	NPM107	NPM344
	11 GT RIM	11 GT CORE	11 GT RIM	12 GT RIM	12 GT CORE	13 GT CORE	81 GT RIM	81 GT CORE	81 GT CORE
SIO2	35.74	35.67	35.71	35.97	36.11	35.62	36.21	36.03	36.10
TIO2	0.09	0.09	0.13	0.26	0.18	0.08	0.11	0.10	0.03
AL2O3	20.45	20.56	20.41	20.19	20.48	20.44	20.74	20.55	20.25
CR2O3	0.01	0.00	0.00	0.00	0.00	0.00	0.00	0.00	0.00
FEO	34.14	35.63	34.79	33.56	33.79	35.32	26.90	23.83	24.49
MNO	6.53	5.53	6.45	6.53	5.56	5.04	15.32	18.05	16.90
MGO	0.93	1.01	0.88	0.93	1.06	1.12	1.16	1.04	1.73
CAO	0.86	0.73	0.88	1.12	1.16	0.78	0.44	0.52	0.81
NA2O	0.00	0.00	0.00	0.00	0.00	0.00	0.00	0.00	0.00
K2O	0.00	0.00	0.00	0.00	0.00	0.00	0.00	0.00	0.00
P2O5	0.00	0.00	0.00	0.00	0.00	0.00	0.00	0.00	0.00
H2O	0.00	0.00	0.00	0.00	0.00	0.00	0.00	0.00	0.00
TOTAL	98.75	99.22	99.25	98.56	98.34	98.40	100.88	100.12	100.31
SI	5.949	5.920	5.930	5.986	5.998	5.944	5.914	5.928	5.922
TI	0.011	0.011	0.016	0.033	0.022	0.010	0.014	0.012	0.004
AL	4.013	4.023	3.996	3.961	4.010	4.021	3.994	3.986	3.916
CR	0.003	0.000	0.000	0.000	0.000	0.000	0.000	0.000	0.000
FE2	4.752	4.946	4.832	4.671	4.694	4.929	3.675	3.279	3.360
MN	0.921	0.777	0.907	0.920	0.782	0.712	2.120	2.515	2.348
MG	0.231	0.250	0.218	0.231	0.262	0.279	0.282	0.255	0.423
CA	0.153	0.130	0.157	0.200	0.206	0.139	0.077	0.092	0.142
NA	0.000	0.000	0.000	0.000	0.000	0.000	0.000	0.000	0.000
K	0.000	0.000	0.000	0.000	0.000	0.000	0.000	0.000	0.000
P	0.000	0.000	0.000	0.000	0.000	0.000	0.000	0.000	0.000
OH	0.000	0.000	0.000	0.000	0.000	0.000	0.000	0.000	0.000

	NPM344	NPM611	NPM611	NPM8A	NPM8A	NPM107	NPM107	NPM344	NPM344
	81 GT RIM	81 GT RIM	81 GT CORE	81 GT CORE	81 GT RIM	82 GT RIM	82 GT CORE	82 GT RIM	82 GT CORE
SIO2	36.12	35.68	35.61	35.83	35.56	35.88	35.83	35.88	35.93
TIO2	0.10	0.03	0.11	0.08	0.03	0.01	0.03	0.04	0.12
AL2O3	20.47	20.84	20.27	20.32	20.42	20.53	20.36	20.42	20.47
CR2O3	0.00	0.00	0.00	0.00	0.00	0.00	0.00	0.00	0.00
FEO	27.44	28.26	28.23	29.48	31.46	26.17	26.38	27.13	24.25
MNO	13.97	11.77	12.32	10.61	9.09	15.99	15.07	13.34	16.87
MGO	1.75	1.63	1.81	1.43	1.50	1.00	1.18	1.68	1.81
CAO	0.72	0.55	0.53	0.61	0.50	0.41	0.40	0.73	0.76
NA2O	0.00	0.00	0.00	0.00	0.00	0.00	0.00	0.00	0.00
K2O	0.00	0.00	0.00	0.00	0.00	0.00	0.00	0.00	0.00
P2O5	0.00	0.00	0.00	0.00	0.00	0.00	0.00	0.00	0.00
H2O	0.00	0.00	0.00	0.00	0.00	0.00	0.00	0.00	0.00
TOTAL	100.57	98.76	98.88	98.36	98.56	99.99	99.25	99.22	100.21
SI	5.907	5.910	5.913	5.966	5.924	5.921	5.942	5.930	5.893
TI	0.012	0.004	0.014	0.010	0.004	0.001	0.004	0.005	0.015
AL	3.947	4.070	3.968	3.989	4.011	3.994	3.980	3.979	3.958
CR	0.000	0.000	0.000	0.000	0.000	0.000	0.000	0.000	0.000
FE2	3.753	3.915	3.920	4.105	4.383	3.612	3.659	3.750	3.327
MN	1.935	1.652	1.733	1.496	1.283	2.235	2.117	1.868	2.344
MG	0.427	0.402	0.448	0.355	0.372	0.246	0.292	0.414	0.442
CA	0.126	0.098	0.094	0.109	0.089	0.072	0.071	0.129	0.134
NA	0.000	0.000	0.000	0.000	0.000	0.000	0.000	0.000	0.000
K	0.000	0.000	0.000	0.000	0.000	0.000	0.000	0.000	0.000
P	0.000	0.000	0.000	0.000	0.000	0.000	0.000	0.000	0.000
OH	0.000	0.000	0.000	0.000	0.000	0.000	0.000	0.000	0.000

	NPM8A	NPM8A	NPM344	NPM344	NPM8A	NPM8A	NPM108	NPM108	NPM108
	82 GT RIM	82 GT CORE	83 GT CORE	83 GT RIM	83 GT CORE	83 GT RIM	CR1 GT CORE	CR1 GT CORE	CR1 GT RIM
SIO2	35.75	35.67	35.81	35.70	35.68	36.31	36.55	36.18	36.20
TIO2	0.07	0.11	0.07	0.00	0.16	0.09	0.00	0.12	0.09
AL2O3	20.42	20.68	20.01	20.65	20.73	20.53	20.62	20.70	21.00
CR2O3	0.00	0.00	0.00	0.00	0.00	0.00	0.00	0.00	0.00
FEO	31.34	31.87	24.11	27.85	32.73	28.07	28.53	28.80	28.22
MNO	8.92	8.63	16.84	13.40	6.69	12.69	9.09	8.91	9.57
MGO	1.62	1.73	1.86	1.73	2.00	1.26	2.33	2.32	2.03
CAO	0.51	0.45	0.79	0.67	0.59	0.61	2.00	2.08	1.78
NA2O	0.00	0.00	0.00	0.00	0.00	0.00	0.00	0.00	0.00
K2O	0.00	0.00	0.00	0.00	0.00	0.00	0.00	0.00	0.00
P2O5	0.00	0.00	0.00	0.00	0.00	0.00	0.00	0.00	0.00
H2O	0.00	0.00	0.00	0.00	0.00	0.00	0.00	0.00	0.00
TOTAL	98.63	99.14	99.49	100.00	98.58	99.56	99.12	99.11	98.89
SI	5.940	5.900	5.921	5.874	5.909	5.976	5.978	5.928	5.938
TI	0.009	0.014	0.009	0.000	0.020	0.011	0.000	0.015	0.011
AL	4.000	4.033	3.900	4.006	4.048	3.984	3.976	3.999	4.061
CR	0.000	0.000	0.000	0.000	0.000	0.000	0.000	0.000	0.000
FE2	4.355	4.409	3.334	3.833	4.533	3.864	3.902	3.947	3.871
MN	1.255	1.209	2.358	1.868	0.939	1.769	1.259	1.237	1.330
MG	0.401	0.426	0.458	0.424	0.494	0.309	0.568	0.567	0.496
CA	0.091	0.080	0.140	0.118	0.105	0.108	0.350	0.365	0.313
NA	0.000	0.000	0.000	0.000	0.000	0.000	0.000	0.000	0.000
K	0.000	0.000	0.000	0.000	0.000	0.000	0.000	0.000	0.000
P	0.000	0.000	0.000	0.000	0.000	0.000	0.000	0.000	0.000
OH	0.000	0.000	0.000	0.000	0.000	0.000	0.000	0.000	0.000

	NPM108	NPM108	NPM108
	CR2 GT RIM	CR2 GT RIM	CR3 GT CORE
SIO2	36.49	37.16	36.22
TIO2	0.05	0.03	0.14
AL2O3	20.75	20.78	20.57
CR2O3	0.00	0.00	0.00
FEO	28.15	28.78	28.22
MNO	9.51	9.01	9.08
MGO	2.18	2.37	2.36
CAO	2.11	2.16	2.16
NA2O	0.00	0.00	0.00
K2O	0.00	0.00	0.00
P2O5	0.00	0.00	0.00
H2O	0.00	0.00	0.00
TOTAL	99.24	100.29	98.75
SI	5.963	5.999	5.948
TI	0.006	0.004	0.017
AL	3.998	3.955	3.982
CR	0.000	0.000	0.000
FE2	3.847	3.886	3.876
MN	1.316	1.232	1.263
MG	0.531	0.570	0.578
CA	0.369	0.374	0.380
NA	0.000	0.000	0.000
K	0.000	0.000	0.000
P	0.000	0.000	0.000
OH	0.000	0.000	0.000

B-5: Microprobe analyses of plagioclase (recalculated to 32 oxygens)

	NPM11	NPM11	NPM2	NPM2	NPM533	NPM533	NPM582	NPM582	NPM11
	11 PL CORE	11 PL RIM	11 PL CORE	11 PL RIM	11 PL CORE	11 PL RIM	11 PL CORE	11 PL RIM	12 PL CORE
SIO2	59.91	59.23	62.80	63.59	58.96	60.10	59.68	61.03	58.65
TIO2	0.00	0.00	0.00	0.00	0.00	0.00	0.00	0.00	0.00
AL2O3	25.50	25.98	23.08	23.14	26.05	24.85	25.44	24.15	26.22
CR2O3	0.00	0.00	0.00	0.00	0.00	0.00	0.00	0.00	0.00
FEO	0.00	0.02	0.12	0.07	0.02	0.05	0.11	0.11	0.10
MNO	0.00	0.00	0.00	0.00	0.00	0.00	0.00	0.00	0.00
MGO	0.00	0.00	0.01	0.04	0.00	0.01	0.00	0.00	0.00
CAO	6.81	7.93	4.87	4.62	7.79	7.46	7.29	6.07	8.05
NA2O	7.73	7.13	8.88	9.28	7.14	7.53	6.71	8.37	7.11
K2O	0.14	0.09	0.11	0.11	0.30	0.29	0.14	0.21	0.11
P2O5	0.00	0.00	0.00	0.00	0.00	0.00	0.00	0.00	0.00
H2O	0.00	0.00	0.00	0.00	0.00	0.00	0.00	0.00	0.00
TOTAL	100.09	100.38	99.87	100.85	100.26	100.29	99.37	99.94	100.24
SI	10.663	10.536	11.138	11.166	10.513	10.703	10.678	10.873	10.465
TI	0.000	0.000	0.000	0.000	0.000	0.000	0.000	0.000	0.000
AL	5.351	5.449	4.826	4.790	5.476	5.218	5.366	5.072	5.516
CR	0.000	0.000	0.000	0.000	0.000	0.000	0.000	0.000	0.000
FE2	0.000	0.003	0.018	0.010	0.003	0.007	0.016	0.016	0.015
MN	0.000	0.000	0.000	0.000	0.000	0.000	0.000	0.000	0.000
MG	0.000	0.000	0.003	0.010	0.000	0.003	0.000	0.000	0.000
CA	1.299	1.512	0.925	0.869	1.488	1.424	1.398	1.159	1.539
NA	2.668	2.459	3.054	3.160	2.469	2.600	2.328	2.891	2.460
K	0.032	0.020	0.025	0.025	0.068	0.066	0.032	0.048	0.025
P	0.000	0.000	0.000	0.000	0.000	0.000	0.000	0.000	0.000
OH	0.000	0.000	0.000	0.000	0.000	0.000	0.000	0.000	0.000

	NPM11	NPM2	NPM2	NPM533	NPM533	NPM582	NPM582	NPM11	NPM11
	12 PL RIM	12 PL CORE	12 PL RIM	12 PL CORE	12 PL RIM	12 PL CORE	12 PL RIM	13 PL RIM	13 PL CORE
SIO2	59.54	64.00	64.17	59.58	58.97	61.37	61.03	59.41	59.30
TIO2	0.00	0.00	0.00	0.00	0.00	0.00	0.00	0.00	0.00
AL2O3	25.64	23.33	23.27	25.53	26.05	23.30	24.22	25.20	25.41
CR2O3	0.00	0.00	0.00	0.00	0.00	0.00	0.00	0.00	0.00
FEO	0.14	0.10	0.12	0.05	0.00	0.00	0.12	0.09	0.00
MNO	0.00	0.00	0.00	0.00	0.00	0.00	0.00	0.00	0.00
MGO	0.00	0.01	0.00	0.00	0.00	0.00	0.00	0.00	0.00
CAO	7.48	4.21	4.34	7.57	8.03	5.97	5.84	7.23	7.83
NA2O	7.52	9.15	8.75	7.05	6.72	8.07	8.05	7.46	7.41
K2O	0.20	0.22	0.17	0.20	0.12	0.12	0.11	0.11	0.18
P2O5	0.00	0.00	0.00	0.00	0.00	0.00	0.00	0.00	0.00
H2O	0.00	0.00	0.00	0.00	0.00	0.00	0.00	0.00	0.00
TOTAL	100.52	101.02	100.82	99.98	99.89	98.83	99.37	99.50	100.13
SI	10.587	11.199	11.231	10.626	10.530	11.018	10.903	10.650	10.588
TI	0.000	0.000	0.000	0.000	0.000	0.000	0.000	0.000	0.000
AL	5.375	4.813	4.802	5.368	5.484	4.932	5.101	5.326	5.349
CR	0.000	0.000	0.000	0.000	0.000	0.000	0.000	0.000	0.000
FE2	0.021	0.015	0.018	0.007	0.000	0.000	0.018	0.013	0.000
MN	0.000	0.000	0.000	0.000	0.000	0.000	0.000	0.000	0.000
MG	0.000	0.003	0.000	0.000	0.000	0.000	0.000	0.000	0.000
CA	1.425	0.789	0.814	1.447	1.536	1.148	1.118	1.389	1.498
NA	2.593	3.104	2.969	2.438	2.327	2.809	2.788	2.593	2.565
K	0.045	0.049	0.038	0.046	0.027	0.027	0.025	0.025	0.041
P	0.000	0.000	0.000	0.000	0.000	0.000	0.000	0.000	0.000
OH	0.000	0.000	0.000	0.000	0.000	0.000	0.000	0.000	0.000

	NPM2	NPM2	NPM533	NPM533	NPM582	NPM582	NPM546	NPM546	NPM546
	13 PL RIM	13 PL CORE	13 PL RIM	13 PL CORE	13 PL CORE	13 PL RIM	21 PL RIM	21 PL CORE	22 PL CORE
SIO2	63.97	62.09	57.24	58.99	57.54	61.13	61.69	63.78	61.37
TIO2	0.00	0.00	0.00	0.00	0.00	0.00	0.00	0.00	0.00
AL2O3	23.73	24.13	27.00	26.16	25.80	24.44	23.84	22.97	24.01
CR2O3	0.00	0.00	0.00	0.00	0.00	0.00	0.00	0.00	0.00
FEO	0.18	0.13	0.15	0.07	0.11	0.18	0.02	0.10	0.13
MNO	0.00	0.00	0.00	0.00	0.00	0.00	0.00	0.00	0.00
MGO	0.00	0.00	0.02	0.02	0.01	0.03	0.01	0.00	0.00
CAO	4.48	5.96	8.92	8.02	9.31	6.37	5.97	4.15	5.67
NA2O	8.90	7.86	6.44	6.78	6.84	8.45	8.36	9.06	8.28
K2O	0.12	0.12	0.12	0.24	0.10	0.10	0.31	0.15	0.16
P2O5	0.00	0.00	0.00	0.00	0.00	0.00	0.00	0.00	0.00
H2O	0.00	0.00	0.00	0.00	0.00	0.00	0.00	0.00	0.00
TOTAL	101.38	100.29	99.89	100.28	99.71	100.70	100.20	100.21	99.62
SI	11.152	10.975	10.275	10.508	10.374	10.822	10.951	11.239	10.940
TI	0.000	0.000	0.000	0.000	0.000	0.000	0.000	0.000	0.000
AL	4.877	5.028	5.714	5.494	5.484	5.101	4.989	4.772	5.046
CR	0.000	0.000	0.000	0.000	0.000	0.000	0.000	0.000	0.000
FE2	0.026	0.019	0.023	0.010	0.017	0.027	0.003	0.015	0.019
MN	0.000	0.000	0.000	0.000	0.000	0.000	0.000	0.000	0.000
MG	0.000	0.000	0.005	0.005	0.003	0.008	0.003	0.000	0.000
CA	0.837	1.129	1.716	1.531	1.799	1.208	1.136	0.784	1.083
NA	3.008	2.694	2.242	2.342	2.391	2.901	2.877	3.096	2.862
K	0.027	0.027	0.027	0.055	0.023	0.023	0.070	0.034	0.036
P	0.000	0.000	0.000	0.000	0.000	0.000	0.000	0.000	0.000
OH	0.000	0.000	0.000	0.000	0.000	0.000	0.000	0.000	0.000

	NPM546	NPM546	NPM546	NPM558	NPM558	NPM468	NPM468	NPM468	NPM468
	22 PL RIM	23 PL CORE	23 PL RIM	24 PL CORE	24 PL RIM	31 PL CORE	31 PL RIM	32 PL RIM	32 PL CORE
SIO2	61.52	60.40	61.54	62.15	62.59	66.56	66.54	66.23	66.57
TIO2	0.00	0.00	0.00	0.00	0.00	0.00	0.00	0.00	0.00
AL2O3	23.77	24.68	24.15	23.36	23.10	21.09	21.31	21.17	21.49
CR2O3	0.00	0.00	0.00	0.00	0.00	0.00	0.00	0.00	0.00
FEO	0.11	0.11	0.18	0.12	0.17	0.00	0.09	0.12	0.11
MNO	0.00	0.00	0.00	0.00	0.00	0.00	0.00	0.00	0.00
MGO	0.00	0.00	0.00	0.00	0.01	0.00	0.00	0.00	0.00
CAO	5.67	6.47	5.92	5.48	5.32	2.01	1.75	1.75	2.19
NA2O	8.39	7.93	8.09	8.45	8.95	10.54	10.96	10.65	10.60
K2O	0.26	0.25	0.25	0.20	0.23	0.09	0.05	0.09	0.08
P2O5	0.00	0.00	0.00	0.00	0.00	0.00	0.00	0.00	0.00
H2O	0.00	0.00	0.00	0.00	0.00	0.00	0.00	0.00	0.00
TOTAL	99.72	99.84	100.13	99.76	100.37	100.29	100.70	100.01	101.04
SI	10.965	10.779	10.923	11.055	11.083	11.649	11.612	11.629	11.583
TI	0.000	0.000	0.000	0.000	0.000	0.000	0.000	0.000	0.000
AL	4.995	5.192	5.054	4.899	4.822	4.351	4.384	4.382	4.408
CR	0.000	0.000	0.000	0.000	0.000	0.000	0.000	0.000	0.000
FE2	0.016	0.016	0.027	0.018	0.025	0.000	0.013	0.018	0.016
MN	0.000	0.000	0.000	0.000	0.000	0.000	0.000	0.000	0.000
MG	0.000	0.000	0.000	0.000	0.003	0.000	0.000	0.000	0.000
CA	1.083	1.237	1.126	1.044	1.009	0.377	0.327	0.329	0.408
NA	2.899	2.744	2.784	2.914	3.073	3.577	3.708	3.626	3.576
K	0.059	0.057	0.057	0.045	0.052	0.020	0.011	0.020	0.018
P	0.000	0.000	0.000	0.000	0.000	0.000	0.000	0.000	0.000
OH	0.000	0.000	0.000	0.000	0.000	0.000	0.000	0.000	0.000

	NPM468	NPM468	NPM441	NPM441	NPM458	NPM458	NPM477	NPM477	NPM542
	33 PL CORE	33 PL RIM	41 PL RIM	41 PL CORE	41 PL CORE	41 PL RIM	41 PL RIM	41 PL CORE	41 PL CORE
SIO2	66.38	62.95	67.52	66.96	62.93	63.75	68.12	66.36	66.29
TIO2	0.00	0.00	0.00	0.00	0.00	0.00	0.00	0.00	0.00
AL2O3	21.37	22.82	20.11	19.88	22.86	22.95	20.32	20.69	21.87
CR2O3	0.00	0.00	0.00	0.00	0.00	0.00	0.00	0.00	0.00
FEO	0.02	0.10	0.17	0.06	0.15	0.14	0.19	0.15	0.04
MNO	0.00	0.00	0.00	0.00	0.00	0.00	0.00	0.00	0.00
MGO	0.00	0.00	0.00	0.00	0.00	0.00	0.01	0.00	0.00
CAO	1.78	3.66	1.47	1.19	4.31	4.06	1.16	1.98	2.97
NA2O	10.45	9.82	10.97	11.21	9.10	9.24	10.70	9.69	9.93
K2O	0.09	0.04	0.10	0.08	0.10	0.10	0.13	0.17	0.07
P2O5	0.00	0.00	0.00	0.00	0.00	0.00	0.00	0.00	0.00
H2O	0.00	0.00	0.00	0.00	0.00	0.00	0.00	0.00	0.00
TOTAL	100.09	99.39	100.34	99.38	99.45	100.24	100.63	99.04	101.17
SI	11.629	11.203	11.806	11.817	11.193	11.235	11.844	11.728	11.520
TI	0.000	0.000	0.000	0.000	0.000	0.000	0.000	0.000	0.000
AL	4.414	4.788	4.145	4.136	4.793	4.768	4.165	4.311	4.481
CR	0.000	0.000	0.000	0.000	0.000	0.000	0.000	0.000	0.000
FE2	0.003	0.015	0.025	0.009	0.022	0.021	0.028	0.022	0.006
MN	0.000	0.000	0.000	0.000	0.000	0.000	0.000	0.000	0.000
MG	0.000	0.000	0.000	0.000	0.000	0.000	0.003	0.000	0.000
CA	0.334	0.698	0.275	0.225	0.821	0.767	0.216	0.375	0.553
NA	3.550	3.389	3.719	3.836	3.138	3.157	3.607	3.321	3.346
K	0.020	0.009	0.022	0.018	0.023	0.022	0.029	0.038	0.016
P	0.000	0.000	0.000	0.000	0.000	0.000	0.000	0.000	0.000
OH	0.000	0.000	0.000	0.000	0.000	0.000	0.000	0.000	0.000

	NPM542	NPM558	NPM558	NPM580	NPM580	NPM441	NPM441	NPM458	NPM458
	41 PL RIM	41 PL RIM	41 PL CORE	41 PL CORE	41 PL RIM	42 PL RIM	42 PL CORE	42 PL CORE	42 PL RIM
SIO2	65.55	62.11	61.02	65.45	67.75	66.08	66.21	62.09	63.46
TIO2	0.00	0.00	0.00	0.00	0.00	0.00	0.00	0.00	0.00
AL2O3	21.60	23.28	24.13	21.98	19.66	20.41	20.58	23.50	22.63
CR2O3	0.00	0.00	0.00	0.00	0.00	0.00	0.00	0.00	0.00
FEO	0.14	0.06	0.16	0.17	0.14	0.22	0.04	0.03	0.14
MNO	0.00	0.00	0.00	0.00	0.00	0.00	0.00	0.00	0.00
MGO	0.01	0.03	0.00	0.04	0.02	0.00	0.01	0.00	0.00
CAO	2.99	5.48	6.75	3.54	1.19	1.81	1.52	5.18	3.90
NA2O	9.82	8.75	8.24	9.59	10.63	10.49	10.98	8.76	9.48
K2O	0.16	0.18	0.13	0.16	0.10	0.16	0.20	0.15	0.15
P2O5	0.00	0.00	0.00	0.00	0.00	0.00	0.00	0.00	0.00
H2O	0.00	0.00	0.00	0.00	0.00	0.00	0.00	0.00	0.00
TOTAL	100.27	99.89	100.43	100.93	99.49	99.17	99.54	99.71	99.76
SI	11.509	11.045	10.839	11.435	11.908	11.705	11.689	11.044	11.249
TI	0.000	0.000	0.000	0.000	0.000	0.000	0.000	0.000	0.000
AL	4.471	4.880	5.053	4.527	4.074	4.262	4.283	4.928	4.729
CR	0.000	0.000	0.000	0.000	0.000	0.000	0.000	0.000	0.000
FE2	0.021	0.009	0.024	0.025	0.021	0.033	0.006	0.004	0.021
MN	0.000	0.000	0.000	0.000	0.000	0.000	0.000	0.000	0.000
MG	0.003	0.008	0.000	0.010	0.005	0.000	0.003	0.000	0.000
CA	0.563	1.044	1.285	0.663	0.224	0.344	0.288	0.987	0.741
NA	3.343	3.017	2.838	3.249	3.623	3.603	3.758	3.021	3.258
K	0.036	0.041	0.029	0.036	0.022	0.036	0.045	0.034	0.034
P	0.000	0.000	0.000	0.000	0.000	0.000	0.000	0.000	0.000
OH	0.000	0.000	0.000	0.000	0.000	0.000	0.000	0.000	0.000

	NPM477	NPM477	NPM542	NPM542	NPM580	NPM580	NPM441	NPM441	NPM458
	42 PL RIM	42 PL CORE	42 PL CORE	42 PL RIM	42 PL CORE	42 PL RIM	43 PL CORE	43 PL RIM	43 PL CORE
SIO2	66.15	65.76	65.35	66.73	64.34	64.01	66.56	67.72	63.45
TIO2	0.00	0.00	0.00	0.00	0.00	0.00	0.00	0.00	0.00
AL2O3	21.47	21.20	21.56	20.30	21.78	21.62	20.29	20.00	23.31
CR2O3	0.00	0.00	0.00	0.00	0.00	0.00	0.00	0.00	0.00
FEO	0.09	0.15	0.18	0.18	0.04	0.13	0.04	0.07	0.16
MNO	0.00	0.00	0.00	0.00	0.00	0.00	0.00	0.00	0.00
MGO	0.00	0.03	0.00	0.01	0.00	0.00	0.04	0.03	0.00
CAO	2.81	2.69	3.08	1.91	3.81	3.62	1.97	1.17	4.16
NA2O	10.10	10.18	9.94	10.35	9.61	9.63	11.17	10.49	9.47
K2O	0.12	0.27	0.11	0.10	0.14	0.20	0.10	0.06	0.17
P2O5	0.00	0.00	0.00	0.00	0.00	0.00	0.00	0.00	0.00
H2O	0.00	0.00	0.00	0.00	0.00	0.00	0.00	0.00	0.00
TOTAL	100.74	100.28	100.22	99.58	99.72	99.21	100.17	99.54	100.72
SI	11.553	11.556	11.491	11.754	11.393	11.398	11.697	11.882	11.156
TI	0.000	0.000	0.000	0.000	0.000	0.000	0.000	0.000	0.000
AL	4.421	4.392	4.469	4.216	4.547	4.539	4.204	4.137	4.832
CR	0.000	0.000	0.000	0.000	0.000	0.000	0.000	0.000	0.000
FE2	0.013	0.022	0.026	0.027	0.006	0.019	0.006	0.010	0.024
MN	0.000	0.000	0.000	0.000	0.000	0.000	0.000	0.000	0.000
MG	0.000	0.008	0.000	0.003	0.000	0.000	0.010	0.008	0.000
CA	0.526	0.506	0.580	0.360	0.723	0.691	0.371	0.220	0.784
NA	3.420	3.469	3.389	3.535	3.299	3.325	3.806	3.569	3.228
K	0.027	0.061	0.025	0.022	0.032	0.045	0.022	0.013	0.038
P	0.000	0.000	0.000	0.000	0.000	0.000	0.000	0.000	0.000
OH	0.000	0.000	0.000	0.000	0.000	0.000	0.000	0.000	0.000

	NPM477	NPM477	NPM542	NPM542	NPM558	NPM558	NPM580	NPM580	NPM405
	43 PL RIM	43 PL CORE	33 PL RIM	33 PL CORE	43 PL RIM	43 PL CORE	43 PL CORE	43 PL RIM	5A1 PL CORE
SIO2	66.25	66.80	66.19	65.74	61.86	61.30	64.92	64.37	54.82
TIO2	0.00	0.00	0.00	0.00	0.00	0.00	0.00	0.00	0.00
AL2O3	20.86	21.07	20.41	20.89	23.34	23.88	21.71	21.72	29.12
CR2O3	0.00	0.00	0.00	0.00	0.00	0.00	0.00	0.00	0.00
FEO	0.03	0.11	0.13	0.13	0.12	0.20	0.19	0.12	0.17
MNO	0.00	0.00	0.00	0.00	0.00	0.00	0.00	0.00	0.00
MGO	0.00	0.01	0.01	0.00	0.00	0.01	0.02	0.00	0.00
CAO	2.35	2.22	2.05	2.59	5.42	6.43	3.55	3.74	10.58
NA2O	10.58	10.24	10.19	10.11	8.43	8.20	9.69	9.63	5.50
K2O	0.11	0.20	0.07	0.07	0.17	0.15	0.18	0.21	0.08
P2O5	0.00	0.00	0.00	0.00	0.00	0.00	0.00	0.00	0.00
H2O	0.00	0.00	0.00	0.00	0.00	0.00	0.00	0.00	0.00
TOTAL	100.18	100.65	99.05	99.53	99.34	100.17	100.26	99.79	100.27
SI	11.632	11.655	11.720	11.613	11.047	10.901	11.431	11.398	9.855
TI	0.000	0.000	0.000	0.000	0.000	0.000	0.000	0.000	0.000
AL	4.318	4.334	4.261	4.350	4.914	5.006	4.507	4.534	6.172
CR	0.000	0.000	0.000	0.000	0.000	0.000	0.000	0.000	0.000
FE2	0.004	0.016	0.019	0.019	0.018	0.030	0.028	0.018	0.026
MN	0.000	0.000	0.000	0.000	0.000	0.000	0.000	0.000	0.000
MG	0.000	0.003	0.003	0.000	0.000	0.003	0.005	0.000	0.000
CA	0.442	0.415	0.389	0.490	1.037	1.225	0.670	0.710	2.038
NA	3.602	3.464	3.499	3.463	2.919	2.827	3.308	3.306	1.917
K	0.025	0.045	0.016	0.016	0.039	0.034	0.040	0.047	0.018
P	0.000	0.000	0.000	0.000	0.000	0.000	0.000	0.000	0.000
OH	0.000	0.000	0.000	0.000	0.000	0.000	0.000	0.000	0.000

	NPM405	NPM406	NPM406	NPM407	NPM407	NPM485	NPM485	NPM405	NPM405
	5A1 PL RIM	5A1 PL RIM	5A1 PL CORE	5A1 PL CORE	5A1 PL RIM	5A1 PL RIM	5A1 PL CORE	5A2 PL RIM	5A2 PL CORE
SIO2	61.33	58.40	58.23	56.19	56.58	61.00	61.60	60.67	52.77
TIO2	0.00	0.00	0.00	0.00	0.00	0.00	0.00	0.00	0.00
AL2O3	25.06	25.94	26.75	27.98	27.16	24.25	24.93	25.19	30.44
CR2O3	0.00	0.00	0.00	0.00	0.00	0.00	0.00	0.00	0.00
FEO	0.17	0.10	0.11	0.13	0.12	0.11	0.08	0.18	0.12
MNO	0.00	0.00	0.00	0.00	0.00	0.00	0.00	0.00	0.00
MGO	0.00	0.00	0.00	0.00	0.00	0.00	0.00	0.00	0.00
CAO	5.21	8.13	8.43	10.19	9.68	5.10	4.92	6.20	12.17
NA2O	8.73	7.22	6.53	6.33	6.35	8.49	8.32	8.26	4.94
K2O	0.09	0.05	0.04	0.10	0.09	0.16	0.09	0.06	0.08
P2O5	0.00	0.00	0.00	0.00	0.00	0.00	0.00	0.00	0.00
H2O	0.00	0.00	0.00	0.00	0.00	0.00	0.00	0.00	0.00
TOTAL	100.59	99.84	100.09	100.92	99.98	99.11	99.94	100.56	100.52
SI	10.830	10.470	10.396	10.040	10.179	10.919	10.906	10.742	9.521
TI	0.000	0.000	0.000	0.000	0.000	0.000	0.000	0.000	0.000
AL	5.217	5.482	5.630	5.894	5.760	5.117	5.203	5.258	6.475
CR	0.000	0.000	0.000	0.000	0.000	0.000	0.000	0.000	0.000
FE2	0.025	0.015	0.016	0.019	0.018	0.016	0.012	0.027	0.018
MN	0.000	0.000	0.000	0.000	0.000	0.000	0.000	0.000	0.000
MG	0.000	0.000	0.000	0.000	0.000	0.000	0.000	0.000	0.000
CA	0.986	1.562	1.613	1.951	1.866	0.978	0.933	1.176	2.353
NA	2.989	2.510	2.260	2.193	2.215	2.947	2.856	2.836	1.728
K	0.020	0.011	0.009	0.023	0.021	0.037	0.020	0.014	0.018
P	0.000	0.000	0.000	0.000	0.000	0.000	0.000	0.000	0.000
OH	0.000	0.000	0.000	0.000	0.000	0.000	0.000	0.000	0.000

	NPM406	NPM407	NPM407	NPM485	NPM485	NPM405	NPM405	NPM406	NPM406
	5A2 PL RIM	5A2 PL CORE	5A2 PL RIM	5A2 PL CORE	5A2 PL RIM	5A3 PL CORE	5A3 PL RIM	5A3 PL CORE	5A3 PL RIM
SIO2	54.16	57.04	57.15	61.62	60.93	60.40	59.80	54.59	59.97
TIO2	0.00	0.00	0.00	0.00	0.00	0.00	0.00	0.00	0.00
AL2O3	29.12	27.66	27.82	24.55	25.09	25.75	25.77	28.47	25.63
CR2O3	0.00	0.00	0.00	0.00	0.00	0.00	0.00	0.00	0.00
FEO	0.04	0.03	0.14	0.13	0.11	0.13	0.08	0.09	0.17
MNO	0.00	0.00	0.00	0.00	0.00	0.00	0.00	0.00	0.00
MGO	0.00	0.00	0.00	0.00	0.00	0.00	0.00	0.00	0.00
CAO	11.51	9.13	9.40	4.54	5.07	6.12	6.48	11.31	7.18
NA2O	5.17	6.30	6.35	8.64	8.32	8.21	8.02	5.71	7.43
K2O	0.06	0.10	0.11	0.03	0.13	0.07	0.07	0.03	0.06
P2O5	0.00	0.00	0.00	0.00	0.00	0.00	0.00	0.00	0.00
H2O	0.00	0.00	0.00	0.00	0.00	0.00	0.00	0.00	0.00
TOTAL	100.06	100.26	100.97	99.51	99.65	100.68	100.22	100.20	100.44
SI	9.779	10.199	10.165	10.953	10.838	10.678	10.631	9.854	10.641
TI	0.000	0.000	0.000	0.000	0.000	0.000	0.000	0.000	0.000
AL	6.198	5.830	5.834	5.145	5.261	5.367	5.401	6.059	5.362
CR	0.000	0.000	0.000	0.000	0.000	0.000	0.000	0.000	0.000
FE2	0.006	0.004	0.021	0.019	0.016	0.019	0.012	0.014	0.025
MN	0.000	0.000	0.000	0.000	0.000	0.000	0.000	0.000	0.000
MG	0.000	0.000	0.000	0.000	0.000	0.000	0.000	0.000	0.000
CA	2.227	1.749	1.791	0.865	0.966	1.159	1.234	2.188	1.365
NA	1.810	2.184	2.190	2.978	2.869	2.814	2.764	1.999	2.556
K	0.014	0.023	0.025	0.007	0.030	0.016	0.016	0.007	0.014
P	0.000	0.000	0.000	0.000	0.000	0.000	0.000	0.000	0.000
OH	0.000	0.000	0.000	0.000	0.000	0.000	0.000	0.000	0.000

	NPM407	NPM407	NPM485	NPM485	NPM538	NPM538	NPM539	NPM560	NPM560
	5A3 PL RIM	5A3 PL CORE	5A3 PL RIM	5A3 PL CORE	71 PL CORE	71 PL RIM	71 PL RIM	71 PL RIM	71 PL CORE
SIO2	58.56	56.61	61.19	61.50	64.24	63.93	65.37	63.53	59.17
TIO2	0.00	0.00	0.00	0.00	0.00	0.00	0.00	0.00	0.00
AL2O3	26.49	27.02	25.05	24.39	21.06	21.66	22.30	22.36	25.30
CR2O3	0.00	0.00	0.00	0.00	0.00	0.00	0.00	0.00	0.00
FEO	0.24	0.12	0.08	0.10	0.20	0.12	0.06	0.12	0.16
MNO	0.00	0.00	0.00	0.00	0.00	0.00	0.00	0.00	0.00
MGO	0.00	0.00	0.00	0.00	0.00	0.00	0.00	0.00	0.00
CAO	8.71	9.75	5.25	4.76	3.06	3.16	2.87	4.22	7.86
NA2O	6.79	6.56	8.53	8.75	9.81	9.92	10.15	9.39	6.91
K2O	0.12	0.08	0.13	0.11	0.13	0.14	0.10	0.19	0.14
P2O5	0.00	0.00	0.00	0.00	0.00	0.00	0.00	0.00	0.00
H2O	0.00	0.00	0.00	0.00	0.00	0.00	0.00	0.00	0.00
TOTAL	100.91	100.14	100.23	99.61	98.50	98.93	100.85	99.81	99.54
SI	10.402	10.179	10.835	10.941	11.500	11.406	11.418	11.266	10.612
TI	0.000	0.000	0.000	0.000	0.000	0.000	0.000	0.000	0.000
AL	5.547	5.728	5.229	5.116	4.444	4.556	4.592	4.675	5.349
CR	0.000	0.000	0.000	0.000	0.000	0.000	0.000	0.000	0.000
FE2	0.036	0.018	0.012	0.015	0.030	0.018	0.009	0.018	0.024
MN	0.000	0.000	0.000	0.000	0.000	0.000	0.000	0.000	0.000
MG	0.000	0.000	0.000	0.000	0.000	0.000	0.000	0.000	0.000
CA	1.658	1.879	0.996	0.907	0.587	0.604	0.537	0.802	1.510
NA	2.338	2.287	2.929	3.018	3.405	3.432	3.438	3.229	2.403
K	0.027	0.018	0.029	0.025	0.030	0.032	0.022	0.043	0.032
P	0.000	0.000	0.000	0.000	0.000	0.000	0.000	0.000	0.000
OH	0.000	0.000	0.000	0.000	0.000	0.000	0.000	0.000	0.000

	NPM566	NPM583	NPM583	NPM538	NPM538	NPM539	NPM539	NPM560	NPM560
	71 PL CORE	71 PL RIM	71 PL CORE	72 PL CORE	72 PL RIM	72 PL RIM	72 PL CORE	72 PL RIM	72 PL CORE
SIO2	63.08	62.54	60.40	64.39	64.68	63.38	63.19	60.73	60.09
TIO2	0.00	0.00	0.00	0.00	0.00	0.00	0.00	0.00	0.00
AL2O3	23.25	23.74	24.77	21.49	21.83	23.70	23.60	24.27	23.61
CR2O3	0.00	0.00	0.00	0.00	0.00	0.00	0.00	0.00	0.00
FEO	0.13	0.13	0.17	0.14	0.11	0.12	0.07	0.12	0.14
MNO	0.00	0.00	0.00	0.00	0.00	0.00	0.00	0.00	0.00
MGO	0.00	0.00	0.00	0.00	0.00	0.00	0.00	0.00	0.00
CAO	4.26	5.42	6.93	3.25	2.96	4.48	4.38	6.85	6.74
NA2O	9.47	8.60	7.61	10.09	9.85	9.11	9.27	7.91	8.10
K2O	0.18	0.12	0.14	0.09	0.15	0.11	0.16	0.11	0.11
P2O5	0.00	0.00	0.00	0.00	0.00	0.00	0.00	0.00	0.00
H2O	0.00	0.00	0.00	0.00	0.00	0.00	0.00	0.00	0.00
TOTAL	100.37	100.55	100.02	99.45	99.58	100.90	100.67	99.99	98.79
SI	11.137	11.033	10.759	11.433	11.443	11.115	11.113	10.823	10.852
TI	0.000	0.000	0.000	0.000	0.000	0.000	0.000	0.000	0.000
AL	4.839	4.937	5.202	4.498	4.553	4.900	4.893	5.099	5.027
CR	0.000	0.000	0.000	0.000	0.000	0.000	0.000	0.000	0.000
FE2	0.019	0.019	0.025	0.021	0.016	0.018	0.010	0.018	0.021
MN	0.000	0.000	0.000	0.000	0.000	0.000	0.000	0.000	0.000
MG	0.000	0.000	0.000	0.000	0.000	0.000	0.000	0.000	0.000
CA	0.806	1.025	1.323	0.618	0.561	0.842	0.825	1.308	1.304
NA	3.242	2.942	2.628	3.474	3.379	3.098	3.161	2.733	2.836
K	0.041	0.027	0.032	0.020	0.034	0.025	0.036	0.025	0.025
P	0.000	0.000	0.000	0.000	0.000	0.000	0.000	0.000	0.000
OH	0.000	0.000	0.000	0.000	0.000	0.000	0.000	0.000	0.000

	NPM566	NPM566	NPM583	NPM583	NPM538	NPM538	NPM539	NPM560	NPM560
	72 PL RIM	72 PL CORE	72 PL CORE	72 PL RIM	73 PL RIM	73 PL CORE	73 PL CORE	73 PL CORE	73 PL RIM
SIO2	62.62	62.09	58.82	62.54	64.05	64.28	64.91	58.31	63.39
TIO2	0.00	0.00	0.00	0.00	0.00	0.00	0.00	0.00	0.00
AL2O3	22.60	23.20	25.21	23.27	22.15	21.93	22.80	25.47	22.33
CR2O3	0.00	0.00	0.00	0.00	0.00	0.00	0.00	0.00	0.00
FEO	0.13	0.10	0.16	0.14	0.15	0.14	0.10	0.14	0.12
MNO	0.00	0.00	0.00	0.00	0.00	0.00	0.00	0.00	0.00
MGO	0.00	0.00	0.00	0.00	0.00	0.00	0.00	0.00	0.00
CAO	4.22	4.98	7.79	5.29	3.58	3.12	3.30	8.12	4.07
NA2O	9.55	9.00	7.53	8.36	9.60	10.10	10.03	7.03	9.44
K2O	0.12	0.15	0.14	0.24	0.14	0.15	0.15	0.12	0.12
P2O5	0.00	0.00	0.00	0.00	0.00	0.00	0.00	0.00	0.00
H2O	0.00	0.00	0.00	0.00	0.00	0.00	0.00	0.00	0.00
TOTAL	99.24	99.52	99.65	99.84	99.67	99.72	101.29	99.19	99.47
SI	11.184	11.072	10.569	11.101	11.347	11.384	11.315	10.520	11.272
TI	0.000	0.000	0.000	0.000	0.000	0.000	0.000	0.000	0.000
AL	4.759	4.877	5.340	4.870	4.626	4.579	4.685	5.417	4.681
CR	0.000	0.000	0.000	0.000	0.000	0.000	0.000	0.000	0.000
FE2	0.019	0.015	0.024	0.021	0.022	0.021	0.015	0.021	0.018
MN	0.000	0.000	0.000	0.000	0.000	0.000	0.000	0.000	0.000
MG	0.000	0.000	0.000	0.000	0.000	0.000	0.000	0.000	0.000
CA	0.808	0.952	1.500	1.006	0.680	0.592	0.616	1.570	0.775
NA	3.307	3.112	2.623	2.877	3.298	3.468	3.390	2.459	3.255
K	0.027	0.034	0.032	0.054	0.032	0.034	0.033	0.028	0.027
P	0.000	0.000	0.000	0.000	0.000	0.000	0.000	0.000	0.000
OH	0.000	0.000	0.000	0.000	0.000	0.000	0.000	0.000	0.000

	NPM566	NPM566	NPM583	NPM583	NPM361	NPM361	NPM537	NPM537	NPM361
	73 PL RIM	73 PL CORE	73 PL CORE	73 PL RIM	81 PL CORE	81 PL RIM	81 PL RIM	81 PL CORE	82 PL RIM
SIO2	62.80	63.49	59.80	61.46	65.19	65.94	64.85	63.76	66.06
TIO2	0.00	0.00	0.00	0.00	0.00	0.00	0.00	0.00	0.00
AL2O3	21.90	22.30	25.14	23.50	22.80	22.17	22.73	23.14	21.60
CR2O3	0.00	0.00	0.00	0.00	0.00	0.00	0.00	0.00	0.00
FEO	0.19	0.05	0.19	0.14	0.05	0.07	0.10	0.08	0.05
MNO	0.00	0.00	0.00	0.00	0.00	0.00	0.00	0.00	0.00
MGO	0.00	0.00	0.00	0.00	0.00	0.00	0.00	0.00	0.00
CAO	4.11	3.75	7.23	5.59	3.41	2.74	3.33	4.00	2.18
NA2O	9.82	9.83	7.78	8.88	9.66	10.21	9.84	8.95	10.69
K2O	0.13	0.15	0.13	0.13	0.09	0.14	0.09	0.15	0.12
P2O5	0.00	0.00	0.00	0.00	0.00	0.00	0.00	0.00	0.00
H2O	0.00	0.00	0.00	0.00	0.00	0.00	0.00	0.00	0.00
TOTAL	98.95	99.57	100.27	99.70	101.20	101.27	100.94	100.08	100.70
SI	11.259	11.281	10.655	10.970	11.349	11.464	11.331	11.237	11.543
TI	0.000	0.000	0.000	0.000	0.000	0.000	0.000	0.000	0.000
AL	4.629	4.671	5.281	4.945	4.679	4.544	4.682	4.808	4.450
CR	0.000	0.000	0.000	0.000	0.000	0.000	0.000	0.000	0.000
FE2	0.028	0.007	0.028	0.021	0.007	0.010	0.015	0.012	0.007
MN	0.000	0.000	0.000	0.000	0.000	0.000	0.000	0.000	0.000
MG	0.000	0.000	0.000	0.000	0.000	0.000	0.000	0.000	0.000
CA	0.790	0.714	1.380	1.069	0.636	0.510	0.623	0.755	0.408
NA	3.414	3.387	2.688	3.073	3.261	3.442	3.334	3.058	3.622
K	0.030	0.034	0.030	0.030	0.020	0.031	0.020	0.034	0.027
P	0.000	0.000	0.000	0.000	0.000	0.000	0.000	0.000	0.000
OH	0.000	0.000	0.000	0.000	0.000	0.000	0.000	0.000	0.000

	NPM537	NPM361	NPM361	NPM537	NPM491	NPM491	NPM8B	NPM8B	NPM491
	82 PL CORE	83 PL CORE	83 PL RIM	83 PL CORE	91 PL RIM	91 PL CORE	91 PL CORE	91 PL RIM	92 PL CORE
SIO2	63.95	66.35	64.85	64.18	67.85	68.17	65.26	68.19	67.76
TIO2	0.00	0.00	0.00	0.00	0.00	0.00	0.00	0.00	0.00
AL2O3	22.84	21.85	20.99	23.19	19.81	20.06	21.78	20.38	20.42
CR2O3	0.00	0.00	0.00	0.00	0.00	0.00	0.00	0.00	0.00
FEO	0.09	0.13	1.88	0.07	0.04	0.03	0.10	0.07	0.08
MNO	0.00	0.00	0.00	0.00	0.00	0.00	0.00	0.00	0.00
MGO	0.00	0.00	0.00	0.00	0.00	0.00	0.00	0.00	0.00
CAO	3.43	2.11	1.73	3.73	0.08	0.22	2.43	0.53	0.27
NA2O	9.79	10.50	9.47	9.98	11.62	11.52	10.59	11.46	11.22
K2O	0.10	0.17	0.55	0.18	0.08	0.12	0.12	0.08	0.19
P2O5	0.00	0.00	0.00	0.00	0.00	0.00	0.00	0.00	0.00
H2O	0.00	0.00	0.00	0.00	0.00	0.00	0.00	0.00	0.00
TOTAL	100.20	101.11	99.47	101.33	99.48	100.12	100.28	100.71	99.94
SI	11.269	11.539	11.543	11.210	11.919	11.900	11.470	11.846	11.850
TI	0.000	0.000	0.000	0.000	0.000	0.000	0.000	0.000	0.000
AL	4.745	4.480	4.405	4.775	4.103	4.128	4.513	4.174	4.210
CR	0.000	0.000	0.000	0.000	0.000	0.000	0.000	0.000	0.000
FE2	0.013	0.019	0.280	0.010	0.006	0.004	0.015	0.010	0.012
MN	0.000	0.000	0.000	0.000	0.000	0.000	0.000	0.000	0.000
MG	0.000	0.000	0.000	0.000	0.000	0.000	0.000	0.000	0.000
CA	0.648	0.393	0.330	0.698	0.015	0.041	0.458	0.099	0.051
NA	3.345	3.541	3.268	3.380	3.958	3.899	3.609	3.860	3.804
K	0.022	0.038	0.125	0.040	0.018	0.027	0.027	0.018	0.042
P	0.000	0.000	0.000	0.000	0.000	0.000	0.000	0.000	0.000
OH	0.000	0.000	0.000	0.000	0.000	0.000	0.000	0.000	0.000

	NPM491	NPM8B	NPM8B	NPM491	NPM491	NPM8B	NPM8B	NPM107	NPM107
	92 PL RIM	92 PL RIM	92 PL CORE	93 PL CORE	93 PL RIM	93 PL RIM	93 PL CORE	GB1 PL RIM	GB1 PL CORE
SIO2	68.74	65.68	65.87	68.76	68.40	67.39	65.82	67.50	65.57
TIO2	0.00	0.00	0.00	0.00	0.00	0.00	0.00	0.00	0.00
AL2O3	19.97	21.78	21.72	20.57	20.45	21.10	21.79	19.36	20.89
CR2O3	0.00	0.00	0.00	0.00	0.00	0.00	0.00	0.00	0.00
FEO	0.08	0.08	0.04	0.04	0.07	0.12	0.13	0.12	0.04
MNO	0.00	0.00	0.00	0.00	0.00	0.00	0.00	0.00	0.00
MGO	0.00	0.00	0.00	0.00	0.00	0.00	0.00	0.00	0.00
CAO	0.14	2.45	2.18	0.46	0.21	1.22	2.28	0.56	2.01
NA2O	10.87	10.25	10.42	11.13	11.25	11.03	10.51	11.20	10.92
K2O	0.13	0.11	0.15	0.11	0.11	0.10	0.16	0.09	0.10
P2O5	0.00	0.00	0.00	0.00	0.00	0.00	0.00	0.00	0.00
H2O	0.00	0.00	0.00	0.00	0.00	0.00	0.00	0.00	0.00
TOTAL	99.93	100.35	100.38	101.07	100.49	100.96	100.69	98.83	99.53
SI	11.979	11.512	11.536	11.875	11.881	11.704	11.508	11.943	11.598
TI	0.000	0.000	0.000	0.000	0.000	0.000	0.000	0.000	0.000
AL	4.103	4.500	4.485	4.188	4.188	4.320	4.492	4.038	4.356
CR	0.000	0.000	0.000	0.000	0.000	0.000	0.000	0.000	0.000
FE2	0.012	0.012	0.006	0.006	0.010	0.017	0.019	0.018	0.006
MN	0.000	0.000	0.000	0.000	0.000	0.000	0.000	0.000	0.000
MG	0.000	0.000	0.000	0.000	0.000	0.000	0.000	0.000	0.000
CA	0.026	0.460	0.409	0.085	0.039	0.227	0.427	0.106	0.381
NA	3.673	3.483	3.538	3.727	3.789	3.714	3.563	3.842	3.745
K	0.029	0.025	0.034	0.024	0.024	0.022	0.036	0.020	0.023
P	0.000	0.000	0.000	0.000	0.000	0.000	0.000	0.000	0.000
OH	0.000	0.000	0.000	0.000	0.000	0.000	0.000	0.000	0.000

	NPM344	NPM344	NPM484	NPM484	NPM611	NPM611	NPM8A	NPM8A	NPM107
	GB1 PL RIM	GB1 PL CORE	GB1 PL CORE	GB1 PL RIM	GB1 PL RIM	GB1 PL CORE	GB1 PL RIM	GB1 PL CORE	GB2 PL RIM
SIO2	64.60	64.94	61.18	62.56	65.03	65.15	66.96	64.57	66.80
TIO2	0.00	0.00	0.00	0.00	0.00	0.00	0.00	0.00	0.00
AL2O3	21.95	21.11	24.88	23.33	21.92	22.02	19.96	21.22	20.65
CR2O3	0.00	0.00	0.00	0.00	0.00	0.00	0.00	0.00	0.00
FEO	0.10	0.14	0.17	0.18	0.12	0.05	0.06	0.15	0.17
MNO	0.00	0.00	0.00	0.00	0.00	0.00	0.00	0.00	0.00
MGO	0.00	0.00	0.00	0.00	0.00	0.00	0.00	0.00	0.00
CAO	2.99	2.58	6.10	4.62	2.86	2.86	0.76	2.38	1.28
NA2O	10.33	10.73	8.30	9.27	9.74	10.15	11.17	10.25	11.08
K2O	0.13	0.22	0.16	0.10	0.06	0.11	0.11	0.11	0.17
P2O5	0.00	0.00	0.00	0.00	0.00	0.00	0.00	0.00	0.00
H2O	0.00	0.00	0.00	0.00	0.00	0.00	0.00	0.00	0.00
TOTAL	100.10	99.72	100.79	100.06	99.73	100.34	99.02	98.68	100.15
SI	11.396	11.504	10.805	11.089	11.467	11.439	11.839	11.521	11.714
TI	0.000	0.000	0.000	0.000	0.000	0.000	0.000	0.000	0.000
AL	4.565	4.409	5.180	4.875	4.557	4.558	4.161	4.464	4.269
CR	0.000	0.000	0.000	0.000	0.000	0.000	0.000	0.000	0.000
FE2	0.015	0.021	0.025	0.027	0.018	0.007	0.009	0.022	0.025
MN	0.000	0.000	0.000	0.000	0.000	0.000	0.000	0.000	0.000
MG	0.000	0.000	0.000	0.000	0.000	0.000	0.000	0.000	0.000
CA	0.565	0.490	1.154	0.877	0.540	0.538	0.144	0.455	0.241
NA	3.533	3.686	2.842	3.186	3.330	3.455	3.829	3.546	3.767
K	0.029	0.050	0.036	0.023	0.013	0.025	0.025	0.025	0.038
P	0.000	0.000	0.000	0.000	0.000	0.000	0.000	0.000	0.000
OH	0.000	0.000	0.000	0.000	0.000	0.000	0.000	0.000	0.000

	NPM107	NPM344	NPM344	NPM484	NPM484	NPM611	NPM611	NPM8A	NPM8A
	GB2 PL CORE	GB2 PL CORE	GB2 PL RIM	GB2 PL CORE	GB2 PL RIM	GB2 PL RIM	GB2 PL CORE	GB2 PL RIM	GB2 PL CORE
SIO2	65.35	64.51	63.71	62.32	61.95	65.47	64.43	64.51	65.00
TIO2	0.00	0.00	0.00	0.00	0.00	0.00	0.00	0.00	0.00
AL2O3	20.47	22.99	22.33	23.80	24.09	21.50	21.78	21.80	21.98
CR2O3	0.00	0.00	0.00	0.00	0.00	0.00	0.00	0.00	0.00
FEO	0.06	0.10	0.15	0.06	0.17	0.12	0.08	0.11	0.03
MNO	0.00	0.00	0.00	0.00	0.00	0.00	0.00	0.00	0.00
MGO	0.00	0.00	0.00	0.00	0.00	0.00	0.00	0.00	0.00
CAO	2.19	3.40	3.41	5.34	5.81	2.54	2.79	2.85	3.07
NA2O	10.43	9.66	9.53	8.81	8.73	10.24	9.74	10.27	10.00
K2O	0.09	0.18	0.18	0.20	0.14	0.12	0.15	0.12	0.11
P2O5	0.00	0.00	0.00	0.00	0.00	0.00	0.00	0.00	0.00
H2O	0.00	0.00	0.00	0.00	0.00	0.00	0.00	0.00	0.00
TOTAL	98.59	100.84	99.31	100.53	100.89	99.99	98.97	99.66	100.19
SI	11.652	11.288	11.324	11.008	10.927	11.525	11.456	11.421	11.432
TI	0.000	0.000	0.000	0.000	0.000	0.000	0.000	0.000	0.000
AL	4.303	4.742	4.679	4.956	5.009	4.462	4.566	4.550	4.557
CR	0.000	0.000	0.000	0.000	0.000	0.000	0.000	0.000	0.000
FE2	0.009	0.015	0.022	0.009	0.025	0.018	0.012	0.016	0.004
MN	0.000	0.000	0.000	0.000	0.000	0.000	0.000	0.000	0.000
MG	0.000	0.000	0.000	0.000	0.000	0.000	0.000	0.000	0.000
CA	0.418	0.637	0.649	1.011	1.098	0.479	0.532	0.541	0.579
NA	3.606	3.277	3.284	3.017	2.986	3.495	3.358	3.525	3.410
K	0.020	0.040	0.041	0.045	0.032	0.027	0.034	0.027	0.025
P	0.000	0.000	0.000	0.000	0.000	0.000	0.000	0.000	0.000
OH	0.000	0.000	0.000	0.000	0.000	0.000	0.000	0.000	0.000

	NPM107	NPM107	NPM344	NPM344	NPM484	NPM484	NPM611	NPM611	NPM8A
	GB3 PL RIM	GB3 PL CORE	GB3 PL RIM	GB3 PL CORE	GB3 PL RIM	GB3 PL CORE	GB3 PL RIM	GB3 PL CORE	GB3 PL RIM
SIO2	67.68	66.12	64.18	65.51	64.61	60.72	65.14	63.64	64.98
TIO2	0.00	0.00	0.00	0.00	0.00	0.00	0.00	0.00	0.00
AL2O3	19.84	20.80	21.77	21.40	22.12	24.27	21.53	21.89	21.94
CR2O3	0.00	0.00	0.00	0.00	0.00	0.00	0.00	0.00	0.00
FEO	0.00	0.00	0.15	0.16	0.11	0.14	0.13	0.16	0.15
MNO	0.00	0.00	0.00	0.00	0.00	0.00	0.00	0.00	0.00
MGO	0.00	0.00	0.00	0.00	0.00	0.00	0.00	0.00	0.00
CAO	0.50	1.93	3.00	2.48	3.70	6.24	2.69	3.32	3.01
NA2O	11.58	10.73	10.05	10.08	9.61	8.30	10.46	9.77	10.20
K2O	0.08	0.13	0.11	0.10	0.09	0.18	0.12	0.12	0.11
P2O5	0.00	0.00	0.00	0.00	0.00	0.00	0.00	0.00	0.00
H2O	0.00	0.00	0.00	0.00	0.00	0.00	0.00	0.00	0.00
TOTAL	99.68	99.71	99.26	99.73	100.24	99.85	100.07	98.90	100.39
SI	11.883	11.653	11.409	11.551	11.375	10.835	11.481	11.362	11.421
TI	0.000	0.000	0.000	0.000	0.000	0.000	0.000	0.000	0.000
AL	4.107	4.322	4.562	4.448	4.591	5.106	4.474	4.608	4.546
CR	0.000	0.000	0.000	0.000	0.000	0.000	0.000	0.000	0.000
FE2	0.000	0.000	0.022	0.024	0.016	0.021	0.019	0.024	0.022
MN	0.000	0.000	0.000	0.000	0.000	0.000	0.000	0.000	0.000
MG	0.000	0.000	0.000	0.000	0.000	0.000	0.000	0.000	0.000
CA	0.094	0.364	0.571	0.469	0.698	1.193	0.508	0.635	0.567
NA	3.942	3.667	3.464	3.446	3.280	2.872	3.575	3.382	3.476
K	0.018	0.029	0.025	0.022	0.020	0.041	0.027	0.027	0.025
P	0.000	0.000	0.000	0.000	0.000	0.000	0.000	0.000	0.000
OH	0.000	0.000	0.000	0.000	0.000	0.000	0.000	0.000	0.000

	NPM8A
	GB3 PL CORE
SIO2	64.78
TIO2	0.00
AL2O3	21.94
CR2O3	0.00
FEO	0.08
MNO	0.00
MGO	0.00
CAO	3.09
NA2O	10.38
K2O	0.11
P2O5	0.00
H2O	0.00
TOTAL	100.38
SI	11.398
TI	0.000
AL	4.551
CR	0.000
FE2	0.012
MN	0.000
MG	0.000
CA	0.583
NA	3.541
K	0.025
P	0.000
OH	0.000

Appendix C:

C-1 Electron Microprobe

Major element analyses for biotite, muscovite, garnet, amphibole and plagioclase were obtained using an automated JEOL 733 Electron Microprobe at Dalhousie University, Halifax. The system uses a wavelength dispersive spectrometer and operates at 15 Kv and 5 nA. Matrix effects are corrected on-line using a Tracor Northern ZAF matrix correction procedure. Analystical uncertainty is 1 to 1.5 wt. % for the major elements. Raw data was recalcuated to cations using a BASIC computer progran (Richard, 1986, unpubl.) based on OH values for hydrous minerals and number of oxygens suggested by Deer et al. 1966.

C-2 Analytical Methods and Sample Selection of Whole Rock chemical samples.

i- Sample Pulverization

Forty eight granitic samples and three lamprophyre samples were collected from the PMP for analyses. Specimens were broken down into cubes (approx. 3x3 cm^2) using a Cutrock (rock vice). All weathered or contaminated surfaces were removed. Fresh fragments were deposited in a Dayton Tow Crusher (model 4K 731) which has thick ceramic plates that were frequently cleaned to eliminate contamination from plate chips. The mafic lamprophyre dyke samples were the last to be processed in an attempt to reduce contamination to the more felsic granitic samples.

The samples were then split using a Soiltest splitter. A final proportion weighing approximately 150-300 grams was then pulverized in a Siebtechnik tungsten carbide ring mill (mode TS 250) until the majority of the sample was less than -100 mesh.

ii- Majors and Traces

The samples analysed at St. Mary's were analysed for 10 major and minor element oxides and fifteen trace elements on a Philips DW 1400 sequential x-ray fluorescence spectrometer using a Phanode x-ray tube. Major oxide determinations were carried out on fused glass discs while trace elements were done on pressed powder pellets. International standards with recommended values from Abbey (1983) as well as in-house standards were used for calibration. Analytical precision as determined on replicate analyses is generally better than 5% for the major oxides and between 5-10 % for trace elements. Loss on ignition (LOI) was determined by heating the sample for 1.5 hours at 1050 C in an electric furnace.

All of the trace element and some major element analyseswas done at St. Mary's University by K. Cameron. The remaining major element analyses were done at McGill University in Montreal by S.T. Ahmedali. The following samples were analysed for major element oxides at McGill University:NPM:2,8B,10,11,17,32,361,368B,371,440,441,477,485,487,511, 537,538,53,556,558,560,563,566,579,580 and 583.

iii- REE'S (NAA)

Thirteen samples were analysed for eight REEs. They are: Ce,Nd,Sm,Eu,Gd,Tb,Yb and Lu. Lanthanum was not analysed. The

analyses were completed using the neutron activation analyses system at Waterloo University in Kitchener Ontario. Approximately 0.1-0.2 grams of rock powder were weighed accurately and sealed in clean plastic ampoules. The samples were then sent to the Waterloo Nuclear Reactor with two standards.

iv- Precision and accuracy of analyses

The precision and accuracy of the trace and major oxide whole rock analyses from St. Mary's University ,the major oxide whole rock anlyses from McGill University and the REE's whole rock analyses from Waterloo University are summarized below.

St. Mary's University-major and traces

Unfortunately no International Standard was available to test the accuracy of the work from St. Mary's. Internal Standards and repeat samples were completed to determine the precision of the analyses.

Table C-1 St. Mary's University

Error Analysis for Rb, Sr, Ba, SiO_2, Al_2O_3, CaO and MgO

Element	Quoted detection limit		Obtained value	Repeat value	Percent Deviation
Rb					
	5-10%	NPM485	132	135	2.3
		NPM361	125	126	0.8
		NPM539	128	129	0.8
		NPM544	128	126	-1.6
Sr					
	5-20%	NPM485	2567	2557	-0.4
		NPM361	86	84	-2.3
		NPM539	151	149	-1.3
		NPM544	337	338	0.3
Ba					
	5-10%	NPM485	1920	1913	-0.4
		NPM361	316	309	-2.2
		NPM539	399	380	-4.8
		NPM544	484	478	-1.2
SiO_2					
	<5%	NPM544	67.79	67.53	-0.4
		NPM584	67.62	68.14	0.8
Al_2O_3					
	<5%	NPM544	16.21	16.22	0.06
		NPM584	16.13	16.25	0.7
CaO					
	<5%	NPM544	2.76	2.77	0.4
		NPM584	3.13	3.12	-0.3
MgO					
	<5%	NPM544	1.80	1.62	-10.0
		NPM584	1.45	1.46	0.7

note: no international standard for St. Mary's University analyses

TABLE C-2 St. Mary's University

Comparison with Internal Standards for Rb,Sr,Ba, SiO_2,Al_2O_3,CaO and MgO.

Element		Quoted detection value	Accepted value	Obtained value	% Deviation from accepted value
Rb					
	5-10%	HFL-1	214+/-0.90	216.00	0.9
		GDV-1A	63+/-0.79	62.00	-1.6
Sr					
	5-10%	HFL-1	204+/-0.67	206.00	0.98
		GDV-1A	217+/-1.07	215.00	-0.92
Ba					
	5-10%	HFL-1	891+/-6.86	902.00	1.2
		GDV-1A	338+/-2.41	356.00	5.3
SiO_2					
	<5%	HFL-1	59.29+/-0.17	59.23	-0.1
		GDV-1A	74.83+/-0.30	74.68	-0.2
Al_2O_3					
	<5%	HFL-1	22.08+/-0.10	22.25	0.8
		GDV-1A	12.15+/-0.09	12.21	0.5
CaO	<5%	HFL-1	0.23+/-0.01	0.23	0.0
		GDV-1A	1.05+/-0.02	1.05	0.0
MgO	<5%	HFL-1	1.93+/-0.09	1.93	0.0
		GDV-1A	1.51+/-0.06	1.61	6.6

* HFL-1	*GDV-1A
trace N=25	trace N=25
major N=12	major N=15

McGill University analysed only for whole rock major element oxides. Tables C-3 and C-4 compare the international standards G-2 (granite) and Nim-1 (granite) with the analyses obtained by McGill University.

Table C-3

G-2 GRANITE

ABBEY 1983 RECOMMENDED	OBTAINED MCGILL	PERCENT DEVIATION
SiO_2 69.22	69.05	0.25
TiO_2 0.48	0.48	0.00
Al_2O_3 15.40	15.48	0.52
Fe_{03} 2.69	2.70	0.37
MnO 0.03	0.03	0.00
MgO 0.75	0.72	4.00
CaO 1.96	2.00	2.04
Na_2O 4.06	4.08	0.49
K_2O 4.46	4.45	0.22
P_2O_5 0.13	0.13	0.00
V 36	38	5.56
Cr_2O_3 8	15	87.50
Ni 3.5	10	185.71
BaO 1900	1880	1.05

Table C-4

NIM-1 GRANITE

	SARM 1 1979 RECOMMENDED	OBTAINED McGILL	PERCENT DEVIATION
SiO_2	75.70	72.23	0.62
TiO_2	0.09	0.09	0.00
Al_2O_3	12.08	12.20	0.99
Fe_2O_3	2.02	1.99	1.49
MnO	0.02	0.02	0.00
MgO	0.06	0.01	83.33
CaO	0.78	1.42	82.05
Na_2O	3.36	3.25	3.27
K_2O	4.99	4.97	0.40
P_2O_5	0.01	0.01	0.00
V	2	10	400.00
Cr_2O_3	12	15	25.00
Ni	8	15	87.50
BaO	120	153	27.50

Waterloo University analysed the REEs of thirteen whole rock samples from the PMP. The precision of these analyses are discussed below in a comparison of the recommended results with those obtained by Waterloo University.

TABLE C-5 Waterloo University

Comparison of REE's + Ba + Th with International Standards

GSP-1 (granodiorite)

	RECOMMENDED (1984)	OBTAINED WATERLOO	PERCENT DEVIATION
Ce	400	508.28	27
Nd	190	260.17	36.9
Sm	26.8	32.96	22.9
Eu	2.4	2.72	13.3
Tb	1.36	0.81	-40.4
Yb	1.7	2.19	28.8
Th	105	127.87	21.7
Ba	1310	970.87	-25.88
Hf	15.0	17.04	13.60

TABLE C-6 Waterloo University
NIM-G granite

	(1984)	RECOMMENDED WATERLOO	OBTAINEDPERCENT DEVIATION
Ce	195	204.26	4.7
Nd	72	80.40	11.2
Sm	15.8	15.07	-4.6
Eu	0.35	0.34	-2.8
Gd	14	16.16	15.4
Tb	3	4.60	53.3
Yb	14.2	14.46	1.8
Lu	2	1.98	-1.0
Th	51	18.05	-64.6
Ta	4.5	4.45	-1.1
Ba	120	78.74	-34.38
Hf	12	12.11	0.91

TABLE C-7 WATERLOO UNIVERSITY -NAA-

repeatability

NPM458

NPM458	REPEAT	% deviation
CE	56.80	55.56	-2.1
ND	29.23	29.24	0.03
SM	6.39	6.33	0.93
EU	0.83	0.84	1.2
GD	5.25	6.42	22.2
TB	0.67	0.72	7.4
YB	2.03	2.16	6.4
LU	0.27	0.28	3.7
TH	12.86	12.89	0.23
TA	1.01	1.04	2.9
BA	241.42	249.82	3.4
HF	4.91	4.83	1.6

v- Sample Selections

Approximately three hundred hand specimens representing all of the rock types from the PMP were collected during the 1985 field season. Approximately one hundred and fifty thin sections were made of these samples in order to detail the petrographic variations and mineral assemblages present. One hundred and thirty-one of the samples were slabbed and stained and point counted (ie. for quartz,kspar and plagioclase). On the basis of this data, 51 samples were chose as being representative samples for chemical analysis. The samples were also selected in an attempt to obtain geographic and Unit coverage and a volumetric representation of each within the PMP.

APPENDIX D-1

Major element analyses (all analyses as percentage), CIPW and Mesonorm values of whole rock chemica l samples.

LEGEND for Major(D-1), Trace(D-2) and REE(D-3) analyses:
line #1= Unit and sample number ie; 1NPM533= Unit 1 sample NPM533
TiO_2 wt. % results from the Major whole rock element table were used in the graphs within the text.

	1NPM11	1NPM2	1NPM484	1NPM487	1NPM533	1NPM544	1NPM565	1NPM582	1NPM584
SIO2	67.23	70.78	73.83	70.33	63.65	67.53	70.01	66.24	68.14
TIO2	0.55	0.41	0.13	0.37	0.68	0.51	0.35	0.63	0.50
AL2O3	16.87	15.40	14.18	15.92	17.67	16.22	15.62	17.00	16.25
FE2O3	3.86	3.16	3.00	3.09	4.64	3.44	2.53	3.76	3.86
FEO	0.00	0.00	0.00	0.00	0.00	0.00	0.00	0.00	0.00
MNO	0.06	0.06	0.10	0.05	0.09	0.08	0.05	0.07	0.07
MGO	1.40	1.19	0.66	1.03	2.02	1.62	1.18	1.56	1.46
CAO	3.23	2.09	1.62	2.74	4.02	2.77	2.05	3.94	3.12
NA2O	3.62	3.92	3.77	4.05	3.97	4.10	4.41	3.94	4.02
K2O	2.41	2.14	2.11	1.94	2.12	2.12	2.90	1.55	1.73
P2O5	0.17	0.22	0.06	0.17	0.19	0.19	0.14	0.30	0.13
H2O+	0.58	0.88	0.50	0.61	0.30	0.70	0.40	0.50	0.50
H2O-	0.00	0.00	0.00	0.00	0.00	0.00	0.00	0.00	0.00
CO2	0.00	0.00	0.00	0.00	0.00	0.00	0.00	0.00	0.00
CL	0.00	0.00	0.00	0.00	0.00	0.00	0.00	0.00	0.00
F	0.00	0.00	0.00	0.00	0.00	0.00	0.00	0.00	0.00
TOTAL	99.98	100.25	99.96	100.30	99.35	99.28	99.64	99.49	99.78
A/CNK	1.17	1.23	1.24	1.16	1.09	1.15	1.11	1.11	1.15
CIPW NORM									
QZ	28.59	34.46	39.74	32.62	21.42	27.95	27.61	27.61	29.79
OR	14.32	12.76	12.53	11.53	12.57	12.62	17.21	9.21	10.27
AB	30.81	33.46	32.06	34.48	33.69	34.94	37.46	33.51	34.18
AN	15.00	9.01	7.68	12.56	18.76	12.59	9.29	17.68	14.70
WO	0.00	0.00	0.00	0.00	0.00	0.00	0.00	0.00	0.00
DI	0.00	0.00	0.00	0.00	0.00	0.00	0.00	0.00	0.00
HY	3.50	2.99	1.65	2.58	5.04	4.06	2.95	3.90	3.65
MT	0.00	0.00	0.00	0.00	0.00	0.00	0.00	0.00	0.00
IL	0.13	0.13	0.21	0.11	0.19	0.17	0.11	0.15	0.15
HM	3.88	3.19	3.01	3.11	4.65	3.46	2.54	3.78	3.88
TN	0.00	0.00	0.00	0.00	0.00	0.00	0.00	0.00	0.00
PF	0.00	0.00	0.00	0.00	0.00	0.00	0.00	0.00	0.00
RU	0.49	0.35	0.02	0.32	0.58	0.42	0.29	0.55	0.42
AP	0.40	0.51	0.14	0.40	0.44	0.44	0.33	0.70	0.30
CO	2.85	3.39	2.90	2.59	1.99	2.61	1.84	2.40	2.41
OL	0.00	0.00	0.00	0.00	0.00	0.00	0.00	0.00	0.00
LC	0.00	0.00	0.00	0.00	0.00	0.00	0.00	0.00	0.00
NE	0.00	0.00	0.00	0.00	0.00	0.00	0.00	0.00	0.00
KP	0.00	0.00	0.00	0.00	0.00	0.00	0.00	0.00	0.00
AC	0.00	0.00	0.00	0.00	0.00	0.00	0.00	0.00	0.00
NS	0.00	0.00	0.00	0.00	0.00	0.00	0.00	0.00	0.00
KS	0.00	0.00	0.00	0.00	0.00	0.00	0.00	0.00	0.00
CS	0.00	0.00	0.00	0.00	0.00	0.00	0.00	0.00	0.00
MESONORM									
QZ	30.50	35.92	40.51	33.95	24.36	30.16	29.25	29.79	31.81
AB	30.66	33.20	31.93	34.30	33.63	34.73	37.35	33.37	34.05
OR	10.63	9.60	10.75	8.82	7.37	8.40	14.16	5.12	6.49
AN	14.91	8.93	7.64	12.48	18.70	12.50	9.25	17.58	14.62
CO	2.82	3.35	2.88	2.56	1.97	2.58	1.82	2.37	2.38
BI	5.34	4.52	2.60	3.92	7.64	6.12	4.42	5.97	5.54
HB	0.00	0.00	0.00	0.00	0.00	0.00	0.00	0.00	0.00
MT	0.00	0.00	0.00	0.00	0.00	0.00	0.00	0.00	0.00
HM	3.86	3.16	3.00	3.09	4.64	3.44	2.53	3.76	3.86
IL	0.52	0.39	0.12	0.35	0.65	0.48	0.33	0.60	0.47
CC	0.00	0.00	0.00	0.00	0.00	0.00	0.00	0.00	0.00

	1NPM593	2NPM546	3NPM542	4NPM17	4NPM32	4NPM368B	4NPM371	4NPM440	4NPM441
SIO2	70.20	63.53	74.26	70.09	73.30	72.96	75.72	68.15	73.72
TIO2	0.47	0.36	0.11	0.42	0.14	0.24	0.26	0.52	0.14
AL2O3	15.69	20.13	14.65	15.53	15.01	14.64	12.51	15.25	14.64
FE2O3	2.59	2.33	0.73	2.79	1.21	2.08	1.68	3.70	1.21
FEO	0.00	0.00	0.00	0.00	0.00	0.00	0.00	0.00	0.00
MNO	0.05	0.05	0.02	0.05	0.05	0.05	0.04	0.07	0.04
MGO	1.22	1.25	0.51	0.84	0.30	0.47	0.39	1.40	0.26
CAO	1.30	4.13	0.92	2.17	0.82	1.81	1.01	3.67	0.83
NA2O	3.94	5.82	4.49	4.18	3.87	4.35	2.72	3.68	3.92
K2O	3.32	1.54	3.62	3.19	4.37	2.82	4.62	2.97	4.28
P2O5	0.20	0.14	0.13	0.30	0.31	0.22	0.21	0.20	0.31
H2O+	0.70	0.60	0.30	0.41	0.65	0.42	0.55	0.52	0.63
H2O-	0.00	0.00	0.00	0.00	0.00	0.00	0.00	0.00	0.00
CO2	0.00	0.00	0.00	0.00	0.00	0.00	0.00	0.00	0.00
CL	0.00	0.00	0.00	0.00	0.00	0.00	0.00	0.00	0.00
F	0.00	0.00	0.00	0.00	0.00	0.00	0.00	0.00	0.00
TOTAL	99.68	99.88	99.74	99.97	100.03	100.06	99.71	100.13	99.98
A/CNK	1.26	1.07	1.13	1.09	1.19	1.08	1.11	0.96	1.16
CIPW NORM									
QZ	30.75	13.54	32.02	28.63	32.95	33.04	40.28	26.25	33.46
OR	19.76	9.16	21.46	18.93	25.99	16.73	27.45	17.64	25.45
AB	33.57	49.54	38.11	35.51	32.96	36.96	23.14	31.30	33.38
AN	5.18	19.69	3.73	8.84	2.06	7.57	3.66	16.39	2.11
WO	0.00	0.00	0.00	0.00	0.00	0.00	0.00	0.00	0.00
DI	0.00	0.00	0.00	0.00	0.00	0.00	0.00	0.00	0.00
HY	3.06	3.13	1.27	2.10	0.75	1.17	0.98	3.50	0.65
MT	0.00	0.00	0.00	0.00	0.00	0.00	0.00	0.00	0.00
IL	0.11	0.11	0.04	0.11	0.11	0.11	0.09	0.15	0.09
HM	2.61	2.34	0.73	2.80	1.22	2.09	1.69	3.72	1.22
TN	0.00	0.00	0.00	0.00	0.00	0.00	0.00	0.42	0.00
PF	0.00	0.00	0.00	0.00	0.00	0.00	0.00	0.00	0.00
RU	0.42	0.31	0.09	0.37	0.08	0.18	0.22	0.27	0.10
AP	0.47	0.33	0.30	0.70	0.72	0.51	0.49	0.47	0.72
CO	3.75	1.72	1.98	1.98	3.18	1.67	1.71	0.00	2.80
OL	0.00	0.00	0.00	0.00	0.00	0.00	0.00	0.00	0.00
LC	0.00	0.00	0.00	0.00	0.00	0.00	0.00	0.00	0.00
NE	0.00	0.00	0.00	0.00	0.00	0.00	0.00	0.00	0.00
KP	0.00	0.00	0.00	0.00	0.00	0.00	0.00	0.00	0.00
AC	0.00	0.00	0.00	0.00	0.00	0.00	0.00	0.00	0.00
NS	0.00	0.00	0.00	0.00	0.00	0.00	0.00	0.00	0.00
KS	0.00	0.00	0.00	0.00	0.00	0.00	0.00	0.00	0.00
CS	0.00	0.00	0.00	0.00	0.00	0.00	0.00	0.00	0.00
MESONORM									
QZ	32.34	15.32	32.66	29.75	33.16	33.59	40.63	27.66	33.61
AB	33.37	49.30	38.03	35.40	32.78	36.84	23.04	31.17	33.20
OR	16.48	5.95	20.13	16.61	24.99	15.38	26.20	14.75	24.56
AN	5.14	19.57	3.71	8.80	2.04	7.54	3.63	15.69	2.09
CO	3.72	1.68	1.97	1.96	3.16	1.65	1.70	0.00	2.78
BI	4.64	4.67	1.88	3.30	1.25	1.90	1.61	4.16	1.09
HB	0.00	0.00	0.00	0.00	0.00	0.00	0.00	1.74	0.00
MT	0.00	0.00	0.00	0.00	0.00	0.00	0.00	0.00	0.00
HM	2.59	2.33	0.73	2.79	1.21	2.08	1.68	3.70	1.21
IL	0.45	0.34	0.10	0.40	0.13	0.23	0.25	0.49	0.13
CC	0.00	0.00	0.00	0.00	0.00	0.00	0.00	0.00	0.00

	4NPM458	4NPM469	4NPM472	4NPM477	4NPM511	4NPM535	4NPM536	4NPM543	4NPM548
SIO2	72.26	70.16	73.35	72.61	73.48	71.33	71.77	64.24	72.73
TIO2	0.31	0.48	0.13	0.32	0.17	0.32	0.25	0.76	0.21
AL2O3	14.90	15.60	15.17	14.58	14.84	15.27	15.20	17.78	15.10
FE2O3	2.13	2.63	1.11	1.83	1.49	2.19	1.97	3.69	1.39
FEO	0.00	0.00	0.00	0.00	0.00	0.00	0.00	0.00	0.00
MNO	0.05	0.04	0.05	0.04	0.04	0.05	0.06	0.05	0.04
MGO	0.84	1.22	0.66	0.49	0.32	1.04	0.86	1.91	0.75
CAO	1.88	1.38	0.77	0.85	1.28	1.61	1.59	3.27	0.87
NA2O	4.54	3.65	4.28	2.96	3.99	4.08	4.66	4.42	3.99
K2O	2.29	3.92	4.03	5.18	3.74	3.45	3.13	2.47	4.22
P2O5	0.17	0.21	0.29	0.27	0.21	0.21	0.24	0.24	0.23
H2O+	0.20	0.70	0.30	0.73	0.55	0.40	0.40	0.50	0.30
H2O-	0.00	0.00	0.00	0.00	0.00	0.00	0.00	0.00	0.00
CO2	0.00	0.00	0.00	0.00	0.00	0.00	0.00	0.00	0.00
CL	0.00	0.00	0.00	0.00	0.00	0.00	0.00	0.00	0.00
F	0.00	0.00	0.00	0.00	0.00	0.00	0.00	0.00	0.00
TOTAL	99.57	99.99	100.14	99.86	100.11	99.95	100.13	99.33	99.83
A/CNK	1.11	1.22	1.18	1.21	1.15	1.14	1.09	1.12	1.19
CIPW NORM									
QZ	32.35	29.95	31.31	34.02	33.51	30.10	28.79	20.00	31.13
OR	13.56	23.33	23.89	30.83	22.22	20.47	18.57	14.67	25.01
AB	38.49	31.10	36.32	25.23	33.95	34.66	39.59	37.59	33.86
AN	8.23	5.51	1.93	2.47	5.01	6.64	6.35	14.73	2.82
WO	0.00	0.00	0.00	0.00	0.00	0.00	0.00	0.00	0.00
DI	0.00	0.00	0.00	0.00	0.00	0.00	0.00	0.00	0.00
HY	2.09	3.06	1.65	1.23	0.80	2.60	2.15	4.78	1.87
MT	0.00	0.00	0.00	0.00	0.00	0.00	0.00	0.00	0.00
IL	0.11	0.09	0.11	0.09	0.09	0.11	0.13	0.11	0.09
HM	2.13	2.65	1.11	1.84	1.50	2.20	1.98	3.71	1.39
TN	0.00	0.00	0.00	0.00	0.00	0.00	0.00	0.00	0.00
PF	0.00	0.00	0.00	0.00	0.00	0.00	0.00	0.00	0.00
RU	0.25	0.44	0.07	0.28	0.13	0.26	0.18	0.71	0.17
AP	0.39	0.49	0.67	0.63	0.49	0.49	0.56	0.56	0.53
CO	1.94	3.36	3.06	3.22	2.41	2.40	1.83	2.47	2.94
OL	0.00	0.00	0.00	0.00	0.00	0.00	0.00	0.00	0.00
LC	0.00	0.00	0.00	0.00	0.00	0.00	0.00	0.00	0.00
NE	0.00	0.00	0.00	0.00	0.00	0.00	0.00	0.00	0.00
KP	0.00	0.00	0.00	0.00	0.00	0.00	0.00	0.00	0.00
AC	0.00	0.00	0.00	0.00	0.00	0.00	0.00	0.00	0.00
NS	0.00	0.00	0.00	0.00	0.00	0.00	0.00	0.00	0.00
KS	0.00	0.00	0.00	0.00	0.00	0.00	0.00	0.00	0.00
CS	0.00	0.00	0.00	0.00	0.00	0.00	0.00	0.00	0.00
MESONORM									
QZ	33.52	31.54	32.18	34.49	33.79	31.52	29.94	22.74	32.13
AB	38.45	30.92	36.25	25.07	33.80	34.56	39.47	37.44	33.80
OR	11.36	20.03	22.16	29.25	21.22	17.75	16.30	9.70	23.04
AN	8.21	5.47	1.92	2.45	4.97	6.61	6.32	14.65	2.81
CO	1.92	3.34	3.05	3.20	2.39	2.39	1.81	2.44	2.93
BI	3.22	4.62	2.48	2.00	1.31	3.92	3.28	7.22	2.82
HB	0.00	0.00	0.00	0.00	0.00	0.00	0.00	0.00	0.00
MT	0.00	0.00	0.00	0.00	0.00	0.00	0.00	0.00	0.00
HM	2.13	2.63	1.11	1.83	1.49	2.19	1.97	3.69	1.39
IL	0.29	0.46	0.12	0.30	0.16	0.30	0.24	0.72	0.20
CC	0.00	0.00	0.00	0.00	0.00	0.00	0.00	0.00	0.00

	4NPM549	4NPM551	4NPM556	4NPM558	4NPM578	4NPM580	4NPM581	5ANPM485	5ANPM612
SIO2	67.10	68.49	70.33	68.27	70.93	72.79	71.45	51.95	46.23
TIO2	0.65	0.42	0.46	0.60	0.29	0.14	0.32	1.22	1.08
AL2O3	16.42	15.98	15.25	16.24	15.31	14.89	15.61	12.07	10.71
FE2O3	3.31	2.85	2.61	3.27	2.16	0.96	2.29	7.89	10.01
FEO	0.00	0.00	0.00	0.00	0.00	0.00	0.00	0.00	0.00
MNO	0.05	0.06	0.04	0.04	0.04	0.03	0.06	0.12	0.15
MGO	1.70	1.43	1.02	1.33	0.97	0.30	0.95	12.98	15.63
CAO	2.46	2.35	1.74	2.27	1.88	0.85	1.76	5.92	6.69
NA2O	3.94	3.97	3.56	3.76	4.21	2.56	4.63	1.29	1.01
K2O	3.42	3.69	4.24	3.66	3.17	6.30	3.09	4.29	4.01
P2O5	0.21	0.16	0.20	0.21	0.20	0.32	0.27	0.84	0.75
H2O+	0.30	0.30	0.46	0.72	0.40	0.61	0.50	1.29	2.50
H2O-	0.00	0.00	0.00	0.00	0.00	0.00	0.00	0.00	0.00
CO2	0.00	0.00	0.00	0.00	0.00	0.00	0.00	0.00	0.00
CL	0.00	0.00	0.00	0.00	0.00	0.00	0.00	0.00	0.00
F	0.00	0.00	0.00	0.00	0.00	0.00	0.00	0.00	0.00
TOTAL	99.56	99.70	99.91	100.37	99.56	99.75	100.93	99.86	98.77
A/CNK	1.12	1.08	1.12	1.14	1.11	1.18	1.10	0.69	0.59
CIPW NORM									
QZ	23.95	24.63	28.84	26.32	29.52	32.62	28.41	0.41	0.00
OR	20.27	21.87	25.17	21.78	18.81	37.46	18.35	25.68	24.31
AB	33.44	33.69	30.26	32.04	35.76	21.79	39.37	11.06	8.77
AN	10.86	10.64	7.36	9.96	8.05	2.14	7.00	14.65	13.17
WO	0.00	0.00	0.00	0.00	0.00	0.00	0.00	0.00	0.00
DI	0.00	0.00	0.00	0.00	0.00	0.00	0.00	4.45	9.81
HY	4.24	3.57	2.55	3.33	2.42	0.75	2.38	30.67	10.80
MT	0.00	0.00	0.00	0.00	0.00	0.00	0.00	0.00	0.00
IL	0.11	0.13	0.09	0.09	0.09	0.06	0.13	0.26	0.33
HM	3.32	2.86	2.62	3.29	2.17	0.97	2.30	7.99	10.27
TN	0.00	0.00	0.00	0.00	0.00	0.00	0.00	2.70	2.29
PF	0.00	0.00	0.00	0.00	0.00	0.00	0.00	0.00	0.00
RU	0.60	0.35	0.42	0.56	0.25	0.11	0.25	0.00	0.00
AP	0.49	0.37	0.47	0.49	0.47	0.75	0.63	1.97	1.78
CO	2.27	1.56	2.12	2.48	2.02	3.09	2.10	0.00	0.00
OL	0.00	0.00	0.00	0.00	0.00	0.00	0.00	0.00	17.22
LC	0.00	0.00	0.00	0.00	0.00	0.00	0.00	0.00	0.00
NE	0.00	0.00	0.00	0.00	0.00	0.00	0.00	0.00	0.00
KP	0.00	0.00	0.00	0.00	0.00	0.00	0.00	0.00	0.00
AC	0.00	0.00	0.00	0.00	0.00	0.00	0.00	0.00	0.00
NS	0.00	0.00	0.00	0.00	0.00	0.00	0.00	0.00	0.00
KS	0.00	0.00	0.00	0.00	0.00	0.00	0.00	0.00	0.00
CS	0.00	0.00	0.00	0.00	0.00	0.00	0.00	0.00	0.00
MESONORM									
QZ	26.40	26.67	30.21	28.10	30.83	32.85	29.66	11.61	2.77
AB	33.37	33.63	30.15	31.85	35.66	21.68	39.22	10.93	8.55
OR	15.86	18.20	22.39	18.17	16.28	36.42	15.81	7.13	7.45
AN	10.83	10.61	7.32	9.88	8.02	2.12	6.96	5.11	-2.55
CO	2.25	1.55	2.11	2.46	2.00	3.08	2.08	0.00	0.00
BI	6.42	5.36	3.92	5.08	3.64	1.20	3.63	27.29	24.38
HB	0.00	0.00	0.00	0.00	0.00	0.00	0.00	27.31	44.95
MT	0.00	0.00	0.00	0.00	0.00	0.00	0.00	0.00	0.00
HM	3.31	2.85	2.61	3.27	2.16	0.96	2.29	7.89	10.01
IL	0.62	0.40	0.44	0.57	0.28	0.13	0.30	1.16	1.03
CC	0.00	0.00	0.00	0.00	0.00	0.00	0.00	0.00	0.00

	5ANPM6156	NPM538	7NPM464	7NPM539	7NPM545	7NPM560	7NPM563	7NPM566	7NPM579
SIO2	52.01	74.50	69.03	71.32	69.28	70.27	71.12	72.72	72.64
TIO2	1.08	0.09	0.48	0.36	0.43	0.35	0.32	0.22	0.26
AL2O3	12.01	14.69	15.58	15.57	15.75	15.76	15.18	14.64	14.61
FE2O3	8.03	0.81	3.03	2.41	3.15	2.54	2.25	1.47	1.47
FEO	0.00	0.00	0.00	0.00	0.00	0.00	0.00	0.00	0.00
MNO	0.21	0.02	0.06	0.06	0.05	0.07	0.04	0.03	0.03
MGO	10.05	0.34	1.22	0.89	1.00	0.77	0.71	0.34	0.34
CAO	10.80	0.92	2.21	2.14	2.47	2.81	1.92	0.86	0.86
NA2O	2.38	3.35	4.51	4.35	4.18	4.44	4.07	2.85	2.85
K2O	0.67	4.75	2.80	2.87	2.31	2.25	3.49	5.86	5.86
P2O5	0.64	0.14	0.31	0.19	0.32	0.22	0.23	0.18	0.18
H2O+	1.50	0.56	0.40	0.37	0.40	0.42	0.50	0.47	0.47
H2O-	0.00	0.00	0.00	0.00	0.00	0.00	0.00	0.00	0.00
CO2	0.00	0.00	0.00	0.00	0.00	0.00	0.00	0.00	0.00
CL	0.00	0.00	0.00	0.00	0.00	0.00	0.00	0.00	0.00
F	0.00	0.00	0.00	0.00	0.00	0.00	0.00	0.00	0.00
TOTAL	99.38	100.17	99.63	100.53	99.34	99.90	99.83	99.64	99.57
A/CNK	0.49	1.19	1.08	1.10	1.14	1.06	1.09	1.16	1.16
CIPW NORM									
QZ	5.70	34.94	26.51	29.76	30.36	29.41	29.71	32.02	31.94
OR	4.02	28.23	16.61	17.02	13.71	13.35	20.73	34.79	34.79
AB	20.45	28.50	38.31	36.94	35.51	37.73	34.61	24.23	24.23
AN	20.40	3.67	8.97	9.41	10.20	12.56	8.06	3.11	3.11
WO	0.00	0.00	0.00	0.00	0.00	0.00	0.00	0.00	0.00
DI	20.84	0.00	0.00	0.00	0.00	0.00	0.00	0.00	0.00
HY	15.74	0.85	3.05	2.22	2.50	1.92	1.78	0.85	0.85
MT	0.00	0.00	0.00	0.00	0.00	0.00	0.00	0.00	0.00
IL	0.46	0.04	0.13	0.13	0.11	0.15	0.09	0.06	0.06
HM	8.15	0.81	3.04	2.42	3.16	2.55	2.26	1.48	1.48
TN	2.10	0.00	0.00	0.00	0.00	0.00	0.00	0.00	0.00
PF	0.00	0.00	0.00	0.00	0.00	0.00	0.00	0.00	0.00
RU	0.00	0.07	0.41	0.29	0.38	0.27	0.28	0.19	0.23
AP	1.51	0.33	0.72	0.44	0.74	0.51	0.54	0.42	0.42
CO	0.00	2.71	1.86	1.87	2.65	1.44	1.77	2.48	2.45
OL	0.00	0.00	0.00	0.00	0.00	0.00	0.00	0.00	0.00
LC	0.00	0.00	0.00	0.00	0.00	0.00	0.00	0.00	0.00
NE	0.00	0.00	0.00	0.00	0.00	0.00	0.00	0.00	0.00
KP	0.00	0.00	0.00	0.00	0.00	0.00	0.00	0.00	0.00
AC	0.00	0.00	0.00	0.00	0.00	0.00	0.00	0.00	0.00
NS	0.00	0.00	0.00	0.00	0.00	0.00	0.00	0.00	0.00
KS	0.00	0.00	0.00	0.00	0.00	0.00	0.00	0.00	0.00
CS	0.00	0.00	0.00	0.00	0.00	0.00	0.00	0.00	0.00
MESONORM									
QZ	-4.76	35.24	28.20	30.97	31.72	30.42	30.61	32.36	32.28
AB	20.16	28.37	38.20	36.84	35.40	37.61	34.47	24.14	24.14
OR	18.95	27.21	13.39	14.63	11.04	11.23	18.76	33.68	33.66
AN	-9.21	3.65	8.93	9.37	10.16	12.50	8.02	3.09	3.09
CO	0.00	2.69	1.84	1.85	2.63	1.42	1.75	2.48	2.45
BI	********	1.28	4.67	3.45	3.86	3.06	2.76	1.39	1.42
HB	85.36	0.00	0.00	0.00	0.00	0.00	0.00	0.00	0.00
MT	0.00	0.00	0.00	0.00	0.00	0.00	0.00	0.00	0.00
HM	8.03	0.81	3.03	2.41	3.15	2.54	2.25	1.47	1.47
IL	1.03	0.09	0.46	0.34	0.41	0.33	0.30	0.21	0.25
CC	0.00	0.00	0.00	0.00	0.00	0.00	0.00	0.00	0.00

	7NPM583	8NPM10	8NPM361	8NPM537	9NPM491	9NPM8B
SIO2	72.85	73.99	75.07	74.56	73.94	73.09
TIO2	0.35	0.14	0.10	0.09	0.02	0.04
AL2O3	15.02	14.76	14.13	14.22	15.33	15.50
FE2O3	2.38	1.02	0.78	0.77	0.64	1.07
FEO	0.00	0.00	0.00	0.00	0.00	0.00
MNO	0.04	0.02	0.02	0.02	0.12	0.22
MGO	0.72	0.28	0.13	0.16	0.41	0.08
CAO	2.35	1.70	1.12	1.25	0.33	0.37
NA2O	3.58	3.12	4.10	3.84	5.58	3.10
K2O	2.19	4.48	3.77	4.44	2.45	5.69
P2O5	0.15	0.06	0.16	0.11	0.33	0.15
H2O+	0.64	0.38	0.44	0.27	0.70	0.74
H2O-	0.00	0.00	0.00	0.00	0.00	0.00
CO2	0.00	0.00	0.00	0.00	0.00	0.00
CL	0.00	0.00	0.00	0.00	0.00	0.00
F	0.00	0.00	0.00	0.00	0.00	0.00
TOTAL	100.27	99.95	99.82	99.73	99.85	100.05
A/CNK	1.20	1.13	1.10	1.06	1.23	1.30
CIPW NORM						
QZ	38.20	34.94	34.80	32.71	31.72	33.03
OR	13.02	26.57	22.38	26.31	14.58	33.87
AB	30.49	26.50	34.84	32.58	47.55	26.42
AN	10.75	8.07	4.53	5.50	0.00	0.86
WO	0.00	0.00	0.00	0.00	0.00	0.00
DI	0.00	0.00	0.00	0.00	0.00	0.00
HY	1.80	0.70	0.32	0.40	1.03	0.20
MT	0.00	0.00	0.00	0.00	0.34	0.61
IL	0.09	0.04	0.04	0.04	0.04	0.08
HM	2.40	1.02	0.78	0.77	0.41	0.66
TN	0.00	0.00	0.00	0.00	0.00	0.00
PF	0.00	0.00	0.00	0.00	0.00	0.00
RU	0.31	0.12	0.08	0.07	0.00	0.00
AP	0.35	0.14	0.37	0.26	5.85	0.35
CO	2.86	1.83	1.65	1.09	3.52	3.95
OL	0.00	0.00	0.00	0.00	0.00	0.00
LC	0.00	0.00	0.00	0.00	0.00	0.00
NE	0.00	0.00	0.00	0.00	0.00	0.00
KP	0.00	0.00	0.00	0.00	0.00	0.00
AC	0.00	0.00	0.00	0.00	0.00	0.00
NS	0.00	0.00	0.00	0.00	0.00	0.00
KS	0.00	0.00	0.00	0.00	0.00	0.00
CS	0.00	0.00	0.00	0.00	0.00	0.00
MESONORM						
QZ	39.02	35.20	34.82	32.84	32.31	32.89
AB	30.32	26.43	34.73	32.52	47.26	26.26
OR	11.03	25.73	21.90	25.79	13.37	33.14
AN	10.67	8.04	4.51	5.48	-0.52	0.85
CO	2.83	1.82	1.64	1.08	3.67	3.93
BI	2.81	1.11	0.56	0.66	1.71	0.82
HB	0.00	0.00	0.00	0.00	0.00	0.00
MT	0.00	0.00	0.00	0.00	0.00	0.00
HM	2.38	1.02	0.78	0.77	0.64	1.07
IL	0.33	0.13	0.10	0.09	0.02	0.04
CC	0.00	0.00	0.00	0.00	0.00	0.00

D-2: Trace Element analyses of whole rock chemical samples (all analyses in ppm.)

	1NPM11	1NPM2	1NPM484	1NPM487	1NPM533	1NPM544	1NPM565	1NPM582	1NPM584
BA	718.00	397.00	446.00	440.00	601.00	484.00	400.00	314.00	475.00
RB	82.00	74.00	65.00	60.00	71.00	128.00	112.00	59.00	62.00
SR	370.00	200.00	304.00	312.00	474.00	337.00	225.00	213.00	385.00
Y	10.00	14.00	17.00	20.00	17.00	20.00	17.00	27.00	11.00
ZR	150.00	127.00	108.00	121.00	182.00	141.00	102.00	389.00	156.00
NB	11.00	10.00	10.00	9.00	12.00	10.00	13.00	11.00	9.00
TH	0.00	9.00	24.00	6.00	0.00	13.00	5.00	4.00	10.00
PB	18.00	22.00	19.00	24.00	8.00	17.00	15.00	13.00	16.00
GA	18.00	18.00	16.00	18.00	22.00	23.00	21.00	18.00	18.00
ZN	59.00	47.00	40.00	43.00	61.00	65.00	57.00	66.00	54.00
CU	16.00	0.00	3.00	2.00	7.00	4.00	2.00	19.00	8.00
NI	7.00	9.00	6.00	10.00	10.00	14.00	9.00	8.00	2.00
TIO2	0.73	0.47	0.11	0.40	0.76	0.57	0.37	0.61	0.49
V	68.00	52.00	0.00	31.00	77.00	58.00	37.00	50.00	37.00
CR	18.00	47.00	10.00	15.00	21.00	24.00	18.00	16.00	14.00

	1NPM593	2NPM546	3NPM542	4NPM17	4NPM32	4NPM368B	4NPM371	4NPM440	4NPM441
BA	768.00	175.00	451.00	645.00	374.00	316.00	409.00	494.00	386.00
RB	115.00	75.00	132.00	124.00	181.00	126.00	170.00	134.00	1.80
SR	194.00	389.00	84.00	184.00	64.00	106.00	66.00	207.00	9.00
Y	13.00	11.00	10.00	20.00	14.00	20.00	20.00	17.00	67.00
ZR	190.00	123.00	47.00	179.00	69.00	137.00	99.00	169.00	73.00
NB	9.00	8.00	6.00	13.00	12.00	10.00	10.00	11.00	11.00
TH	35.00	10.00	3.00	9.00	6.00	5.00	13.00	13.00	2.00
PB	26.00	14.00	18.00	26.00	26.00	16.00	25.00	12.00	24.00
GA	20.00	22.00	18.00	19.00	20.00	19.00	19.00	22.00	21.00
ZN	58.00	50.00	29.00	57.00	43.00	60.00	56.00	74.00	49.00
CU	0.00	7.00	0.00	0.00	0.00	0.00	3.00	6.00	1.00
NI	7.00	6.00	6.00	10.00	4.00	16.00	17.00	16.00	13.00
TIO2	0.49	0.57	0.10	0.53	0.14	0.25	0.28	0.56	0.13
V	36.00	36.00	3.00	38.00	4.00	16.00	11.00	55.00	7.00
CR	19.00	32.00	8.00	20.00	9.00	12.00	10.00	42.00	9.00

	4NPM458	4NPM469	4NPM472	4NPM477	4NPM511	4NPM535	4NPM536	4NPM543	4NPM548
BA	364.00	823.00	427.00	696.00	261.00	383.00	316.00	683.00	334.00
RB	96.00	152.00	179.00	152.00	152.00	139.00	137.00	112.00	186.00
SR	139.00	161.00	64.00	113.00	70.00	124.00	102.00	278.00	70.00
Y	22.00	14.00	17.00	16.00	16.00	15.00	17.00	17.00	15.00
ZR	186.00	200.00	66.00	160.00	92.00	115.00	117.00	220.00	88.00
NB	10.00	7.00	10.00	9.00	10.00	9.00	11.00	7.00	9.00
TH	9.00	38.00	7.00	27.00	5.00	12.00	7.00	28.00	12.00
PB	16.00	22.00	20.00	27.00	21.00	17.00	19.00	11.00	22.00
GA	18.00	22.00	17.00	19.00	22.00	22.00	19.00	26.00	21.00
ZN	49.00	81.00	44.00	50.00	53.00	57.00	60.00	88.00	51.00
CU	2.00	6.00	0.00	3.00	0.00	6.00	0.00	4.00	0.00
NI	9.00	9.00	16.00	14.00	12.00	9.00	9.00	10.00	10.00
TIO2	0.30	0.49	0.13	0.32	0.17	0.32	0.24	0.78	0.20
V	18.00	34.00	6.00	13.00	8.00	27.00	15.00	71.00	14.00
CR	14.00	24.00	11.00	8.00	7.00	21.00	13.00	47.00	16.00

	4NPM549	4NPM551	4NPM556	4NPM558	4NPM578	4NPM580	4NPM581	5ANPM485	5ANPM612
BA	929.00	812.00	781.00	901.00	497.00	774.00	461.00	1920.00	1311.00
RB	139.00	121.00	166.00	137.00	130.00	234.00	156.00	132.00	167.00
SR	223.00	330.00	163.00	226.00	137.00	102.00	116.00	2567.00	420.00
Y	15.00	18.00	16.00	17.00	19.00	19.00	19.00	23.00	21.00
ZR	206.00	123.00	151.00	217.00	140.00	60.00	151.00	421.00	135.00
NB	8.00	10.00	7.00	8.00	9.00	8.00	10.00	30.00	12.00
TH	32.00	3.00	26.00	44.00	3.00	1.00	13.00	0.00	4.00
PB	15.00	13.00	22.00	21.00	17.00	21.00	18.00	0.00	7.00
GA	23.00	19.00	26.00	25.00	20.00	20.00	21.00	19.00	16.00
ZN	91.00	47.00	83.00	90.00	56.00	33.00	61.00	105.00	89.00
CU	10.00	5.00	4.00	8.00	0.00	3.00	0.00	41.00	38.00
NI	10.00	11.00	16.00	14.00	12.00	18.00	13.00	194.00	79.00
TIO2	0.64	0.48	0.50	0.61	0.28	0.13	0.36	1.22	1.07
V	53.00	52.00	38.00	45.00	24.00	6.00	24.00	144.00	181.00
CR	32.00	19.00	20.00	33.00	14.00	8.00	20.00	551.00	957.00

	5ANPM6156NPM538	7NPM464	7NPM539	7NPM545	7NPM560	7NPM563	7NPM566	7NPM579
BA	394.00	244.00	730.00	399.00	318.00	283.00	546.00	963.00	598.00
RB	19.00	133.00	137.00	128.00	112.00	98.00	123.00	157.00	150.00
SR	598.00	63.00	219.00	151.00	130.00	184.00	157.00	118.00	152.00
Y	28.00	11.00	22.00	16.00	24.00	15.00	17.00	16.00	13.00
ZR	248.00	39.00	202.00	128.00	229.00	210.00	146.00	112.00	137.00
NB	18.00	8.00	12.00	9.00	12.00	10.00	10.00	10.00	9.00
TH	3.00	2.00	7.00	11.00	10.00	0.00	8.00	14.00	14.00
PB	2.00	24.00	15.00	22.00	13.00	17.00	23.00	29.00	26.00
GA	15.00	21.00	20.00	22.00	19.00	22.00	20.00	22.00	20.00
ZN	110.00	23.00	63.00	57.00	83.00	60.00	59.00	44.00	54.00
CU	16.00	0.00	6.00	0.00	3.00	4.00	1.00	0.00	1.00
NI	22.00	9.00	12.00	13.00	11.00	9.00	11.00	13.00	13.00
TIO2	0.96	0.05	0.49	0.34	0.42	0.34	0.32	0.21	0.26
V	240.00	1.00	32.00	30.00	37.00	27.00	21.00	5.00	19.00
CR	1046.00	6.00	14.00	25.00	13.00	12.00	21.00	7.00	16.00

	7NPM583	8NPM10	8NPM361	8NPM537	9NPM491	9NPM8B
BA	657.00	972.00	316.00	460.00	4.00	181.00
RB	69.00	77.00	125.00	143.00	165.00	178.00
SR	197.00	229.00	86.00	111.00	3.00	30.00
Y	22.00	10.00	15.00	15.00	8.00	11.00
ZR	209.00	53.00	70.00	76.00	32.00	37.00
NB	8.00	6.00	7.00	5.00	14.00	10.00
TH	12.00	1.00	3.00	9.00	4.00	2.00
PB	18.00	29.00	25.00	22.00	15.00	36.00
GA	19.00	14.00	15.00	16.00	20.00	19.00
ZN	53.00	16.00	26.00	23.00	43.00	18.00
CU	1.00	0.00	0.00	0.00	0.00	0.00
NI	4.00	3.00	10.00	8.00	8.00	5.00
TIO2	0.37	0.18	0.08	0.08	0.00	0.03
V	24.00	16.00	4.00	3.00	1.00	0.00
CR	14.00	12.00	9.00	3.00	5.00	9.00

D-3: REE analyses of thirteen whole rock samples (in ppm)

EREE= E7REE excluding Gd

	1NPM533	1NPM582	1NPM584	3NPM542	4NPM458	4NPM477	4NPM558	5ANPM612	7NPM539
LA	0.00	0.00	0.00	0.00	0.00	0.00	0.00	0.00	0.00
CE	38.51	49.30	67.96	17.54	56.80	72.29	113.46	60.79	43.41
PR	0.00	0.00	0.00	0.00	0.00	0.00	0.00	0.00	0.00
ND	18.98	27.09	29.41	8.17	29.23	44.93	65.54	33.52	22.98
SM	3.88	5.96	5.19	2.03	6.39	10.18	13.50	6.52	4.63
EU	1.21	1.30	1.34	0.46	0.83	0.59	1.17	1.82	0.75
GD	4.57	4.94	0.00	0.00	5.25	0.00	15.70	5.01	3.81
TB	0.41	0.81	0.32	0.19	0.67	0.48	1.51	0.70	0.47
DY	0.00	0.00	0.00	0.00	0.00	0.00	0.00	0.00	0.00
HO	0.00	0.00	0.00	0.00	0.00	0.00	0.00	0.00	0.00
ER	0.00	0.00	0.00	0.00	0.00	0.00	0.00	0.00	0.00
TM	0.00	0.00	0.00	0.00	0.00	0.00	0.00	0.00	0.00
YB	1.38	3.07	0.87	0.69	2.03	1.11	1.15	1.68	1.70
LU	0.20	0.43	0.10	0.10	0.27	0.12	0.15	0.24	0.23
BA	391.21	209.55	343.63	360.47	241.42	477.21	605.45	816.66	284.15
CO	0.00	0.00	0.00	0.00	0.00	0.00	0.00	0.00	0.00
CR	0.00	0.00	0.00	0.00	0.00	0.00	0.00	0.00	0.00
CS	0.00	0.00	0.00	0.00	0.00	0.00	0.00	0.00	0.00
HF	5.11	8.47	3.68	1.81	4.91	4.41	6.52	3.95	3.53
SC	0.00	0.00	0.00	0.00	0.00	0.00	0.00	0.00	0.00
TA	0.58	0.77	0.44	0.45	1.01	1.01	0.00	0.53	1.20
TH	6.49	7.67	10.75	3.56	12.86	28.17	26.42	4.87	9.36
U	0.00	0.00	0.00	0.00	0.00	0.00	0.00	0.00	0.00
E REE	45.59	60.87	75.78	21.01	66.99	84.77	130.94	71.75	51.19

	7NPM560	7NPM566	7NPM583	9NPM8B
LA	0.00	0.00	0.00	0.00
CE	13.04	48.70	56.93	6.03
PR	0.00	0.00	0.00	0.00
ND	7.11	25.55	25.59	2.88
SM	1.81	6.00	5.36	0.87
EU	0.75	0.64	1.17	0.13
GD	2.35	3.31	0.00	0.00
TB	0.34	0.54	0.53	0.18
DY	0.00	0.00	0.00	0.00
HO	0.00	0.00	0.00	0.00
ER	0.00	0.00	0.00	0.00
TM	0.00	0.00	0.00	0.00
YB	1.49	0.60	2.04	1.22
LU	0.21	0.07	0.29	0.18
BA	0.00	652.13	436.34	119.59
CO	0.00	0.00	0.00	0.00
CR	0.00	0.00	0.00	0.00
CS	0.00	0.00	0.00	0.00
HF	4.79	3.03	5.27	1.60
SC	0.00	0.00	8.00	0.00
TA	0.98	0.50	0.57	1.30
TH	1.76	10.16	15.10	0.91
U	0.00	0.00	0.00	0.00
E REE	17.64	56.55	66.32	8.61

APPENDIX E Ar^{40}/Ar^{39} Laboratory Procedures

E-1 Mineral Separation (revised from Elias(1986))

Representative samples of up to a few kilograms in weight were first trimmed of weathered surfaces, then comminuted in a steel jaw crusher. Where the grain size warranted, final pulverization waas performed in a tungsten carbide shatter box. Appropriate size fractions were screened (mesh size=) thoroughly washed in tap water, then dried under a 60 watt bulb. Mineral separation was completed in a Franz magnetic separator. Hand picking of individual grains was necessary to attain high purity.

E-2 Argon Dating Procedure (revised from Elias (1986))

Samples were packed into small thin-walled aluminum discs or simply wrapped in aluminum foil. Samples and standards were stacked in aluminum canisters. Most of the canisters were lined with 1.0 mm of cadmium metal to absorb therm neutrons. Interspersed among the samples were a number of flux monitors, normally 8-10 per canister. Two flux monitors were used: (i) the Dalhousie University laboratory standard, NS 231, which has an apparent K-Ar age of 368 +/-5 Ma (Reynolds et al 1973) and (ii) the hornblende standard MMHb-1 which has a 519 Ma argon age (Alexander et al. 1978, Roddick, 1983). Replicate analyses of these standards over the corse of the present study have shown that the above two ages are consistent with each other to within 0.5%, a value which is substantially smaller than the

estimated uncertainties in either age.

After irradiation, samples were stored for a few weeks to permit safer handling. Each sample was subsequently loaded into a quartz boat and placed in a quartz extraction tube connected to a glass vacuum line. The quartz tube was heated to a maximum of 1200 degress C by means of a Lindberg (type 59344) furnace. Temperature within the furnace was monitored by a "Paltinel" thermocouple. The gas was extracted in a stepwise fashion, usually at 50 degree intervals, purified over a Ti sponge getter, and leaked directly into the chamber of a substantially modified mass spectrometer.

Analyses were accomplished by sequentially scanning for masses 36, 37, 39 and 40. Mass 37 was omitted for samples with low Ca/K ratios, and mass 38 was not recorded for any samples. A peack hopping procedure was executed automatically and the amplified signal fed into an on-line Apple 11e microcomputer. Each mass was measured 15 times. Peak positions were relocated before the first, sixth and eleventh measurements.

Amplified signals arriving from the mass spectrometer were digitized and the following mass ratios calculated: 36/39, 37/39, 40/39. The measured isotopic ratios often vary significantly over the duration of 15 dterminations (about 45 minutes). Consequently, a linear extrapolation of ratios was made back to zero time, when the gas was first let into the mass spectrometer. In calculating the ratio 40Ar/39Ar, a correction was made for the tailing of the 40Ar peak at the 39Ar position. Very occasionally, the 40Ar tail was observed to extend over to the 36 Ar position, in which case a

correction was performed manually.

Summary sheets for the four PMP samples analysed for this study, follow on the next pages.

$^{40}Ar/^{39}Ar$ spectrum of four samples analysed from the PMP

S-612 HORNBLENDE SUMMARY

TEMP. (DEG.C)	mV Ar39	% Ar39	AGE (Ma)	% ATMOS.	Ar37/Ar39	% I.I.C.
			J = 2.557E-03			
200-650	4.9	5.7	315.2 +/- 18.9	83.3	1.7	.2
650-725	6.1	7.2	353.4 +/- 12.4	76	1	.1
725-800	5.3	6.1	380 +/- 17.1	83.4	2.7	.3
800-850	5.8	6.7	371 +/- 12.3	78.3	3.4	.4
850-900	9	10.4	412.4 +/- 6.2	67.3	7	.9
900-950	25	29.1	460.5 +/- 3.4	42.9	30.9	4
950-980	14.3	16.6	411.6 +/- 2	40.9	46.8	6.5
980-1010	6.2	7.2	371.8 +/- 7.9	58.7	41.2	6.1
1010-1050	5.7	6.6	342.4 +/- 8.1	76	41.5	6.4
1050-1100	3.3	3.9	351.1 +/- 31	86.3	45.9	7

TOTAL GAS AGE = 402.2 MY. +/- 10 MY. (2.5 %) =

% I.I.C. - INTERFERING ISOTOPES CORRECTION

ERROR ESTIMATES AT ONE SIGMA LEVEL

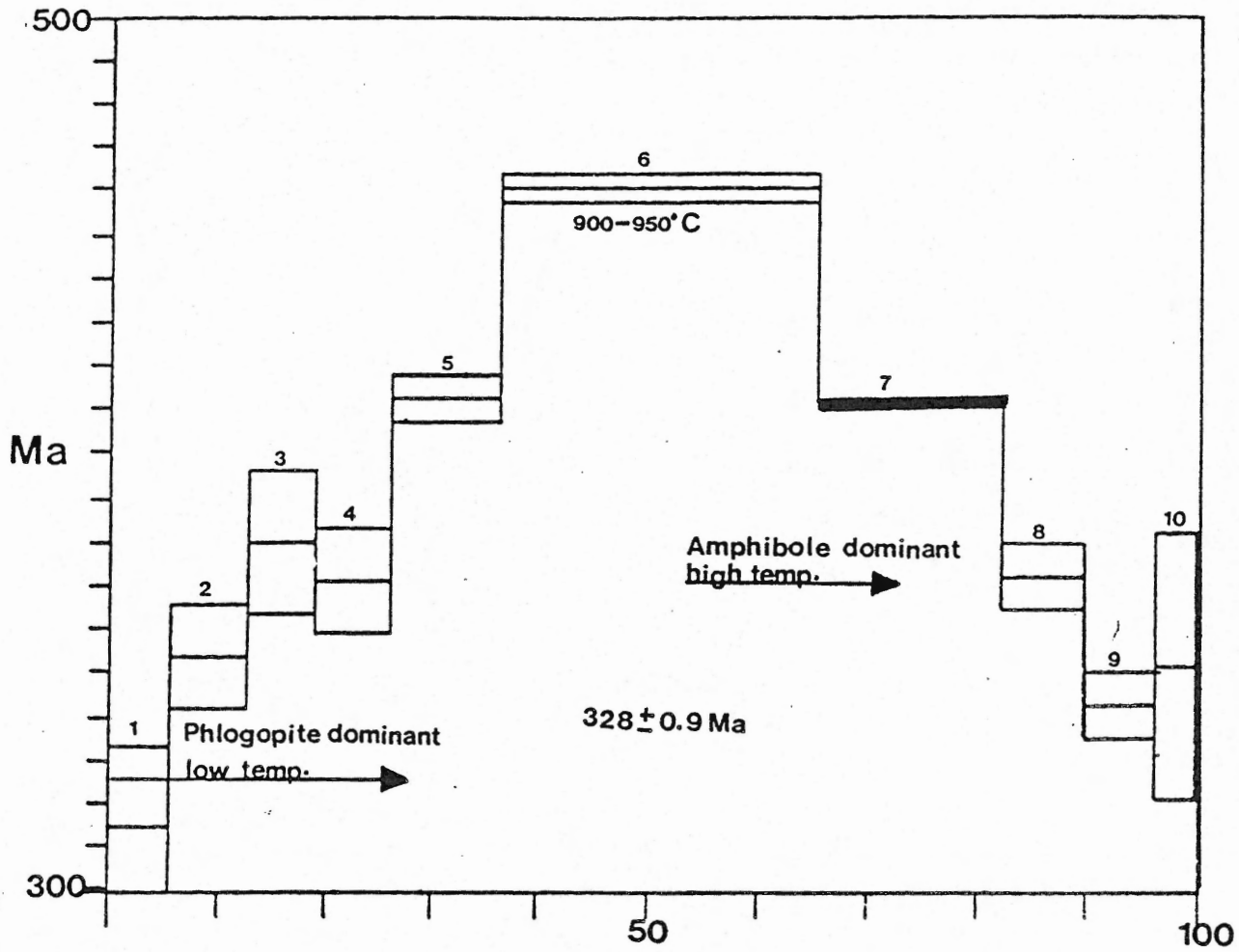
500
300
Ma
50
100
1
2
3
4
5
6
7
8
9
10
900–950°C
Amphibole dominant
high temp.
Phlogopite dominant
low temp.
328±0.9 Ma
% cumulative of 39Ar

NPM612

S-581 BIOTITE SUMMARY

TEMP.(DEG.C)	mV Ar39	% Ar39	AGE(Ma)	% ATMOS.	Ar37/Ar39	% I.I.C.
			J = 2.53E-03			
200-600	139	18.3	291.8 +/- .3	16.7	0	0
600-650	216.4	28.5	315.7 +/- .2	5.5	0	0
650-700	123.9	16.3	313.7 +/- .2	8.3	0	0
700-750	34	4.4	310.1 +/- 1	21.2	0	0
750-800	29.5	3.9	310 +/- .9	33.4	0	0
800-850	39	5.1	314.3 +/- .6	28.8	0	0
850-900	70.4	9.3	313.9 +/- .3	17.5	0	0
900-950	78.2	10.3	312.3 +/- .4	15.7	0	0
950-1000	19.6	2.5	310.5 +/- 1.4	39	0	0
1000-1050	6.3	.8	300.4 +/- 5.3	62.1	0	0

TOTAL GAS AGE = 309.7 MY. +/- .5 MY.(.1 %)

% I.I.C. - INTERFERING ISOTOPES CORRECTION

ERROR ESTIMATES AT ONE SIGMA LEVEL

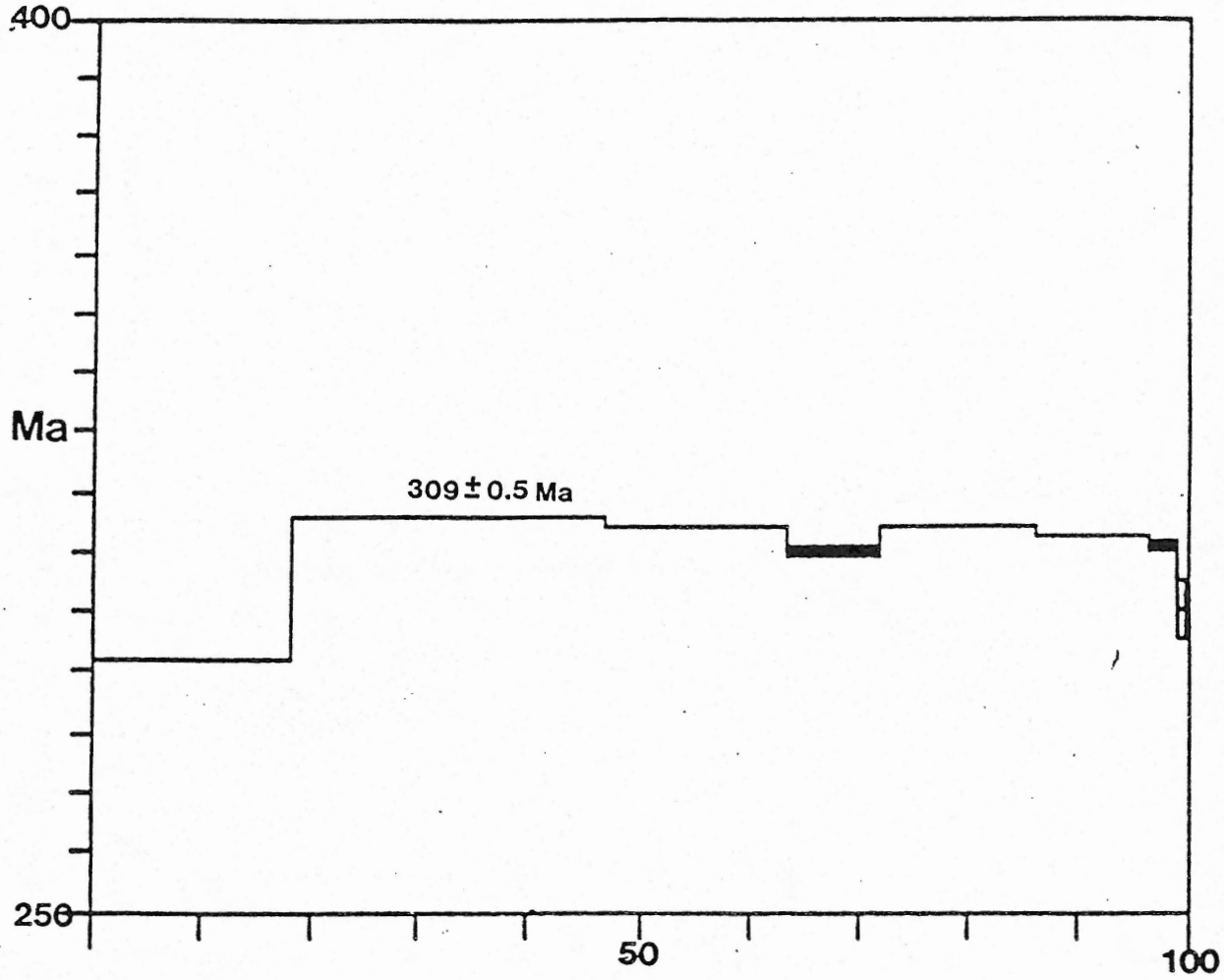

NPM581

S-533 BIOTITE SUMMARY

TEMP.(DEG.C)	mV Ar39	% Ar39	AGE(Ma)	% ATMOS.	Ar37/Ar39	% I.I.C.
			J = 2.527E-03			
200-550	53.5	7.1	298.8 +/- .6	33.9	0	0
550-600	105.4	14	320.9 +/- .3	10.6	0	0
600-650	162.4	21.6	321.7 +/- .2	6.9	0	0
650-700	164.9	22	321.1 +/- .6	7	0	0
700-750	70	9.3	320 +/- .4	14.5	0	0
750-800	26.6	3.5	314.9 +/- 1.4	26	0	0
800-850	51.7	6.9	321.6 +/- .5	27.1	0	0
850-900	44.1	5.8	321.2 +/- .5	18	0	0
900-950	46.4	6.1	319.4 +/- .6	38.1	0	0
950-1000	17	2.2	318.5 +/- 2.1	55.6	0	0
1000-1050	6.8	.9	314.4 +/- 5.4	69	0	0

TOTAL GAS AGE = 319.1 MY. +/- .7 MY.(.2 %)

% I.I.C. - INTERFERING ISOTOPES CORRECTION

ERROR ESTIMATES AT ONE SIGMA LEVEL

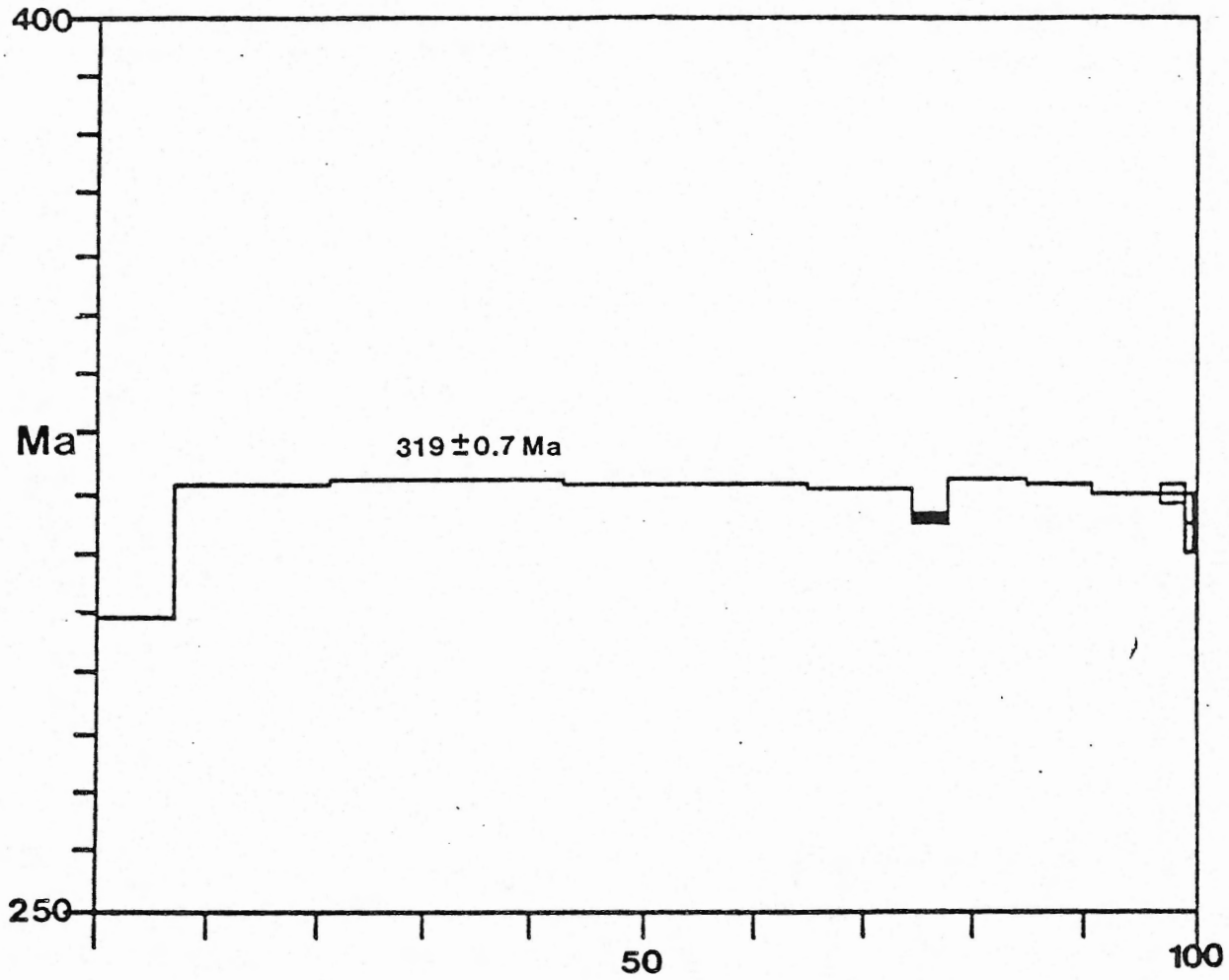

NPM533

NPM485 - phlogopite

TEMP. (DEG.C)	mV Ar39	% Ar39	AGE (Ma)	% ATMOS.	Ar37/Ar39	% I.I.C.
			J = 2.512E-03			
200-550	12.6	2.2	213.1 +/- 2.1	59.7	0	0
550-650	98	17.6	329.8 +/- .4	10.7	0	0
650-700	110	19.8	330.6 +/- .2	7.8	0	0
700-750	66	11.8	329.4 +/- 1.2	12.1	0	0
750-800	47.4	8.5	330.2 +/- 1.3	21.6	0	0
800-850	21.7	3.9	329.6 +/- .9	27.6	0	0
850-900	46	8.2	336.1 +/- .6	26.9	.4	0
900-950	65.9	11.8	332.7 +/- .5	21.7	0	0
950-1000	52.8	9.5	330. +/- .6	30	0	0
1000-1050	20.9	3.7	327.9 +/- 1.2	47.2	0	0
1050-1150	13.5	2.4	326.4 +/- 4.6	69.6	0	0

TOTAL GAS AGE = 328.1 MY. +/- .9 MY. (.3 %)

% I.I.C. - INTERFERING ISOTOPES CORRECTION

ERROR ESTIMATES AT ONE SIGMA LEVEL

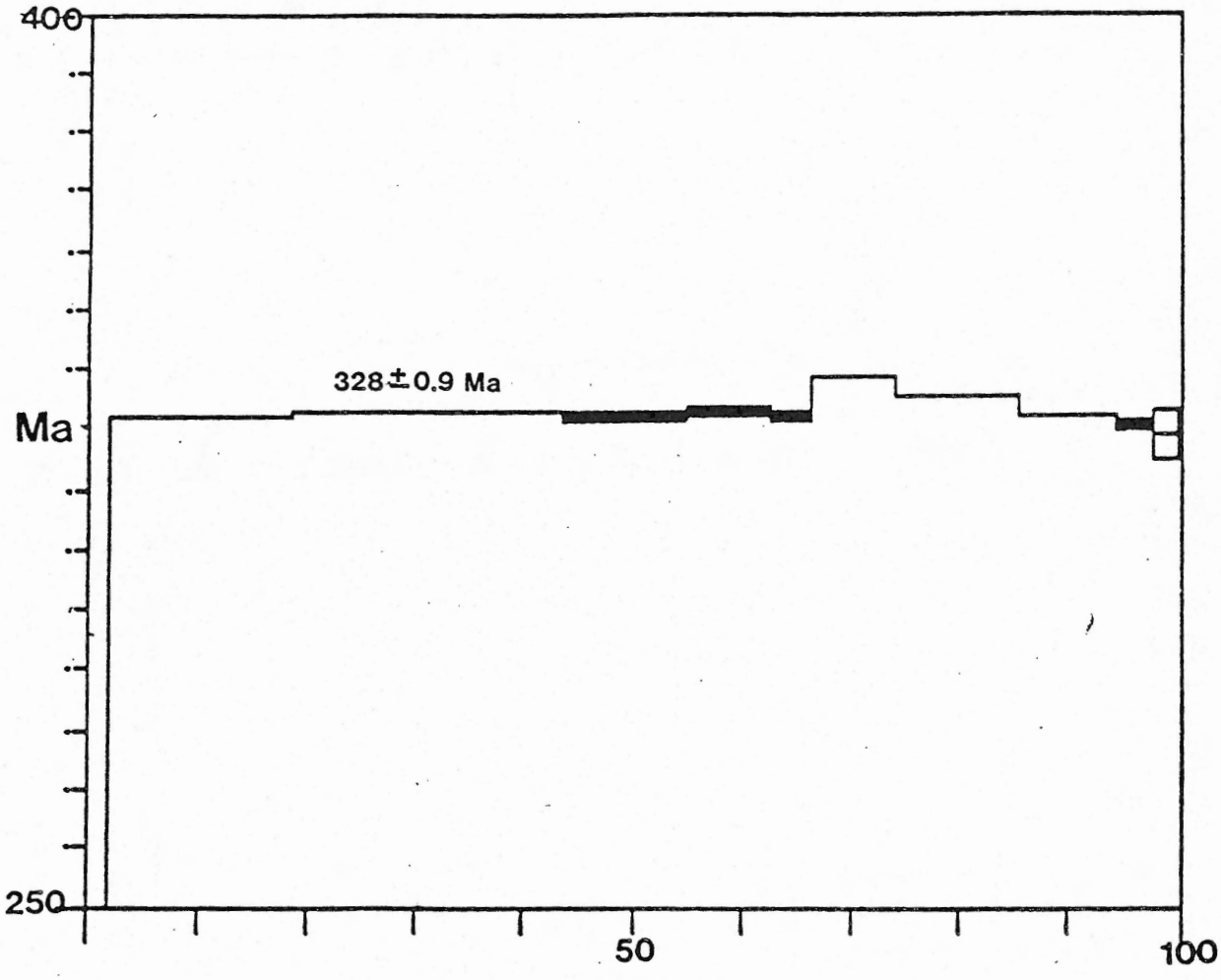

NPM485

REFERENCES

Abbott, R.N. Jr., 1981, AFM liquidus projections for granitic magmas, with special reference to hornblende, biotite and garnet: in The Canadian Mineralogist, 19, Part 1, "Peraluminous Granites", D.B. Clarke, ed., pp. 103-110.

Allan, B.D. and Clarke, D.B., 1981. Occurrence and origin of garnets in the South Mountain Batholith, Nova Scotia: in The Canadian Mineralogist, 19, Part 1, "Peraluminous Granites", D.B. Clarke, ed., pp. 19-24.

Anderson, J.L. and Rowley, M.C., 1981. Synkinematic intrusion of peraluminous and associated metaluminous granitic magmas, Whipple Mountains California: in The Canadian Mineralogist, 19, Part 1, "Peraluminous Granites", D.B. Clarke, ed., pp. 83-102.

Aoki, K., 1963. The kaersutites and oxykaersutites from alkalic rocks of Japan and surrounding areas: Journal of Petrology, 4, pp. 198-210.

Asquith, G.B., 1973. Flow differentiation in Tertiary lamprophyres (camptonites), Sacramento Mountains, New Mexico: Journal of Geology, 81, pp. 643-647.

Auigs, J., 1972. "Nickel": in The Encyclopedia of Geochemistry and Environmental Sciences. R.W. Fairbridge, ed.

Berger, G.W. and York, D., 1981. Geothermometry from $^{40}Ar/^{39}Ar$ dating experiments: Geochim. Cosmochim. Acta. 45, pp. 795-811.

Bachinski, S.W. and Scott, R.B., 1979. Rare-earth and other trace element contents and the origin of minettes: Geochim. Cosmocim. Acta. 43, pp. 93-100.

Bailey, S.W., 1984. Classification and Structures of Micas. in Reviews in Mineralogy, vol. 13, Micas, S.W. Bailey ed., Mineralogical Society of America.

Bouseily, El. A.M. and Sokkary, El. A.A., 1975. The relation between Rb, Ba and Sr in granitic rock: Chemical Geology, 16, pp. 207-219.

Bradley, D.C., 1982. Subsidence in Late Paleozoic basins in the Northern Appalachians: Tectonics, 1, pp. 107-123.

Brown, G.C. and Fyfe, W.S., 1970. The production of granitic melts during ultrametamorphism: Contributions to Mineralogy and Petrology, 28, pp. 310-318.

Buddington, A.F., 1959. Granite emplacement with special reference to North America: Geological Society of America Bulletin, 70, pp. 671-747.

Burkast-Baumann, I., 1972. "Vanadium": The Encyclopedia of Geochemistry Environmental Sciences. Fairbridge, R.W., ed. Van Nostrand Reinhold Co., N.Y. Volume IVA. p1235-1237

Cameron, K.L., 1975. An experimental study of actinolite-cummingtonite phase relations with notes on the synthesis of Fe-rich anthophyllite: American Mineralogist, 60, pp. 375-390.

Cann, J.R., 1970. Upward movement of granitic magma: Geological Magazine, 107, pp. 335-340.

Carmichael, I.S.E. and Turner, F.J. and Verhoogen, J., 1974. Igneous Petrology, McGraw-Hill, New York.

Chappell, B.W., 1984. Source rocks of I- and S-type granites in the Lachlan Belt,, southeastern Australia: Phil. Trans. Royal Society London, A310, pp. 693-707.

Chappell, B.W. and White, A.J.R., 1974. Two contrasting granite types: Pacific Geology, 8, pp. 173-174.

Chatterjee, A.K., Strong, D.F., Clarke, D.B. and Keppie, J.D., 1985. Geology and Geochemistry of the Carboniferous Wedgeport Pluton Hosting Sn-W Mineralization. Chapter 11, pp. 201-216. in Guide to the Granites and Mineral Deposits of Southwestern Nova Scotia. Eds. A.K. Chatterjee and D.B. Clarke, Nova Scotia Department of Mines and Energy, Preprint of Paper 85-3.

Clarke, D.B., 1976. The Tertiary volcanic province of Baffin Bay: Geological Association of Canada, Special Paper 16, pp. 445-460.

Clarke, D.B., 1981. Introduction: in The Canadian Mineralogist, 19, Part 1, "Peraluminous Granites", D.B. Clarke, ed., pp. 1-3.

Clarke, D.B., Barr, S.M. and Donohoe, H.V., 1980. Granitoid and other plutonic rocks of Nova Scotia: in IGCP Conference Proceedings "The Caledonides in the U.S.A.", pp. 107-115.

Clarke, D.B., Halliday, A.N., 1980. Strontium Isotope Geology of the South Mountain Batholith, Nova Scotia: Geochemical et Cosmochimica Acta, 44, pp. 1045-1058

Clarke, D.B. and Halliday, A.N., 1985. Sm/Nd isotopic investigation of the age and origin of the Meguma Zone metasedimentary rocks: Canadian Journal Earth Sciences, 22, pp. 102-107.

Clarke, D.B., Muecke, G.K. and de Albuquerque, C.A.R., 1980. Igneous and Metamorphic Geology of Southern Nova Scotia. GAC-MAC Field Guide, No. 21, 1980.

Clarke, D.B., Muecke, G.K., 1985. Review of the Petrochemistry and origin of the South Mountain Batholith and associated plutons, Nova Scotia, Canada: in "High Heat Production (HHP) granites, hydrothermal circulation and ore genesis" , The Institute of Mining and Metallurgy, London England, pp. 41-55.

Clemens, J.D., Wall, V.J. and Clarke, D.B., 1983. Models for granitoid evolution and source compositions: restite - R.I.P.?: Geological Society of Australia Abstracts, 9 , 178-179.

Conrad, W.K., Nicholls, J.A. and Wall, V.J., 1986. Water Saturated and Undersaturated Melting of Metaluminous and Peraluminous Model Crustal Composition at 10 Kbar: The Origin of Rhyolitic Magmas in the Taupo Volcanic Zone. In press.

Cormier, R.F. and Smith, T.E., 1973. Radiometric ages of granitic rocks, southwestern Nova Scotia: Canadian Journal of Earth Sciences, 10, pp. 1201-1211.

Currie, K.L. and Pajari, G.E. Jr., 1981. Anatectic peraluminous granites from the Carmanville area, northeastern Newfoundland: in The Canadian Mineralogist, 19, Part 1, "Peraluminous Granites", D.B. Clarke, ed., pp. 147-162.

Curtis, C.D., 1972. "Zinc": in The Encyclopedia of Geochemistry and Environmental Sciences. Ed. Fairbridge, R.W. Van Nostrand Reinhold Co. N.Y. Volume IVA p1293-1295

Dallmeyer, R.D. and Keppie, J.D., 1984. Geochronological constraints on the Accretion of the Meguma Terrane with North America: in GSA Abstracts. 19th Annual Meeting-Northeastern Section, GSA. March 15-17.

Dallmeyer, R.D., Sutter, J.F. and Baker, D.J., 1975. Incremental $^{40}Ar/^{39}Ar$ ages of biotite and hornblende from the northeastern. Reading Prong: Their bearing on late Proterozoic thermal and tectonic history: Geological Society of America Bulletin, 86, pp. 1435-1443.

Dallmeyer and Keppie, 1986. Polyphase Late Paleozoic Tectonothermal Evolution of the Meguma Terrane, Nova Scotia (abastract) in Abstracts with Programs, 1986, 21st Annual Meeting Northeastern Section, Geological Society of America, Vol,18 No. 1, p.11.

de Albuquerque, C.A.R., 1977. Geochemistry of the tonalitic and granitic rocks of the Nova Scotia Southern plutons: Geochem. et Cosmochim Acta. 41, pp. 1-13.

de Albuquerque, C.A.R., 1979. Origin of the plutonic mafic rocks of southern Nova Scotia: Geological Society of America Bulletin 90, pp. 719-731.

Deer, W.A., Howie, R.A. and Zussman, J., 1966. An Introduction to the Rock Forming Minerals. Longman Group Limited.

Deer, W.A., Howie, R.A. and Zussman, J., 1962. Rock-Forming Minerals, 3, Sheet Silicates. Longmans, Green & Co. Ltd.

Donohoe, H.V. and Wallace, P.I., 1978. Anatomy of the Cobequid Fault and its relations to the Glooscap and Cabot Fault systems (abstract). in Geological Association of Canada Annual Meeting, Toronto, pp. 391.

Eisbacher, G.H., 1969. Displacement and stress field along part of the Cobequid Fault, N.S.: Canadian Journal of Earth Sciences, 6, pp. 1095-1104.

Elias, P., 1986. Thermal History of the Meguma Terrane: A study based on ^{40}Ar-^{39}Ar and Fission Track Dating. Unpublished Ph.D. thesis, Dalhousie University, Halifax, N.S., pp. 403.

Fairbairn, H.W., Hurley, P.M., Pinson, W.H., and Cormier, R.F., 1960. Age of the granitic rocks of Nova Scotia: Geological Society of America Bulletin, 71, pp. 399-414.

Faribault, E.R., 1913-14. Geology of the Port Mouton Map - Area, Queens County, Nova Scotia: Canada Geological Survey - Summary Report 1913-14.

Faure, G., 1970. "Strontium", Chapter 38. in Handbook of Geochemistry. K.H. Wedepohl (Ed.). Volume II-4. Elements Kr(36) to Ba(56). p38-B-1 to 38-B-32.

Ferry, J.M., 1980. A comparative study of geothermometers and geobarometers in pelitic schists from south-central Maine: American Mineralogist, 65, pp. 720-732.

Ferry, J.M. and Spears, F.S., 1978. Experimental Calibration of the Positioning of Fe and Mg Between Biotite and Garnet: Contributions to Mineralogical Petrology, 66, pp. 113-117.

Fleck, R.D., Sutter, J.F. and Elliot, E., 1977. Interpretation of discordant $^{40}Ar/^{39}Ar$ age-spectrum of Mesozoic tholeiites from Antarctica: Geochim. Cosmochim. Acta. 41, pp. 15-32.

Foslie, S., 1945. Hastingsites and amphiboles from the epidote-amphibolite facies: Norsk, Geol. Tiddsskr, 25, pp. 74.

Frenzel, G., 1971. Die Mineralparagenese der Albersweiler Lampropyre: Neues Jahrb Mineral ABlt. 115, pp. 164-191.

Geldon, A.L., 1972. Petrology of the lamprophyre pluton near Dead River: in Sims. P. and Mudrey, G.B. (Eds.). Geology of Minnesota, 153-159. St. Paul: Geological Survey of Minnesota.

Gilbert, M.C., Helz, R.T., Popp, R.K., and Spear, F.S., 1982. Experimental Studies of Amphibole Stability, pp. 228-267. In Veblen, D.R. and Ribbe, P.H. (editors),Reviews in Mineralogy, vol. 9B, Amphiboles: Petrology and Experimental Phase Relations.

Giles, P.S., 1985. A major Post-Visean Sinistral Shear Zone- New Perspectives on Devonian and Carboniferous Rocks of Southern Nova Scotia: in Guide to the Granites and Mineral Deposits of S.W. N.S. Eds. A.K. Chatterjee and D.B. Clarke, NSDME - Paper 85-3.

Giles, P.S. and Chatterjee, A.K., 1986. Peraluminous Granites of the Liscomb Complex: in J.L. Bates and D.R. MacDonald (editors), Mines and Minerals Branch Report of Activities NSDME Report 87-1, p95-98.

Goad, B.E. and Cerny, P., 1981. Peraluminous pegmatitic granites and their pegmatite aureoles in the Winnipeg River district, southeastern Manitoba: in The Canadian Mineralogist, 19, Part 1, "Peraluminous Granites", D.B. Clarke, ed., pp. 177-194.

Gornitz, V., 1972. "Niobium", The Encyclopedia of Geochemistry and Environmental Sciences. Ed. Fairbridge, R.W. Van Nostrand Reinhold Co., N.Y. Volume IVA. p793-795.

Green, T.H., 1977. Garnet in silicic liquids and it's possible use as P-T indicator: Contributions to Mineralogical Petrology, 65, 59-67.

Greenland, L.P., 1972. The Encyclopedia of Geochemistry and environmental Sciences. Ed. Fairbridge, R.W. Van Nostrand Reinhold Co., N.Y. Volume IVA.

Greenland, L.P., 1970. An equation for trace element distribution during magmatic crystallization: American Mineralogist, 55, pp. 455-465.

Hall, A., 1965. The origin of accessory garnet in the Donegal garnet: Mineralogical Magazine, 35, pp. 628-633.

Halliday, A.N., Stephens, W.E. and Harman, R.S., 1981. Isotopic and chemical constrains on the development of peraluminous Caledonian and Acadian granites: in The Canadian Mineralogist, 19, Part 1, "Peraluminous Granites", D.B. Clarke, ed., pp. 204-216.

Ham, L., 1983. Determination of Chemical Composition of Different Types of White Mica within Nova Scotia Granites. Dalhousie University, Internal Report.

Hammarstrom, J.M. and Zen, E-An, 1986. Aluminum in hornblende: An empirical igneous geobarometer: American Mineralogist, 71, pp. 1297-1313.

Hanson, G.N, 1978. The application of trace elements to the petrogenesis of igneous rocks of granitic composition: Earth and Planetary Science Letters, 38, pp. 26-43.

Harrison, T.M., 1981. The diffusion of ^{40}Ar in hornblende: Contributions to Mineralogical Petrology, 78, pp. 324-331.

Harrison, T.M. and McDougall, I., 1980. Investigations of an intrusive contact, northwest Nelson, New Zealand - II: Diffusion of radiogenic and excess ^{40}Ar in hornblende revealed by $^{40}Ar/^{39}Ar$ age spectrum analysis: Geochim. Cosmochim. Acta 44, pp. 2005-2020.

Harrison, T.M., Duncan, I.J. and McDougall, I., 1985. Diffusion of ^{40}Ar in biotite: Temperature, pressure and compositional effects: Geochim. Cosmochim. Acta. 49, pp. 2461-2468.

Haskin, L.A., Frey, F.A., Schmitt, R.A. and Smith, R.H, 1966. "Meteoric, Solar and Terrestrial Rare Earth Distributions", in (Ahrens, L.H. et al. editors) "Physics and Chemistry of the Earth", 7, Oxford, Pergamon Press, pp. 167-321.

Hawthorne, F.C., 1981. Chapter Crystal Chemistry of the Amphiboles: in Veblen, P.R., 1981. Reviews in Mineralogy, 9A, 1981. Amphiboles and other Hydrous Pyriboles-Mineralogy. Mineralogical Society of America

Helz, R.T., 1979. Alkali exchange between hornblende and melt: a temperature sensitive reaction: American Mineralogist, 64, pp. 933-965.

Henderson, P. (Ed.), 1984. Rare Earth Element Geochemistry Developments in Geochemistry 2. Elsevier Science Publication Amsterdam.

Henderson, P., Nolan, J., Cunningham, G.C. and Lowry, R.K., 1985. Structural controls and mechanisms of diffusion in natural silicate melts: Contributions to Mineralogical Petrology, 89, pp. 263-272.

Hermann, A.G., 1970. Yhrium and lanthanidis: in Wedepohl, K.H. ed. Handbook of Geochemistry, 39, pp. 57-71 E1-19. Springer-Verlag, Berlin Heidleberg, N.Y.

Hill, J.D., 1986. Granitoid plutons in the Canso area,Nova Scotia: in Current Research, Part A., GSC Paper 86-1A, pp. 185-192.

Hoinkes, Georg, 1986. Effect of grossular-content in garnet on the partitioning of Fe + Mg between garnet and biotite: Contributions to Mineralogical Petrology, 92 p. 393-399.

Hope, T.L., 1987. Geology and Metamorphism in the Port Mouton-Lockeport Area, Queens and Shelburne Counties, Nova Scotia. Unpubl. MSc thesis, Acadia University, 165p

Hope, T.L. and Woodend, S.L., 1986. Geological Mapping and igneous and metamorphic petrology, Queen's and Shelburne counties, Nova Scotia: in Current Research Part A, GSC Paper 86-1A, pp. 429-433.

Huang, W.L. and Wyllie, P.J., 1975. Melting reactions in the system $NaAlSi_3O_8$-$kAlSi_3O_8$-SiO_2 to 35 Kbars, dry and with excess water: Journal of Geology, 83, pp. 737-748.

Hyndman, D.W., 1981. Controls on source and depth of emplacement of granitic magmas: Geology, 9, No. 6, pp. 244-249.

Indares, A. and Martignole, J., 1985. Evolution of P-T conditions during a high-grade metamorphic event in the Maniwaki area (Grenville Province): Canadian Journal of Earth Sciences, 21, pp. 853-863.

Indares, A. and Martignole, J., 1985. Biotite-garnet geothermometry in granulite facies rocks: Evaluation of equilibrium criteria: Canadian Minerlaogist, 23, pp. 187-193

James, R.S. and Hamilton, D.L., 1969. Phase relations in the system $NaAlSi_3O_8$-$kAlSi_3O_8$-$CaAl_2Si_2O_8$-SiO_2 at 1 Kbar H_2O vapour pressure: Contributions to Mineralogy and Petrology, 21, pp. 111-141.

Jamieson, R.A., 1981. Metamorphism during ophiolite emplacement. The petrology of the St. Anthony Complex: Journal of Petrology, 22, pp. 397-449.

Jamieson, R.A., 1974. The contact of the South Mountain Batholith Near Mount Uniacke, Nova Scotia. Honours thesis, Dalhousie University, 1974.

Jensen, L.R., 1976. The Torbrook Formation (Lower Devonian, Nova Scotia): Maritime Sediments., 12, pp. 107-118.

Karlo, J.F., 1982. Average composition of an alkali basalt, pp. 44.2. in AGI Data Sheets for Geology in the Field, Laboratory and Office, American Geological Institute.

Kay, R., 1972. "Yttrium"; in The Encyclopedia of Geochemistry and Environmental Sciences. Ed. Fairbridge, R.W. Van Nostrand Reinhold Co., N.Y. Volume IVA. p1290-1292.

Keppie, J.D., 1977. Structural history of preCarboniferous rocks of Southern Nova Scotia: in Geological Society of America Abstracts Program, 9, pp. 283.

Keppie, J.D., 1982. The Minas Geofracture: in Major structural zones and faults of the northern Appalachians. Edited by P. St. Julien and J. Beland. G.A.C. Special Paper 24, pp. 263-280.

Keppie, J.D. and Cormier, R.F., 1983. Tectonothermal evolution of the Meguma Terrane: Radiometric Controls. in GSA Abstracts with Programs 15, pp. 136, 1983.

Keppie, J.D., Odom, L. and Cormier, R.F., 1983. Tectonothermal evolution of the Meguma Terrane: radiometric controls: Geological Society of America, Abstracts with Programs, 15, pp. 136.

Keppie, J.D. and Muecke, G.K., 1979. Metamorphic Map of Nova Scotia. Nova Scotia Department of Mines, Halifax, N.S.

Kerrick, D.M., 1970. Contact metamorphism in some areas of the Sierra Nevada, California: in Bull. Geol. Society of America, 81, pp. 2913-2938.

King, L.H., Hyndman, R.D. and Keen, C.E., 1975. Geological Development of the Continental Margin of Atlantic Canada: Geoscience Canada, 2, 26-35.

Kretz, R., 1973. Kinetics of the crystallization of garnet at two localities near Yellowknife: Canadian Mineralogist, 12, pp 1-20.

Krogh, T.E. and Keppie, J.D., 1986. Detrital Zircon Ages Indicating a North African Provenance for the Goldenville Formation of Nova Scotia: in GSA/MAC Joint Annual Meeting, May 19-21, Program with Abstracts VII.

Kubilius, W.P., 1983. Sulfur Isotopic Evidence for Country Rock Contamination of Granitoids in Southwestern Nova Scotia. M.Sc. Unpublished thesis; Pennsylvania State University, Department of Geosciences.

Laird, J. and Albee, A.L., 1981. Pressure, temperature and time indicators in mafic schist: Their application to reconstructing the polymetamorphic history of Vermont: American Journal of Science, 281, pp. 127-175.

Leake, B.E., 1967. Zoned garnets from the Galway granite and its aplites: Earth Planetary Science Letters, 3 pp. 311-316.

Leake, B.E., 1978. Nomenclature of amphiboles: American Mineralogist, 63, pp. 1023-1052.

Lees, G.J., 1974. Petrochemistry of the mica lamprophyres (minettes) of Jersey. In Proc. Ussher Soc. 3, pp. 149 -155.

Liew, M.Y.C., 1979. Geochemical Studies of the Goldenville Formation at Taylor Head, Nova Scotia. M.Sc. thesis, Dalhousie University, Halifax, N.S.

Longstaffe, F.J., Smith, T.E. and Muehlenbadis, K., 1979. Oxygen isotope evidence for the genesis of upper Paleozoic granitoids of southwestern Nova Scotia: Canadian Journal of Earth Sciences, 17, pp. 132-141.

Longstaffe, F.J., Cerny, P. and Muehlenbachs, K., 1981. Oxygen-isotope geochemistry of the rocks in the Winnipeg River pegmatite district, southeastern Manitoba: in The Canadian Mineralogist, 19, Part 1, "Peraluminous Granites", D.B. Clarke, ed., pp.195-204.

Luth, W.C., Jahns, R.H. and Tuttle, O.F., 1964. The granite system at pressures of 4 to 10 Kbars: Journal of Geophysics Research, 69, pp. 759-773.

MacDonald, D., 1988. Examination of a zoned Pegmatite and Host Rocks at Port Joli Nova Scotia. Unpubl. BSc thesis. Dalhousie U. March 5, 1988.

MacDonald, M.A., 1981. The Mineralogy, petrology and geochemistry of the Musquodoboit Batholith. M.Sc. Thesis, Dalhousie University.

MacDonald, M.A. and Clarke, D.B., 1985. The petrology, geochemistry and economic potential of the Musquodoboit Batholith: Canadian Journal of Earth Sciences, pp. 1633-1642.

MacDonald, R., Thorpe, R.S., Gaskarth, J.W. and Grindrod, A.R., 1985. Multi-component origin of Caledonian lamprophyres of northern England: Mineralogical Magazine, 49, No. 353.

MacLeod, J.L., 1981. Tin, Port Mouton Queens County, Nova Scotia. Esso Resources Canada Limited. in Nova Scotia Department of Mines and Energy Assessment Report. 20P/15C, 51-N-17 (01)

MacMichael, T.P., 1975. The origin of the lead-zinc-silver ores and the alteration of the surrounding granites at the Dunbrack Mine, Musquodoboit Harbour, N.S. B.Sc. thesis (Hons.) Dalhousie University, Halifax, N.S.

Maksaev, V., 1986. The Origin of Banding in the Mountain Island Granite, Southern Nova Scotia. Unpublished Internal Report, Dalhousie University, Halifax, N.S.

Mamet, B.L., 1970. Carbonate microfacies of the Windsor Group (Carboniferous, Nova Scotia and New Brunswick: Geological Survey of Canada Paper 70-21.

Manning, D.A.C., 1983. Chemical variation in garnets from aplites and pegmatites, peninsular Thailand: Mineralogical Magazine, Sept., 47, pp. 353-358.

Manning, D.A.C. and Pichavant, M., 1983. The role of fluorine and boron in the generation of granitic melts: in M.P. Atherton and C.D. Gribble (editors), "Migmatites, Melting, and Metamorphism", Shiva Publ., pp. 94-109.

Martin, R.F. and Bowden, P., 1981. Peraluminous granites produced by rock-fluid interaction in the Ririwai nonorogenic ring-complex, Nigeria: Mineralogical evidence: in The Canadian Mineralogist, 19, Part 1, "Peraluminous Granites", D.B. Clarke, ed., pp. 65-84.

Mason, B.H., 1982. Principles of geochemistry. B. Mason, C.B. Moore, 4th Ed. New York: Wiley.

Mason, B., 1968. Kaersutite from San Carlos, Arizona, with comments on the paragenesis of this mineral: Mineralogical Magazine, 36, pp. 997-1002.

Mauger, R.L., 1982. Petrology of a Mesozoic biotite lamprophyre dyke near Concorde, North Carolina. in Geological Society of America Abstracts, program 14, pp. 38.

McKenzie, C.B., 1974. Petrology of the South Mountain Batholith, Western Nova Scotia. Unpublished M.Sc. thesis, Dalhousie University, Halifax, N.S.

McKenzie, C.B. and Clarke, D.B., 1975. Petrology of the South Mountain Batholith, Nova Scotia: Canadian Journal of Earth Sciences, 12, pp. 1209-1218.

McNally, R.N., 1972. "Zirconium", in The Encyclopedia of Geochemistry and Environmental Sciences. Ed. Fairbridge, R.W. Van Nostrand Reinhold Co., N.Y. Volume IVA. p1294-1295.

Merrett, D., 1987. The migmatites of Port Mounton. Unpublished Honours BSc thesis, Dalhousie University.

Metsis, D. and Cheyes, F., 1962. Varieties of Lamprophyre: Carnegie Institution of Washington Yearbook '62, pp. 156-157.

Mielke, P. and Winkler, H.G.F., 1979. Eine besser Berechnung der Mesonorm fuer granitische Gesteine: Newes Jahrb: Miner. Monatsh, No. 10, pp. 471-480.

Miller, C.F., 1985. Are strongly peraluminous magma derived from pelitic sedimentary sources?: Journal of Geology, 93, pp. 673-689.

Miller, C.F. and Stoddard, E.F., 1978. Origin of garnet in granitic rocks; an example of the role of Mn from thed Woman-Piute range, California: Geol. Assoc. Can/ Mineral. Assoc. Can, Program with Abstr., 3, p. 456.

Miller, C.F., Stoddard, E.F., Bradfish, L.J. and Dollase, W.A., 1981. Composition of plutonic muscovite: genetic implications: Canadian Mineralogy, 19, pp. 25-34.

Miyashiro, A., 1973. Metamorphism and metamorphic belts. Second ed., Allen & Urwin Ltd., 1973.

Moore, W.S. and Swami, S.K., 1972. "Thorium". in Encyclopedia of Geochemistry and Environmental Sciences. Ed. Fairbridge, R.W.

Muecke, G.K. and Clarke, D.B., 1981. Geochemical Evolution of the South Mountain Batholith, Nova Scotia: Rare-Earth-Element Evidence: Canadian Mineralogist, 19, pp. 133-145.

Muecke, 1984. Metamorphic evolution of the Meguma Terrane, N.S. GSA abstracts. 19th Annual Meeting- Northeastern Section, GSA. March 15-17

Oba, T., 1980. Phase relations in the tremolite-pargasite join: Contributions to Mineralogy and Petrology, 71, pp. 247-256.

Oldale, H.R., 1959. Beryllium, Port Mouton, Queens County, Nova Scotia, Preliminary Report. Nova Scotia Department of Mines, Address File 20P/15C 08-N-18(01).

O'Reilly, G.A., (in progress). Geology and Geochmistry of the Sangster Lake and Larry's River plutons, Guysborough County, Nova Scotia. MSc thesis, Dalhousie U. Halifax N.S.

O'Reilly, G.A., 1976. The Petrology of the Brenton Pluton Yarmouth County, N. S. Unpublished B.Sc. (Honours) thesis. Dalhousie University, Halifax, N.S.

Orville, P.M., 1963. Alkali ion exchange between vapor and feldspar phases: American Journal of Sciences, 61, pp. 201-237.

Palmer, M.G.B., 1979. Uranium Path Lake, Queens County, Nova Scotia, Can-Lake Exploratons Limited (For E and B explorations limited). Nova Scotia Department of Mines and Energy assessment report. 20P/15B, 54-N-29 (01).

Pearce, J.A., 1982. in Andesites (R.S. Thorpe Ed.) John Wiley & Sons, pp. 525-548. Trace element characteristics of lavas from destructive plate boundaries.

Pearce, J.A., 1983. Continental Basalts & Mantle xenoliths C.J. Hawkesworth and M.J. Norny, eds.) Shive Publ. pp. 230-249.

Phillips, W.J., 1956. Minor intrusive suite associated with the Crifell-Dalbeattie granodiorite complex: Proc. Geol. Assoc., 67, pp. 103-121.

Phillips, G.N., Wall, V.J. and Clemens, J.D., 1981. Petrology of the Strathbogie batholith - a corlierite- bearing granite: Canadian Mineralogy, 19, pp. 47-63.

Pilkey, O., 1972. "Barium". in The Encyclopedia of Geochemistry and Environmental Sciences. R.W. Fairbridge, Ed. Van Nostrand and Reinhold Co. N.Y. Volume IVA. p62-67.

Piwinskii, A.J. and Wyllie, P.J., 1968. Experimental studies of igneous rock series: a zoned pluton in the Wallowa batholith, Oregon: Journal of Geology, 76, pp. 205-234.

Piwinskii, A.J. and Wyllie, P.J., 1970. Experimental studies of igneous rock series "Felsic Body Suite" from the Needle Point Pluton, Wablowa batholith, Oregon: Journal of Geology, 78, pp. 52-76.

Poole, W.H., 1967. Tectonic evolution of the Appalachian region of Canada: in E.R.W. Neale and H. Williams (Eds.), Geological Association of Canada Special Paper, 4, pp. 9-51.

Poole, W.H., Sanford, B.V., Williams, H. and Kelley, D.G., 1970. Geology of southeastern Canada. in Geology and Economic Minerals of Canada: R.J.W. Douglas, Ed. Geological Survey of Canada, Economic Geology, Report 1 (5th Ed.), pp. 229-304.

Poole, W.H., 1971. Graptolites, copper and potassium argon in Goldenville Formation, N.S. in Report of Activities, Part A, GSC of Canada, Paper 71-1A, pp. 9-11.

Puchelt, H., 1978. "Barium", Chapter 56. in Handbook of Geochemistry. K.W. Wedepohl, Ed. Spring-Verlag Berlin-Heidleberg. Volume II-4. p56-a-1 to 56-A-22.

Purdy, J.W. and Jager, E., 1976. K-Ar ages on rock-forming minerals from the Central Alps: Mem. Inst., Geol. Mineral. Univ. Padova, 30, pp. 1-31.

Raase, P, 1974. Al and Ti contents of hornblend Indicators of pressure and temperature of regional metamorphism: Contributions to Mineralogy and Petrology. 45, 231-236.

Rast, N., 1984. The Alleghenian orogeny in eastern North America. in Variscan Tectonics of the North Atlantic Region. Ed. Hutton, D.H.W. and Sanderson, D.J., 1984. Blackwell Scientific Publications, The Geology Society.

Read, H.H., 1957. The granite controversy. T. Murby, London.

Reynolds, P.H., Kublick, E.E. and Muecke, G.K., 1973. Potassium-Argon Dating of Slates from the Meguma Group, N.S.: Canadian Journal of Earth Sciences, 10, No. 7, pp. 1059-1067.

Reynolds, P.H. and Muecke, G.K., 1978. Age studies on slates: applicability of the $^{40}Ar/^{39}Ar$ stepwise outgassing method: Earth Planetary Science Letters, 40, pp. 111-118.

Reynolds, P.H., Zentilli, M. and Muecke, G.K., 1981. K-Ar + $^{40}Ar/^{39}Ar$ geochronology of granitoid rocks from southern N.S. and its bearing on the geological evolution of the Meguma Zone of the Appalachians: Canadian Journal of Earth Sciences, 18, 1981.

Reynolds, P.H., Zentilli, M., Elias, P.M. and Muecke, G.K., 1984. The southwestern Meguma Zone, Nova Scotia: an argon study of regional cooling and Hercynian Mineralization. Geological Association of America, Northeastern Section, Abstracts with Programmes, 16, pp. 59.

Reynolds, R.C., 1972. "Rubidium". in The Encyclopedia of Geochemistry and Environmental Sciences, 10A. Van Nostrand and Reinhold Co., N.Y. Volume IVA. p1050-1052.

Richard, L., 1987. Geochemical discrimination of the Peraluminous Devono-Carboniferous Granitoids of Nova Scotia and Morocco. MSc in progress. Dalhousie University, Halifax, Nova Scotia.

Rock, N.M.S., 1977. The Nature and Origin of Lamprophyres; Some Definitions, Distinctions, and Derivations: Earth-Science Reviews, 13, 1977, pp. 123-169.

Rock, N.M.S., 1980. Rare-earth elements and the origin of minettes: a critical comment on a paper by Bachinski and Scott, 1979: Geochim. Cosmochim. Acta, 44, pp. 1385-8.

Rock, N.M.S., 1984. Nature and origin of calc-alkaline lamprophyres: minettes, vogesites, kersantites and spessartites: Trans. of the Royal Society of Edinburgh Earth Sciences, 74, pp. 193-227.

Rock, N.M.S. and Leake, B.E., 1984. The International Mineralogical Association amphibole nomenclature scheme: computerization and its consequences: Mineralogical Magazine, June, 48, pp. 211-227.

Rogers, H.D. (in progress). Geology and Igneous Petrology of Shelburne and eastern Yarmouth Counties, Nova Scotia. Masters thesis, Acadia University, Wolfville, Nova Scotia Canada

Rogers, H.D., 1985. Granitoid Rocks of Shelburne County and Eastern Yarmouth County, Nova Scotia, Chapter 7. in Guide to Granites and Mineral Deposits of Southwestern Nova Scotia. Ed. A.K. Chatterjee and D.B. Clarke; NSDME, Preprint of Paper 85-3.

Ruddock, D.I. and Hamilton, D.L., 1978a. The system $KAlSi_2O_6$-$CaMgSi_2O_6$-SiO_2 at 4 Kb. Prog. Exp. Petrol. Nerc. Publ. Ser. D, 11, pp. 25-27.

Ruddock, D.I. and Hamilton, D.L., 1978b. Stability of carbonate in simple potassium-rich rock model. in Prog. Exp. Petrol. NERC Publ. Ser. D, 11, pp. 28-31.

Schenk, P.E., 1970. Regional variation of the flysch-like Meguma Group (lower Paleozoic) of Nova Scotia, compared to recent sedimentation off the Scotian Shelf: Geological Association of Canada Special Papers, 7, pp. 127-153.

Schenk, P.E., 1978. Synthesis of the Canadian Appalachians; GSC Paper 78-13, pp. 113-136.

Schenk, P.E., 1981. The Meguma Zone of Nova Scotia - A Remnant of Western Europe, South America or Africa? Canadian Society of Petroleum Geology, Memoir 7, pp. 119-148.

Schenk, P.E. and Lane, T.E., 1982. Pre-Acadian sedimentary rock of the Meguma Zone, N.S. - a passive continental margin juxtaposed against a volcanic island arc. in International Association of Sedimentologists, Excursion 5B Guidebook, 85 p.

Schenk, P.E., 1983. The Meguma Terrane of Nova Scotia, Canada - an aid in trans-Atlantic correlation. in P.E.Schenk (Ed.), Regional Trends in the geology of the Appalachian - Caledonian - Hercynian - Mauritanide Oregon. Nato ASI Series. D. Reidal Publishing Co., pp. 121-130.

Slobodskay, R.M., 1972. Indication of injection of magma during formation of granitoid massifs: Int. Geol. Rev., 14, pp. 1351-1358.

Smith, J.G., 1973. A tertiary lamprophyre dyke province in S.E. Alaska: Canadian Journal of Earth Sciences, 10, pp. 408-420.

Smith, T.E., 1974. The geochemistry of the granitic rocks of Halifax Co., Nova Scotia: Canadian Journal of Earth Sciences, 11, pp. 650.

Smith, T.E. and Turek, A., 1976a. The geochemistry and origin of the Devonian granitic rocks in Southwestern, Nova Scotia. in GAC Abstracts, 1, pp. 73.

Smith, T.E., 1979. The geochemistry and origin of the Devonian granitic rocks of southwest Nova Scotia: GSA Bulletin, Part 2, 90, pp. 850-885.

Speer, J.A., 1984. Micas in Igneous Rocks. in S.W. Bailey (editor), Reviews in Mineralogy, vol. 13, Mica Mineralogical Society of America.

Speer, J.A., 1981. Petrology of cordierite- and almandine-bearing granitoid plutons of the southern Appalachian Piedmont, U.S.A. : in The Canadian Mineralogist, 19, Part 1, "Peraluminous Granites", D.B. Clarke, ed., pp. 35-46.

Stallard, V., 1975. Geochemistry of biotites as a guide to the evolution of the S.M.B. Unpublished Honours thesis, Dalhousie University, Halifax, N.S.

Stormer, J.C. Jr, and Nicholls, J., 1978. XLFRAC: A program for the interactive testing of magmatic differentiation models: Computers and Geoscience, 14, pp. 143-159.

Streckeisen, A., 1976. To each plutonic rock its proper name: Earth-Sciences Review, 12, pp. 1-33.

Streckeisen, A, 1979. Classification and nomenclature of volcanic rocks, lamprophyres, carbonatites and melilitic rocks: Geology, 7, pp. 331-5

Strong, D.F. and Hanmer, S.K., 1981. The leucogranites of southern Brittany: origin by faulting, frictional heating, fluid flux and fractional melting: in The Canadian Mineralogist, 19, Part 1, "Peraluminous Granites", D.B. Clarke, ed., pp. 163-176.

Sultan, M., Batiza, R. and Sturchio, N.C., 1986. The origin of small-scale geochemical and mineralogic variations in a granite intrusion. A crystallization and mixing model: Contributions to Mineral Petrology, 93, pp. 513-523.

Sundius, N., 1946. The classification of hornblendes and the solid solution relations in the amphibole group: Arsbok Sueriges Geol. Undersok, 40, No. 4

Taylor, F.C., 1967. Reconnaissance geology of Shelburne map-area, Nova Scotia: Geological Survey of Canada Memoirs, 349.

Taylor, S.R., 1980. Refractory and moderately volati element abundances in the earth, moon and meteorites. in Proc. Lunar Sci. Confr., 11, pp. 333-348.

Trent, D.D., 1981. 'Schlieren in the Sierra Nevada'. Paper presented at 77th Annual Meeting of the GSA, March 27, 1981 at Herniosillo, Sonora, Mexico.

Turekian, K., 1956. "The geochemistry of strontium": Geochim. Cosmochim. Acta, 10, pp. 145-196.

Turekian, K.K. and Wedepohl, W.H., 1961. Distribution of the elements in some major units of the earth's crust: Geological Society of America Bulletin, 72, pp. 175-192.

Turner, F.J. and Verhoogen, J., 1960. Igneous and Metamorphic Petrology. New York : McGraw Hill.

Turner, G., 1968. The distribution of potassium and argon in meteorites. in Origin and Distribution of the Elements. Ed. L.H. Ahrens, pp. 387-397. London : Pergamon, 1178 pp.

Turner, G., 1969. Thermal histories of meteorites by the $^{40}Ar/^{39}Ar$ method. in Meteorite Research, Ed. P.M. Millman, pp. 407-417. Dordrecht : Reidel, 940 pp.

Tuttle, O.F. and Bowen, N.L., 1958. Origin of granite in the light of experimental studies in the system $NaAlSi_3O_8$-$KAlSi_3O_8$-SiO_2-H_2O. Geological Society of America Memoirs, 74, pp. 153.

Vernon, R.H., 1984. Microgranitoid enclaves in granite globules of hybrid magma quenched in a plutonic environment: Nature, 309.

Wall, V.J., Clemons, J.D., and Clarke, D.B., 1987. Model for granitoid evolution and source compositions. Unpublished.

Wampler, J.M., 1972. The Encyclopedia of Geochemistry and Environmental Sciences. Ed. Fairbridge, R.W.

Wark, J.M. and Clarke, D.B., 1980. Geochemical discriminators and the palaeotectonic environment ofthe North Mountain basalts, Nova Scotia: Canadian Journal of Earth Sciences, 12, pp. 1740-1745.

Weagle, M.A., 1983. Study of the Moose Point Pluton, Queen's County, Nova Scotia. B.Sc. Acadia University, April.

Webb, G.W., 1969. Paleozoic wrench faults in Canadian Appalachians. in M. Kay (Ed.). North Atlantic-geology and continental drift. American Association of Petroleum Geology, Memoir 12, pp. 754-786.

White, A.J.R. and Chappell, B.W., 1977. Ultrametamorphism and granitoid genesis: Tectonophysics, 43, pp. 7-22.

William, H., 1979. Appalachian Orogen in Canada: Canadian Journal of Earth Science, v. 16, p762-807.

Wimmenauer, W., 1973b. Lamprophyre, Semilamprophyre and Whibasaltische Gangesteine: Fortschr. Mineral, 51, pp. 3-67.

Wimmenauer, W., 1976. Remarks to the Discussion on Nomenclature of Lamprophyres. Consultative Document IUGS subcommission (unpublished as of 1976).

Winkler, H.G.F., 1976. Petrogenesis of Metamorphic Rocks. 4th edition. 1974, 1976 by Springer-Verlag, New York Inc.

Wones, D.R. and Gilbert, M.C., 1982. Amphiboles in the Igneous Environment, Chapter 3, pp. 355-368. in D.R. Veblen and P.H. Ribbe, editors. Reviews in Mineralogy, vol. 93, Amphiboles: Petrology and Experimental Phase Relations.

Wyllie, P.J., Huang, W., Stern, C.R. and Maale, S., 1976. Granitic magmas: possible and impossible sources, water contents, and crystallization sequences: Canadian Journal of Earth Sciences, 13, 1007-1019.

Wyllie, P.J., 1977. Crustal anatexis: An experimental review: Tectonophysics, 13, pp. 41-71.

Wyllie, P.J., 1983. Experimental and Thermal Constraints on the Deep-seated Parentage of some Granitoid Magmas in Subduction Zones. in Migmatites, Melting and Metamorphism. M.P.A. Horton and G.D. Gribble (Eds.), Shiva Publ. Ltd., 1983, pp. 36-51.

Wyllie, P.J., 1984. Sources of granitoid magmas at convergent plate boundaries: Phys. Earth Planet. Inter., 35, pp. 12-18.

Yamaguchi, Y., 1985. Hornblende-cummingtonite and hornblende-actinolite intergrowths: American Mineralogy, 70, pp. 980-986.

Yoder, H.S. and Tilley, C.E., 1962. Origin of basaltic(?) magmas: An experimental study of natural and synthetic rock systems: Journal of Petrology, 3, pp. 342-532.

Zen, E-An, 1987. Aluminum Enrichment in Silicate Melts by Fractional Crystallization: Some Mineralogic and Petrographic Constraints: Journal of Petrology, 27, No. 5, Oct.

Zen, E-An, 1987. Phase Relations of Peraluminous Granitic Rocks and their Petrogenic Implications. In progress.

Zentilli, M., 1977. Evolution of metallogenic domains in Nova Scotia (abstract). Canadian Institute of Mineral Metallurgy Bulletin, 70, pp. 69.

Zentilli, M. and Reynolds, P.H., 1985. Ar/Ar dating of micas from the East Kemptville tin deposit, Yarmouth County, Nova Scotia: Canadian Journal of Earth Sciences.

MAP 1

Geology of the Port Mouton Pluton, Nova Scotia

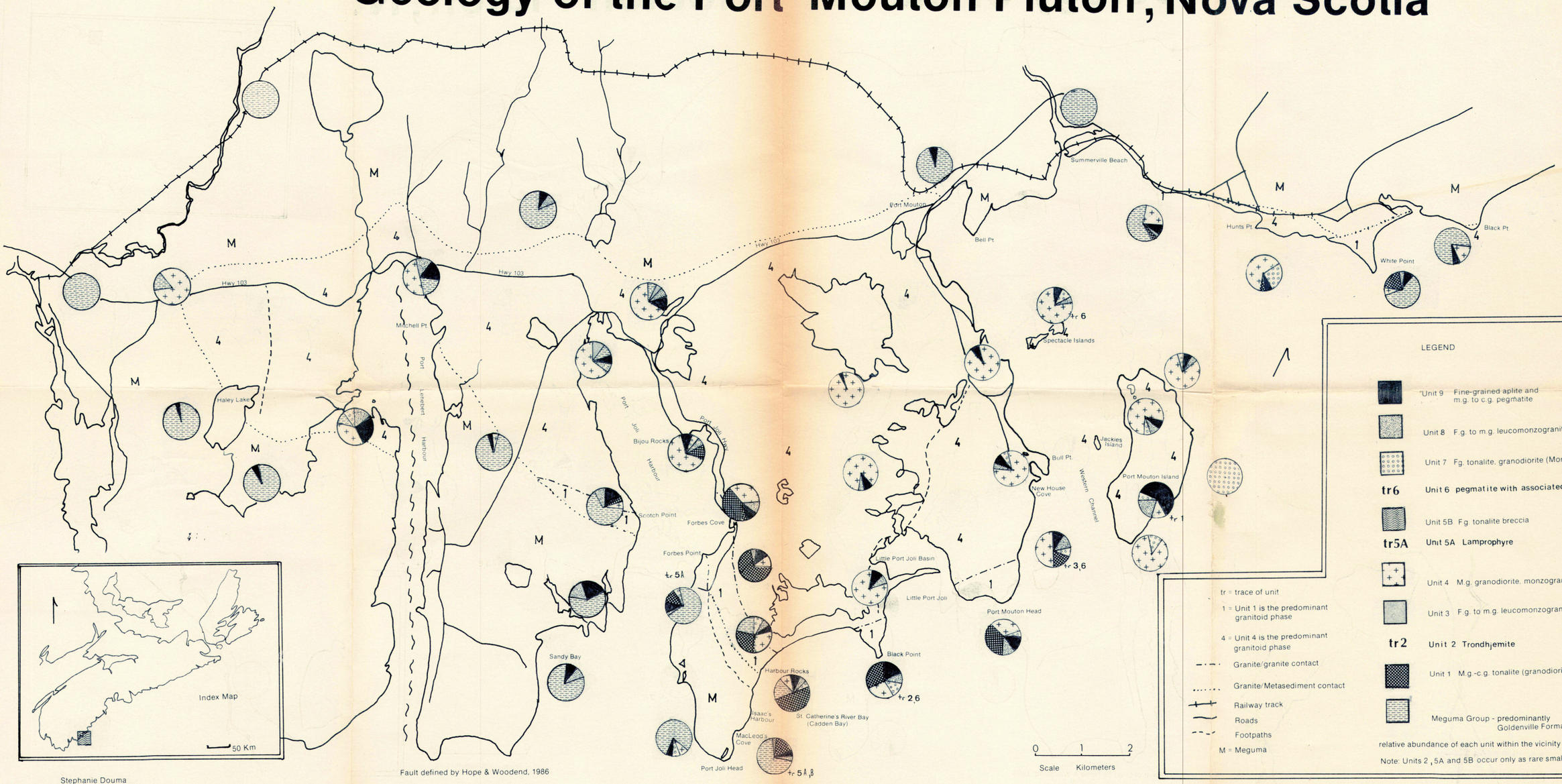

LEGEND

- Unit 9 Fine-grained aplite and m.g. to c.g. pegmatite
- Unit 8 F.g. to m.g. leucomonzogranite
- Unit 7 Fg. tonalite, granodiorite (Monzogranite)
- tr6 Unit 6 pegmatite with associated aplite
- Unit 5B F.g. tonalite breccia
- tr5A Unit 5A Lamprophyre
- Unit 4 M.g. granodiorite, monzogranite
- Unit 3 F.g. to m.g. leucomonzogranite
- tr2 Unit 2 Trondhjemite
- Unit 1 M.g.-c.g. tonalite (granodiorite)
- Meguma Group - predominantly Goldenville Formation

relative abundance of each unit within the vicinity of the pie

Note: Units 2, 5A and 5B occur only as rare small dykes

tr = trace of unit

1 = Unit 1 is the predominant granitoid phase

4 = Unit 4 is the predominant granitoid phase

Granite/granite contact

Granite/Metasediment contact

Railway track

Roads

Footpaths

M = Meguma

Stephanie Douma

MAP 2

Sample Location Map for the Port Mouton Pluton, Nova Scotia